AD-A084 171 UNIVERSAL ENERGY SYSTEMS INC DAYTON OHIO F/G 11/6
SURFACE CHARACTERIZATION OF CHEMICALLY TREATED TITANIUM AND TIT--ETC(U)
FEB 80 A A ROCHE F33615-79-C-5129
UNCLASSIFIED AFWAL -TR-80-4004 NL

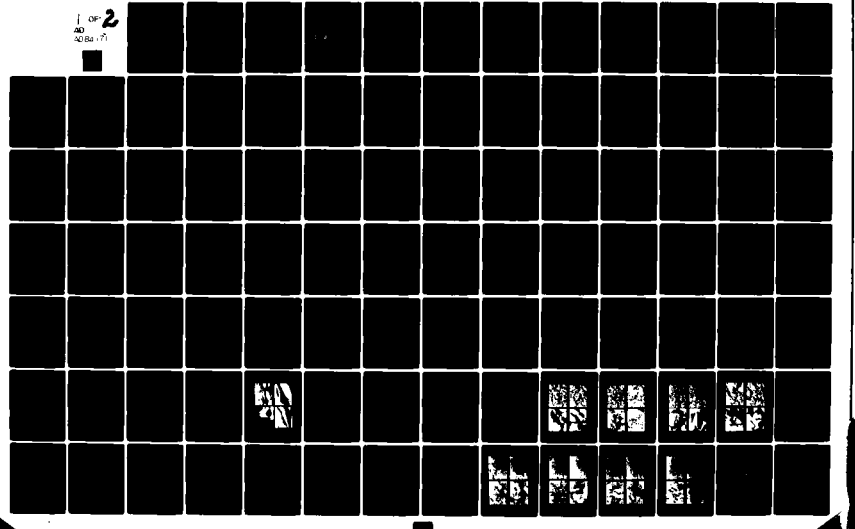

AFWAL-TR-80-4004

(2) LEVEL II

SURFACE CHARACTERIZATION OF CHEMICALLY TREATED TITANIUM AND TITANIUM ALLOYS

A. A. ROCHE
UNIVERSAL ENERGY SYSTEMS, INC.
3195 PLAINFIELD ROAD
DAYTON, OHIO 45432

FEBRUARY 1980

TECHNICAL REPORT AFWAL-TR-80-4004
Interim Report for period 1 May 1979 — 30 November 1979

MATERIALS LABORATORY
AIR FORCE WRIGHT AERONAUTICAL LABORATORIES
AIR FORCE SYSTEMS COMMAND
WRIGHT-PATTERSON AIR FORCE BASE, OHIO 45433

NOTICE

When Government drawings, specifications, or other data are used for any purpose other than in connection with a definitely related Government procurement operation, the United States Government thereby incurs no responsibility nor any obligation whatsoever, and the fact that the Government may have formulated, furnished, or in any way supplied the said drawings, specifications, or other data, is not be be regarded by implication or otherwise as in any manner licensing the holder or any other person or corporations, or conveying any rights or permission to manufacture, use, or sell any patented invention that may in any way be related thereto.

This report has been reviewed by the Information Office (OI) and is releasable to the National Technical Information Service(NTIS). At NTIS, it will be available to the general public, including foreign nations.

This technical report has been reviewed and is approved for publication.

W.L. BAUN, Project Engineer
Mechanics & Surface Interactions Branch
Nonmetallic Materials Division

S.W. TSAI, Chief
Mechanics & Surface Interactions Branch
Nonmetallic Materials Division

FOR THE COMMANDER

J.M. KELBLE, Chief
Nonmetallic Materials Division

"If your address has changed, if you wish to be removed from our mailing list, or if the addressee is no longer employed by your organization, please notify AFWAL/MLBM, W-PAFB, Ohio 45433 to help us maintain a current mailing list".

Copies of this report should not be returned unless return is required by security considerations, contractual obligations, or notice on a specific document.

AIR FORCE/56780/24 April 1980 — 200

SECURITY CLASSIFICATION OF THIS PAGE (When Data Entered)

REPORT DOCUMENTATION PAGE	READ INSTRUCTIONS BEFORE COMPLETING FORM
1. REPORT NUMBER: AFWAL-TR-80-4004	2. GOVT ACCESSION NO.: AD-A084 172 / 3. RECIPIENT'S CATALOG NUMBER:
4. TITLE (and Subtitle): SURFACE CHARACTERIZATION OF CHEMICALLY TREATED TITANIUM AND TITANIUM ALLOYS	5. TYPE OF REPORT & PERIOD COVERED: INTERIM REPORT MAY 1979 – NOVEMBER 1979
	6. PERFORMING ORG. REPORT NUMBER:
7. AUTHOR(s): ALAIN A. ROCHE	8. CONTRACT OR GRANT NUMBER(s): F33615-79-C-5129
9. PERFORMING ORGANIZATION NAME AND ADDRESS: UNIVERSAL ENERGY SYSTEMS, INC. 3195 PLAINFIELD ROAD DAYTON, OHIO 45432	10. PROGRAM ELEMENT, PROJECT, TASK AREA & WORK UNIT NUMBERS:
11. CONTROLLING OFFICE NAME AND ADDRESS: MATERIALS LABORATORY (AFML/MBM) AIR FORCE WRIGHT AERONAUTICAL LABORATORIES WRIGHT PATTERSON AIR FORCE BASE, OHIO 45433	12. REPORT DATE: FEBRUARY 1980 / 13. NUMBER OF PAGES:
14. MONITORING AGENCY NAME & ADDRESS (if different from Controlling Office): SAME AS NO. 11	15. SECURITY CLASS. (of this report): UNCLASSIFIED / 15a. DECLASSIFICATION/DOWNGRADING SCHEDULE:

16. DISTRIBUTION STATEMENT (of this Report)

APPROVED FOR PUBLIC RELEASE;DISTRIBUTION IS UNLIMITED.

17. DISTRIBUTION STATEMENT (of the abstract entered in Block 20, if different from Report)

18. SUPPLEMENTARY NOTES

19. KEY WORDS (Continue on reverse side if necessary and identify by block number)

Surface Characterization	Auger Electron Spectroscopy
Surface Treatment	Secondary Ion Mass Spectroscopy
Titanium	Photoelectron Spectroscopy
Titanium Alloy	Scanning Electron Microscopy
Adhesive Bonding	Auger-Sputter Profile Analysis

20. ABSTRACT (Continue on reverse side if necessary and identify by block number)

A thorough knowledge of adherend surfaces is necessary to adequately evaluate adhesive bond joint performance. Auger Electron Spectroscopy (AES), Secondary Ion Mass Spectroscopy (SIMS), Scanning Electron Microscopy (SEM), and X-Ray Photoelectron Spectroscopy (XPS) were used to characterize the surface topography (roughness, selective etching) composition (relative concentration of alloyed element on surface, contaminated overlayer...) chemical state (titanium or alloy surface oxide, oxy-fluoride...) and oxide thickness of different chemically treated titanium and titanium alloys. Seven alloys and

DD FORM 1 JAN 73 1473 EDITION OF 1 NOV 65 IS OBSOLETE

SECURITY CLASSIFICATION OF THIS PAGE (When Data Entered)

S/N 0102-014-6601

the metal were conditioned with seven different chemical treatments. Data from each treated alloy has been compiled to show physical and chemical effects of each treatment on each alloy.

FOREWORD

This report describes the results of a research program to characterize the effects of surface treatments to titanium alloys for adhesive bonding. This report covers the period from May 1979 through November 1979. Until September, 1979 it was conducted by the Southeastern Center for Electrical Engineering Education (SCEEE), 202 Samford Hall, Auburn University, Auburn, Alabama 36830 at the Air Force Materials Laboratory under Contract F33615-77-C-5003, Contributive Research/Resident Scientist Program, initiated under Task 53B. The work monitor was H.L. Guidrey.

Since October 1979 the program has been conducted by Universal Energy Systems, Inc. (UES), 3195 Plainfield Road, Dayton, Ohio 45432, with the research performed at the Air Force Materials Laboratory at Wright Patterson Air Force Base, Ohio 45433, under Contract F33615-79-C-5129 Contributive Research/Visiting Scientist Program, initiated under Task 10. The work monitor is W. Powell. The Project Engineer for the Air Force was W.L. Baun, Mechanics and Surface Interactions Branch, Nonmetallic Materials Division (AFML/MBM). The research was performed by A.A. Roche. The author submitted this report in December 1979.

ACKNOWLEDGMENTS

Acknowledgment is made to W.L. Baun and J.S. Solomon for their helpful suggestions and discussions. I would also like to thank W.C. Miller, D.E. Hanlin and M.F. Koeing for their contributions to the experimental work.

TABLE OF CONTENTS

TABLE OF CONTENTS (continued)

LIST OF TABLES

LIST OF TABLES (CONTINUED)

LIST OF ILLUSTRATIONS

LIST OF ILLUSTRATIONS (CONTINUED)

FIGURE LIST OF ILLUSTRATIONS (CONTINUED) PAGE

LIST OF ILLUSTRATIONS (CONTINUED)

LIST OF ILLUSTRATIONS (CONTINUED)

I. INTRODUCTION

Advanced aircraft design and performance specifications require the use of high temperature, lightweight materials, such as, titanium and titanium alloys. These materials are used in a number of airframe systems, which can in turn be fabricated in a number of ways, including conventional riveting, adhesive bonding, and weld bonding. The latter two processes are still in the research and development stage. Their anticipated advantages over conventional fabrication processes includes overall weight reduction while maintaining high strength requirements. Three major factors which influence adhesive bond joint performance include prebonding surface conditioning, adhesive formulation, and performance environment.

Titanium has two crystallographic forms: alpha and beta. The alpha (α) phase is a close-packed hexagonal structure while the beta (β) phase is body-centered cubic. There are approximately 30 titanium alloys and there are usually classified into α, α - β or β groups. The principal alloying elements used in the α alloys are AL,O,Sn, and Zr. The principal alloying elements in β alloys, which serve as stabilizers are Mn,Fe, Cr,V, and Mo. The alloys studied in this work are listed in Table I.

The purpose of this work is to establish a data base which can be used to assess the effects of chemical etching on the surface morphology and composition of titanium and titanium alloys. This data will thus be beneficial in establishing whether a particular etch is to be used with a series of surface conditioners or possibly as an exclusive prebonding treatment. Seven common chemical etchants for titanium and seven titanium alloys were investigated. Their respective effects on the metal alloy surfaces were characterized with an Auger Electron Spectrometer (A.E.S.),

TABLE 1

TITANIUM AND TITANIUM ALLOYS COMPOSITION (Ref. 1)

TITANIUM AND ALLOYS	CODE	TYPE	DENSITY	COMPOSITION (WEIGHT %)											
				Al	V	Sn	Mn	Mo	Zr	Si	Cr	Fe	C	N	O
Ti commercially purity	A	α	4.52				0.20					0.30	0.10 to 0.20	0.07	0.15
Ti - 8Al - 1Mo - 1 Sn *	B	α - β near α	4.40	8		1		1							
Ti - 6Al - 4V	C	α - β	4.46	5.5 to 6.75	3.5 to 4.5							0.30	0.10	0.05	0.2
Ti - 5Al - 2.5 Sn	D	α	4.46	4.0 to 6.0		2.0 to 3.0	0.30					0.50	0.15	0.07	0.2
Ti - 5Al - 5Sn - 2Mo-2Zr-0.25 Si*	E	near α - β	4.52	5		5		2	2	0.25					
Ti - 3Al-2.5V	F	α - β	4.49	2.5 to 3.5	2.0 to 3.0							0.25	0.05	0.02	0.12
Ti - 13V - 11Cr - 3Al	G	β metastable	4.84	2.5 to 4.0	12.5 to 14.5						10.00 to 12.00	0.35	0.05 to 0.10	0.05 to 0.08	0.20
Ti - 8Mn	H	α - β	4.74				6.5 to 9.0						0.08 max.	0.05 max.	

* Alloy composition not given

Secondary Ion Mass Spectrometer (SIMS), Scanning Electron Microscopy (SEM), and a X-Ray Photoelectron Spectrometer (XPS). The information obtained from these four techniques is divided into three categories:

- surface chemistry
- elemental depth distribution
- and surface topography

II. EXPERIMENTAL

Titanium and its alloys listed in Table 1 were subjected to the chemical treatments listed in Table 2. After drying, they were analyzed with a PERKIN-ELMER Physical Electronics Industries (PHI) model 540 A Thin Film Analyzer equipped with a single pass Cylindrical Mirror Analyzer (CMA) with a resolution $\Delta E/E \sim 0.6\%$. The coaxial electron gun was operated with a 4 KeV potential at 1.0 to 5.0 μA beam current. A peak-to-peak modulation of 7eV during broad scans (ie, 0-2000 eV) and 3 eV for narrow scans (ie,330-530 eV) was applied to the analyzer for phase sensitive detection. Elemental sputter profiles were constructed using digitally recorded and computer processed N'(E) data(Ref. 2). The ion beam was generated with a PHI model 04-191 Sputter Ion Gun which was operated with a beam potential of 2 KeV and ion current density of approximately 1.9 $\mu A/mm^2$ at 10 mA ion gun emission current or 0.5 $\mu A/mm^2$ at 3 mA ion gun emission current (Data noted *).

The sputtering rate for TiO_2 under the above conditions was determined to be 11.5 nanometers per minute (1 Nanometer (nm) = 3.94×10^{-8} in.) with an ion current density of 1.9 $\mu A/mm^2$ and 2.8 nm/min with an ion current density of 0.5 $\mu A/mm^2$. This was done using a titanium specimen anodized in room temperature tartaric acid (150 g|1) at 100 volts. To determine the oxide thickness, a piece of the anodized specimen was gold coated and bent to produce cracks in the anodic oxide layer and examined with an ISI - 60 Scanning Electron Microscope (S.E.M.). Figure 1 contains the SEM micrographes of the bent specimen and cross sections of the fractured oxide which show the oxide to be 205 ±10nm thick. The AES spectrum of this specimen prior to sputtering is shown in Figure 2. The Ti peak

TABLE 2

SURFACE CHEMICAL TREATMENTS FOR TITANIUM
AND TITANIUM ALLOYS

CODE	DESCRIPTION	TREATMENT
1	Degrease	Sample slurried in acetone, wiped dry, then ultrasonically cleaned in carbon tetrachloride for 5 minutes.
2	Alkaline	Sample submerged in 0.1N sodium hydroxide, room temperature for 2 minutes. Running tap H_2O for 1 minute, standing deionized H_2O for 5 minutes.
3	HNO_3/HF (fluoro-nitric)	Sample submerged in a solution of 170ml nitric acid, 30ml hydrofluroic acid, 800ml distilled water, room temperature for 2 minutes. Rinse as in #2.
4	$Na_3PO_4/NaF/HF$ (fluoro-phosphate)	Sample submerged in a solution of 50g sodium ortho phosphate, 9g sodium fluoride, 26ml hydrofluoric acid, distilled water to 1 liter, room temperature for 2 minutes. Rinse as in #2.
5	NH_4HF_2 (fluoro-ammonium)	Sample submerged in solution of ammonium bifluoride (10g/liter) room temperature for 2 minutes. Rinse as in #2.
6	H_2SO_4/CrO_3 (sulfo-chromium)	Sample submerged in solution of 300g sulfuric acid, 40g chromium acid, distilled water to 1 liter, room temperature for 2 minutes. Rinse as in #2.
7	$HNO_3/HF/H_2O_2/NH_4F,HF$ (fluoro-nitro-ammonium)	Sample submerged in solution of 80ml nitric acid, 20 ml hydrofluoric acid, 20ml hydrogen peroxide (30%), 10ml ammonium bifluoride (saturated), distilled water 500ml, room temperature for 2 minutes. Rinse as in #2.
8	Hot $NaOH/H_2O_2$ (hot alkaline)	Sample submerged in solution of 20g sodium hydroxide, 20ml hydrogen peroxide (30%), distilled water to 1 liter, 65°C temperature (150 F) for 2 minutes. Rinse as in #2.

shapes are characteristic of TiO_2 (Ref. 3-9). Figures 3 and 4 contain the Auger sputter profiles with 10mA and 3mA ion gun emission current respectively. Oxide thickness determinations from sputter profiles were made by multiplying the sputtering time to the oxide metal interface by the predetermined sputtering rate. The sputtering time to reach an interface was chosen as the average between oxygen and titanium sputtering times to the 50% points on their respective profiles.

Secondary Ion Mass Spectroscopy (SIMS) analysis was performed using an EAI/1100 quadrupole mass analyzer fitted with a low resolution double-focussing ion energy filter. Figure 5 contains a schematic drawing of the combined AES - SIMS instrument which allows for simultaneous analysis by both techniques. The same ion gun used for sputter profiling was used as the primary ion beam source for SIMS. Both He^+ and Ar^+ were used as primary ion sources. He^+ was used to obtain SIMS data from surfaces prior to sputter profiling since near static (nonsputtering) conditions can be achieved with the lighter inert gas. During sputter profiles analysis Ar^+ was used. The AES - SIMS analysis of the specimens proceeded as follows:

- AES spectrum (0-2000 eV)
- AES spectrum (330-530 eV)
- SIMS spectrum (He^+)
- AES spectrum after He^+ SIMS (0-2000 eV)
- AES in depth profile(Ar^+)
- SIMS during the sputtering (Ar^+)
- AES spectrum after sputter profiling (0-2000eV)

Pieces of the specimens for SEM analysis were coated with $\sim$ 20 - 50 nm Au in an ISI-PS-2 Sputter coater. All specimens were analyzed with a tilt angle of 15°.

An X-ray Photoelectron Spectrometer (XPS or ESCA) KRATOS ES-300 was used for the analysis of several alloyed titanium samples. Base pressure for the system was 7×10^{-10} torr (9.1×10^{-8} Pa), and all scans were taken at a pressure less than 6×10^{-8} torr (7.8×10^{-6} Pa). Non-monochromatic Mg $K_{\alpha_{1,2}}$ radiation was used at a power setting of 105 watts (15 KV, 7mA). Resolution was determined with a clean silver sample. Using a 1.0 mm exit slit and operating in the fixed 65 eV transmission mode, the full width at half maximum (F W H M) of the Ag $3d^{5/2}$ peak was measured to be 0.92 eV. A Ion Tech B 22b Saddle-Field Ion gun was used for sputter etching. Typical settings were 8KV, 5mA to the cathode and a measured ion current 16 μA impinging on the sample. A constant flow of argon through the ion gun and system was required for sputtering. During this time the pressure in the analysis chamber rose to 2×10^{-4} torr (2.6×10^{-2} Pa). The spectrometer was calibrated for C_{1s} at 285 eV (binding energy).

III. RESULTS

1. TITANIUM (c.p.)

A. Surface Topography

Figures 6 - 9 contain S.E.M. micrographs of commercially pure titanium panels subjected to each of the chemical treatments listed in Table 2. The alpha-numberic code to the right of the micrographs identifies the specimen according to material and treatment codes from Tables 1 and 2, respectively. For example, code A_{1-7} identifies the upper micrographs in Figure 9 as those from c.p. titanium subjected to treatment 1 followed by treatment 7.

Treatments 1-2,1-6,1-7 and 1-8 produce surfaces very similar to the "as received" (treatment 1) surface. Treatments 1-3,1-4, and 1-5 produce surfaces containing microcrystalline particles. This is in agreement with previously reported work (Ref. 3,6, 10-14).

B. Surface Composition

a) Auger Electron Spectroscopy (AES)

AES spectra from specimens subjected to treatments 1 through 1-6 were similar to those previously reported from identically treated titanium (Ref. 6, 14, 15). Figures 10 and 11 contain AES spectra from titanium subjected to treatments 1-7 and 1-8. Table 3 is a semi-quantitative compilation of the elements detected by AES from each of the treated Ti panels. The numbers listed are the Auger peak-to-peak height (APPH) ratio normalized to the Ti_{LMM} peak at $\sim$ 381 eV. Figures 12 and 13 are the expanded spectrum of Ti_{LMM}, Ti_{LMV} and O_{KLL} from specimens A_{1-7} and A_{1-8} respectively. The Ti_{LMV} peaks at approximately 400-425 eV have a subtle difference in their respective shapes. These peaks

reflect the 3d and 4s valence band transitions and are sensitive to the chemical state of titanium (Ref. 5). The Ti_{LMV} peak from A_{1-8} is very similar to that of TiO_2 (Ref. 3-9). The Ti_{LMV} peak shape from A_{1-7} is similar to that from Ti_2O_3 (Ref. 8) and to that reported by Solomon et. al. (Ref. 16) and Mathieu et. al. (Ref. 17) for electron beam induced reduction of TiO_2. Therefore there is some doubt whether: (1) the Ti_{LMV} peak shape difference between A_{1-7} and A_{1-8} reflects a real difference in the Ti chemical state; (2) electron beam reduction occurred; or (3) the oxide layer is very thin and therefore the Ti_{LMV} peak shape simply reflects a mixture of TiO_2+Ti.

b) Secondary Ion Mass Spectroscopy (SIMS)

Figures 14 and 15 contain the + SIMS spectra from specimens A_{1-7} and A_{1-8} respectively obtained with 2kV He+. The differences between these two spectra are subtle. The largest difference is the presence of more contaminant species, attributed to the tap water, on A_{1-8}. Table 4 summarizes the SIMS data from the treated Ti panels. All values listed are normalized to the Ti(m/e = 48) peak.

c) Auger Sputter Profiles Analysis (ASPA)

Figures 16 and 17 contain the Auger Sputter Profiles of C,O, Ti and S from specimens A_{1-7} and A_{1-8} respectively. The profiles in these figures reflect total analysis time. In all cases sputtering was initiated after approximately five minutes analysis time. The difference in initial O and Ti signal levels is attributed to the differences in surface contaminants such as C and S.

Table 5 lists the oxide thickness on each of the pretreated panels. Because of the uncertainties of sputtering and O-Ti diffusion, the oxide metal interfacial width is listed in Table 5 as the

TABLE 3 : AES ELEMENTAL I.D. OF TREATED TITANIUM (c.p.)

TREATMENT	ELEMENT IDENTIFICATION											
	Ti (381 eV)	O	C	P	Cu	Si	Na	F	S	Cl	K	Ca
1	1	2.8	1.6				0.2		0.15	0.25	x	0.25
1-2	1	2.2	0.9	x		x	x		x	x		x
1-3	1	2	0.6		0.3	x			x	x		x
1-4	1	1.2	0.3	0.2			0.3	0.8	x	x		0.12
1-5	1	1.8	0.3	x					x	x		x
1-6	1	2.4	0.9				x	x	x	x		x
1-7	1	2	0.3						x	x		x
1-8	1	2.3	0.9				x		x	x		x

(x APPH RATIO < 0.1)

TABLE 4 : SIMS ELEMENTAL I.D. OF TREATED TITANIUM (c.p.)

TREATMENT	m/e / positive ion identification										
	16 O	19 F	23 Na	31 P	39 K	40 Ca	48 Ti	59 CaF	64 TiO	67 TiF	86 TiF_2
1	0.2	x	>6		>6	0.7	1		0.4		
1-2	x	x	1.6	x	0.5	0.4	1		0.36		
1-3	x	x	0.6		x	0.1	1		0.25		
1-4		0.23	5.2	x	0.25	1	1	x	0.12	0.10	x
1-5	x	x	1.2	x	0.20	x	1		0.26		
1-6	x	x	1.3		0.35	0.2	1		0.41		
1-7	x	x	0.7		x	x	1		0.23		
1-8	x	x	0.9		0.1	0.7	1		0.33		

(x VALUE < 0.1)

TABLE 5: CARBON DISTRIBUTION, OXIDE AND INTERFACIAL THICKNESS DETERMINED BY AUGER SPUTTER PROFILE ANALYSIS FROM TREATED Ti (c.p.)

TREATMENT	1	1-2	1-3	1-4	1-5	1-6	1-7	1-8
THICKNESS (nm)	16.6	5.7	6.7	82.5	19.4	13.5	7.0	15.6
INTERFACE O Δt(min)	1.8	0.8	0.8	15.4	8.1	1.6	1.2	1.8
C DISTRIBUTION Δt (min)	0.4	0.4	3.6	7.5	5.5	1.2	0.4	0.6

difference (Δt) between the sputtering time to the 16% and 84% points on the oxygen profile contour at the interface (Ref. 17). It is felt therefore that the Δt values listed in Table 5 provide a semiquantitative comparison of the effects of each treatment on oxide interfacial width. Treatment 1-4 had the thickest oxide layer and the broadest interface between oxide and metal while treatment 1-2 produced the thinnest oxide layer and interface. This is in agreement with their respective SEM micrographs in Figures 6 and 7. Carbon and sulfur were found to be present on the surface of all the treated specimens. Their distribution within the oxide seems to be the greatest when the oxide microstructure resulting from treatment 1-3 and 1-5 (Fig. 7 and 8) is observed. The carbon is most likely an adsorbed species such as CO, CH_n since as shown in Figure 18 most of the carbon is removed with a very gentle sputter with He^+. Like the oxide metal interface, carbon distribution at the surface is listed Table 5 in terms of Δt since it is removed too quickly to define its presence in a discrete layer.

2. Ti-8Al-1Mo-1Sn

A. Surface Topography

Figures 19-22 contain S.E.M. micrographs of treated Ti-8Al-1Mo-1Sn (B) alloy. The most noticeable difference with this alloy compared to Ti - (Fig. 6-9) is the presence of what appears to be a second phase even after chemical treatment. Treatment 1-4 produced the same "sea shell" structure as observed on A_{1-4}. Treatment 1-3, 1-5 and 1-7 produce surfaces with the most distinguishable "plate-like structure" which is probably the result of selective etching (Ref. 12, 18-20). This structure, which results from treatment 1-3,1-5, and 1-7 is characteristic of the alpha and beta phases.

B. Surface Composition

a) Auger Electron Spectroscopy (AES)

Figures 23 and 24 contain the AES spectra from a degreased panel. The spectrum in Figure 24 is an expanded portion of Figure 23 and shows that Sn is not detected, although it would suffer interference by overlapping Ti peaks. Except for treatment 1-4 (Figure 25) the AES spectra from the remaining panels were similar to those for the degreased panel. Figure 26, the expanded spectrum from a panel subjected to treatment 1-4, shows that the Ti_{LMV} peak shapes have some subtle differences compared to Figure 24 which implies a difference in the chemical state of titanium at the surface since any electron beam effects would be the same for both specimens. A semiquantitative compilation of the elements detected by AES in all the treated specimens is presented in Table 6. As Table 6 shows, only one of the alloying element, aluminum, was detected on any of the treated surfaces.

b) Secondary Ion Mass Spectroscopy (SIMS)

Figures 27 and 28 contain the + SIMS spectra for a degreased panel and one subjected to the treatment 1-4. The SIMS spectra from the remaining panels were identical to Figure 27. Table 7 summarizes the SIMS data from the treated panels. All values listed are normalized to the Ti (m/e = 48) peak. The fact that Sn is detected on the degreased panel (Figure 27) shows the importance of having complementary techniques which offset each others possible weaknesses.

c) Auger Sputter Profiles Analysis (ASPA)

Figures 29 and 30 contain the normalized elemental sputter profiles of C,O,Ti, and Al from panels subjected to treatment 1 and 1-4 respectively. In all cases, the increase of Al in the bulk reflects the difference of Al combined with oxygen on the surface versus a metallic state in the bulk. Table 8 lists the oxide thickness on

TABLE 6 : AES ELEMENTAL I.D.OF TREATED Ti-8Al-1Mo-1Sn

TREATMENT	ELEMENT IDENTIFICATION											
	Ti (381 eV)	O	C	P	Cu	Ca	Na	F	S	Cl	K	Al
1	1	2.3	0.7	x		0.2	x		x	x		x
1-2	1	2.0	0.6	x		x			x	x		x
1-3	1	2.3	0.5		0.3			x	0.1	x		x
1-4	1	1.6	0.5	0.1		0.4	0.6	0.7	x	x	x	x
1-5	1	2.0	0.3	x		x		x	x	x		x
1-6	1	2.1	0.8	x		x			x	x		x
1-7	1	2.1	0.5	x	x	x	x	x	x	x		x
1-8	1	2.1	0.3			0.2	x		x	x		x

(x APPH RATIO < 0.1)

TABLE 7 : SIMS ELEMENTAL I.D. OF TREATED Ti-8Al-1Mo-1Sn

TREATMENT	m/e / positive ion identification														
	16 O	19 F	23 Na	27 Al C_2H_3	35 Cl	39 K	40 Ca	48 Ti	59 AlO_2 CaF	64 TiO	67 TiF	86 TiF_2	96 Ti_2	112 Ti_2O	120 Sn
1	x	x	1.9	0.28	x	2.72	0.76	1		0.28			x	x	x
1-2	x	x	0.8	0.29		0.23	0.29	1	x	0.37			x	x	x
1-3	x	x	0.9	0.28	x	0.25	x	1		0.22			x	x	
1-4		0.5	13	0.74		0.12	0.73	1	x	x	0.25	x			
1-5	x	x	1.6	0.14	x	0.23	0.10	1		0.32			x	x	x
1-6		x	0.2	0.39		x	0.12	1		x			x	x	
1-7			0.3	0.26		0.10	x	1		x			x		
1-8			0.4	0.27	x	0.10	0.76	1		x					

(x VALUE < 0.1)

TABLE 8: CARBON DISTRIBUTION, OXIDE AND INTERFACIAL THICKNESS DETERMINED BY AUGER SPUTTER PROFILE ANALYSIS FROM TREATED Ti-8Al-1Mo-1Sn

TREATMENT	1	1-2	1-3	1-4	1-5	1-6	1-7	1-8
THICKNESS (nm)	14.6	15.7	17.8	111.8	17.8	12.2	13.3	7.8
INTERFACE O Δt (min)	1.8	2.3	2.3	10.8	3.1	2.2	1.4	1.4
C DISTRIBUTION Δt (min)	1.0	0.8	1.0	1.4	2.4	0.9	0.7	0.8

each of the pretreated panels. As with Ti c.p. (Table 5), Table 8 compares the carbon distribution and the width of the oxide-metal interface in terms of the Δt of sputtering time.

3. Ti-6Al-4V

The data obtained from this treated alloy are generally in good agreement with previously reported studies (Ref. 6,12,14,15,18-24).

A. Surface Topography

Figures 31-34 contain S.E.M. micrographs of Ti-6Al-4V panels subjected to each of the chemical treatments listed in Table 2. The most noticeable difference with this alloy compared to titanium c.p. (Fig. 6-9) is its smoother surface. Treatment 1-4 did not produce the "sea shell" effect as it did with Ti (c.p.) and Ti-8Al-1Mo-1Sn. In addition the S.E.M. micrographs from this alloy did not reveal the presence of α or β phases at the surface of any of the treated panels.

B. Surface Composition

a) *Auger Electron Spectroscopy* (A.E.S.)

Figures 35 and 36 contain the A.E.S. spectra from the treated panels 1-4 and 1-7. Figures 37 and 38 are expanded portions of Figures 35 and 36, respectively. The spectra from the remaining panels were similar to those for the treated panel 1-7. The Ti_{LMV} peak shape from treatment 1-4 (Fig. 37) is similar to those from 1-4 treated Ti and Ti-8Al-1Mo-1Sn. The detection of small amounts of vanadium by A.E.S. in the presence of titanium is difficult because of the overlapping of the V_{LMM} peaks by much stronger Ti_{LMV} peak. A.E.S. spectra of Ti,V, and Ti-6Al-4V in Figure 39 illustrate this problem (Ref. 15). The problem is further complicated when oxygen is present since a number of oxygen loss peaks can interfere with both Ti and V. Nevertheless except treatment 1-2 and 1-4, V was detected on the surfaces of this treated alloy. Table 9 is a semiquantitative listing of the element detected

TABLE 9: AES ELEMENTAL I.D. OF TREATED Ti-6Al-4V

TREATMENT	ELEMENT IDENTIFICATION											
	Ti (381 eV)	O	C	P	Cu	Ca	Na	F	S	Cl	Al	V
1	1	2.7	0.6			0.2	x		x	x	x	x
1-2	1	2.2	0.9			x	x		x	x	x	
1-3	1	2.3	0.8		0.4				x	0.2	x	x
1-4	1	1.3	0.5	x		0.2	0.5	0.8	x	x	x	
1-5	1	2.2	0.4	x		x		x	x	x	x	x
1-6	1	2.2	0.5					x	x	x	x	x
1-7	1	2.1	0.4	x		x		x	x	x	x	x
1-8	1	2.1	0.4			x		x	x	x	x	x

(x: APPH RATIO < 0.1)

TABLE 10: SIMS ELEMENTAL I.D. OF TREATED Ti-6Al-4V

TREATMENT	m/e / positive ion identification																Al/V
	16 O	19 F	23 Na	27 Al C_2H_3	39 K	40 Ca	46 Na_2	48 Ti	51 V	59 AlO_2 CaF	64 TiO	65 AlF_2 Na_2F	67 TiF VO	70 VF	86 TiF_2	88 TiF_2H_2 $Al_2(OH)_2$	
1	x	x	1.7	0.12	1.9	0.7		1	0.07	x	0.27		x				1.7
1-2	x	x	0.5	0.20	0.1	0.3		1	0.06	x	0.28		x				3.1
1-3	x	x	0.6	0.20	0.3	0.1		1	0.04	x	0.21	x	x				4.6
1-4	x	9	>20	0.73	1.1	1.3	x	1	0.16	1.2	0.19	0.63	1.23	0.1	0.17	x	4.7
1-5	x	x	1.9	0.40	1.0	0.2		1	0.14	x	0.27		x				3.6
1-6	x	x	1.2	0.18	0.7	0.4		1	0.03	x	0.39	x	x				6.1
1-7	x	x	1.0	0.23	0.1	x		1	0.05	x	0.19		x				4.3
1-8	x	x	0.6	0.29	0.2	0.6		1	0.04	x	0.25		x				6.7

(x VALUE <0.1)

TABLE 11: CARBON DISTRIBUTION, OXIDE AND INTERFACIAL THICKNESS DETERMINED BY AUGER SPUTTER PROFILE ANALYSIS FROM TREATED Ti-6Al-4V

TREATMENT	1	1-2	1-3	1-4	1-5	1-6	1-7	1-8
THICKNESS (nm)	5.1	14.3	4.0	35.0	15.2	13.0	4.8	15.8
INTERFACE O Δt (min)	2.8	2.5	3.2	66.2	5.5	4.3	3.8	12.0
C DISTRIBUTION Δt (min)	5.3	5.1	3.9	31.5	8.7	2.6	1.9	7.8

by A.E.S. on all the treated Ti-6Al-4V.

b) Secondary Ion Mass Spectroscopy (SIMS)

Figures 40 and 41 contain the + SIMS spectra for the 1-4 and 1-7 treated Ti-6Al-4V. The SIMS spectra from the remaining panels were identical to Figure 41. Table 10 summarizes semiquantitatively the SIMS data from the treated Ti-6Al-4V panels. Unlike A.E.S., the vanadium at m/e = 51 SIMS peak is not subject to interference by titanium and consequently its detection by SIMS is more reliable. As Table 10 shows, V^+ was detected on all the treated alloy surfaces. The V^+/Ti^+ ratio from the treated surfaces compared to the bulk (Ref. 6), infer that the vanadium concentration on the surface is the same as the bulk, with the exception of treatment 1-4 and 1-5 which show higher ratios of V^+/Ti^+ on the surface. The Al^+/Ti^+ ratios were generally lower for the treated surfaces compared to the bulk ($\sim$ 0.3), again with the exception of treatment 1-4 and 1-5.

c) Auger Sputter Profiles Analysis (ASPA)

Figures 42 and 43 contain the normalized elemental sputter profiles of C, O, Ti, Al and V from panels subjected to treatment 1-4 and 1-7 respectively. Table 11 lists the oxide thickness on each of the pretreated panels, carbon distribution and oxide metal interface width. On all cases the bulk aluminum concentration is higher than the surface. The bulk vanadium concentration is greater than the surface on panels subjected to treatments 1-2, 1-3, and 1-4 and less than the surface concentration on the remaining panels.

4. Ti-5Al-2.5Sn

A. Surface Topography

SEM micrographs of treated Ti-5Al-2.5Sn in Figures 44-47 show fairly rough surfaces (except for treatments 1-3 and 1-7).

The "sea shell" structure produced on Ti with treatment 1-4 is not evident on this alloy treated with 1-4.

B. Surface Composition

a) Auger Electron Spectroscopy (AES)

The spectra in Figure 48 shows that the "as received" surface of this alloy is void of tin. On the other hand, treatment 1-5 produces a Sn rich surface, which is reflected in the spectra in Figure 49. The remaining spectra in Figure 49 also show Sn present in varying amounts on the surfaces of panels subjected to treatment 1-2,1-3 and 1-4. Although the main tin Auger peak is overlapped by titanium, the degree of overlapping is less than that of vanadium, therefore Sn is easily identified in expanded spectra such as those in Figure 49. Included in Figure 49 is the Equilibrum Sputtered (ES) spectrum from this alloy. An ES surface is one which was ion beam etched until no noticeable changes are observed in the AES spectrum. Table 12 is a semiquantitative listing of the elements detected by AES on each of the treated Ti-5AL-2.5Sn panels.

b) Secondary Ion Mass Spectroscopy (SIMS)

The SIMS spectrum from the "as received" surface in Figure 50, like AES, does not show the presence of Sn. Unlike the previous alloys subjected to treatment 1-4, this alloy did not have a fluoride rich surface and therefore the SIMS spectra (Fig. 51) from this specimen does not show Ti-F species such as TiF^+ , TiF_2^+ etc....
Because of its low secondary ion yield (Ref. 25) the detection of tin by SIMS is difficult, especially when a light probing ion such as He^+ is used.
The problem is further complicated by the high sputtering yield of Sn

TABLE 12: AES ELEMENTAL I.D. OF TREATED Ti-5Al-2.5Sn

TREATMENT	ELEMENT IDENTIFICATION											
	Ti (381 eV)	O	C	P	Cu	Ca	Na	F	S	Cl	Al	Sn
1	1	2.1	0.1	x		0.3		x	x	x	x	
1-2	1	3.2	3.3	x		0.3	x	x	0.1	0.2	x	x
1-3	1	2.7	1.8		0.3	x			0.1	0.2	x	x
1-4	1	2.4	1.9	x		0.1		x	x	x	x	x
1-5	x	x	x			x			x	x	x	1
1-6	1	2.7	1.9			x		x	x	x	x	x
1-7	1	2.2	0.3			x		x	x	x	x	x
1-8	1	2.7	1.6			0.4			x	x	x	

(x APPH RATIO < 0.1)

TABLE 13: SIMS ELEMENTAL I.D OF TREATED Ti-5Al-2.5Sn

TREATMENT	m/e / positive ion identification										
	16 O	19 F	23 Na	27 C_2H_3 Al	39 K	40 Ca	48 Ti	64 TiO	96 Ti_2	112 Ti_2O	120 Sn
1	x	x	9.9	0.50	14.4	0.5	1	0.23	x	x	
1-2	x	x	1.5	0.50	1.2	1.0	1	0.25	x	x	x
1-3	x	x	0.5	0.35	0.4	0.2	1	0.16	x	x	x
1-4	x	x	1.2	0.33	0.7	0.6	1	0.20			x
1-5	x	x	1.2	0.33	1.0	0.6	1	0.34			x
1-6	x	x	0.6	0.27	0.3	0.3	1	0.18	x	x	x
1-7	x	x	0.7	0.21	x	0.1	1	0.15	x	x	x
1-8	x	x	1.3	0.63	0.4	2.1	1	0.15			

(x VALUE < 0.1)

TABLE 14: CARBON DISTRIBUTION, OXIDE AND INTERFACIAL THICKNESS DETERMINED BY AUGER SPUTTER PROFILE ANALYSIS FROM TREATED Ti-5Al-2.5Sn

TREATMENT	1	1-2	1-3	1-4	1-5	1-6	1-7	1-8
THICKNESS (nm)	6.2	10.1	7.3	19.2	49.5	5.1	2.3	9.0
INTERFACE O Δt (min)	3.7	3.5	4.3	13.8	30.3	3.7	3.7	6.7
C DISTRIBUTION Δt (min)	5.7	9.1	15.6	25.6	21.7	6.7	2.3	8.3

and Sn oxide (Ref. 26) because surface monolayers of Sn are quickly sputtered away even with He^+ (Fig. 52).

Table 13 is a semiquantitative summary of the SIMS data from the treated Ti-5AL-2.5Sn alloy.

c) Auger Sputter Profiles Analysis (ASPA)

Figures 53 and 54 contain the normalized elemental sputter profiles of C,O,Ti, Al and Sn from panels subjected to treatment 1 and 1-5, respectively. Table 14 lists the oxide thickness and each of the pretreated specimens, carbon distribution and oxide metal interface width. The bulk aluminum concentration is less than the surface in panels subjected to treatments 1 and 1-3, and higher than the surface concentration on the remaining panels. The bulk tin concentration is higher than the surface in the remaining panels and less than the surface concentration on the panels subjected to treatment 1-3 and 1-5.

5. Ti - 5Al - 5Sn - 2Mo - 2Zr - .25Si

A. Surface Topography

The surface of this alloy subjected to treatments 1-2, 1-6 and 1-8 as well as the "as received" alloy are fairly smooth while the 1-3,1-5 and 1-7 treated surfaces show the α and β phase structure (Fig 55-58). The topography of the 1-5 treated alloy (Fig. 57) is very similar to 1-5 treated Ti-5Al-2.5Sn (Fig. 46). The treatment 1-4 produce again "the sea shell surface".

B. Surface Composition

a) Auger Electron Spectroscopy (AES)

This alloy was the most difficult to analyze for treatment effects on surface elemental composition because of severe peak overlapping of Zr and Mo with contaminants such as S and Cl. The spectra in

Figure 59 from the "as received" alloy shows the presence of Al and Sn at the surface by Zr and Mo cannot be seen. Then their presence is not confirmed in the Equilibrium Sputtered (ES) spectrum in Figure 60. Tin was detected on all treated surfaces, with treatment 1-5 producing the highest concentration (Fig. 61). Unlike Ti-5Al-2.5Sn (Fig. 49), the 1-4 treated surface was rich in fluorine (Fig. 62) and the Ti_{LMV} ($\sim$ 421eV) peak shape is different from TiO_2, which was observed for Ti c.p. and alloys A,B and C. Table 15 summarizes the AES elemental data from the treated alloy surfaces. At no time was Zr positively identified.

b) Secondary Ion Mass Spectroscopy (SIMS)

Like AES, the elemental SIMS characterization of this alloy was difficult because the low secondary ion yields and peak overlap problems with Ti_2^+,Zr^+ and Mo^+. Sn was detected on all surfaces while a trace of Zr, but not Mo, was detected on the ES surface (Fig. 63). The SIMS results are tabulated in Table 16. *The 1-4 treated surface (Fig. 64)* did contain fluorine and TiF^+ species were observed.

c) Auger Sputter Profiles Analysis (ASPA)

Figures 65 and 66 contain the normalized elemental sputter profiles of C,O,Ti, Al and Sn from the 1 and 1-5 treated panels. Because the profiles are normalized Sn in Figure 66 appears to decrease to a zero level when, in fact, it approaches the bulk level. This means that the Sn concentration at the surface of the 1-5 treated panel was higher than the bulk. The surface concentration of Sn on the remaining panels was always less than the bulk. Table17 lists the oxide thickness, carbon distribution, and oxide metal interface width for each of the treated panels. On the remaining panels, the bulk aluminum concentration

TABLE 15: AES ELEMENTAL I.D. OF TREATED Ti-5Al-5Sn-2Mo-2Zr-0.25Si

TREATMENT	ELEMENT IDENTIFICATION													
	Ti (381 ev)	O	C	P	Cu	Ca	Na	F	S	Cl	K	Al	Sn	Mo
1	1	2.5	0.6	x		x	x		0.2	x	x	x	x	
1-2	1	2.3	0.9	x		x	x	x	x	x		x	x	
1-3	1	2.2	0.6	x	0.3	x		x	x	0.2		x	x	x
1-4	1	0.9	0.3	0.12		x	0.2	0.8	x	x		x	x	
1-5	x	x	x			x			x	x		x	1	x
1-6	1	2.3	0.7	x		x	x	x	x	x		x	x	
1-7	1	2.2	0.4	x		x	x	x	x	x		x	x	
1-8	1	2.2	0.4			x		x	x	x			x	

(x APPH RATIO < 0.1)

TABLE 16: SIMS ELEMENTAL I.D. OF TREATED Ti-5Al-5Sn-2Mo-2Zr-0.25Si

TREATMENT	m/e / positive ion identification																
	16 O	19 F	23 Na	27 C_2H_3 Al	31 P	39 K	40 Ca	46 Na_2	48 Ti	64 TiO	65 Na_2F	67 TiF	69 Na_3	90 Zr	96 Ti_2	112 Ti_2O	120 Sn
1	x	x	>4.5	0.17		>4.5	0.2		1	0.20					x	x	x
1-2	x	x	1.0	0.19		0.3	0.4		1	0.19				x	x	x	x
1-3	x	x	0.6	0.19		0.2	x		1	0.13				x	x	x	x
1-4	x	11	>18	1.3	x	1.8	1.7	x	1	0.18	x	x	x		x		x
1-5	x	x	2.8	0.26		2.0	0.2		1	0.14				x	x	x	x
1-6	x	x	1.0	0.10		0.4	0.3		1	0.20				x	x	x	x
1-7	x	x	0.5	0.19		0.1	0.2		1	0.18				x	x	x	x
1-8	x	x	0.3	0.24		x	0.4		1	0.20				x	x	x	x

(x VALUE < 0.1)

TABLE 17: CARBON DISTRIBUTION, OXIDE AND INTERFACIAL THICKNESS DETERMINED BY AUGER SPUTTER PROFILE ANALYSIS FROM TREATED Ti-5Al-5Sn-2Mo-2Zr-0.25Si

TREATMENT	1	1-2	1-3	1-4	1-5	1-6	1-7	1-8
THICKNESS (nm)	10.4	4.5	5.6	112.0	20.0	5.1	2.6	3.4
INTERFACE 0 Δt (min)	5.5	3.5	4.3	38.4	12.9	3.7	3.7	4.5
C DISTRIBUTION Δ t (min)	4.3	3.9	3.7	3.5	4.9	3.7	3.7	4.1

(except the 1-8 treated panel) and the bulk tin concentration (except the 1-5 treated panel are higher than the surface.

6. Ti - 3Al - 2.5V

A. Surface Topography

The surface of the Ti-3Al-2.5V alloy subjected to the treatments 1-2,1-6 and 1-8 as well as the "as received" surface are fairly smooth (Fig. 67,69 and 70), while the 1-3,1-5 and 1-7 treated surfaces have a rough texture (Fig 68,69,70). The 1-4 treated surface has the "sea shell" appearance (Fig. 68).

B. Surface Composition

a) Auger Electron Spectroscopy (AES)

The problem of the AES detection of vanadium in the presence of titanium was discussed in section III.3.B.a. However, as shown in Figure 71, there was evidence of vanadium on the surface of the 1-5 treated alloy. AES spectra from all the treated surfaces from this alloy revealed the presence of both Al and V. Figure 72, which contains spectra from a panel subjected to treatment 1-4, shows a fluorine rich surface and a subtle change in the Ti_{LMV} peak shape. Table 18 summarizes the AES elemental data from the treated Ti-3Al-2.5V surfaces.

b) Secondary Ion Mass Spectroscopy (SIMS)

Figure 73 shows the 1-5 treated alloy + SIMS analysis. The spectra from the remaining panels are similar to Figure 73 except the 1-4 panel (Fig. 74) which shows the same fluorine and sodium species like Na_2^+,ALF^+ (m/e = 46), TiF^+ (m/e = 67),Na_3^+ (m/e = 69), VF^+ (m/e = 70), TiF_2^+ (m/e = 86). Table 19 is a semiquantitative summary of the SIMS data from the treated Ti-3Al-2.5V alloy.

TABLE 18: AES ELEMENTAL I.D. OF TREATED Ti-3Al-2.5V

TREATMENT	ELEMENT IDENTIFICATION												
	Ti (381 eV)	O	C	P	Cu	Ca	Na	F	S	Cl	K	Al	V
1	1	2.2	0.4			0.1	x		x	x	x	x	x
1-2	1	4.2	8.7			x				x	x	x	x
1-3	1	2.3	0.5	x	0.43	x			x	0.3		x	x
1-4	1	1.2	0.3	x		0.1	0.3	0.8	x	x		x	x
1-5	1	2.3	0.3			x			x	x		x	x
1-6	1	2.1	0.4			x			x			x	x
1-7	1	2.4	0.6			x			0.2	0.1		x	x
1-8	1	2.0	0.3			x			x	x		x	x

(x APPH RATIO < 0.1)

TABLE 19: SIMS ELEMENTAL I.D. OF TREATED Ti-3Al-2.5V

TREATMENT	m/e / positive ion identification															Al/V
	16 O	19 F	23 Na	27 C_2H_3 Al	35 Cl	39 K	40 Ca	46 Na_2	48 Ti	51 V	64 TiO	67 TiF VO	69 Na_3	70 VF	86 TiF_2 Al_2O_2	
1	x	x	1	0.21		1.5	0.5		1	0.05	0.22	x				4.2
1-2	x	x	0.5	0.23		0.5	0.5		1	0.05	0.23	x				4.6
1-3	x	x	0.6	0.10	x	x	0.1		1	0.02	0.21	x				4.7
1-4	x	>5	>5	0.82		0.2	0.9	x	1	0.10	0.18	x	x	x	x	8.5
1-5	x	x	0.4	x	x	x	0.2		1	x	0.22	x				2.5
1-6	x	x	0.5	0.19		0.3	0.2		1	0.04	0.22	x			x	5.4
1-7	x	x	x	x		x	x		1	x	x	x			x	3.8
1-8	x	x	0.8	0.18		0.2	0.6		1	0.02	0.21	x			x	9.5

(x VALUE < 0.1)

TABLE 20: CARBON DISTRIBUTION, OXIDE AND INTERFACIAL THICKNESS DETERMINED BY AUGER SPUTTER PROFILE ANALYSIS FROM TREATED Ti-3Al-2.5V

TREATMENT	1	1-2	1-3	1-4	1-5	1-6	1-7	1-8
THICKNESS (nm)	1.7	3.4	8.4	50.7	7.9	2.9	2.3	3.1
INTERFACE O Δt (min)	4.5	5.3	6.3	44.8	9.4	3.7	3.7	5.1
C DISTRIBUTION Δt (min)	3.3	2.7	3.7	9.1	5.3	2.4	3.3	3.7

c) Auger Sputter Profiles Analysis (ASPA)

Figures 75 and 76 contain the normalized elemental sputter profiles of C,Ti,O, and V from the panels subjected to treatment 1-5 and 1-7, respectively. Aluminium was not profiled because the signal intensity was too low. The vanadium profile in Figure 75 shows a higher concentration on the surface versus bulk. This was also observed with the SIMS technique by measuring the m/e ratios of 51/48. Vanadium surface concentration was higher than bulk on the 1,1-2,1-3,1-6 and 1-8 treated panels. Although the normalized Al profiles are not shown in Figures 75 and 76 the raw data did show that the aluminium concentration on treated surfaces was less than the bulk. Table 20 lists the oxide thickness, carbon distribution and oxide metal interface width for each of the treated panels.

7. Ti - 13V - 11Cr - 3Al

A. Surface Topography

Figures 77-80 contain SEM micrographs of Ti-13V-11Cr-3Al panels subjected to each of the treatments listed in Table 2. Once again the 1-4 treated surface has a "sea shell" like structure surface and the 1-3 treated surface contains microcrystalline particles. The remaining specimens have fairly smooth, clean surfaces.

B. Surface Composition

a) Auger Electron Spectroscopy (AES)

The spectra in Figure 81 show the presence of vanadium, chromium, and aluminium on the "as received" surface. The remaining spectra are similar to Figure 81. Although the main vanadium and chromium peaks are overlapped by titanium and oxygen, they are observed. The expanded portion of the spectrum from "as received" titanium (c.p.) is

TABLE 21: AES ELEMENTAL I.D. OF TREATED Ti-13V-11Cr-3Al

TREATMENT	ELEMENT IDENTIFICATION													
	Ti (381 eV)	O	C	P	Cu	Ca	Na	F	S	Cl	K	Al	Cr	V
1	1	3.1	1.4	x		0.1	x		0.2	0.3	x	x	x	x
1-2	1	2.8	1.5	x		0.1	x		x	x		x	x	x
1-3	1	3.0	1.2		0.6	x			x	0.4		x	x	x
1-4	1	3.1	1.3	x		0.1	x	0.1	x	x		x	x	x
1-5	1	2.5	0.7						x	x		x	x	x
1-6	1	2.4	0.8			x	x		x	x		x	x	x
1-7	1	2.5	0.8			x			0.1	x		x	x	x
1-8	1	3.5	3.5			0.1	x		x	x		x	x	x

(x APPH RATIO < 0.1)

TABLE 22: SIMS ELEMENTAL I.D. OF TREATED Ti-13V-11Cr-3Al

TREATMENT	m/e / positive ion identification													Al/V	Cr/V
	16 O	19 F	23 Na	27 C_2H_3 Al	35 Cl	39 K	40 Ca	48 Ti	51 V	52 Cr	64 TiO	67 VO	68 CrO		
1	x	x	8.2	0.26	x	>9	0.5	1	0.17	0.13	0.15	x		1.8	1.0
1-2	x	x	0.8	0.22		0.4	0.6	1	0.12	0.13	0.20	x	x	2.1	1.1
1-3	x	x	0.7	0.21	x	0.4	0.2	1	0.17	0.19	0.18	x	x	1.4	1.2
1-4	x	x	>3	0.16	x	0.2	0.5	1	0.18	0.49	0.17	x	x	1.0	2.6
1-5	x	x	0.3	0.16		x	x	1	0.26	0.16	0.19	x	x	0.6	0.6
1-6	x	x	0.5	0.13		0.1	0.2	1	0.12	0.24	0.23	x	x	1.1	2.0
1-7	x	x	0.3	0.15	x	0.1	0.2	1	0.19	0.17	0.19	x	x	0.8	0.9
1-8	x	x	0.9	0.22	x	0.2	0.8	1	0.13	0.35	0.16	x	x	1.8	2.8

(x VALUE < 0.1)

TABLE 23: CARBON DISTRIBUTION, OXIDE AND INTERFACIAL THICKNESS DETERMINED BY AUGER SPUTTER PROFILE ANALYSIS FROM TREATED Ti-13V-11Cr-3Al

TREATMENT	1	1-2	1-3	1-4	1-5	1-6	1-7	1-8
THICKNESS (nm)	9.6	2.3	6.5	6.8	2.3	7.9	4.0	5.7
INTERFACE O Δt (min)	6.9	3.1	8.0	4.7	4.7	4.1	5.1	4.7
C DISTRIBUTION Δt (min)	8.7	2.2	10.8	11.4	4.7	3.3	4.3	5.7

superimposed above the G_1 expanded spectrum to show that the differences between the two spectra are due to vanadium and chromium. The 1-4 treatment (Fig. 82) did not produce a surface rich in fluorine and consequently the Ti_{LMV} peak shape was identical to that of TiO_2. The Equilibrium Sputtered spectrum from this alloy in Figure 83 shows quite clearly the presence of vanadium, chromium, and aluminium in the bulk. Table 21 is a semiquantitative listing of the elements detected by AES on each of the treated Ti-13V-11Cr-3Al panels.

b) Secondary Ion Mass Spectroscopy (SIMS)

Figures 84 and 85 contain the + SIMS spectra from the degreased panel and the specimen subjected to 1-4 treatment. The spectrum from treatment 1-4 reflects the low fluorine concentration by the weak peaks associated with F, such as TiF^+ (m/e = 67), compared to some of the other alloys. Table 22 tabulates the + SIMS data from all the treated panels of this alloy.

c) Auger Sputter Profiles Analysis (ASPA)

Figures 86 and 87 contain the normalized elemental sputter profile of C,O,Ti,V and Cr from the 1 and 1-2 treated panels. The surface concentrations of aluminium, vanadium, and chromium on the all treated panels were less than the bulk. Table 23 lists the oxide thickness, carbon distribution, and oxide metal interface width for each of the treated panels .

8. Ti - 8Mn

A. Surface Topography

The SEM micrographs in Figures 88-91 show the surfaces of the Ti-8Mn alloy subjected to treatment listed in Table 2, to have

TABLE 24: AES ELEMENTAL I.D. OF TREATED Ti-8Mn

TREATMENT	ELEMENT IDENTIFICATION												
	Ti (381 eV)	O	C	P	Cu	Ca	Na	F	S	Cl	K	Mn	Si
1	1	2.7	0.5	x		0.1	x		x	x	x	x	x
1-2	1	2.6	0.6	x		0.1			x	x		x	x
1-3	1	2.6	0.7		0.5	x			0.2	0.5		x	x
1-4	1	1.3	0.1	0.2		x	0.2	0.7	x	x		x	
1-5	1	2.2	0.4			x			x			x	x
1-6	1	2.5	0.4	x		x			x			x	x
1-7	1	2.6	0.5		x	x			0.2	x		x	
1-8	1	2.4	0.2			0.2			x	x		x	

(x APPH RATIO < 0.1)

TABLE 25: SIMS ELEMENTAL I.D OF TREATED Ti-8Mn

TREATMENT	m/e / positive ion identification																	
	16 O	19 F	23 Na	27 C_2H_3	31 P	35 Cl	39 K	40 Ca	46 Na_2	48 Ti	55 Mn	60 SiO_2	64 TiO	65 Na_2F	67 TiF	69 Na_3	71 MnO	74 MnF
1	x	x	>2	x		x	>2	0.4		1	0.09	x	0.28				x	
1-2	x	x	0.6	0.2	x		0.2	0.4		1	0.07	x	0.33				x	
1-3	x	x	0.4	x		x	0.1	x		1	0.08	x	0.22				x	
1-4	x	>7	>7	0.1	x	x	0.9	0.4	x	1	0.10	x	0.29	0.50	1.1	x		x
1-5	x	x	0.3	x		x	0.1	x		1	0.09	x	0.20				x	
1-6	x	x	3.2	x		x	0.1	0.2		1	0.05	x	0.26				x	
1-7	x	x	0.3	x		x	x	0.1		1	0.09	x	0.19				x	
1-8	x	x	0.5	x		x	x	0.5		1	0.12	x	0.35				x	

(x VALUE < 0.1)

TABLE 26: CARBON DISTRIBUTION, OXIDE AND INTERFACIAL THICKNESS DETERMINED BY AUGER SPUTTER PROFILE ANALYSIS FROM TREATED Ti-8Mn

TREATMENT	1	1-2	1-3	1-4	1-5	1-6	1-7	1-8
THICKNESS (nm)	7.9	3.7	2.3	21.4	1.7	2.8	3.4	13.5
INTERFACE O Δt (min)	6.3	4.1	3.7	31.8	4.7	4.1	3.7	12.8
C DISTRIBUTION Δt (min)	4.1	5.7	7.9	11.8	4.7	1.8	1.8	7.7

a granulated crystalline surface structure consisting of α and β phases.

B. Surface Composition

a) Auger Electron Spectroscopy (AES)

Figure 92 contains the spectra of the 1-8 treated panel and ES surface, respectively. Except for 1-4 treatment spectra from the remaining panels are similar to Figure 92. Because of the overlapping with oxygen and fluorine, manganese is difficult, but not impossible to detect. Figure 93 shows a high concentration of F on the surface of the 1-4 treated alloy which affected the Ti_{LMV} peak shape. Table 24 summarizes the AES elemental data from the treated Ti-8Mn alloy.

b) Secondary Ion Mass Spectroscopy (SIMS)

Figures 94 and 95 contain the + SIMS spectra of the 1-4 and 1-8 treated panels. All the remaining panels are similar to Figure 95. Because of the high surface concentration of F a number of fluorine species are evident. The Table 25 summarizes the SIMS data from the treated panels.

c) Auger Sputter Profiles Analysis (ASPA)

Figures 96 and 97 which contain the normalized elemental sputter profiles of C,O,Ti, and Mn from the 1-7 and 1-8 treated panels show the surface concentration of Mn were less than the bulk. The manganese surface concentration of all the treated panels of this alloy was less than the bulk. Table 26 lists the oxide thickness, carbon distribution, and oxide metal interface width for each of the treated panels.

The data obtained from this treated alloy are generally in good agreement with previously reported works (Ref. 6, 15).

IV. DISCUSSION

Table 27 lists the surface oxide thickness for each treated alloy.

1. Treatment 1 (Degrease)

Treatment 1 is not a true chemical treatment which modifies the metal surface. It is simply a degreasing step which strips the "as received" titanium and titanium alloys of gross surface contaminants in order to characterize these surfaces prior to actual chemical treatment. In general, the "as received" surface of the metal and alloys studied were covered with thin carbonous and oxide layers. As shown in Figures 98 and 99 the oxide layer on Ti-6Al-4V was primarily TiO_2. The XPS oxygen spectrum from Ti-6Al-4V in Figure 99 has two main features which correspond to two different chemical states. The peak at approximately 530 eV corresponds to oxygen bound to Ti as TiO_2 and the peak at approximately 533 eV corresponds to oxygen chemically bound to carbon (ie. CO, CO_2, etc...) as an adsorbed layer. The shift in the Ti_{2p} peak (Figure 98) is characteristic of the oxide like TiO_2 on Ti-6Al-4V (Ref. 12, 20).

2. Treatment 1-2 (Degrease and Alkaline)

This treatment had little or no effect on surface topography. The oxide layer on each alloy was identified as TiO_2. In some cases the etching effect of this treatment was insufficient to remove carbon contaminant layers.

3. Treatment 1-3 (Degrease and Fluoro-nitric)

The overall effect of this treatment is the selective etching of the α phase, leaving a thin oxide layer on the remaining β phase. The oxide composition is TiO_2. Oxide thicknesses are generally

Table 27 OXIDE THICKNESS VERSUS CHEMICAL TREATMENTS FOR TITANIUM (c.p.) AND SOME OF ITS ALLOYS

TREATMENT	OXIDE THICKNESS				
	< 5 nm	5-10 nm	10-15 nm	15-20 nm	> 20 nm
DEGREASE	* Ti-3Al-2,5V	* Ti-6Al-4V * Ti-5Al-2.5Sn * Ti-5Al-5Sn-2Mo-2Zr- - .25Si * Ti-13V-11Cr-3Al * Ti-8Mn	* Ti-8Al-1Mo-1Sn	* Ti (c.p.)	
DEGREASE and ALKALINE	* Ti-5Al-5Sn-2Mo-2Zr- - .25Si * Ti-3Al-2.5V * Ti-13V-11Cr-3Al * Ti-8Mn	* Ti (c.p.)	* Ti-6Al-4V * Ti-5Al-2.5Sn	* Ti-8Al-1Mo-1Sn	
DEGREASE and FLUORO-NITRIC	* Ti-6Al-4V * Ti-8Mn	* Ti (c.p.) * Ti-5Al-2.5Sn * Ti-5Al-5Sn-2Mo-2Zr- - .25Si * Ti-3Al-2.5V * Ti-13V-11Cr-3Al		* Ti-8Al-1Mo-1Sn	
DEGREASE and FLUORO-PHOSPHATE		* Ti-13V-11Cr-3Al		* Ti-5Al-2.5Sn	* Ti (c.p.) * Ti-8Al-1Mo-1Sn * Ti-6Al-4V * Ti-5Al-5Sn-2Mo-2Zr- .25Si * Ti-3Al-2.5V * Ti-8Mn
DEGREASE and FLUORO-AMMONIUM	* Ti-13V-11Cr-3Al * Ti-8Mn	* Ti-3Al-2.5V		* Ti (c.p.) * Ti-8Al-1Mo-1Sn * Ti-6Al-4V	* Ti-5Al-2.5Sn * Ti-5Al-5Sn-2Mo-2Zr- .25Si
DEGREASE and SULFO-CHROMIUM	* Ti-3Al-2.5V * Ti-8Mn	* Ti-5Al-2.5Sn * Ti-5Al-5Sn-2Mo- -2Zr- .25Si * Ti-13V-11Cr-3Al	* Ti (c.p.) * Ti-8Al-1Mo-1Sn		
DEGREASE and FLUORO-NITRO- -AMMONIUM	* Ti-6Al-4V * Ti-5Al-2.5Sn * Ti-5Al-5Sn-2Mo-2Zr- - .25Si * Ti-3Al-2.5V * Ti-13V-11Cr-3Al * Ti-8Mn	* Ti (c.p.)	* Ti-8Al-1Mo-1Sn		
DEGREASE and HOT ALKALINE	* Ti-5Al-5Sn-2Mo-2Zr- - .25Si * Ti-3Al-2.5V	* Ti-8Al-1Mo-1Sn * Ti-5Al-2.5Sn * Ti-13V-11Cr-3Al	* Ti-8Mn	* Ti (c.p.) * Ti-6Al-4V	

less than 10nm. (*See note at the end of the discussion)

4. Treatment 1-4 (Degrease and Fluoro-phosphate)

This is a common industrial surface etchant often referred to as a "conversion treatment" because it supposedly changes the rutile TiO_2 oxide layer on unaged panels to the anatase form or the anatase to rutile on aged panels (Ref.21,28). In general, this treatment produced the thickest oxide layers which had a "sea shell" like appearance. The oxides were not pure TiO_2, since in most cases, fluorine was present throughout the oxide layer. Table 28 summarizes the physical and chemical effects of treatment 1-4 on titanium and its alloys. As mentioned above, the oxide layers contained F throughout and as indicated in Table 28 the Ti_{LMV} peak shape was slighty different than TiO_2 (see Figure 100). J.S. Solomon et al.(Ref.16) reported changes in the Ti_{LMV} peak shape from TiO_2 resulting electron beam induced reduction of the oxide (Figure 101). In attempting to determine the chemical state of Ti, O, and F within the oxide layer produced with this treatment possible instrumentally induced artifacts, ie. electron beam effects, had to be investigated. In this work the electron beam current density was less than .7 $\mu A/mm^2$ and with prolonged exposure no changes in the Ti_{LMV} peak shape were observed. Oxide reduction can also be induced by an ion beam bombardment. Comparison of AES spectra before and after ion beam (He^+) bombardment did not show changes in Ti_{LMV} peak shapes. Figure 102 contains the Ti_{LMV} and O_{KLL} AES spectra from fluoro-ammonium (1-5) treated Ti-6Al-4V recorded at various times during Ar^+ ion beam etching. Initially, the Ti_{LMV} peak at $\sim$ 418 eV had a TiO_2 like appearance. With increasing Ar^+

Table 28: PHYSICAL AND CHEMICAL EFFECTS OF FLUORO PHOSPHATE TREATMENT ON TITANIUM (c.p.) AND SOME OF ITS ALLOYS

	MATERIALS							
OBSERVATIONS	Ti(c.p.)	Ti-8Al-1Mo-1Sn	Ti-6Al-4V	Ti-5Al-2.5Sn	Ti-5Al-5Sn 2Mo-2Zr-.25Sn	Ti-3Al-2.5V	Ti-13V-11Cr-3Al	Ti-8Mn
S.E.M. "sea shell" surface	Yes	Yes	No	No	Yes	Yes	Yes	Yes
A.E.S. "TiO_2" peak shape	No	No	No	Yes	No	No	Yes	No
+SIMS TiF^+ m/e=67 AMU	Yes	Yes	Yes	No	Yes	Yes	No	Yes

etching the Ti_{LMV} peak shape gradually changes to a characteristic metallic form. The peak shape at t=75 seconds has a TiO like appearance. However, since the oxide is thin and is being removed at a fairly fast rate, a distinction between possible beam reduction and composite oxide-metal special features cannot be made. Figure 103 also contains Ti_{LMV} and O_{KLL} AES spectra recorded from fluoro-phosphate (1-4) treated Ti-6Al-4V at various times during sputter profile analysis with Ar^+. In this case, the intermediate Ti_{LMV} spectra revealed neither pure TiO_2 nor TiO shapes.

With the assumption that negligeable beam induced reduction is occurring, the data in Figure 37 and Figure 104 suggest that the Ti_{LMV} shape varies with the amount of fluorine, and therefore F is chemically bound to titanium. The unhomogeneous nature of this surface is represented by the different spectra in Figure 104 was previously reported by T. Smith (Ref. 23).

The chemical states of O, F, and Ti on fluoro-phosphate treated surface specimens were investigated with high resolution X-rays Photoelectron Spectrometer (XPS) since this technique is much more sensitive to chemical bonding than Auger Electron Spectroscopy. Figures 105 and 106 contain the respective XPS spectra of oxygen and titanium from treated Ti-6Al-4V and TiO_2 "standard". These spectra were recorded after the carbon overlayer was removed by sputtering. Before sputtering, F_{1s} was recorded and is compared to F_{1s} recorded from the oxide layer in Figure 107. The fluorine on the surface has a higher binding energy than in the oxide. This would be expected if the surface fluorine was chemically bound to

surface contaminants such as C, Ca, Na, and K versus Ti in the oxide. The O_{1s} and Ti_{2p} spectra from the oxide (compared to TiO_2) show shifts to higher binding energies. These shifts along with the F_{1s} shift infer the composition of the oxide layer to be an oxy-fluoride rather than a pure TiO_2 plus contaminants.

5. Treatment 1-5 (Degrease and Fluoro-ammonium)

The general effect of this treatment is to produce a surface with characteristic α and β phases covered with a thin oxide layer. The composition of this oxide layer was found to be TiO_2 except for alloys containing 2.5 and 5 wt% Sn. In those cases the surface oxide was identified as Sn-O by comparing their respective AES spectra in Figures 49 and 61 with the AES spectra in Figure 108 from anodized Sn and Sn metal.

6. Treatment 1-6 (Degrease and Sulpho-chromium)

The effect of this treatment on surface topography was negligible with no apparent evidence of α or β phases. The oxide film produced in each case was identified to be TiO_2.

7. Treatment 1-7 (Degrease and Fluoro nitro-ammonium)

In general this treatment produced the thinnest oxide layer identified as TiO_2. It also produces a surface topography with the characteristic α - β phases on all α - β alloys.

8. Treatment 1-8 (Degrease and Hot alkaline)

This treatment has no apparent effect on surface topography compared to "as received" panels. Characteristic α-β phases are not evident on α - β phase alloys. The major difference between this treatment versus room temperature alkaline (1-2) is that it produces a much cleaner surface. In all cases, the oxide layer produced is TiO_2.

* Note:

The source of the copper found on the surfaces of the etched alloys can be traced to the fluoro-nitric solution, which was previously used to etch the Cu containing 2024T-3 Al alloy. The SEM microphotographs of the treated alloy surfaces have the same characteristic morphology as those treated in a Cu containing fluoro-nitric solution by Baun et.al. (Ref. 6).

V. CONCLUSIONS

Different chemical treatments of various titanium alloys produce significant differences in surface topography, composition, chemical state, and oxide thickness. The effects of these treatments cannot be adequately evaluated using a single characterization technique. In this study it was necessary to thoroughly assess treatment effects. The data base produced will be beneficial in the evaluation of adhesive bond joints of titanium alloy adherents. In general, the influence of surface topography and chemistry on joint strength and durability cannot be predicted. Only after mechanical testing and induced failure can these properties be evaluated. Therefore, it is essential that as much as possible be known about the adherent surface before bonding so that evaluation failure modes can be more easily related to the physical and chemical properties of all components of bonded structures.

REFERENCES

1 R.A. Wood, R.J. Favor, "Titanium Alloys Handbook" MCIC-HB-02 Metals and Ceramics Information Center. December 1972.

2 J.S. Solomon, W.L. Baun, J. Vac. Sci. Tech. 12(1975) 375-378.

3 F. Dalard, C. Montella, J.Gandon, Surf. Tech. 8(1979) 203-224.

4 S. Thomas, Surf. Sci. 55(1976) 754-758.

5 J.S. Solomon, W.L.Baun, Surf. Sci. 51(1975) 228-236.

6 W.L. Baun, N.T. McDevitt, J.S. Solomon, Air Force Materials Laboratory Technical Report AFML-TR-76-29 Part I, II, III, September 1976.

7 K.W. Allen, H.S. Alsalim, W.C. Wake, J. Adhesion, 6(1974), 153-164.

8 H.J. Mathieu, J.B. Mathieu, D.E. McClure, D. Landolt, J. Vac. Sci. Tech. 14, 4(1977) 1023-1028.

9 J.S. Solomon, V. Meyers, American Laboratory March, 1976, 31-40.

10 P.C.S. Hayfield, Titanium Science and Technology, 4(1973), 2405-2418

11 W.L. Baun, N.T. McDevitt, J.S. Solomon, Air Force Materials Laboratory Technical Report AFML-TR-76-18 March 1976.

12 W. Chen, D.W. Dwight, J.P. Wightman, National Aeronautics and Space Administration, Technical Report, N78-26184, February 1978

13 R. Perrier, J.J. Bodu, M. Brunin, Surf. Tech. 8(1979). 463,481.

14 J.S. Solomon, D.L. Hall, D.E. Hanlin, Air Force Materials Laboratory, Technical Report, AFML-TR-79-4100, August 1979.

15 J.S. Solomon, J.A. Mescher, T.J. Wild, T.P. Graham, R.G. Keil, Air Force Materials Laboratory, Technical Report, AFML-TR-76-128, July 1976.

16 J.S. Solomon, M.B. Chamberlain, W.L. Baun, Proceedings of the Microbeam Analysis Society, Ninth Annual Conference, Ottawa, Canada, July 1974 Abstract p. 46A-B.

17 H.J. Mathieu, D. Landolt, Proceedings 7th International Vac. Congr. & 3rd International Conf. Solid Surfaces (Vienna, 1977) p. 2023-2026, R. Debrozemsky, F. Rüdenauer, F. Viehböck, and A. Breth, ed., Debrozemsky, Vienna, 1977.

18 G.W. Lively, Air Force Materials Laboratory, Technical Report, AFML-TR-72-70, October 1972.

19 G.W. Lively, Air Force Materials Laboratory, Technical Report, AFML-TR-73-270, January 1974.

20 T.A. Bush, M.E. Counts, T.C. Ward, J.P. Wightman, National Aeronautics and Space Administration, Technical Report, NAS1-10646-14, November 1973.

21 W.C. Hamilton, G.A. Lyerly, G. Frohnsdorff, Gillette Research Institute, Technical Report No. 4362, June 1972.

22 W.C. Hamilton, Applied Polymer Symposium, 19(1972) p. 105-124.

23 T. Smith, Air Force Materials Laboratory, Technical Report, AFML-TR-74-73 Part II, October 1975.

24 W.W. Ladyman, Air Force Materials Laboratory, Technical Report, AFML-TR-73-270, Part II, August 1975.

25 J. Socha, Surf. Sci., 25(1971), 147.

26 A. Benninghoven, Surf. Sci., 53(1975), 596.

27 L. Ramqvist, K. Harmin, G. Johansson, A. Fahlman, C. Nordling, J. Phys. Chem. 30(1969), 1835.

28 R.F. Wegman, M.C. Ross, S.A.Slota, E.S. Duda, Materials Engineering Laboratory, Picatinny Arsenal, Dover, N.J. Technical Report 4186, Part I, September, 1971.

APPENDIX

RELATIVE ABUNDANCE OF NATURALLY OCCURRING ISOTOPES

(Z = I - 92)

APPENDIX

RELATIVE ABUNDANCES OF NATURALLY OCCURRING ISOTOPES

Z↓	A→	1	2	3	4	5	6	7	8	9	10	11	12	13	14	15	16	17	18	19	20
1	H	99 9	01																		
2	He				100																
3	Li						7 4	92 6													
4	Be									100											
5	B										18 3	81 7									
6	C												98 9	1 1							
7	N														99 6	0 4					
8	O																99 8	0 04	0 20		
9	F																			100	
10	Ne																				90 9

Z↓	A→	21	22	23	24	25	26	27	28	29	30	31	32	33	34	35	36	37	38	39	40
10	(Ne)	0 3	8 8																		
11	Na			100																	
12	Mg				78 6	10 1	11 3														
13	Al							100													
14	Si								92 2	4 7	3 1										
15	P											100									
16	S												95 0	0 8	4 2		0 02				
17	Cl															75 5		24 5			
18	Ar																0 34		0 06		99 6
19	K																			93 1	0 01
20	Ca																				97 0

Z↓	A→	41	42	43	44	45	46	47	48	49	50	51	52	53	54	55	56	57	58	59	60
19	K	6 9																			
20	Ca		0 6	0 1	2 1		003		0 2												
21	Sc					100															
22	Ti						8 0	7 3	74 0	5 5	5 2										
23	V										0 3	99 7									
24	Cr										4 3		83 8	9 6	2 3						
25	Mn															100					
26	Fe														5 8		91 7	2 2	0 3		
27	Co																			100	
28	Ni																		67 8		26 2

Z↓	A→	61	62	63	64	65	66	67	68	69	70	71	72	73	74	75	76	77	78	79	80
28	(Ni)	1 2	3 6		1 2																
29	Cu			69 1		30 9															
30	Zn				48 9		27 8	4 1	18 8		0 6										
31	Ga									60 5		39 5									
32	Ge										20 5		27 4	7 7	36 7		7 7				
33	As															100					
34	Se														0 9		9 0	7 6	23 5		49 8
35	Br																			50 6	
36	Kr																		0 4		23

Z↓	A→	81	82	83	84	85	86	87	88	89	90	91	92	93	94	95	96	97	98	99	100
34	(Se)		9 2																		
35	(Br)	49 4																			
36	(Kr)		11 5	11 5	56 9		17 4														
37	Rb					72 2		27 8													
38	Sr				0 6		9 9	7 0	82 5												
39	Y									100											
40	Zr										51 5	11 2	17 1		17 4		2 8				
41	Nb													100							
42	Mo												15 9		9 1	15 7	16 5	9 5	23 7		9 6
43	Tc	DOES NOT OCCUR NATURALLY																			
44	Ru																5 6		1 9	12 7	12 6

Z↓	A→	101	102	103	104	105	106	107	108	109	110	111	112	113	114	115	116	117	118	119	120
44	(Ru)	17.1	31.6		18.5																
45	Rh			100																	
46	Pd		1.0		11.0	22.2	27.3		26.7		11.8										
47	Ag							51.4		48.6											
48	Cd						1.2		0.9		12.4	12.7	24.1	12.3	28.8		7.6				
49	In													4.3		95.7					
50	Sn												0.9		0.6	0.3	14.2	7.6	24.0	8.6	33.0
51	Sb	DOES NOT OCCUR NATURALLY																			
52	Te																				0.1

Z↓	A→	121	122	123	124	125	126	127	128	129	130	131	132	133	134	135	136	137	138	139	140
50	(Sn)		4.6		6.0																
51	(Sb)	57.3		42.7																	
52	(Te)		2.4	0.9	4.6	7.0	18.7		31.8		34.5										
53	I							100													
54	Xe				0.1		0.1		1.9	26.4	4.1	21.2	26.9		10.4		8.9				
55	Cs													100							
56	Ba										0.1		0.1		2.4	6.6	7.8	11.3	71.7		
57	La																		0.1	99.9	
58	Ce																0.2		0.2		88.5

Z↓	A→	141	142	143	144	145	146	147	148	149	150	151	152	153	154	155	156	157	158	159	160
58	(Ce)		11.1																		
59	Pr	100																			
60	Nd		27.1	12.1	23.8	8.3	17.3		5.8		5.6										
61	Pm	DOES NOT OCCUR NATURALLY																			
62	Sm				3.2			15.1	11.3	13.8	7.5		26.6		22.5						
63	Eu											47.9		52.1							
64	Gd												0.2		2.1	14.7	20.5	15.7	24.9		21.9
65	Tb																			100	
66	Dy																0.1		0.1		2.3

Z↓	A→	161	162	163	164	165	166	167	168	169	170	171	172	173	174	175	176	177	178	179	180
66	(Dy)	18.9	25.5	24.9	28.2																
67	Ho					100															
68	Er		0.1		1.6		33.4	22.9	27.1		14.9										
69	Tm									100											
70	Yb								0.2		3.0	14.3	21.8	16.1	31.9		12.7				
71	Lu															97.4	2.6				
72	Hf														0.2		5.2	18.5	27.1	13.8	35.2
73	Ta																				0.01
74	W																				0.2

Z↓	A→	181	182	183	184	185	186	187	188	189	190	191	192	193	194	195	196	197	198	199	200
73	(Ta)	[illegible]																			
74	(W)	—	[illegible]	[illegible]	[illegible]																
75	Re	—	—	—	—	[illegible]		[illegible]													
76	Os	—	—	—	0.02		[illegible]	[illegible]	[illegible]	16.1	26.4		41.0								
77	Ir	—	—	—	—	—	—	—	—	—	—	38.5		61.5							
78	Pt	—	—	—	—	—	—	—	—	—	0.1		0.8		32.9	33.9	25.2		7.19		
79	Au	—	—	—	—	—	—	—	—	—	—							100			
80	Hg	—	—	—	—	—	—	—	—	—	—						0.2		10.0	16.8	23.1

Z↓	A→	201	202	203	204	205	206	207	208	209	210	211	212	213	214	215	216	217	218	219	220
80	(Hg)	13.2	29.8		6.9																
81	Tl	—	—	29.5		70.5															
82	Pb	—	—	—	1.4		25.2	21.7	51.7												
83	Bi	—	—	—	—	—	—	—	—	100											

84 (Po), 85 (At), 86 (Rn), 87 (Fr), 88 (Ra), 89 (Ac), DO NOT OCCUR NATURALLY

Z↓	A→	221	222	223	224	225	226	227	228	229	230	231	232	233	234	235	236	237	238	239	240
90	Th	—	—	—	—	—	—	—	100												
91	Pa	—	—	—	—	—	—	—	—	100											
92	U	—	—	—	—	—	—	—	—	—	—	—	—	—	0.06	0.7			99.3		

93 (Np), 94 (Pu), 95 (Am), 96 (Cm), 97 (Bk), 98 (Cf), 99 (Es), 100 (Fm) 101 (Md), 102 (No), 103 (Lw), DO NOT OCCUR NATURALLY

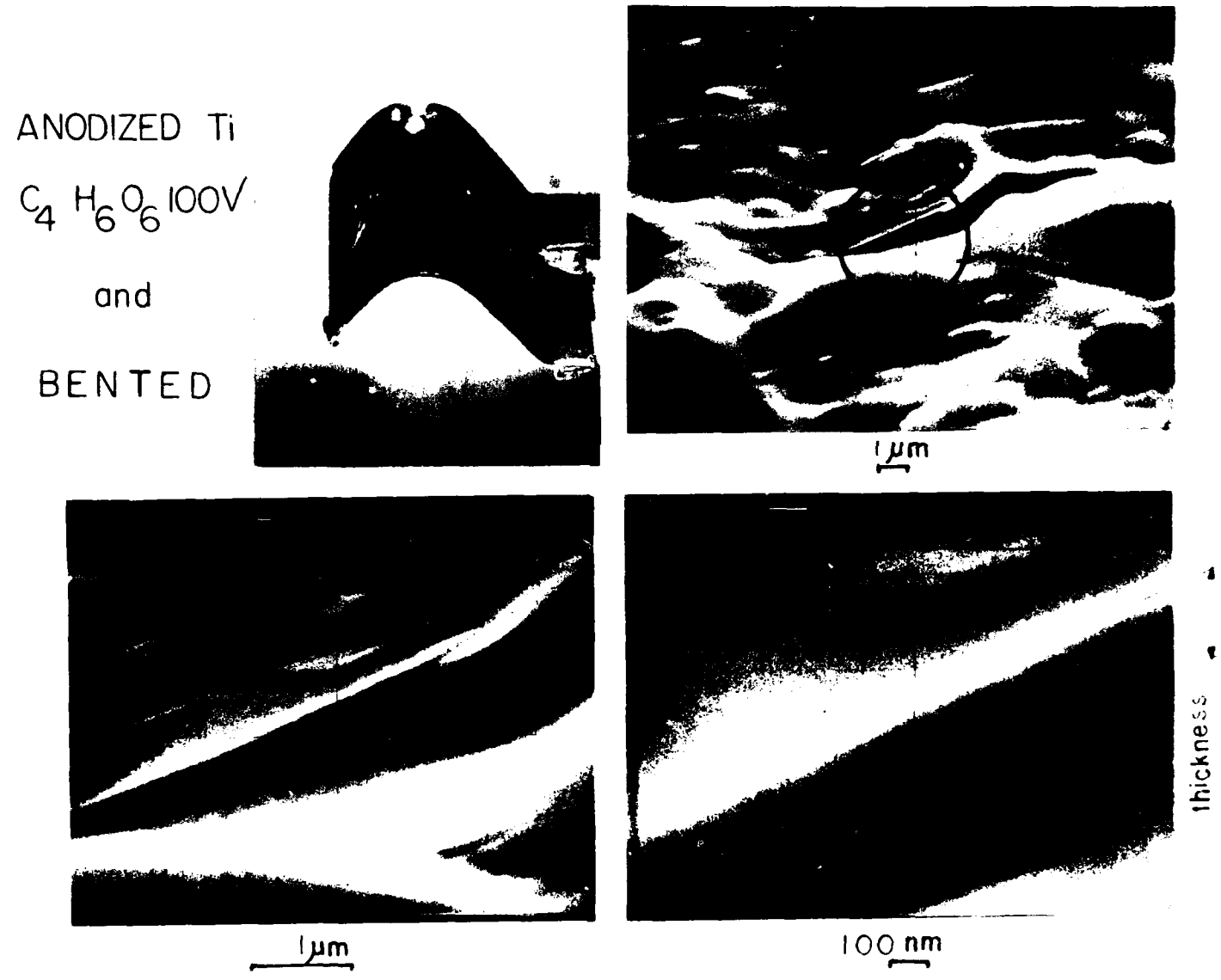

FIG. 1 S.E.M. photomicrographs of anodized titanium (c.p.): determination of the oxide layer thickness

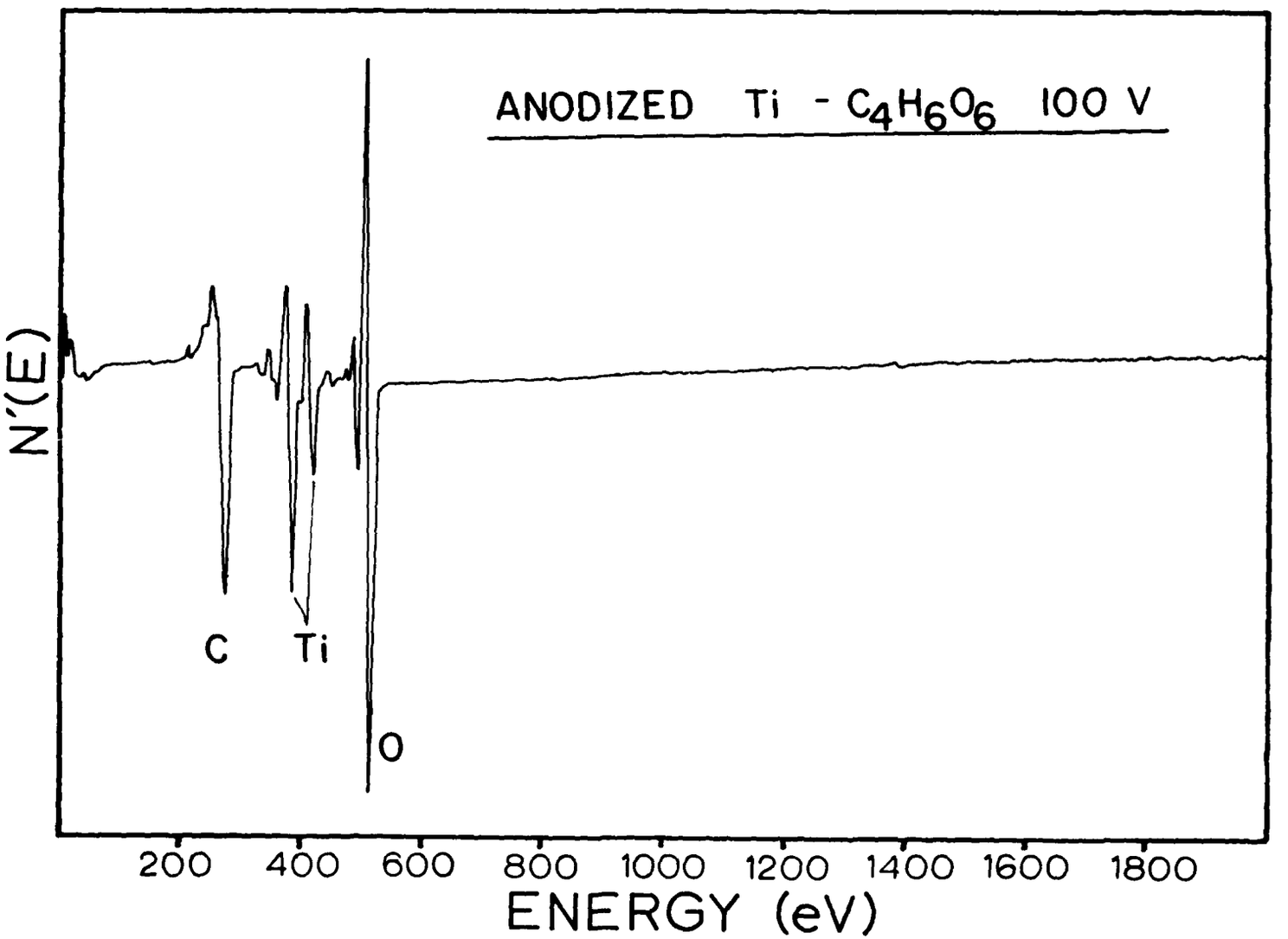

FIG. 2 A.E.S. spectra of anodized titanium (c.p.)

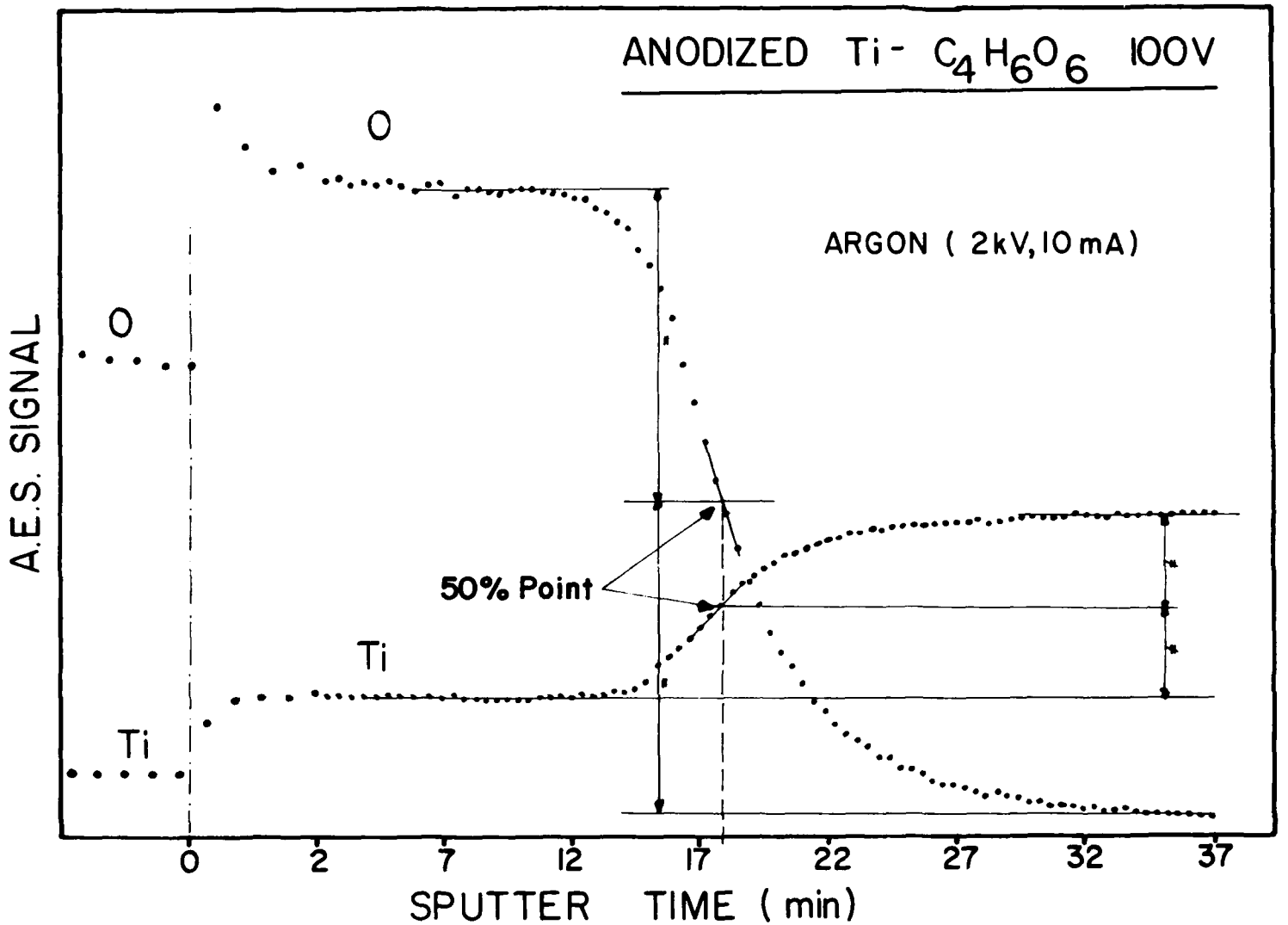

FIG. 3 Auger sputter profiles of anodized titanium (c.p.) with Ar+ (2kV, 10mA)

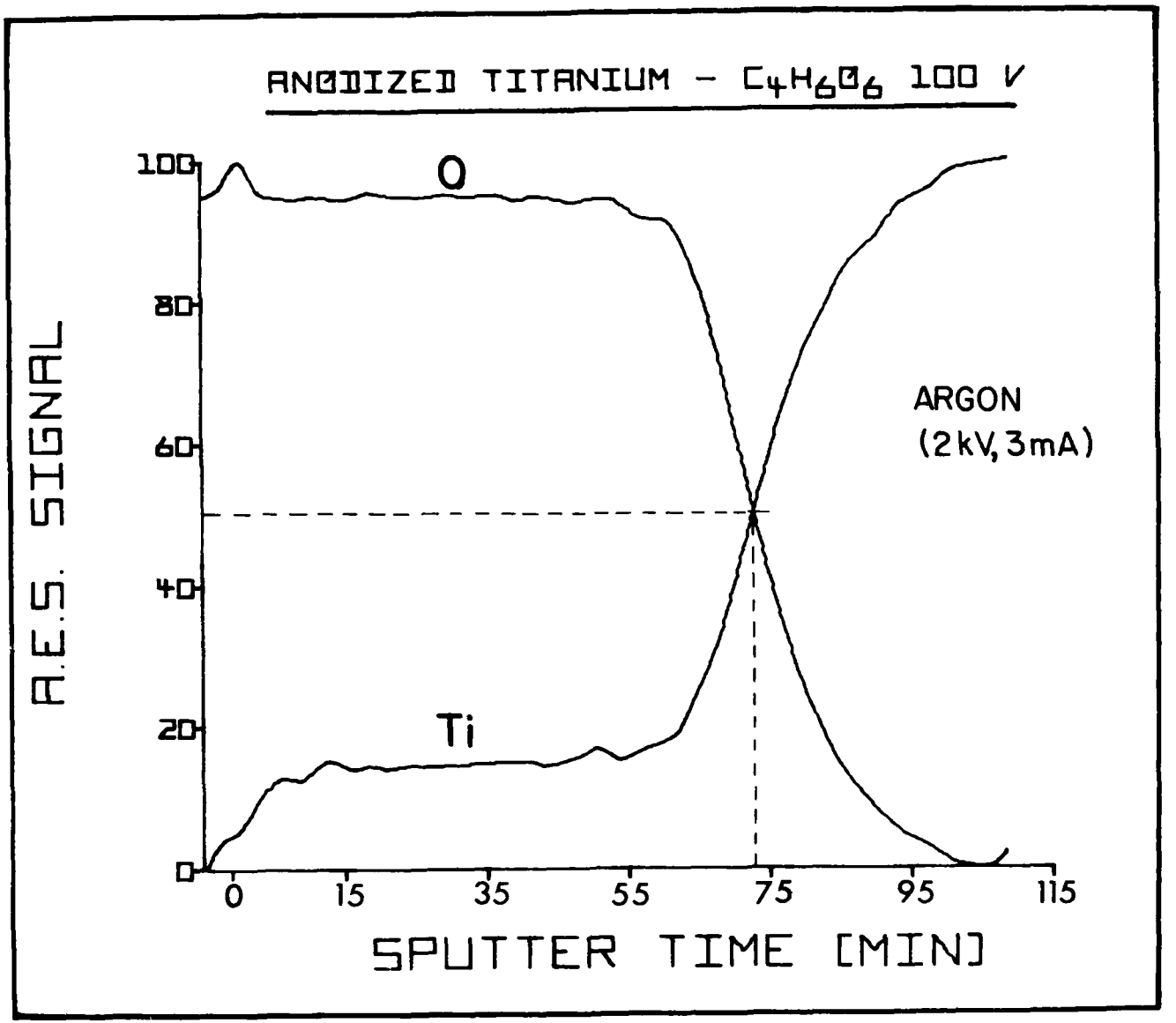

FIG. 4 Auger sputter profiles of anodized titanuim (c.p.) with Ar+ (2kV, 3mA)

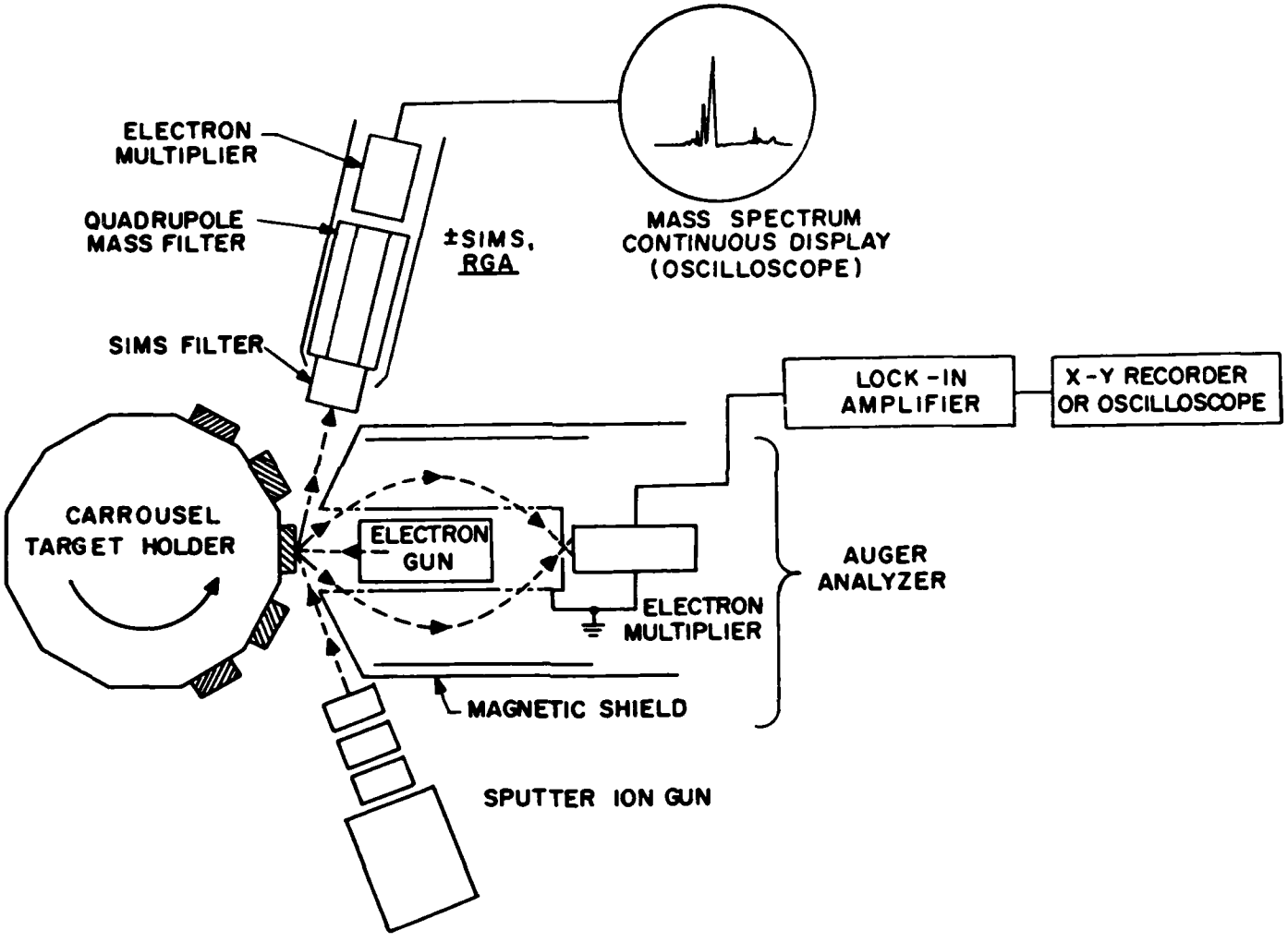

FIG. 5 Schematic drawing of the combined AES-SIMS instrument

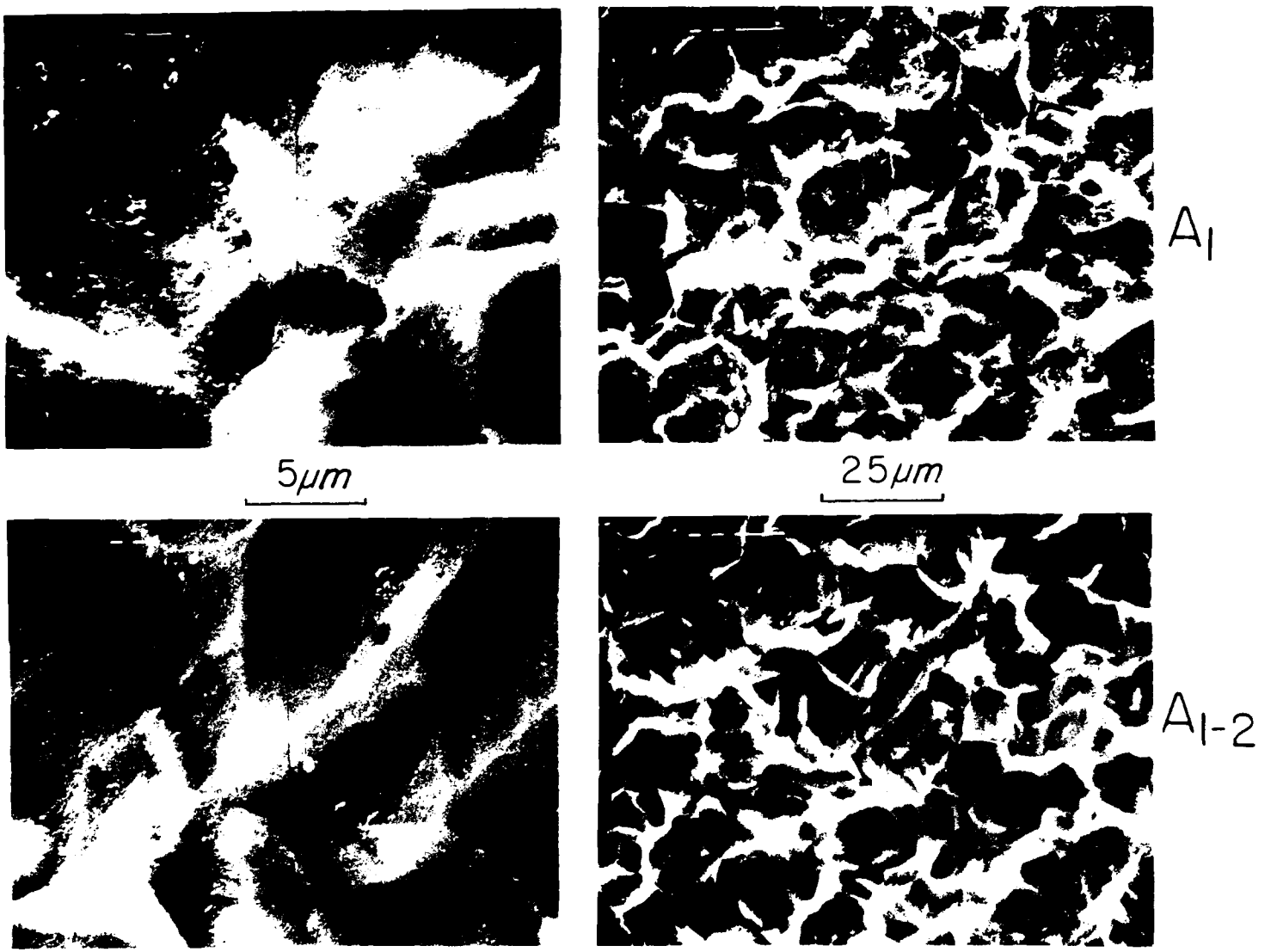

FIG. 6 S.E.M. photomicrographs of titanium (c.p.) subjected to 1 and 1-2 treatments

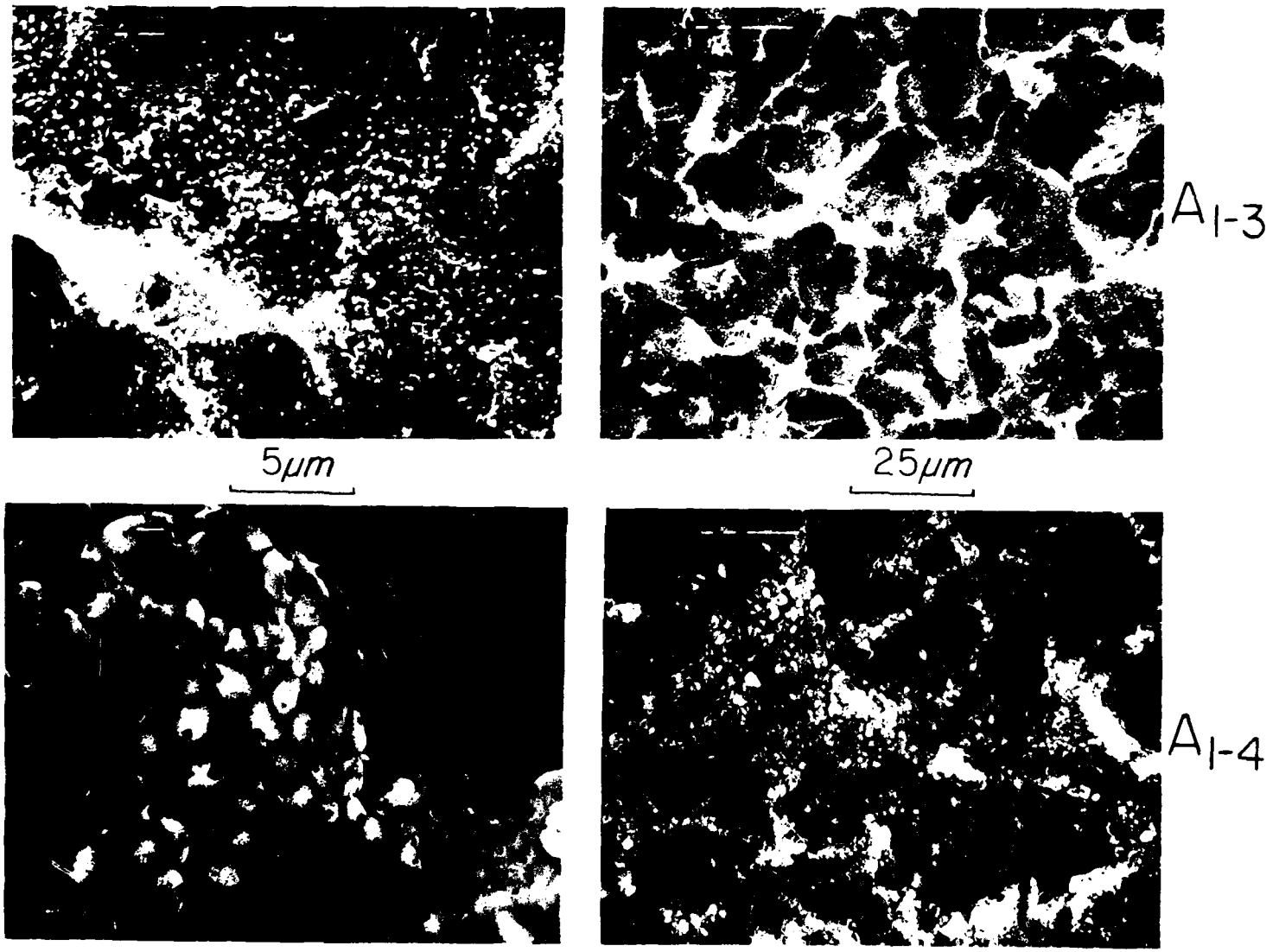

FIG. 7 S.E.M. photomicrographs of titanium (c.p.) subjected to 1-3 and 1-4 treatments

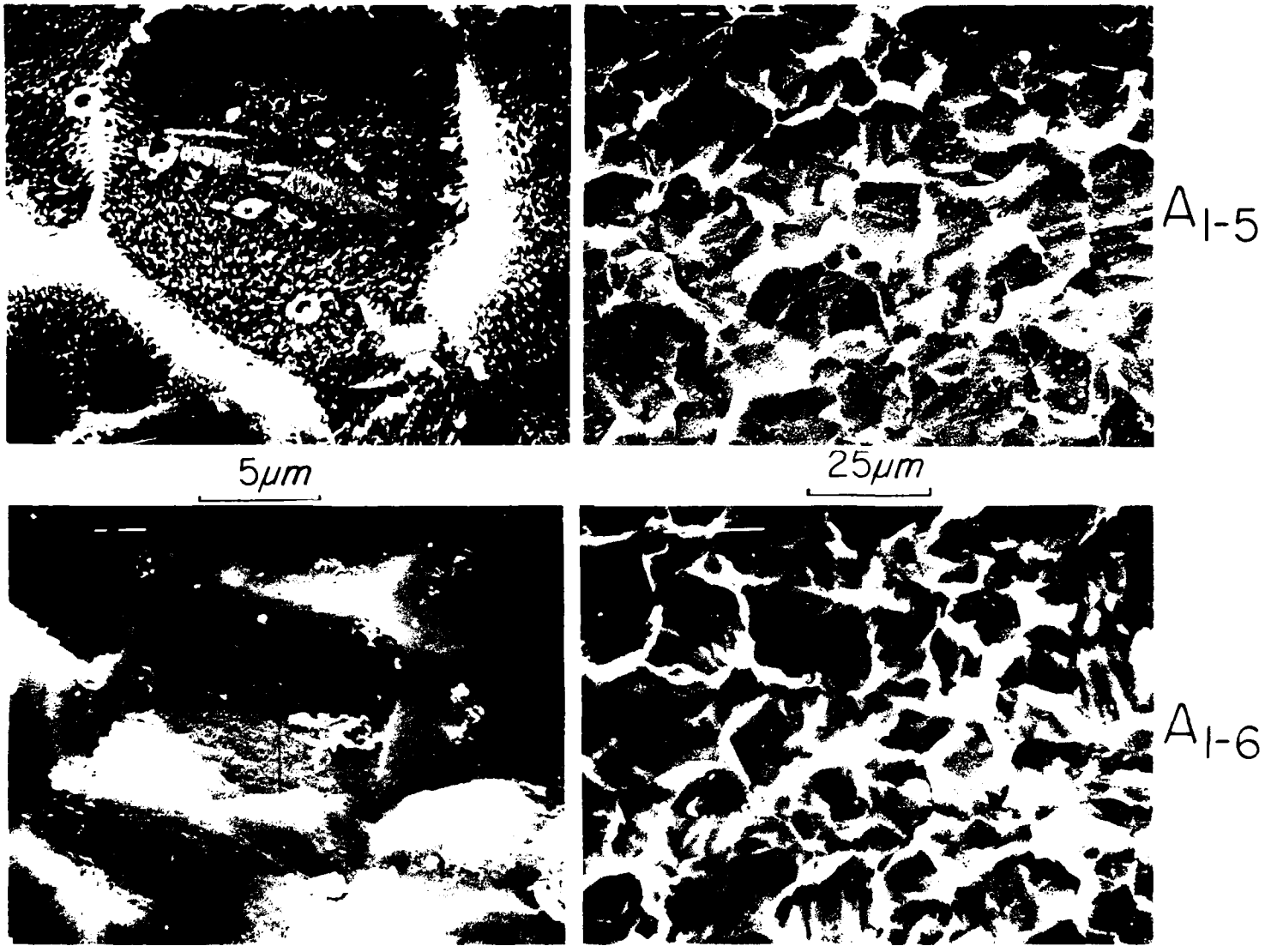

FIG. 8 S.E.M. photomicrographs of titanium (c.p.) subjected to 1-5 and 1-6 treatments

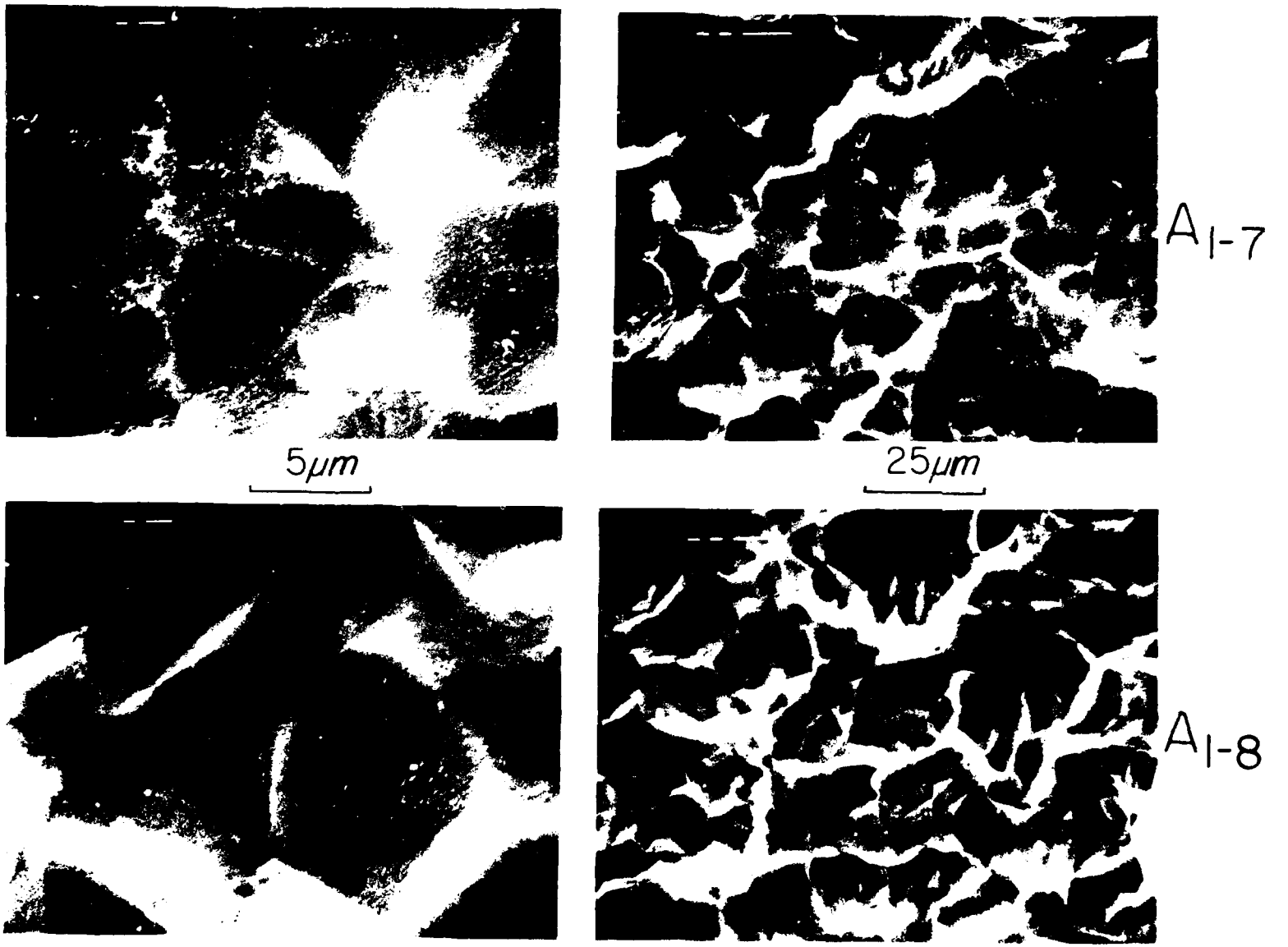

FIG. 9 S.E.M. photomicrographs of titanium (c.p.) subjected to 1-7 and 1-8 treatments

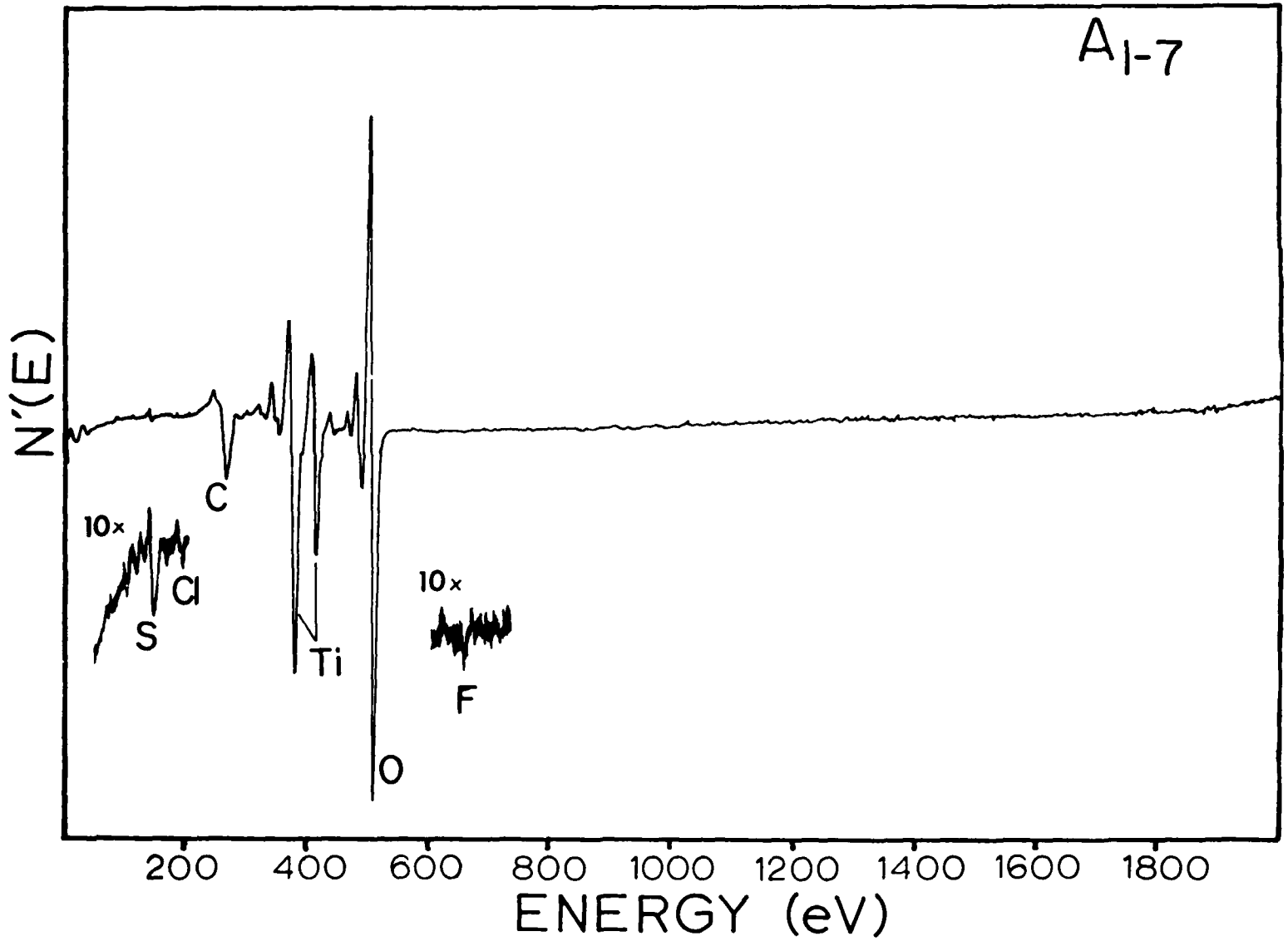

FIG. 10 A.E.S. spectra of titanium (c.p.) subjected to 1-7 treatment (0-2000 eV)

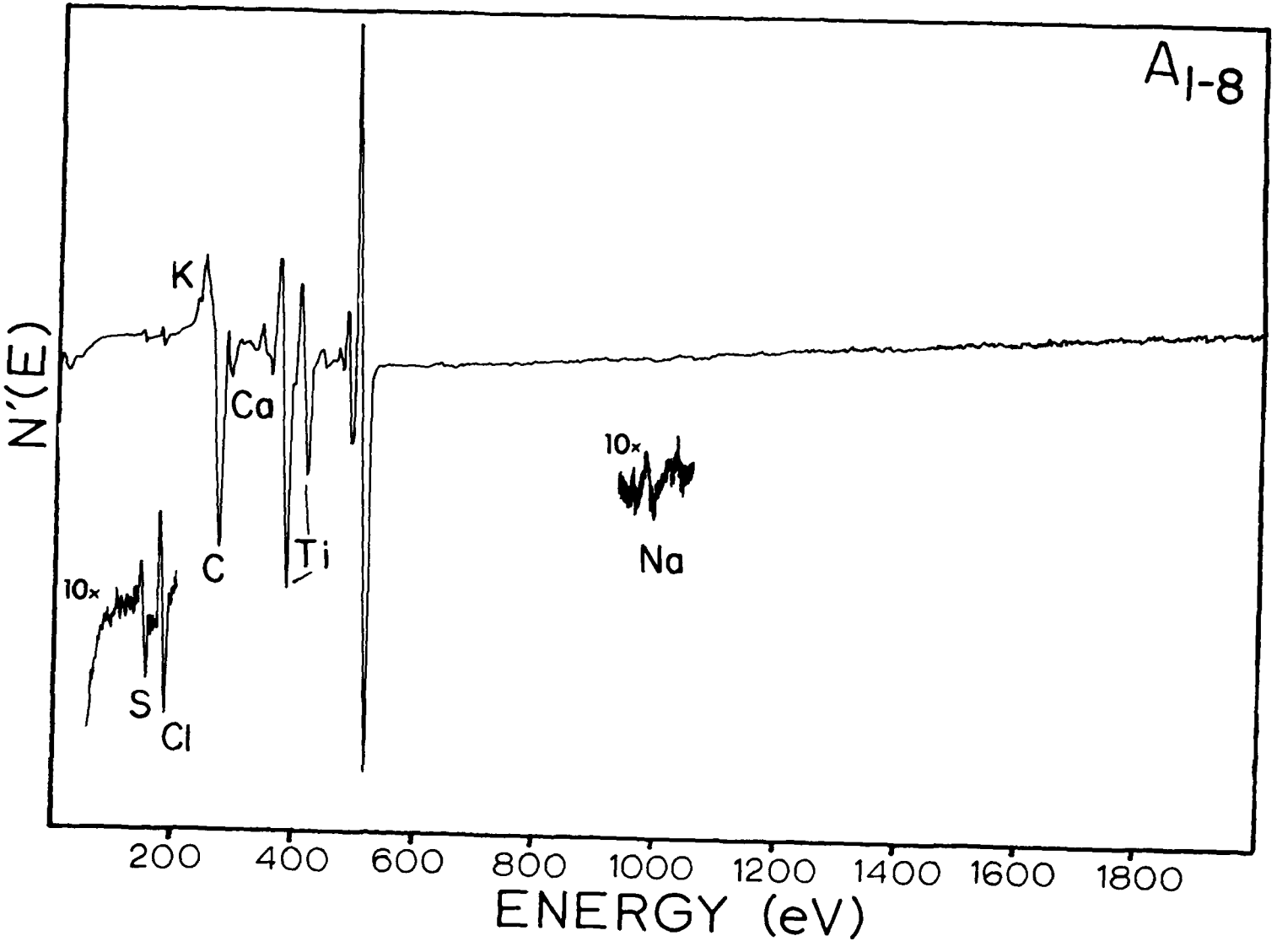

FIG. 11 A.E.S. spectra of titanium (c.p.) subjected to 1-8 treatment (0-2000 eV)

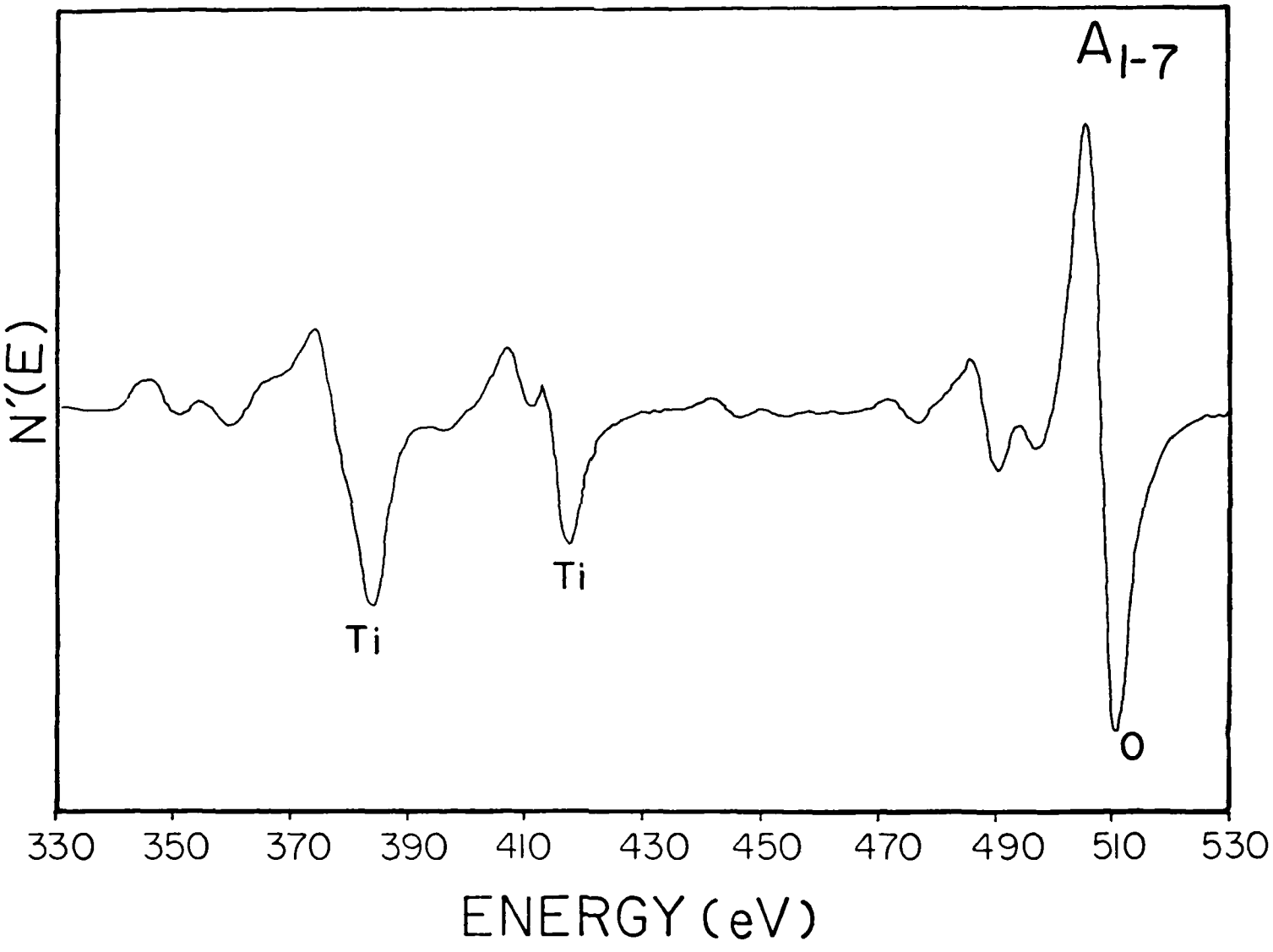

FIG. 12 A.E.S. spectra of titanium (c.p.) subjected to 1-7 treatment (330 - 530 eV)

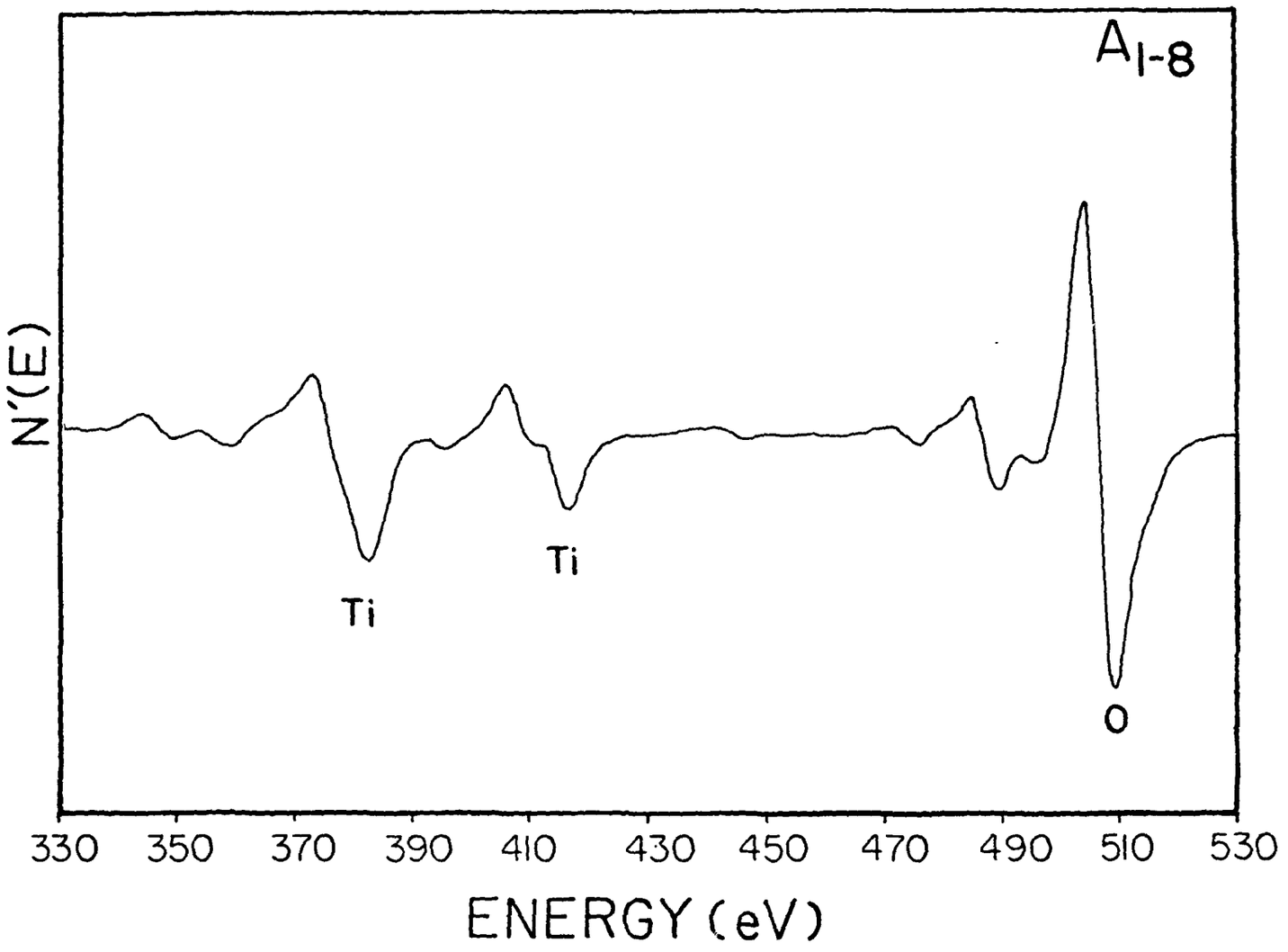

FIG. 13 A.E.S. spectrum of titanium (c.p.) subjected to 1-8 treatment (330 - 530 eV)

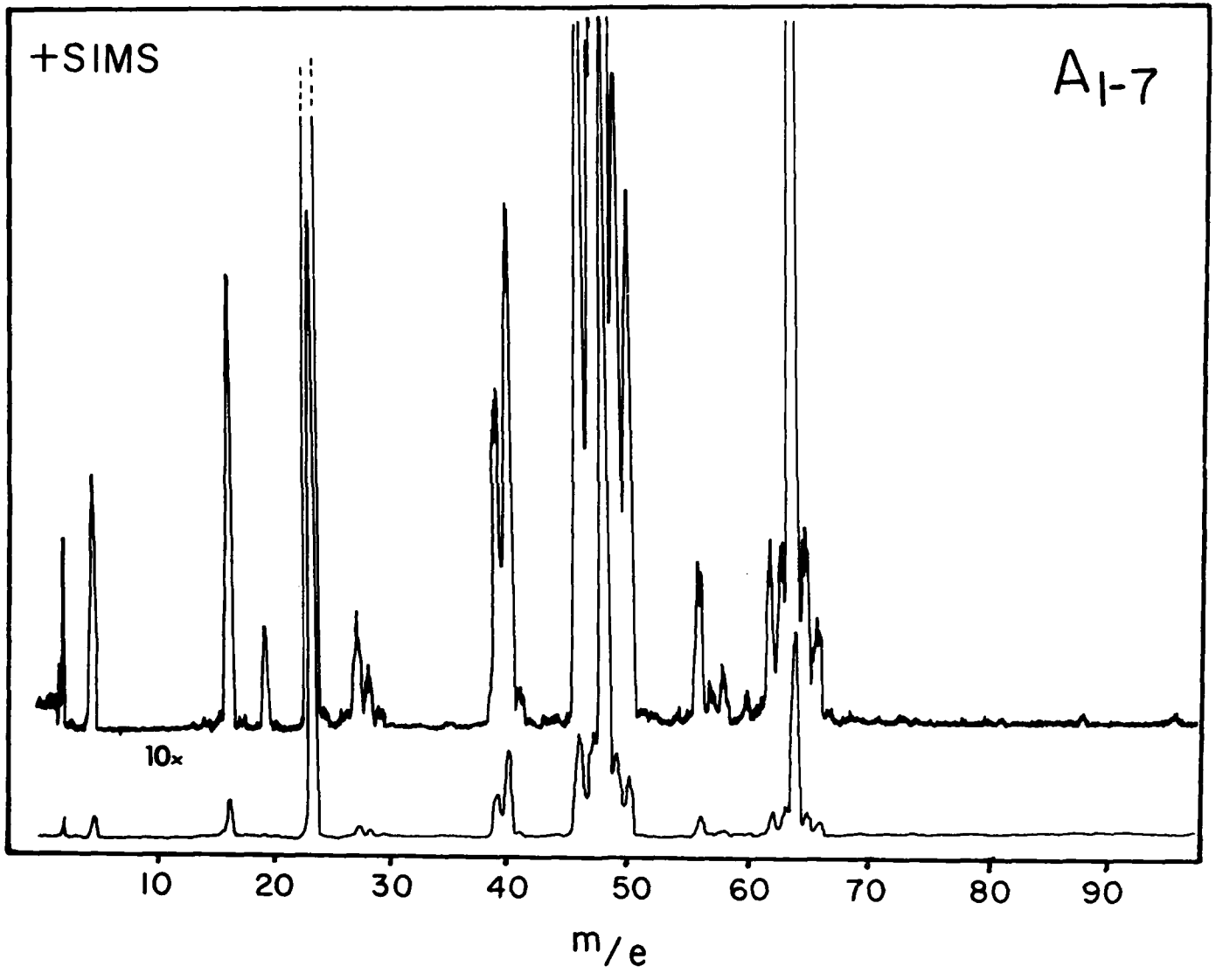

FIG. 14 Positive ion SIMS spectra of titanium (c.p.) subjected to 1-7 treatment

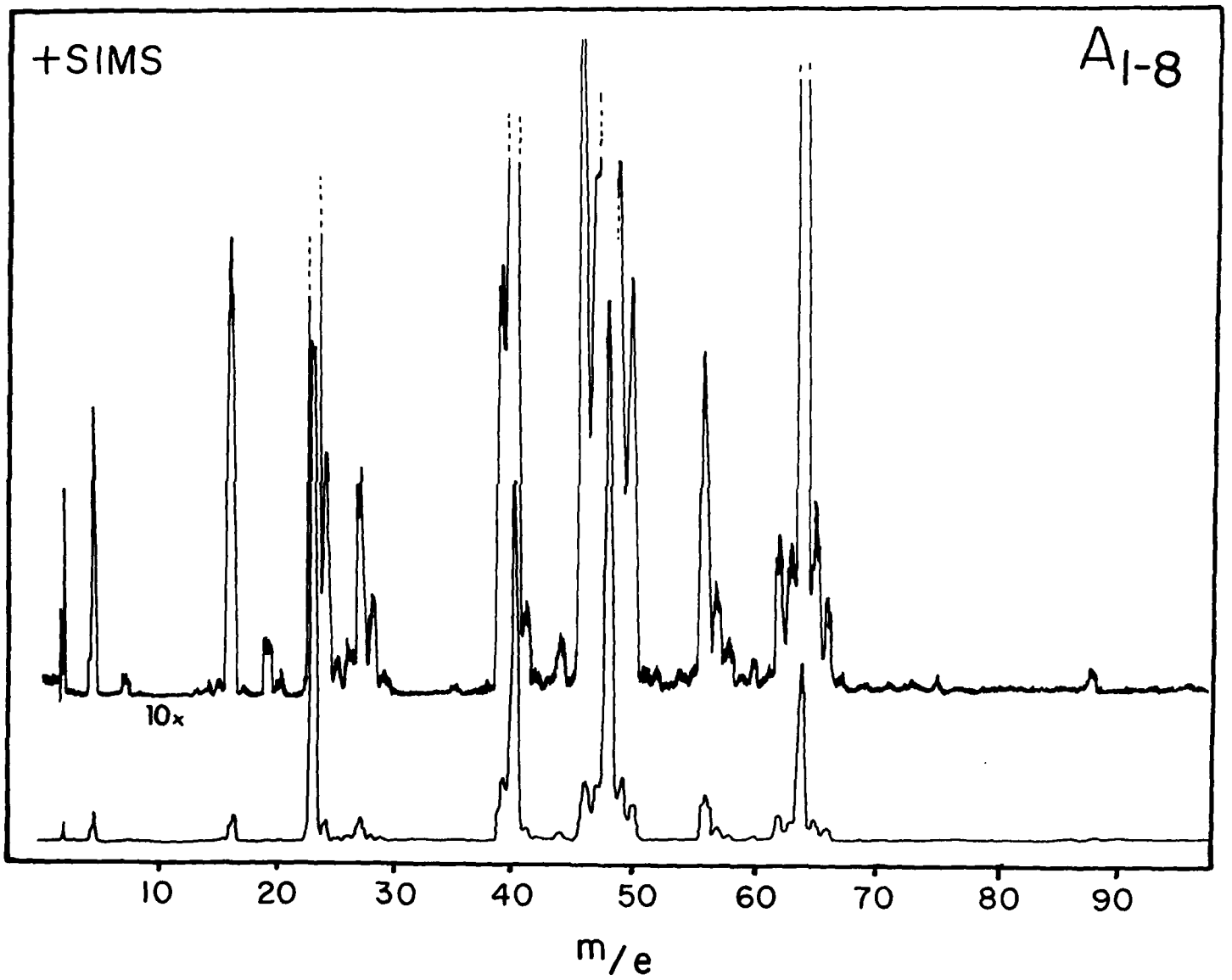

FIG. 15 Positive ion SIMS spectra of titanium (c.p.) subjected to 1-8 treatment

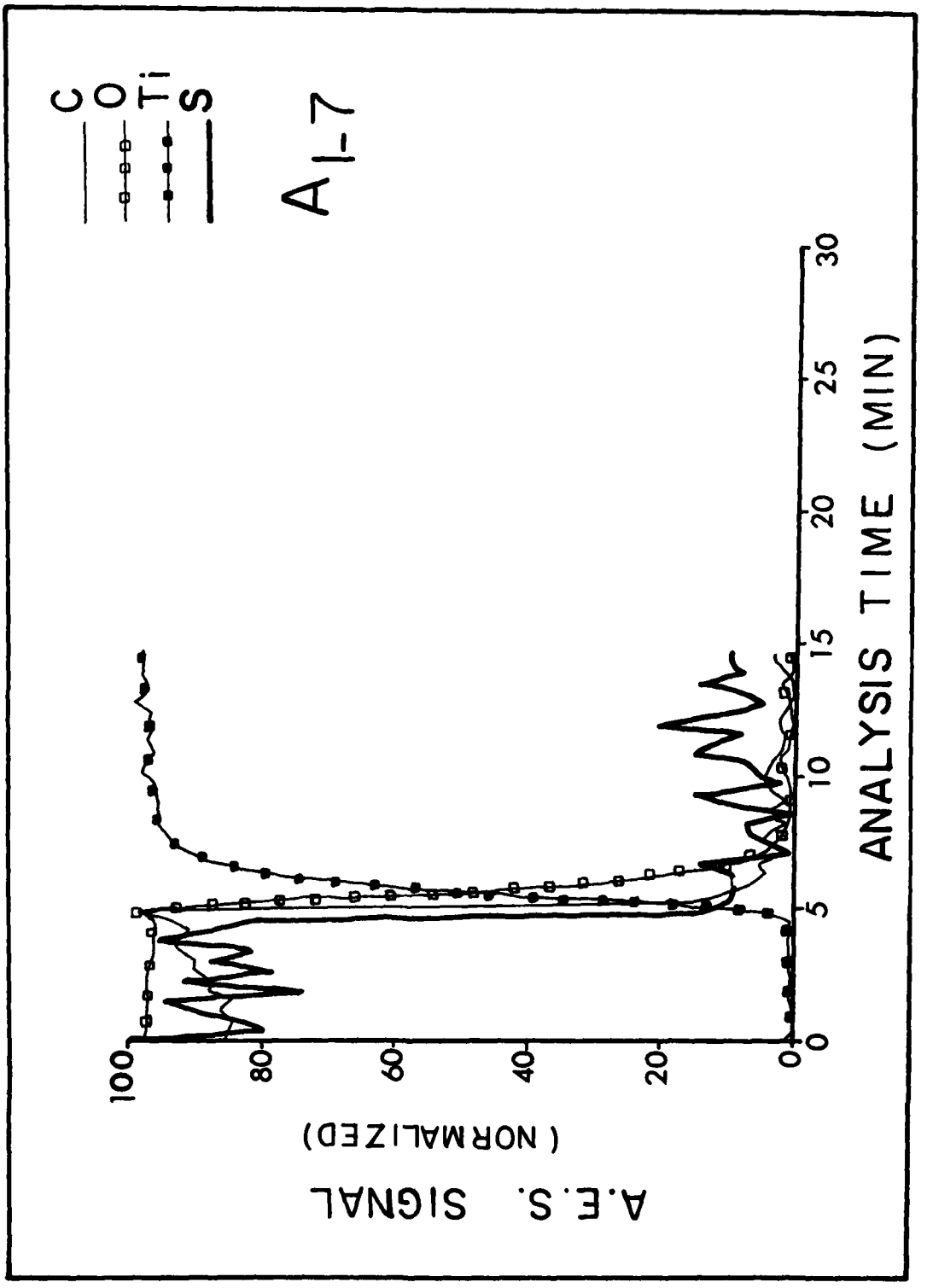

FIG. 16 A.E.S. sputter profiles of titanium (c.p.) subjected to 1-7 treatment

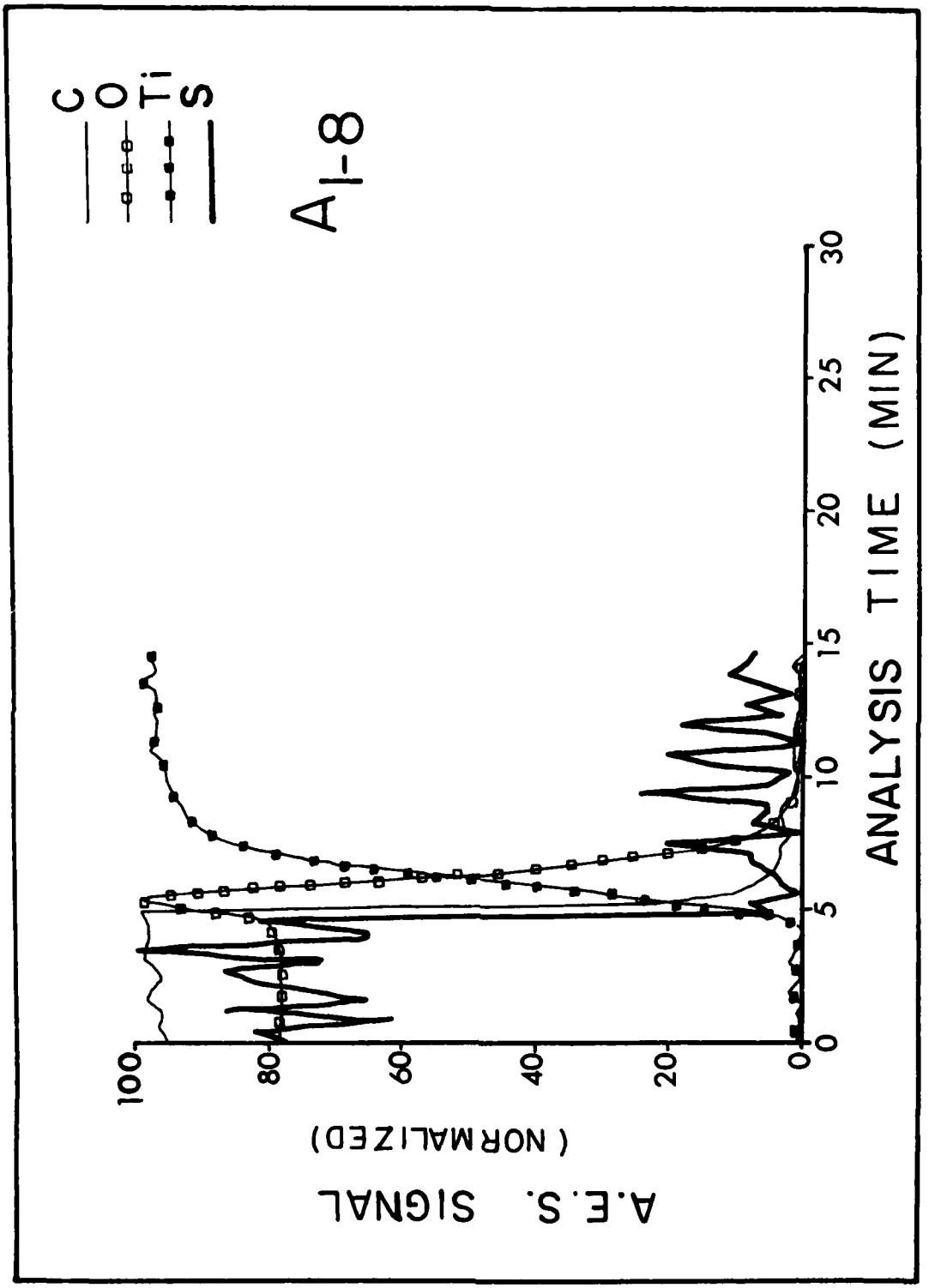

FIG. 17 A.E.S. sputter profiles of titanium (c.p.) subjected to 1-8 treatment

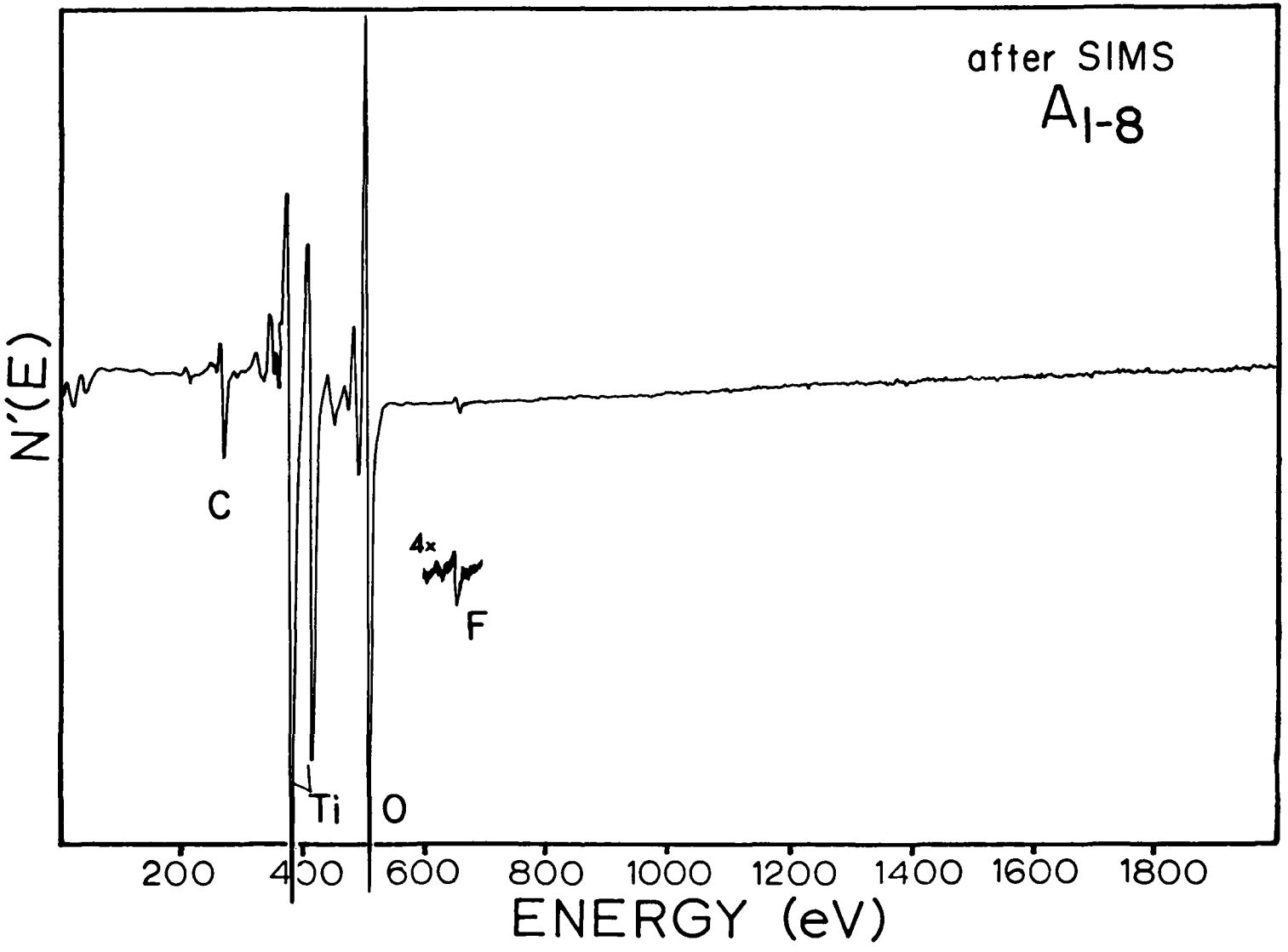

FIG. 18 A.E.S. spectra of titanium (c.p.) subjected to 1-8 treatment following He+ bombardment

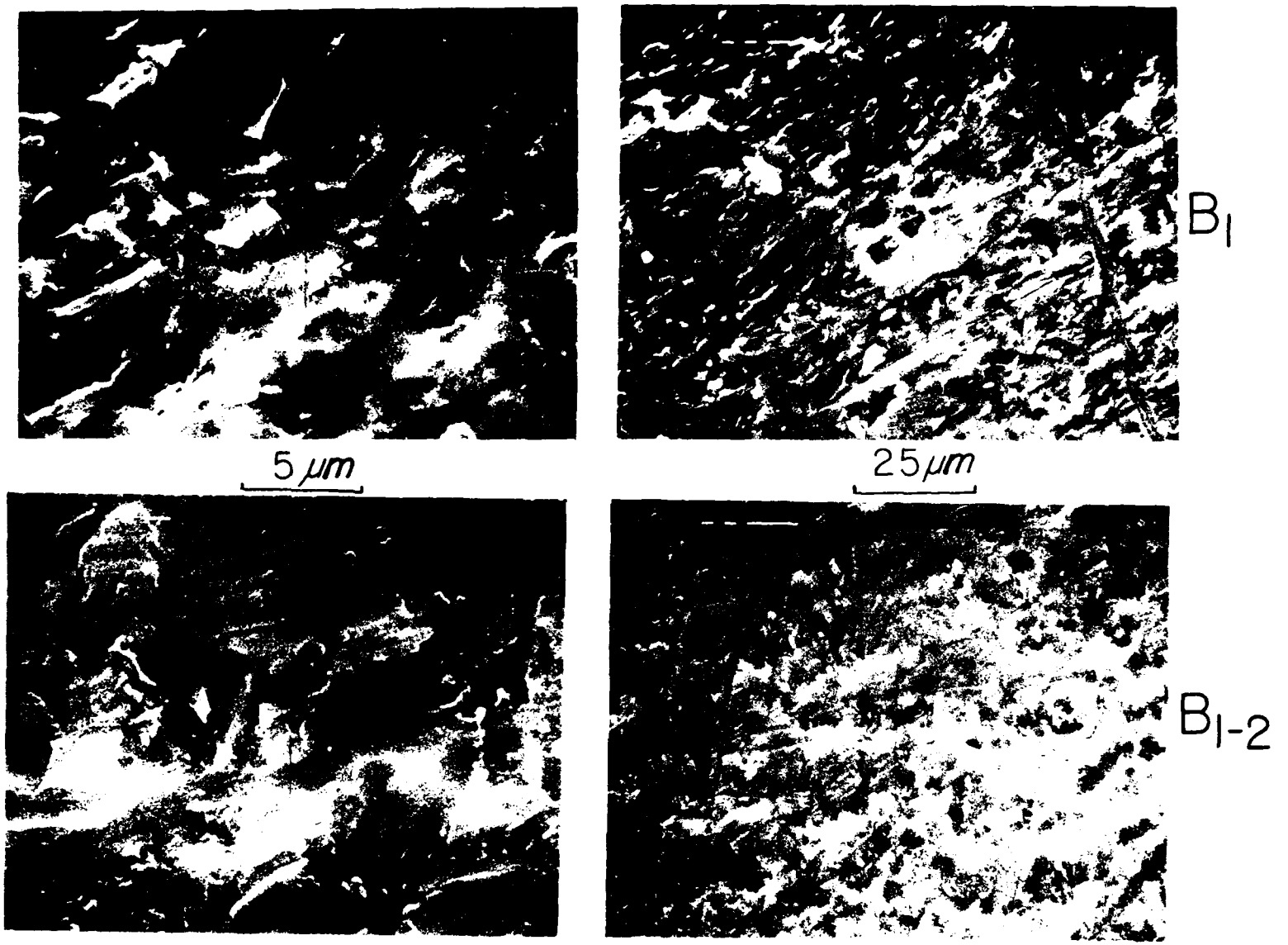

FIG. 19 S.E.M. photomicrographs of Ti-8Al-1Mo-1Sn subjected to 1 and 1-2 treatments

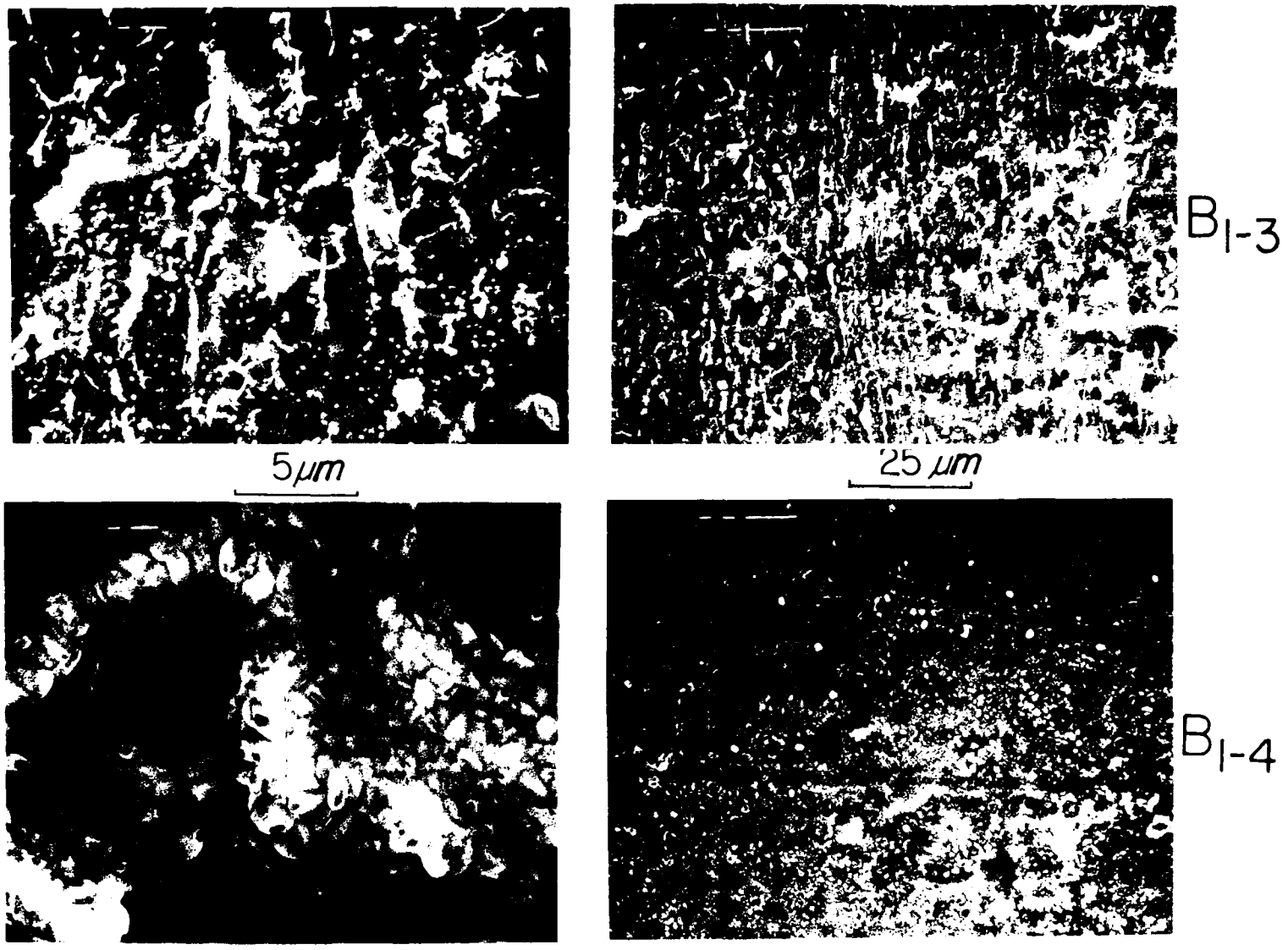

FIG. 20 S.E.M. photomicrographs of Ti-8Al-1Mo-1Sn subjected to 1-3 and 1-4 treatments

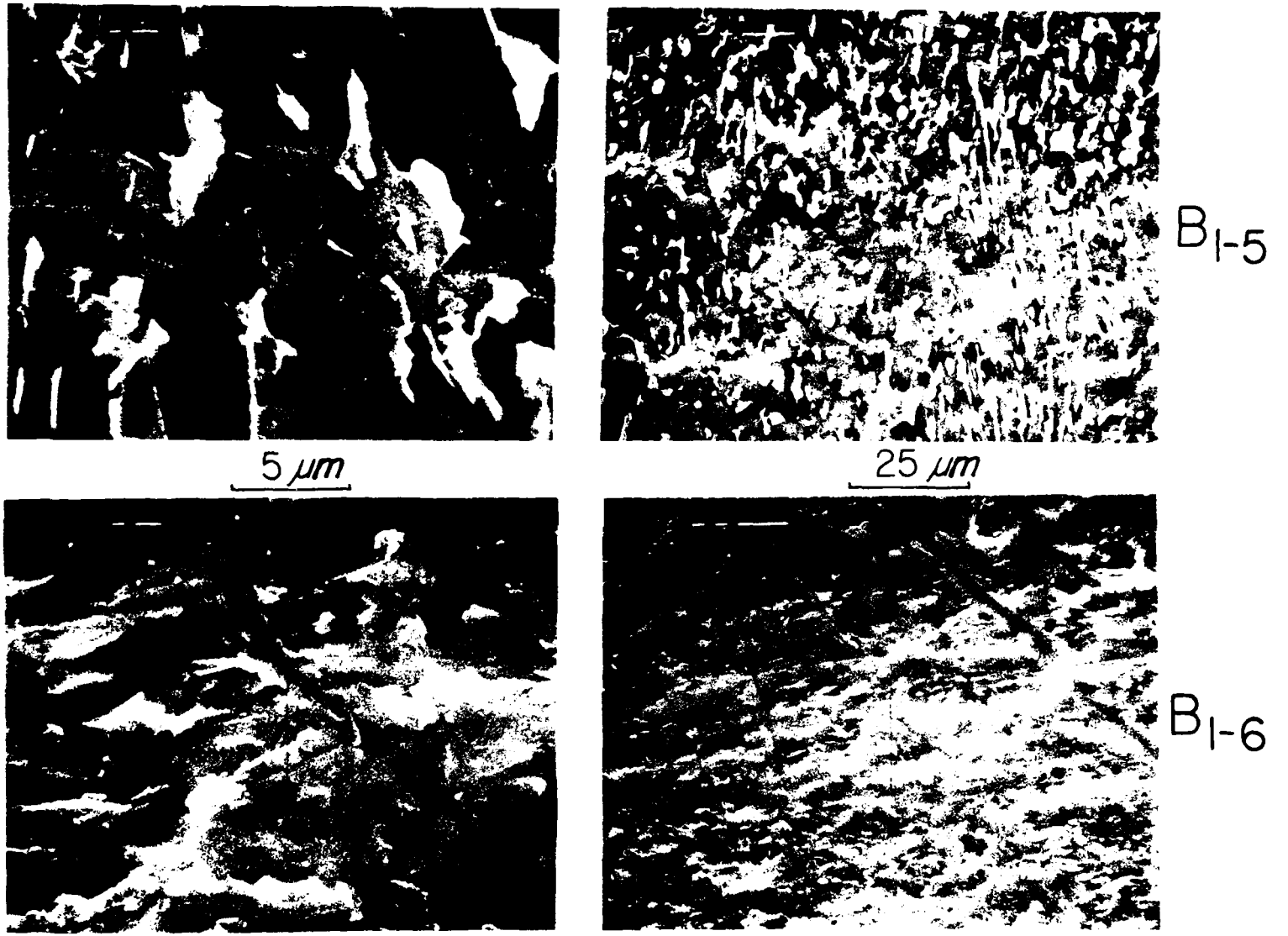

FIG. 21 S.E.M. photomicrographs of Ti-8Al-1Mo-1Sn subjected to 1-5 and 1-6 treatments

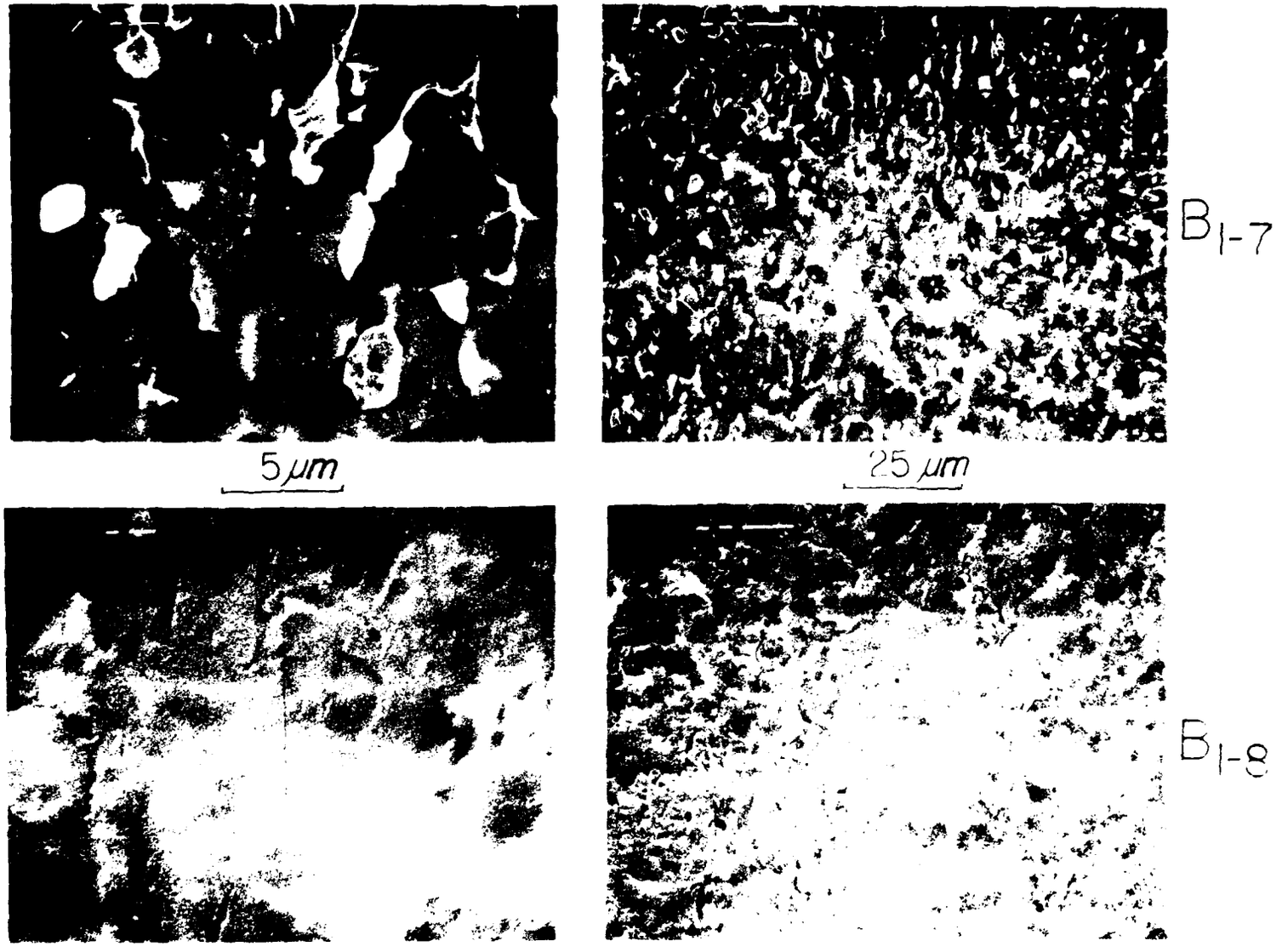

FIG. 22 S.E.M. photomicrographs of Ti-8Al-1Mo-1Sn subjected to 1-7 and 1-8 treatments

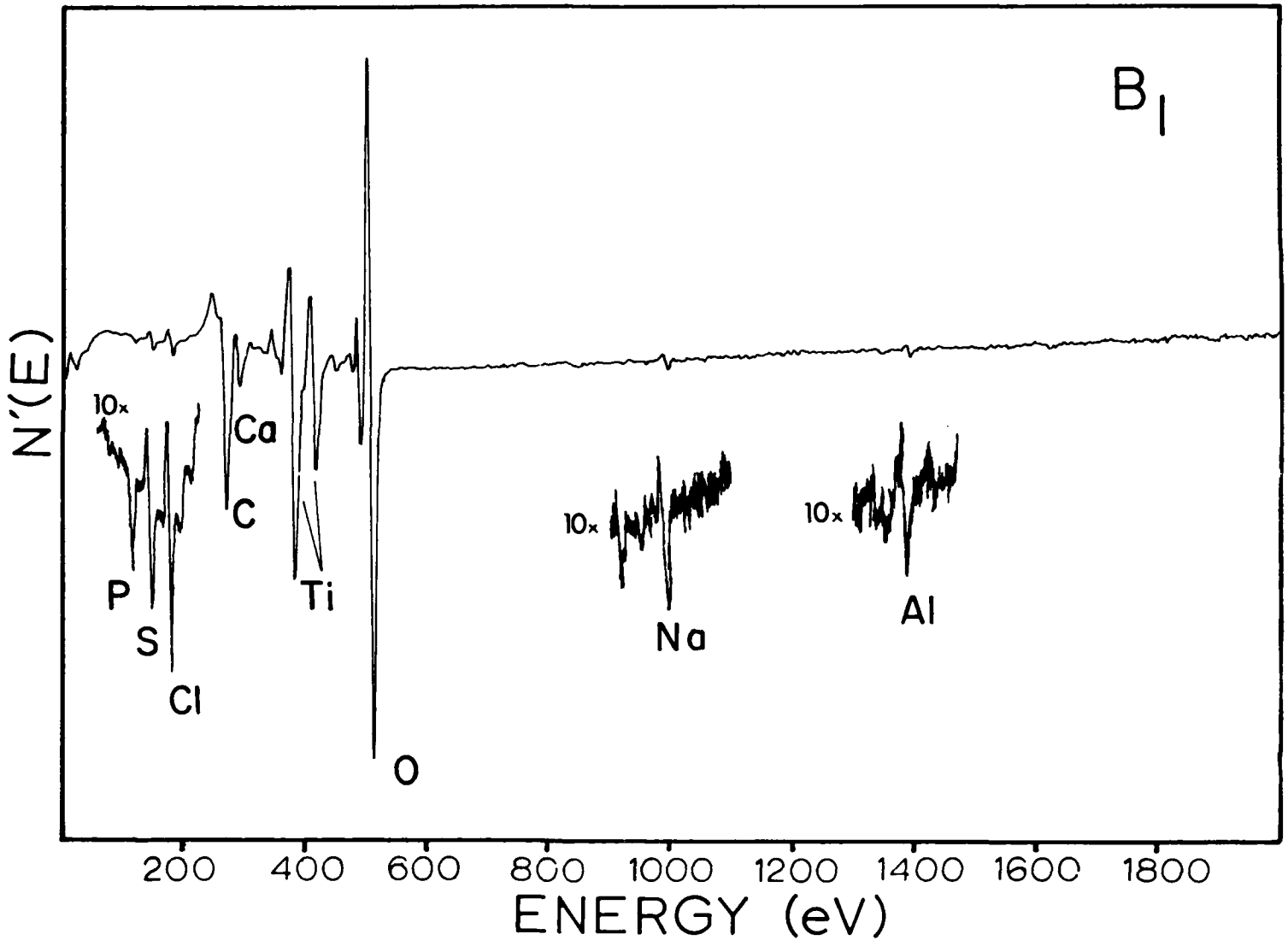

FIG. 23 A.E.S. spectra of Ti-8Al-1Mo-1Sn subjected to 1 treatment (0-2000 eV)

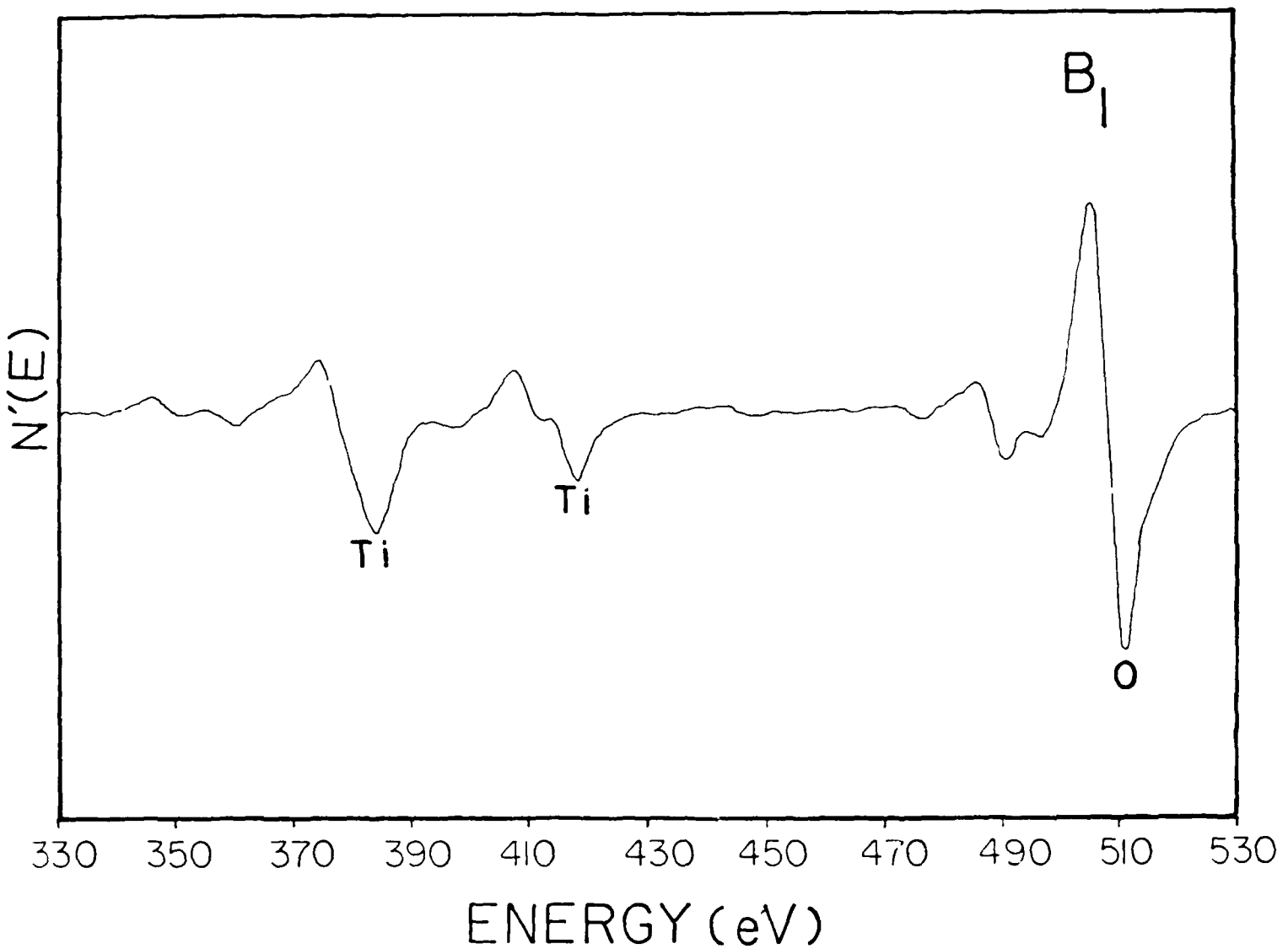

Fig. 24 A.E.S. spectrum of Ti-8Al-1Mo-1Sn subjected to 1 treatment (330 - 530 eV)

AD-A084 171 UNIVERSAL ENERGY SYSTEMS INC DAYTON OHIO F/G 11/6
SURFACE CHARACTERIZATION OF CHEMICALLY TREATED TITANIUM AND TIT--ETC(U)
FEB 80 A A ROCHE F33615-79-C-5129

UNCLASSIFIED AFWAL -TR-80-4004 NL

2 OF 2
AD A084171

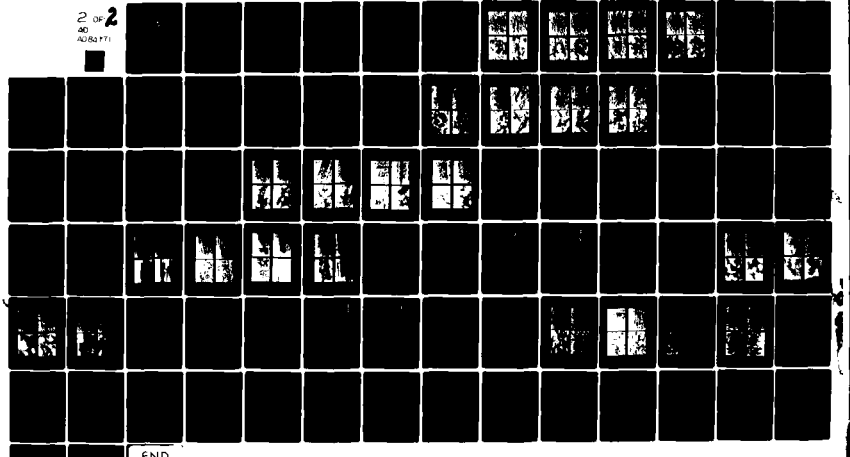

END
DATE FILMED
6-80
DTIC

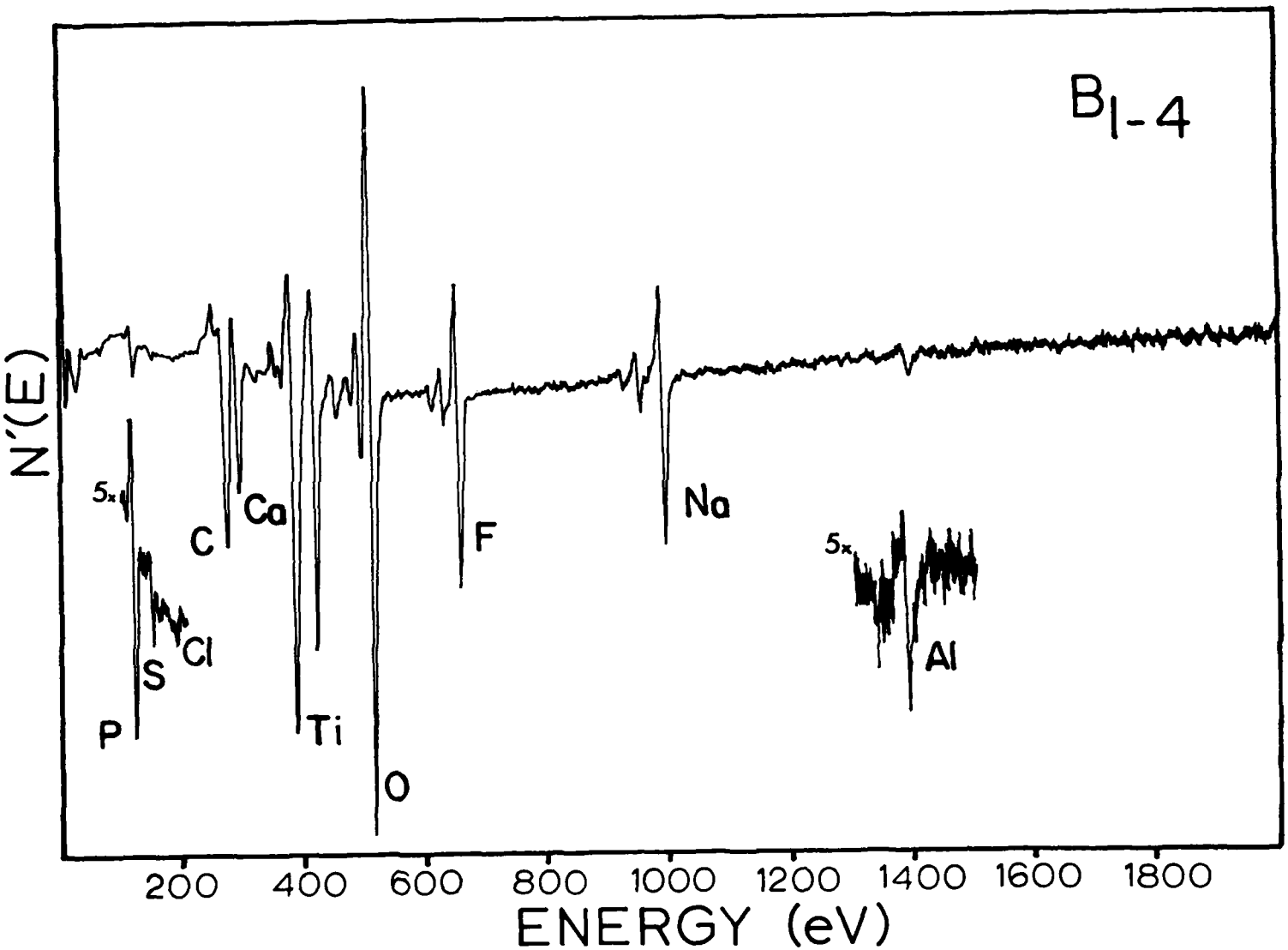

FIG. 25 A.E.S. spectra of Ti-8Al-1Mo-1Sn subjected to 1-4 treatment (0-2000 eV)

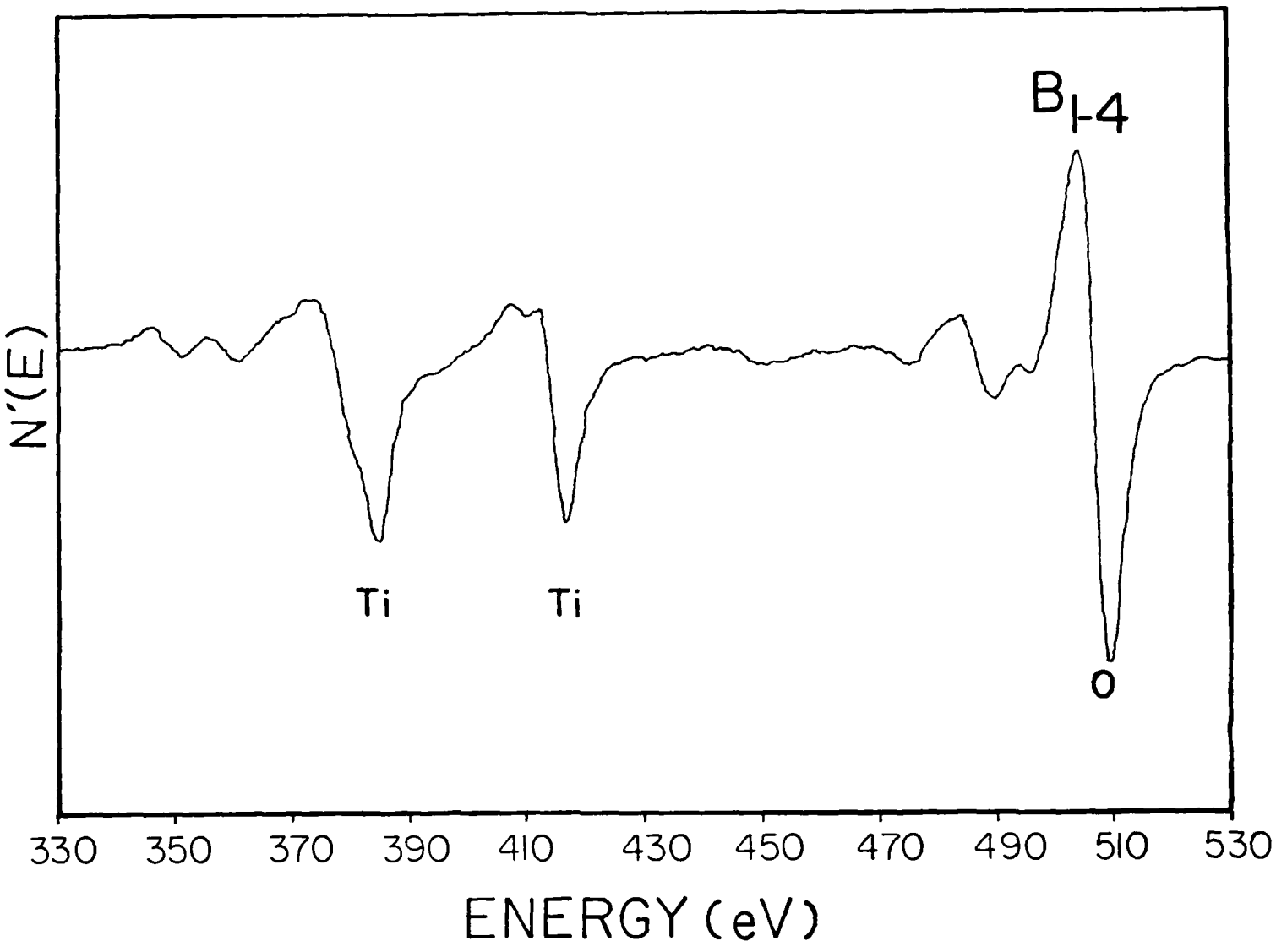

FIG. 26 A.E.S. spectrum of Ti-8Al-1Mo-1Sn subjected to 1-4 treatment (330-530 eV)

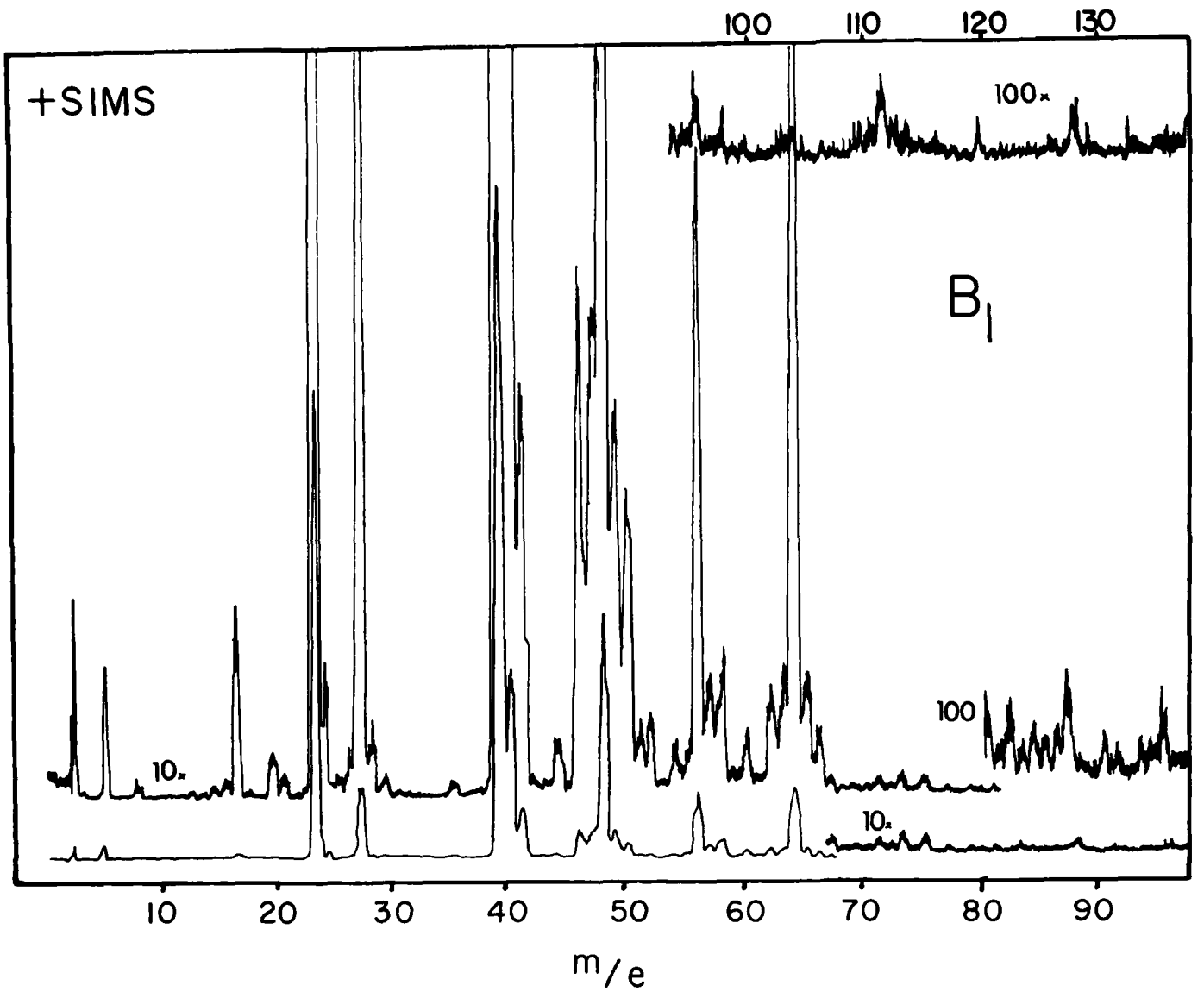

FIG. 27 Positive ion SIMS spectra of Ti-8Al-1Mo-1Sn subjected to 1 treatment

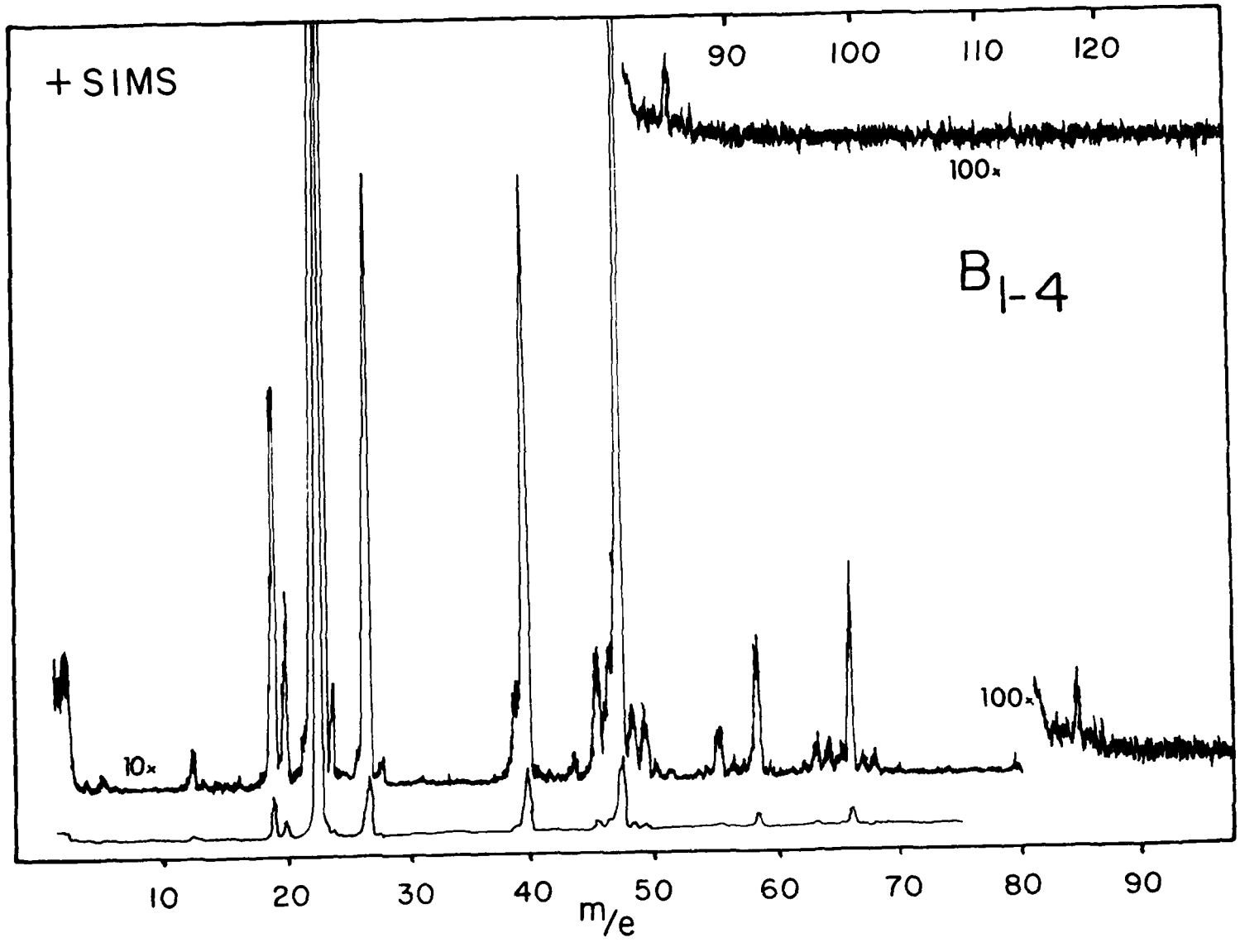

FIG. 28 Positive ion SIMS spectra of Ti-8Al-1Mo-1Sn subjected to 1-4 treatment

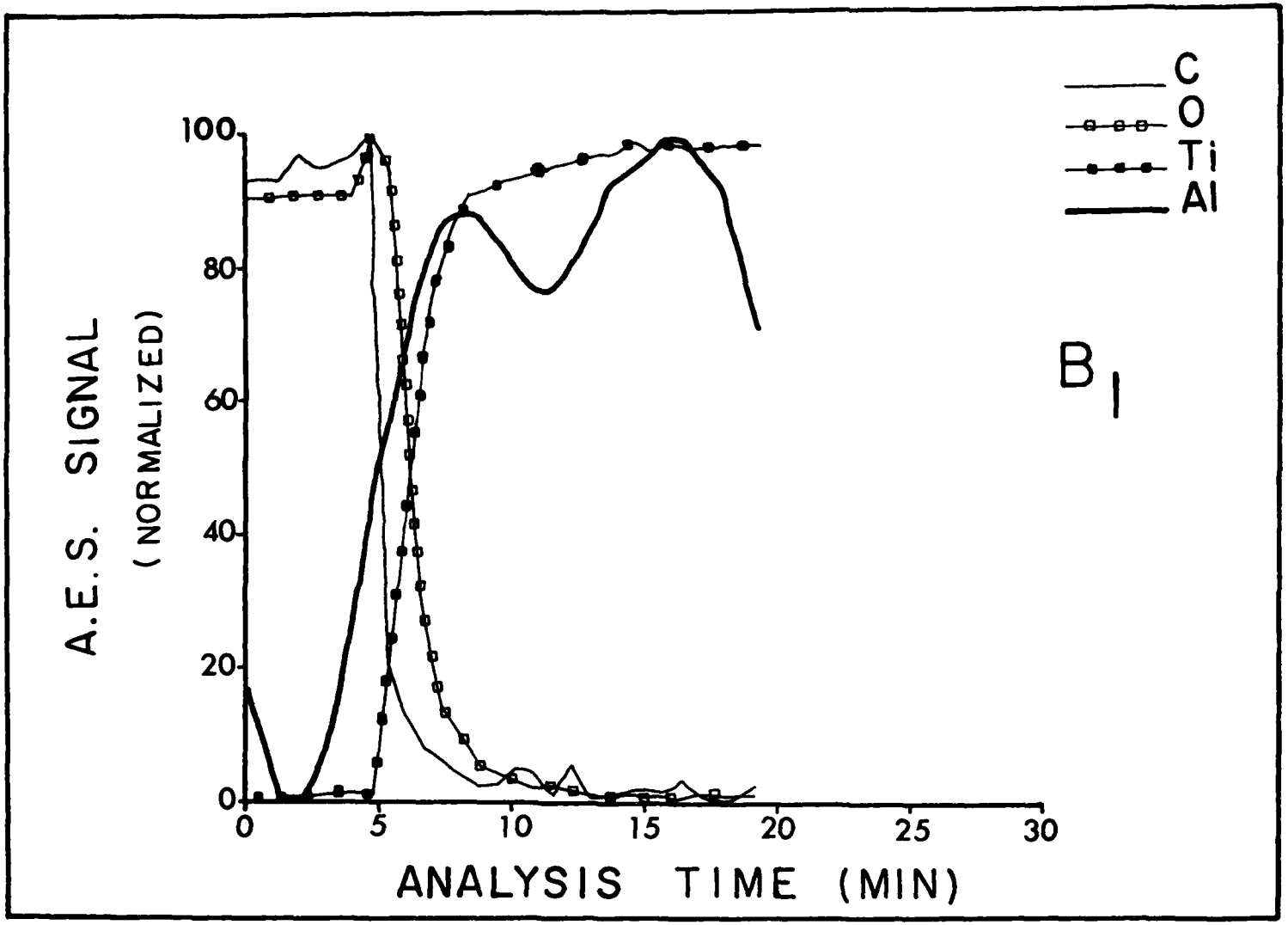

FIG. 29 A.E.S. sputter profiles of Ti-8Al-1Mo-1Sn subjected to 1 treatment

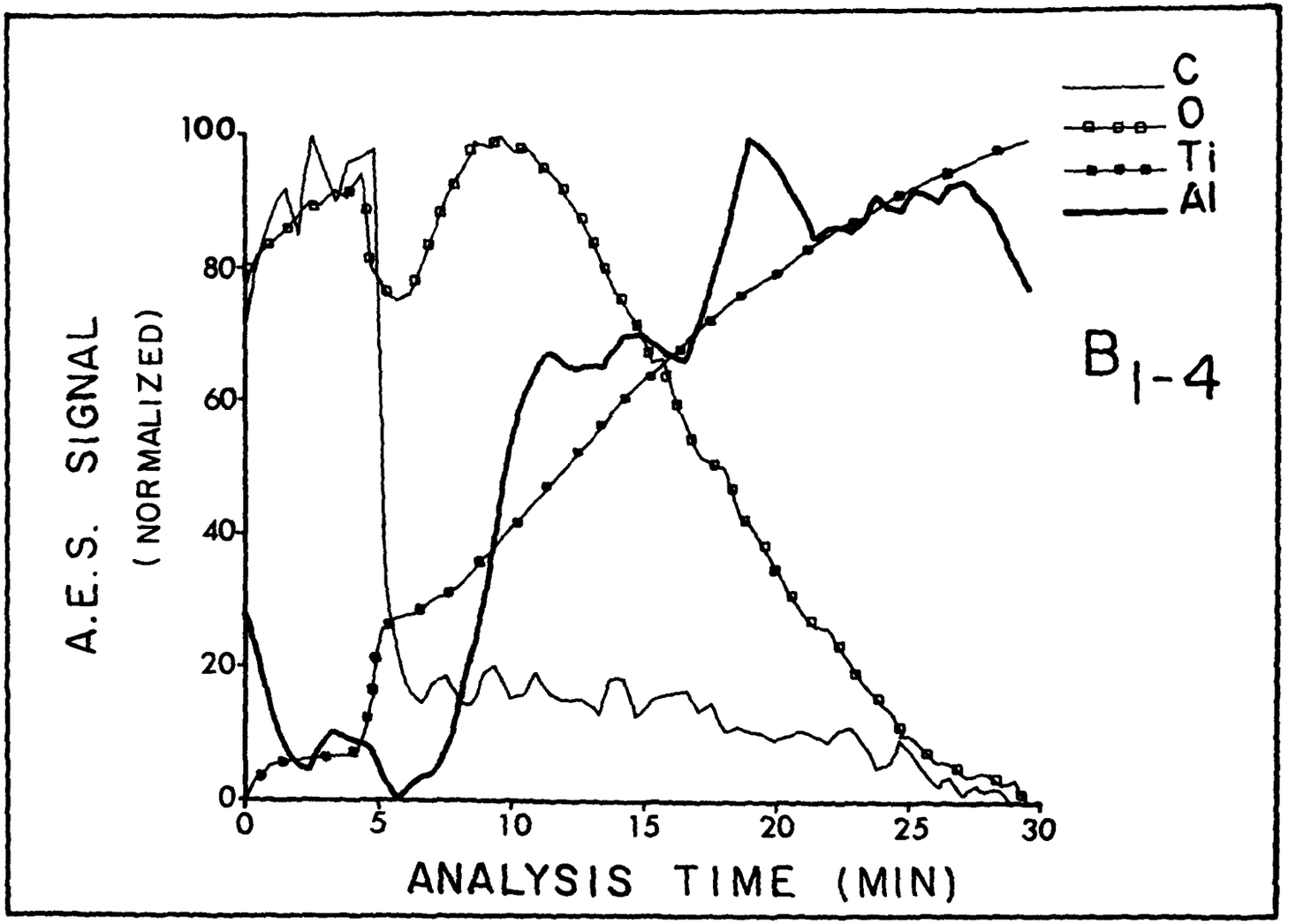

FIG. 30 A.E.S. sputter profiles of Ti-8Al-1Mo-1Sn subjected to 1-4 treatment

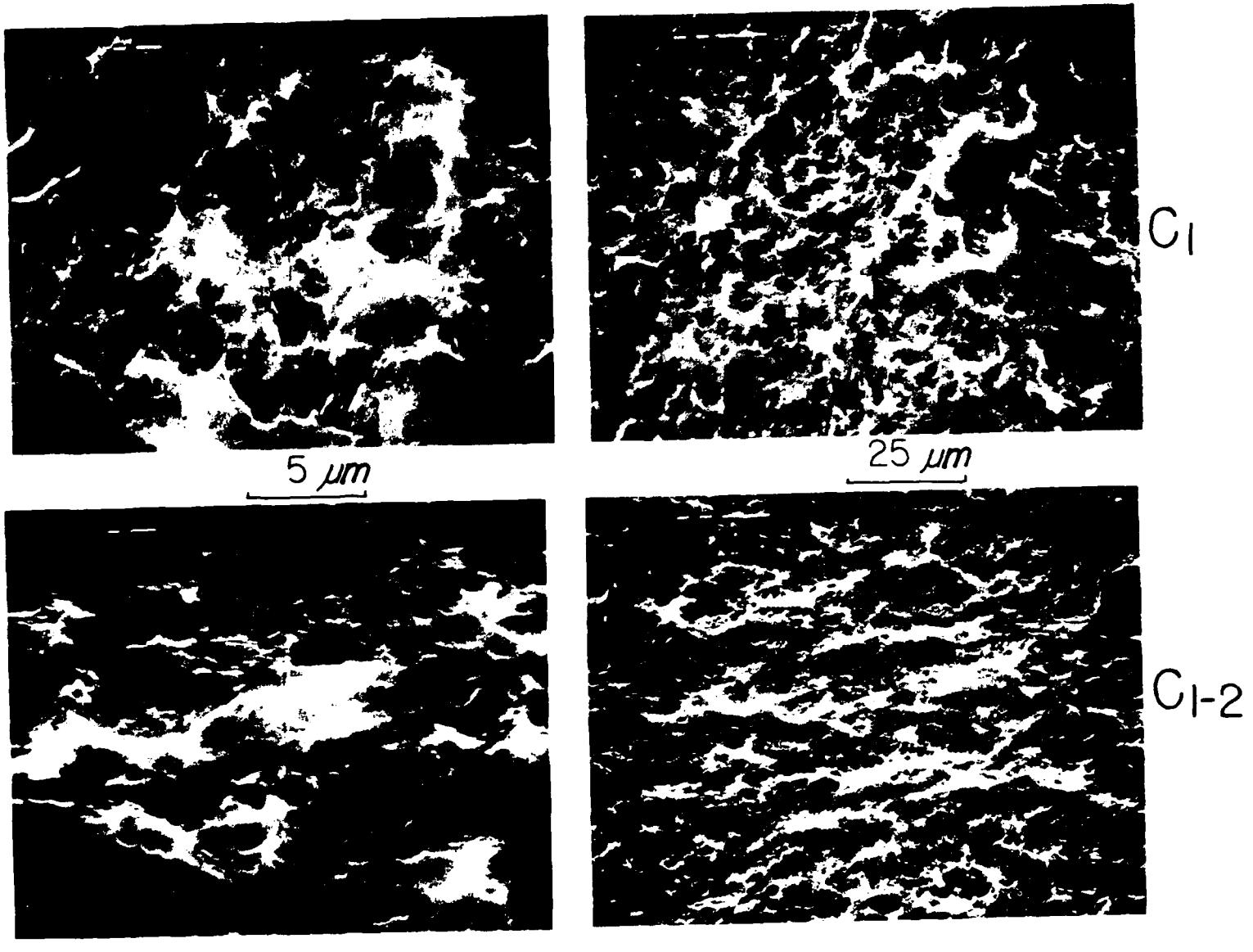

FIG. 31 S.E.M. photomicrographs of Ti-6Al-4V subjected to 1 and 1-2 treatments

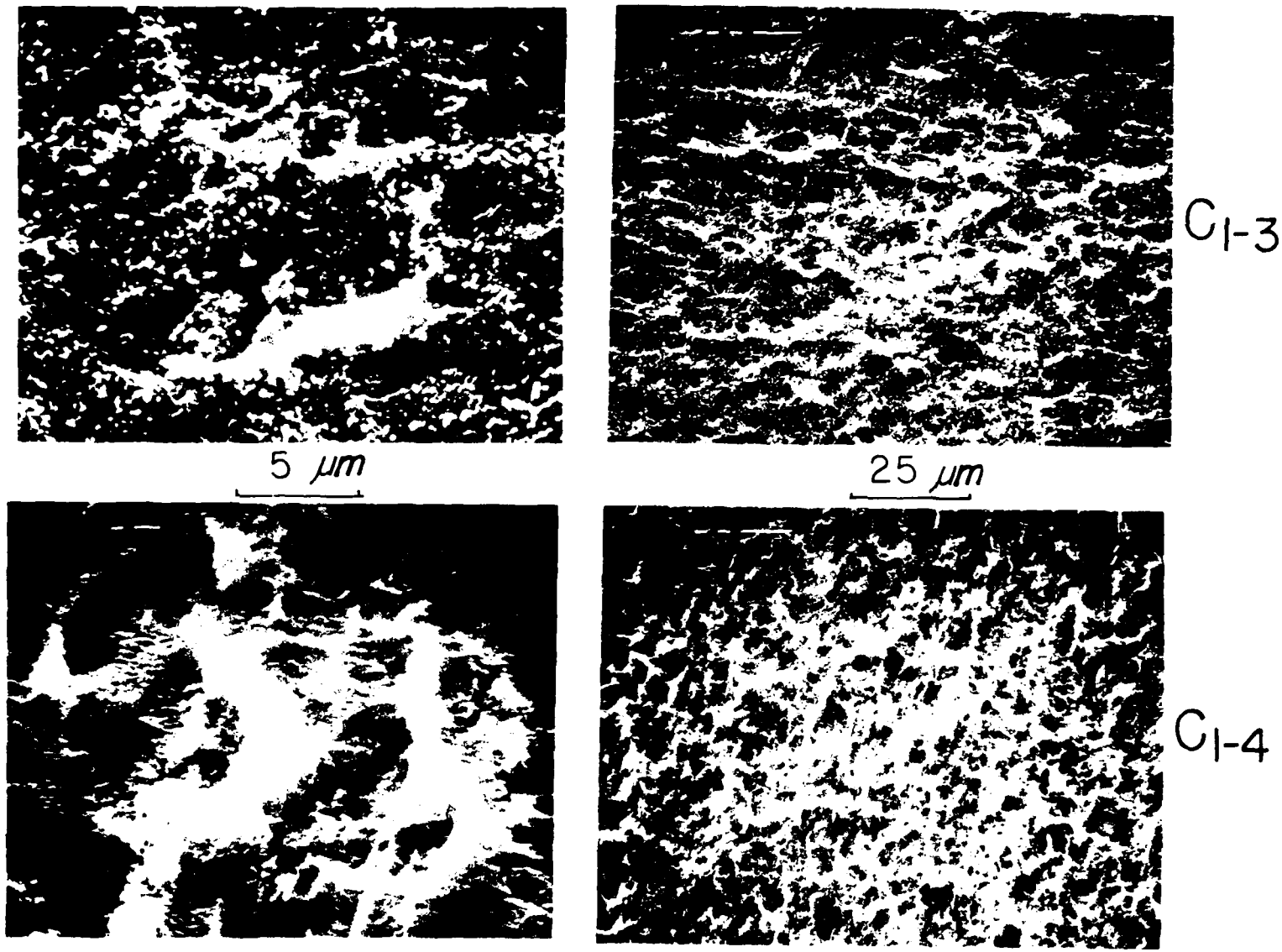

FIG. 32 S.E.M. photomicrographs of Ti-6Al-4V subjected to 1-3 and 1-4 treatments

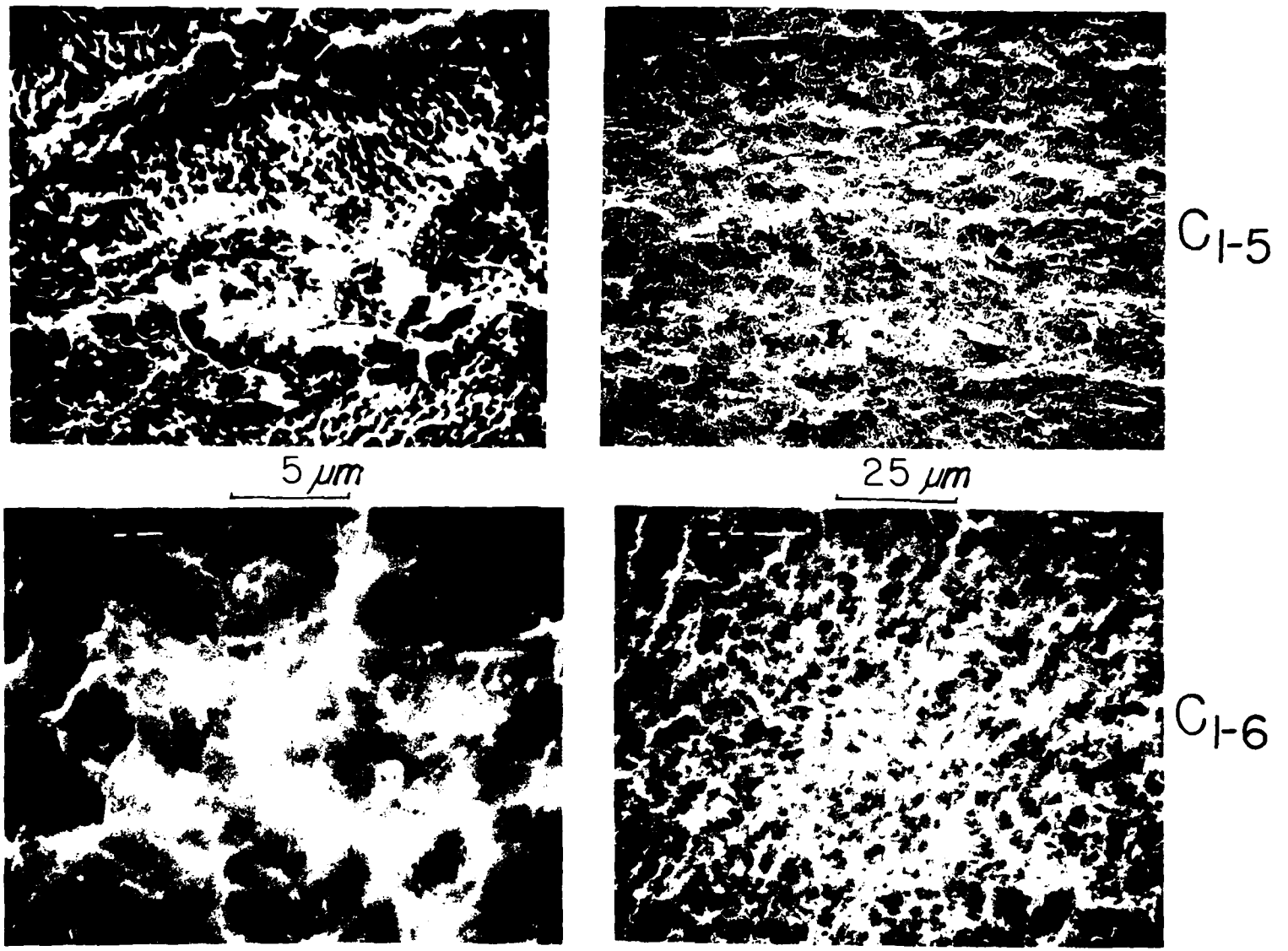

FIG. 33 S.E.M. photomicrographs of Ti-6Al-4V subjected to 1-5 and 1-6 treatments

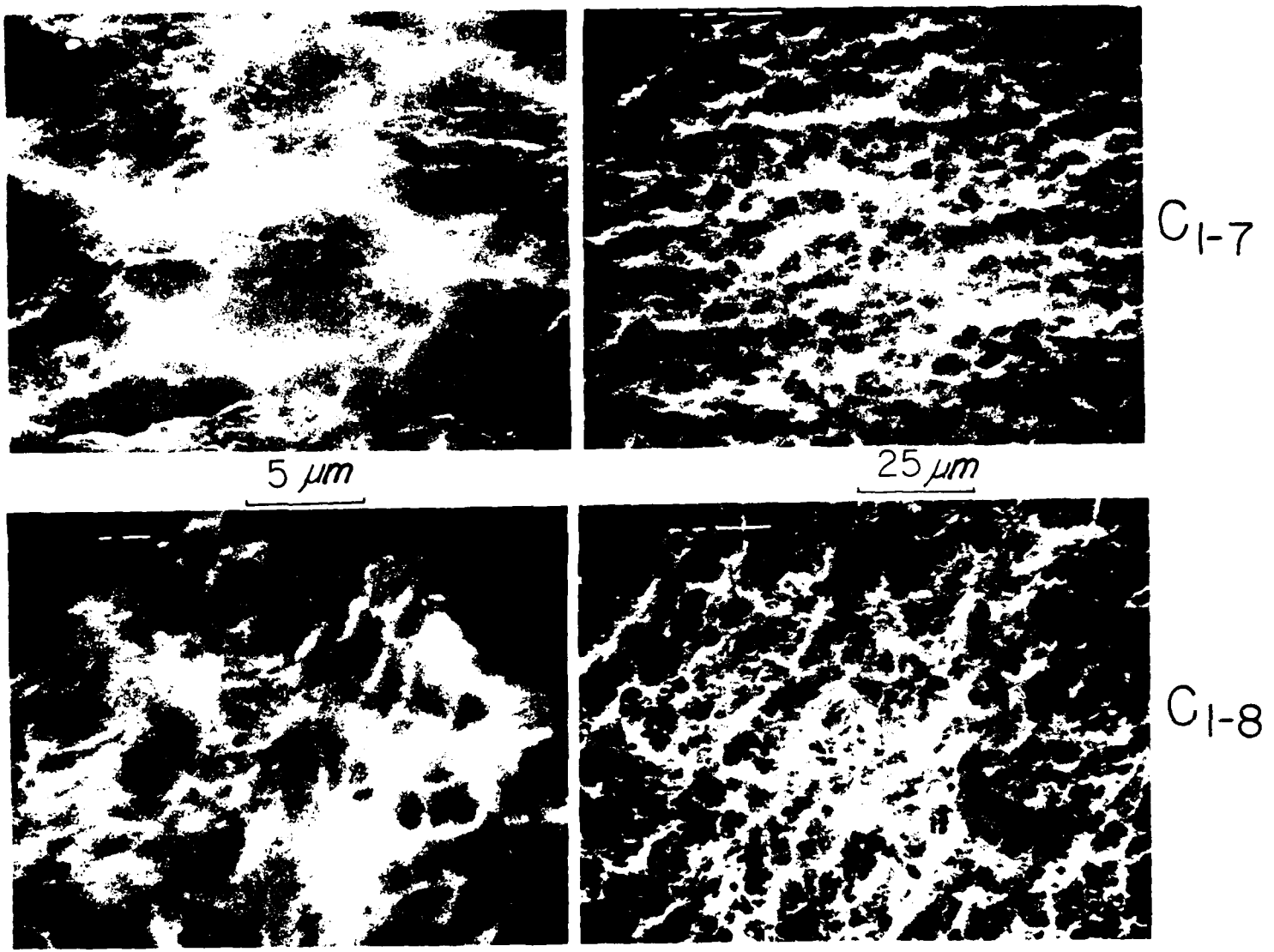

FIG. 34 S.E.M. photomicrographs of Ti-6Al-4V subjected to 1-7 and 1-8 treatments

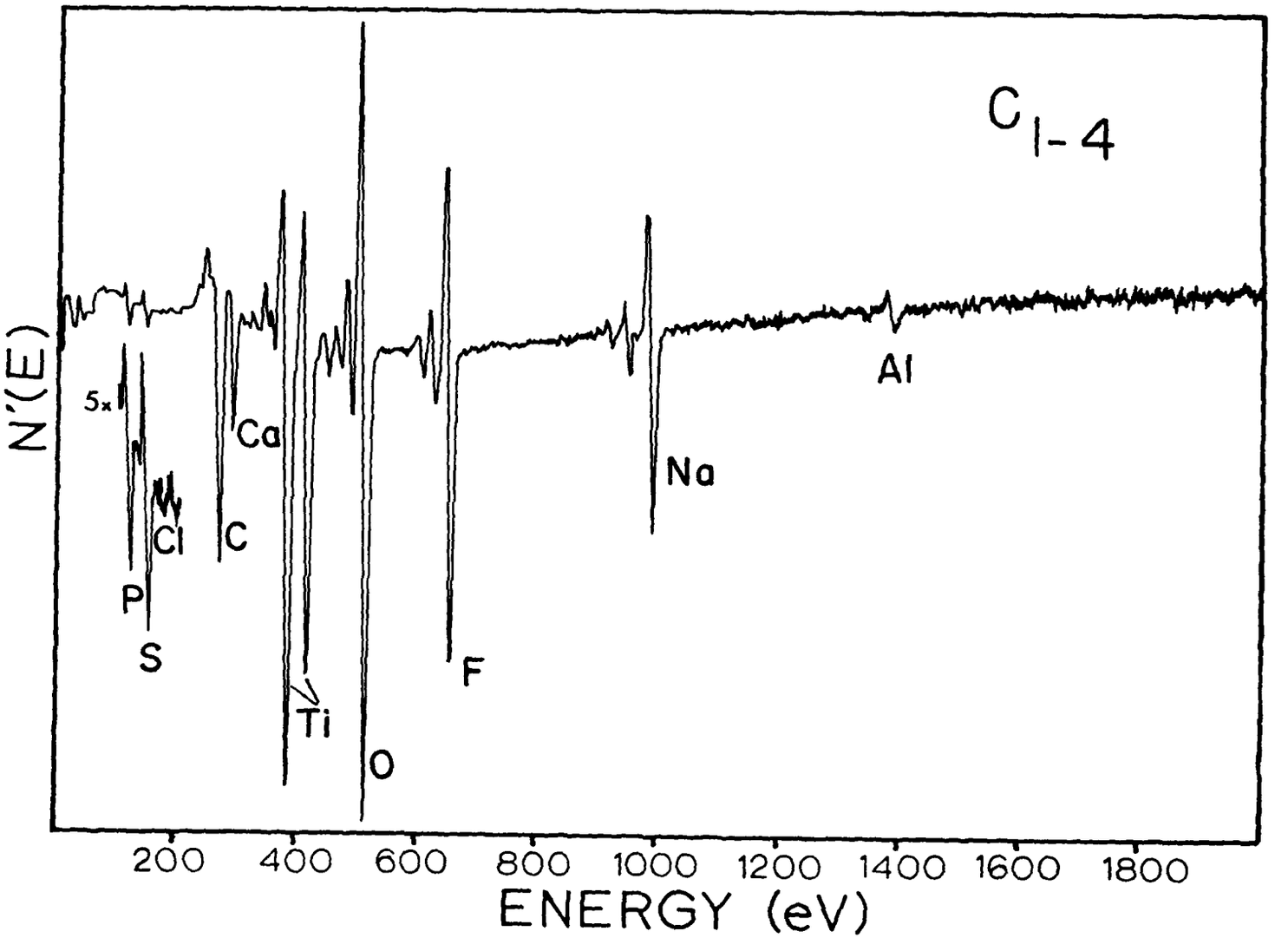

FIG. 35 A.E.S. spectra of Ti-6Al-4V subjected to I-4 treatment (0-2000 eV)

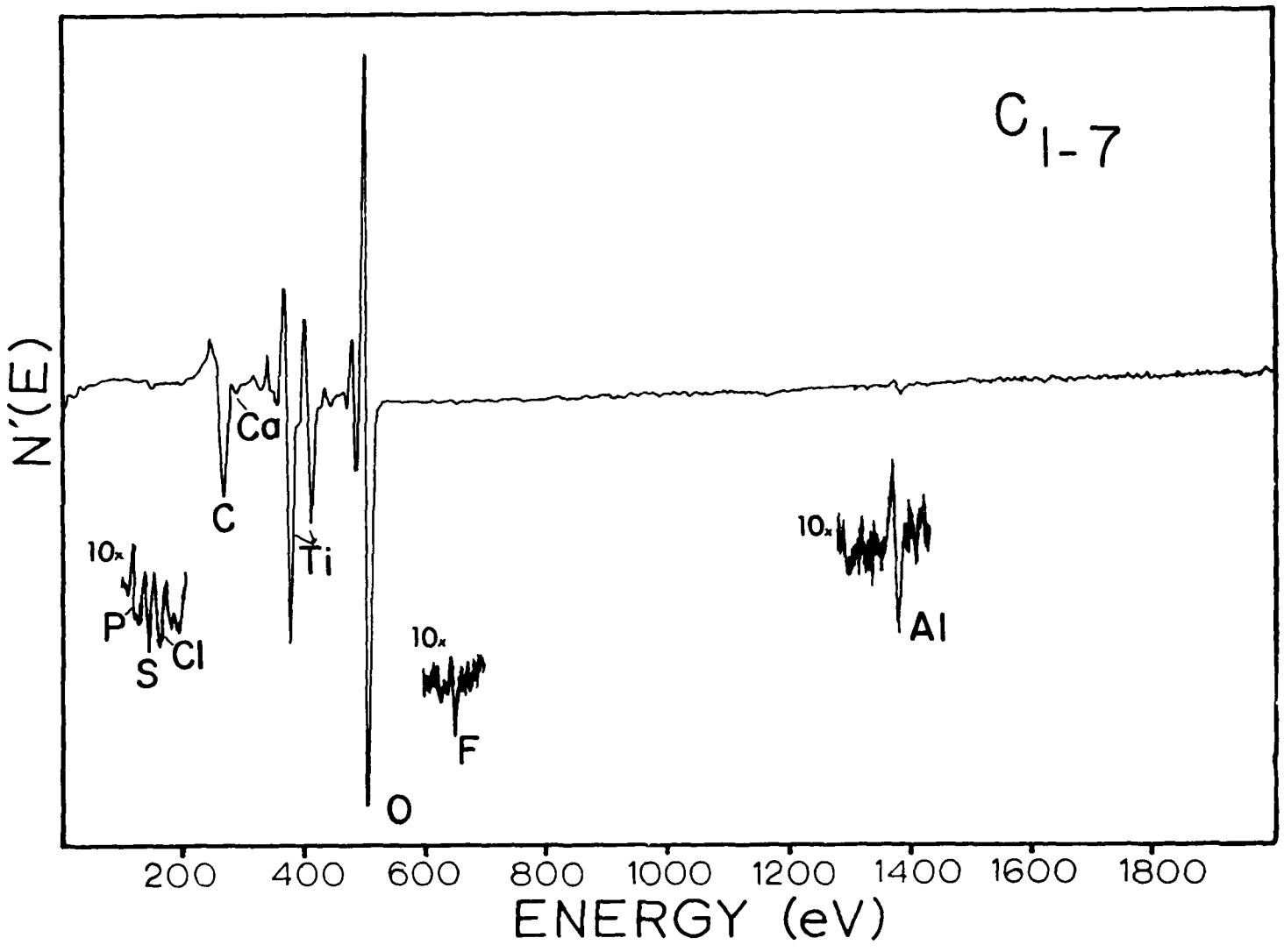

FIG. 36 A.E.S. spectra of Ti-6Al-4V subjected to 1-7 treatment (0-2000 eV)

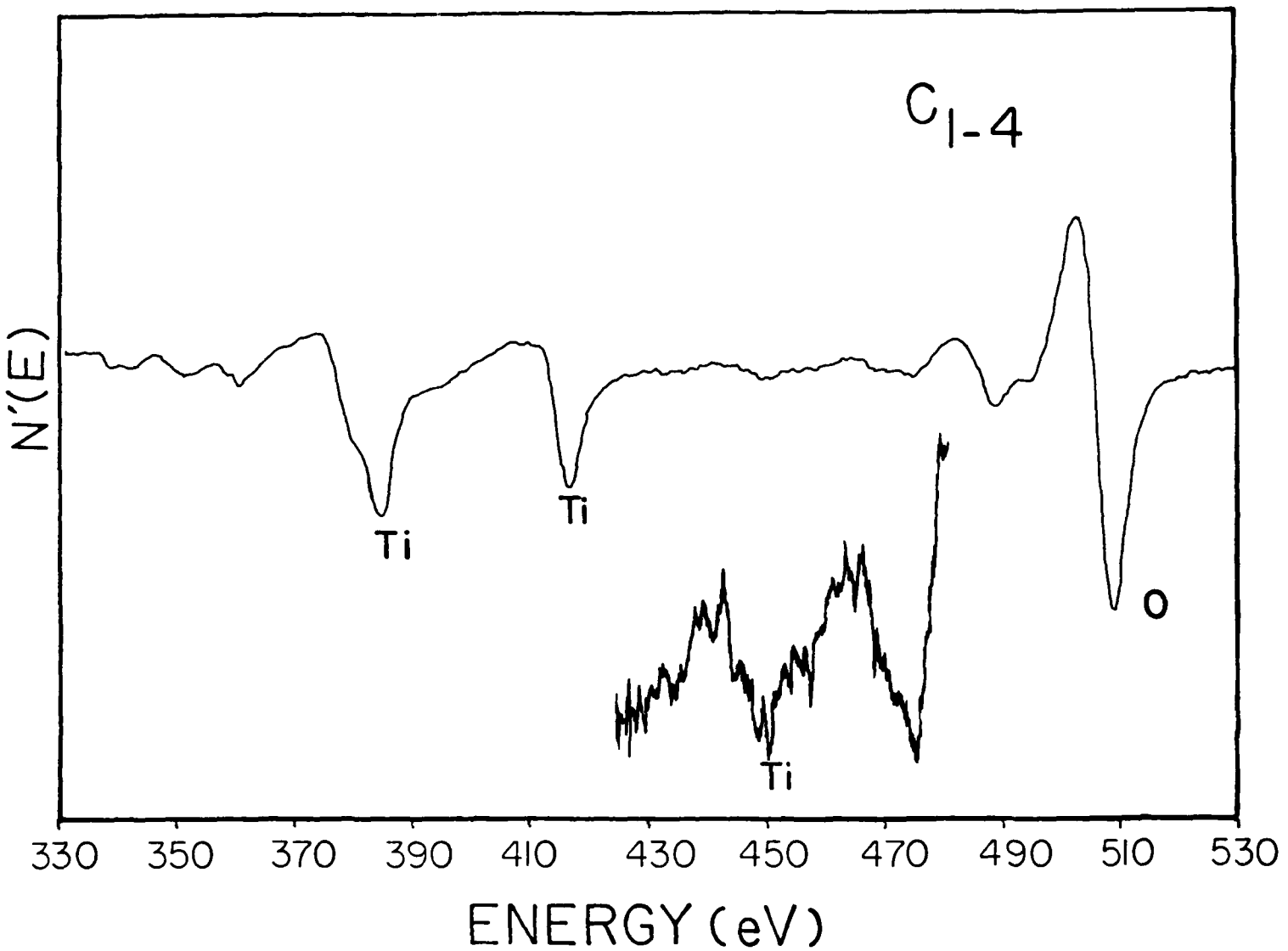

FIG. 37 A.E.S. spectra of Ti-6Al-4V subjected to 1-4 treatment (330-530 eV)

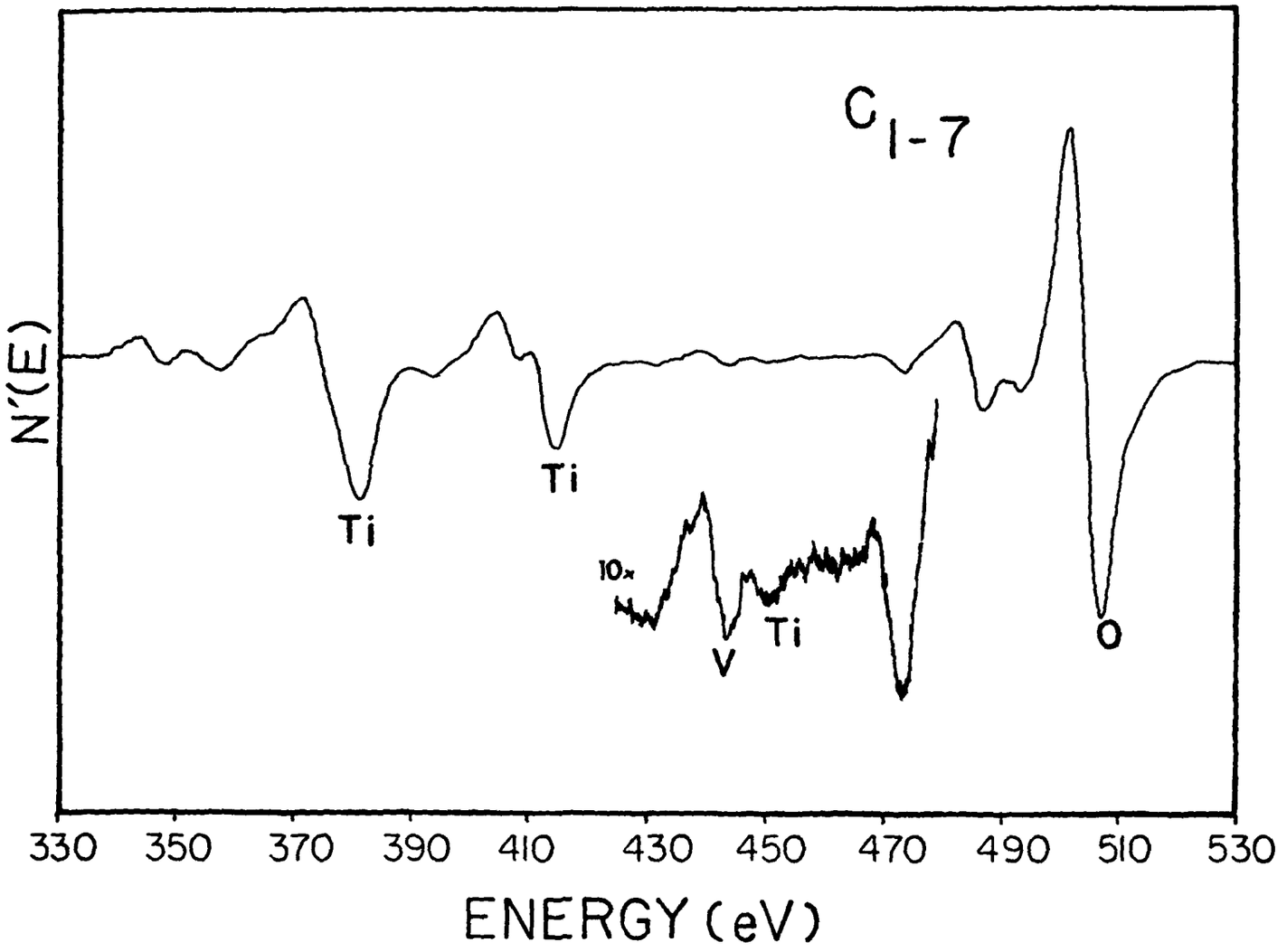

FIG. 38 A.E.S. spectra of Ti-6Al-4V subjected to 1-7 treatment (330-530 eV)

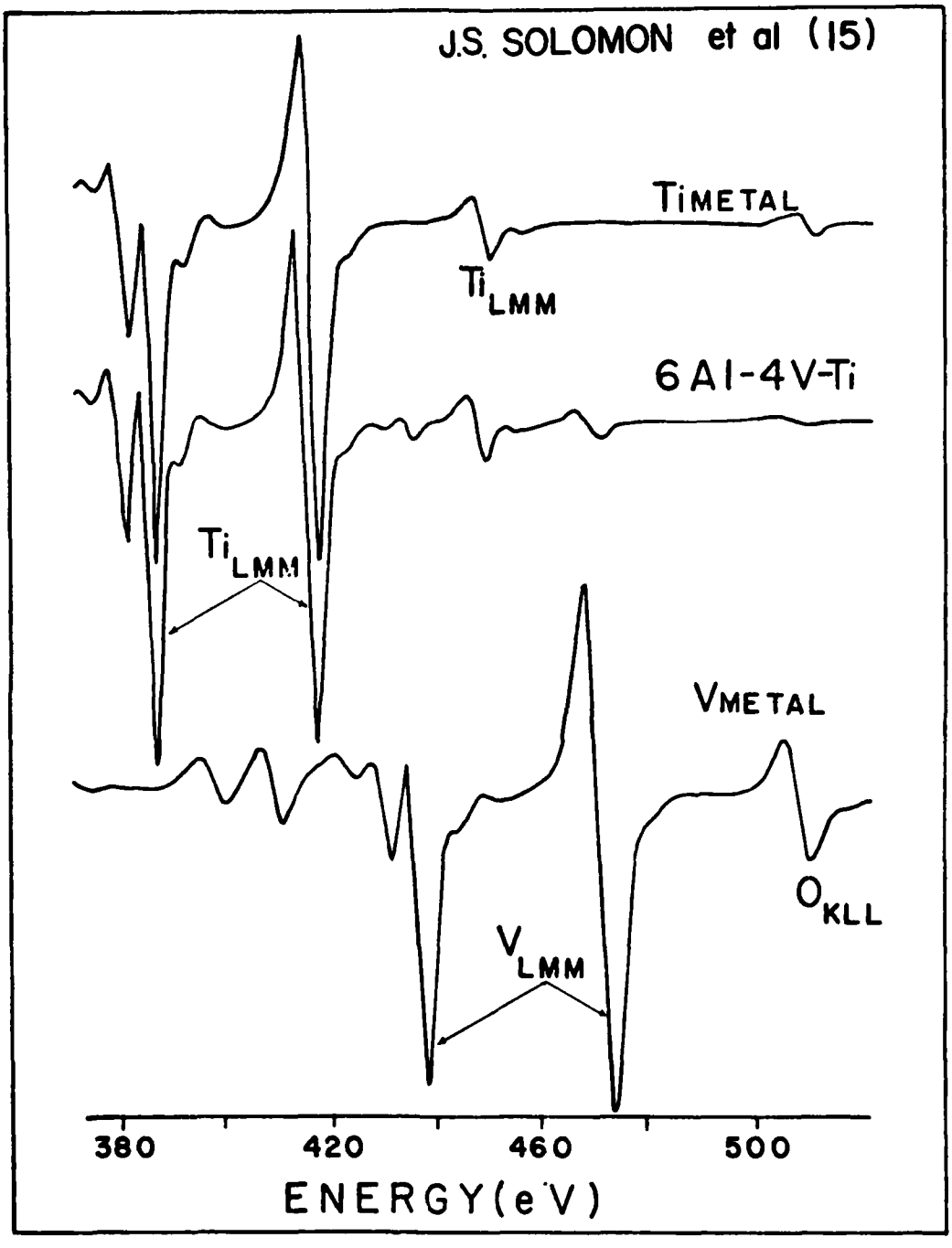

FIG. 39 A.E.S. spectra of titanium (c.p.) metal, vanadium metal and Ti-6Al-4V by J.S. Solomon et.al. (Ref. 15)

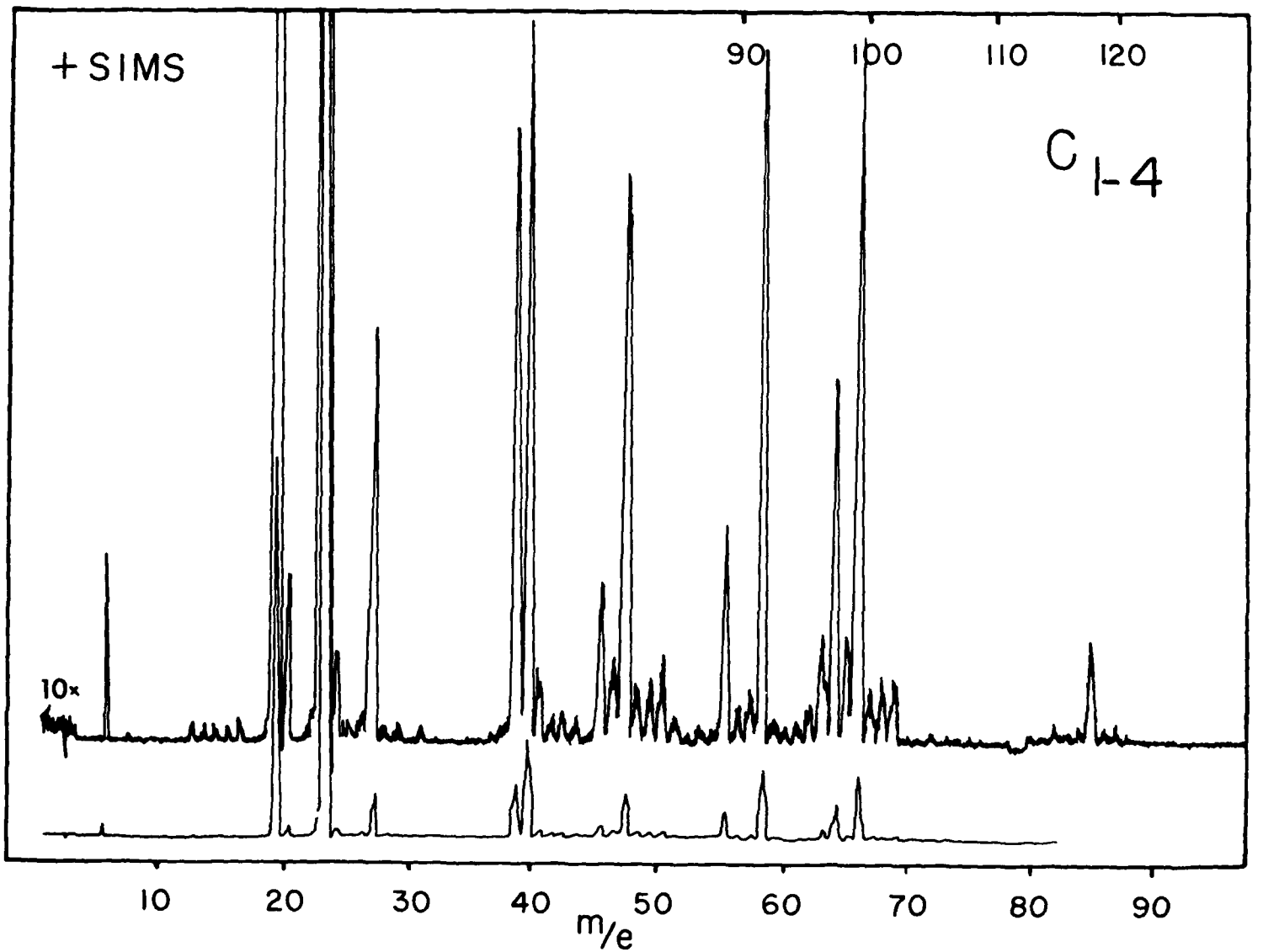

FIG. 40 Positive ion SIMS spectra of Ti-6Al-4V subjected to 1-4 treatment

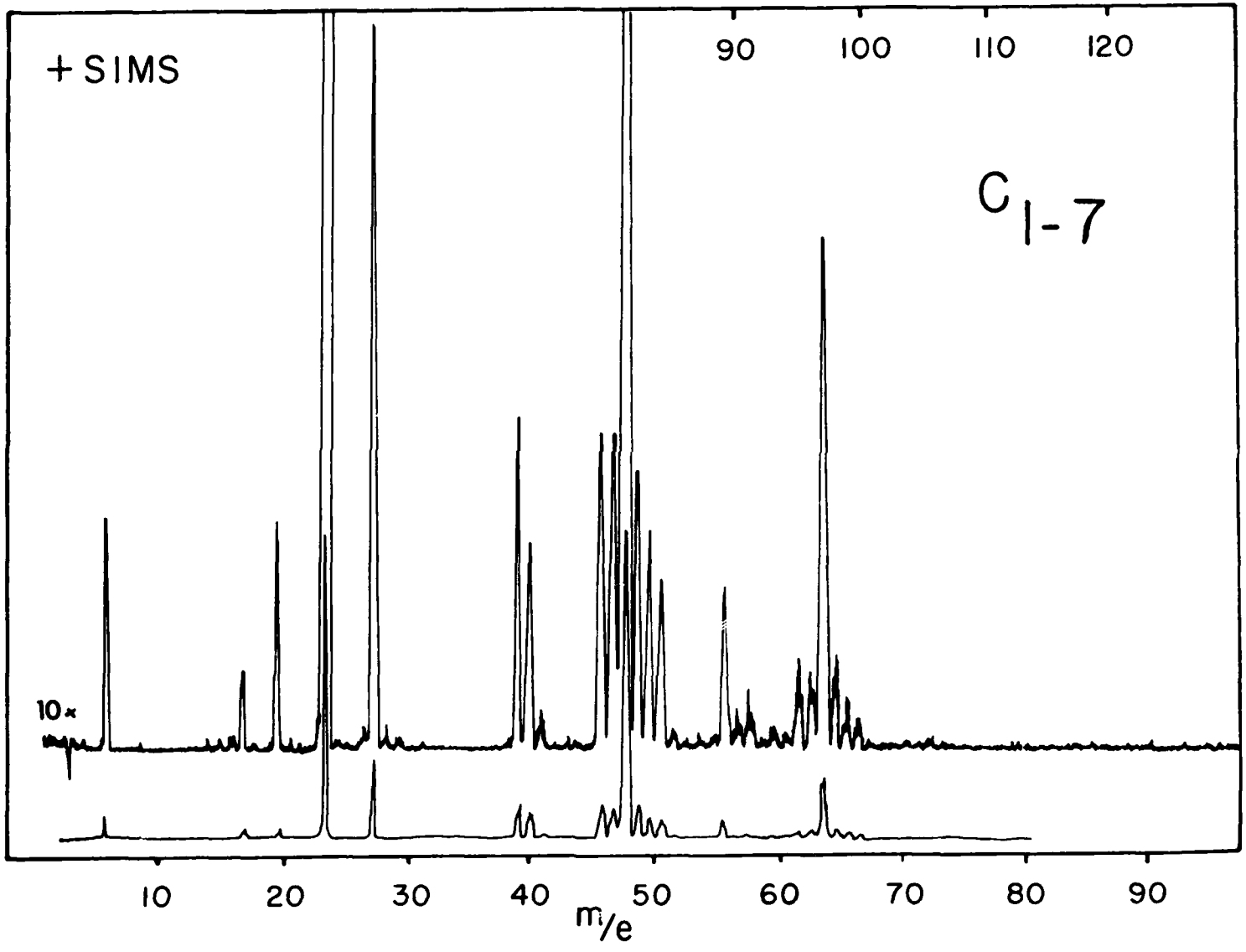

FIG. 41 Positive ion SIMS spectra of Ti-6Al-4V subjected to 1-7 treatment

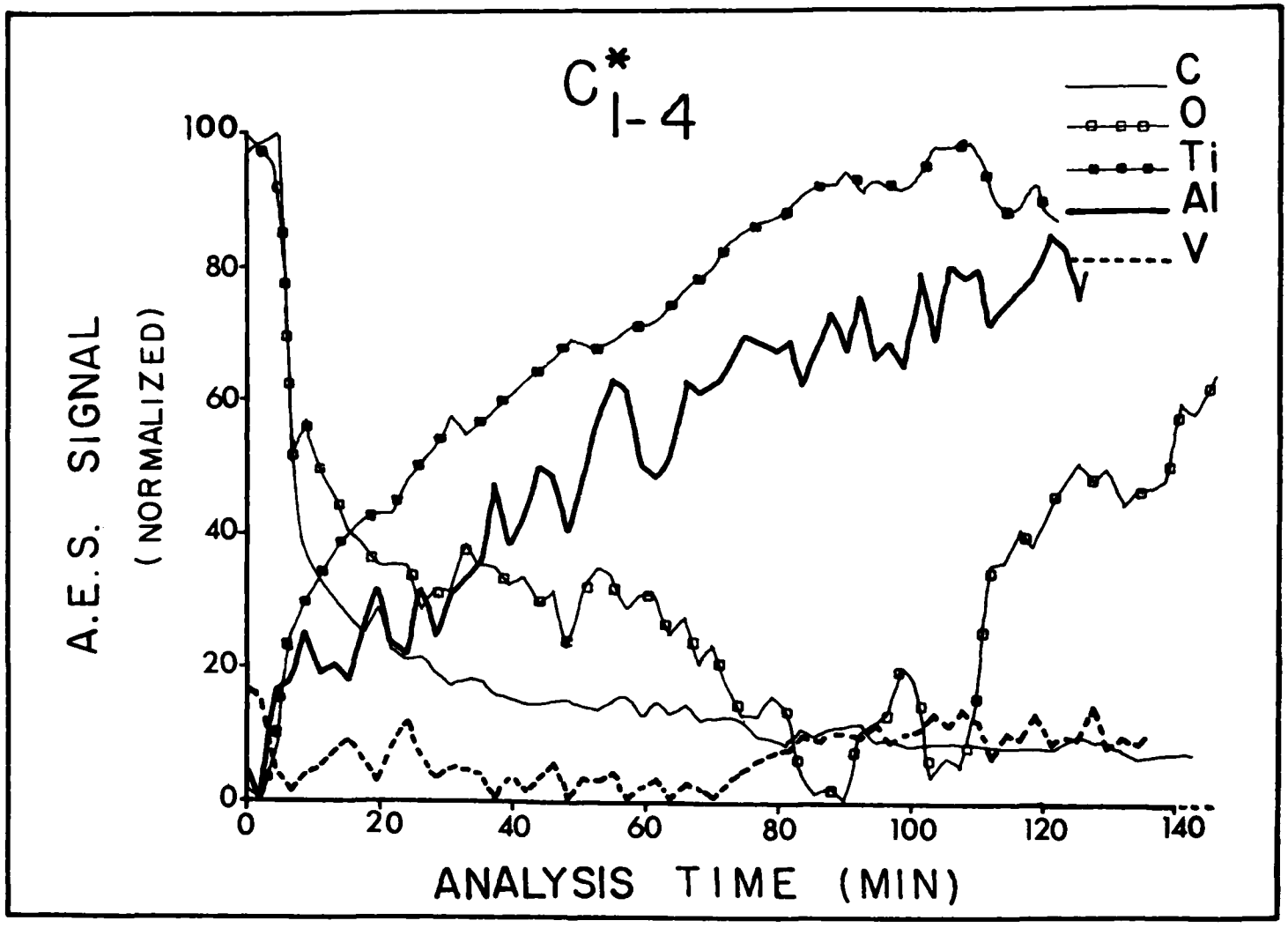

FIG. 42 A.E.S sputter profiles of Ti-6Al-4V subjected to 1-4 treatment

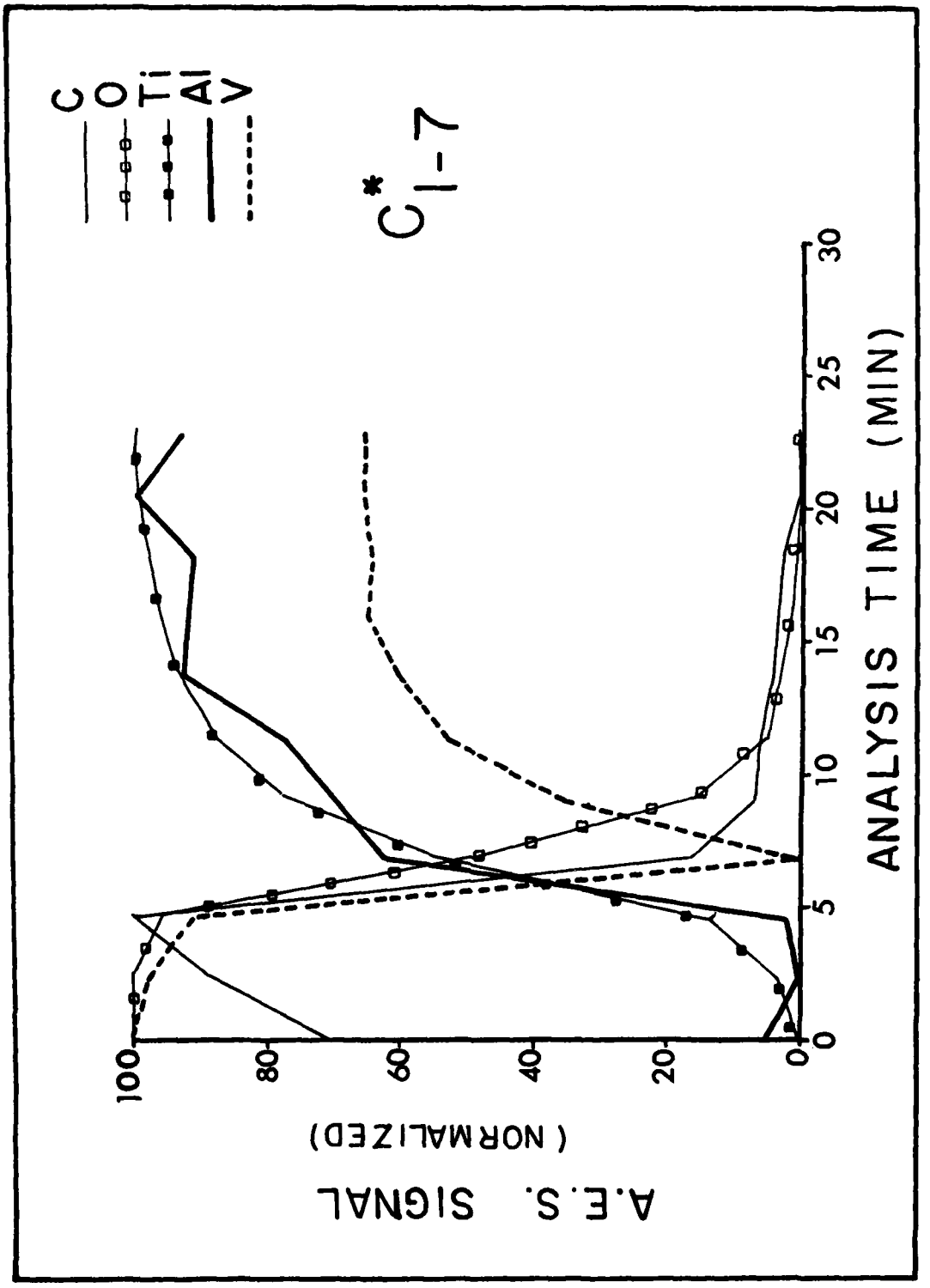

FIG. 43 A.E.S. sputter profiles of Ti-6Al-4V subjected to 1-7 treatment

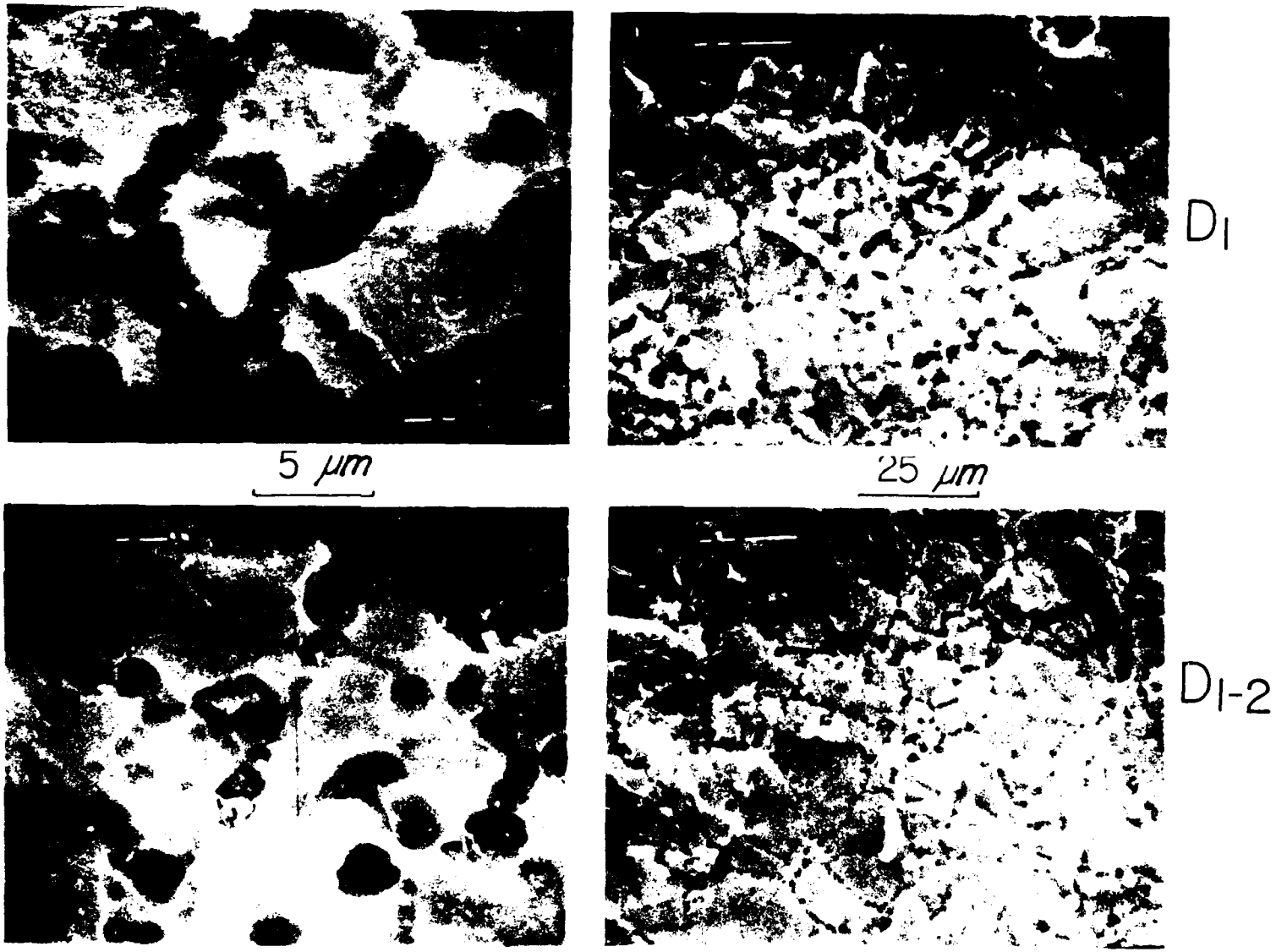

FIG. 44 S.E.M. photomicrographs of Ti-5Al-2.5Sn subjected to 1 and 1-2 treatments

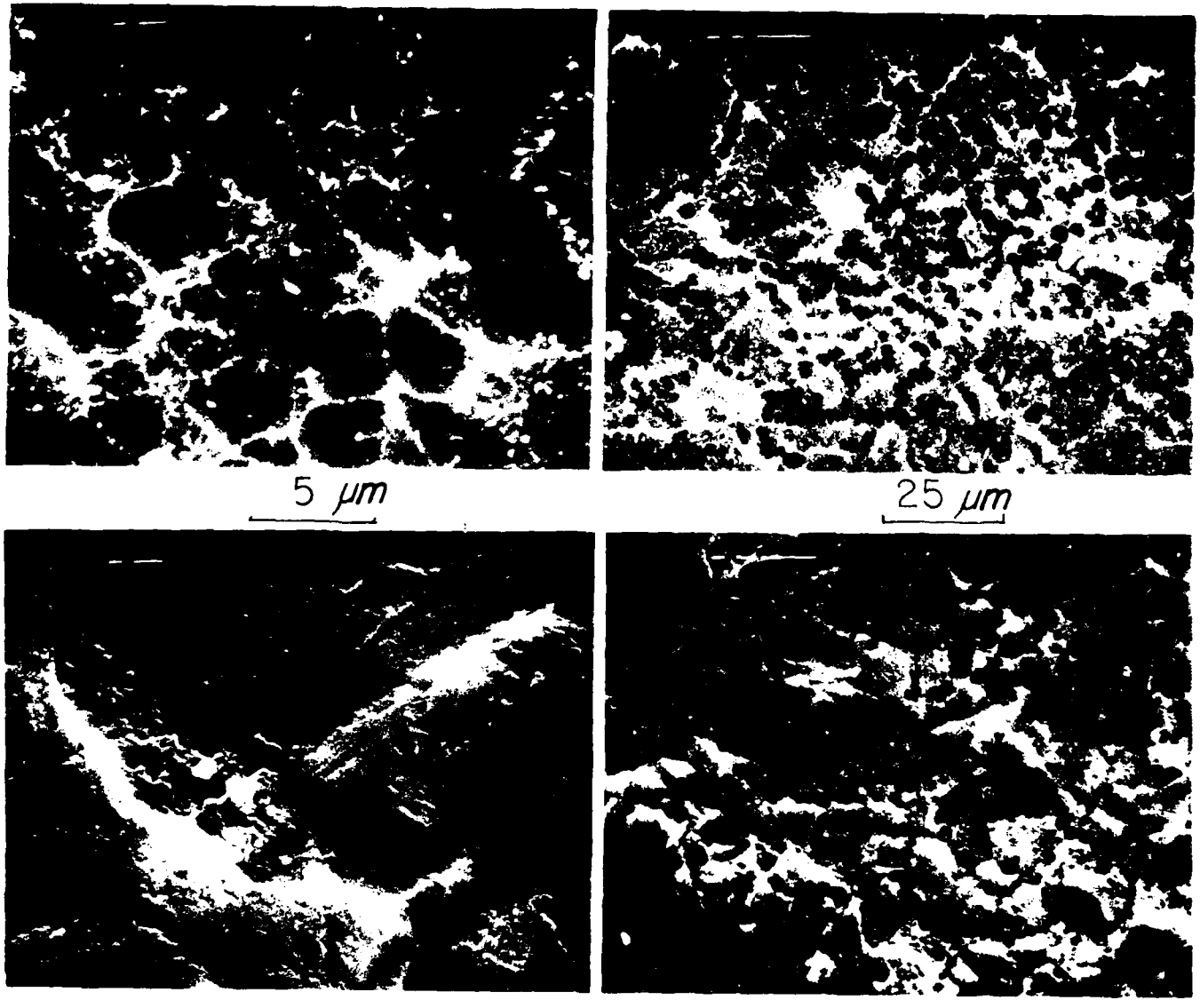

FIG. 45 S.E.M. photomicrographs of Ti-5Al-2.5Sn subjected to 1-3 and 1-4 treatments

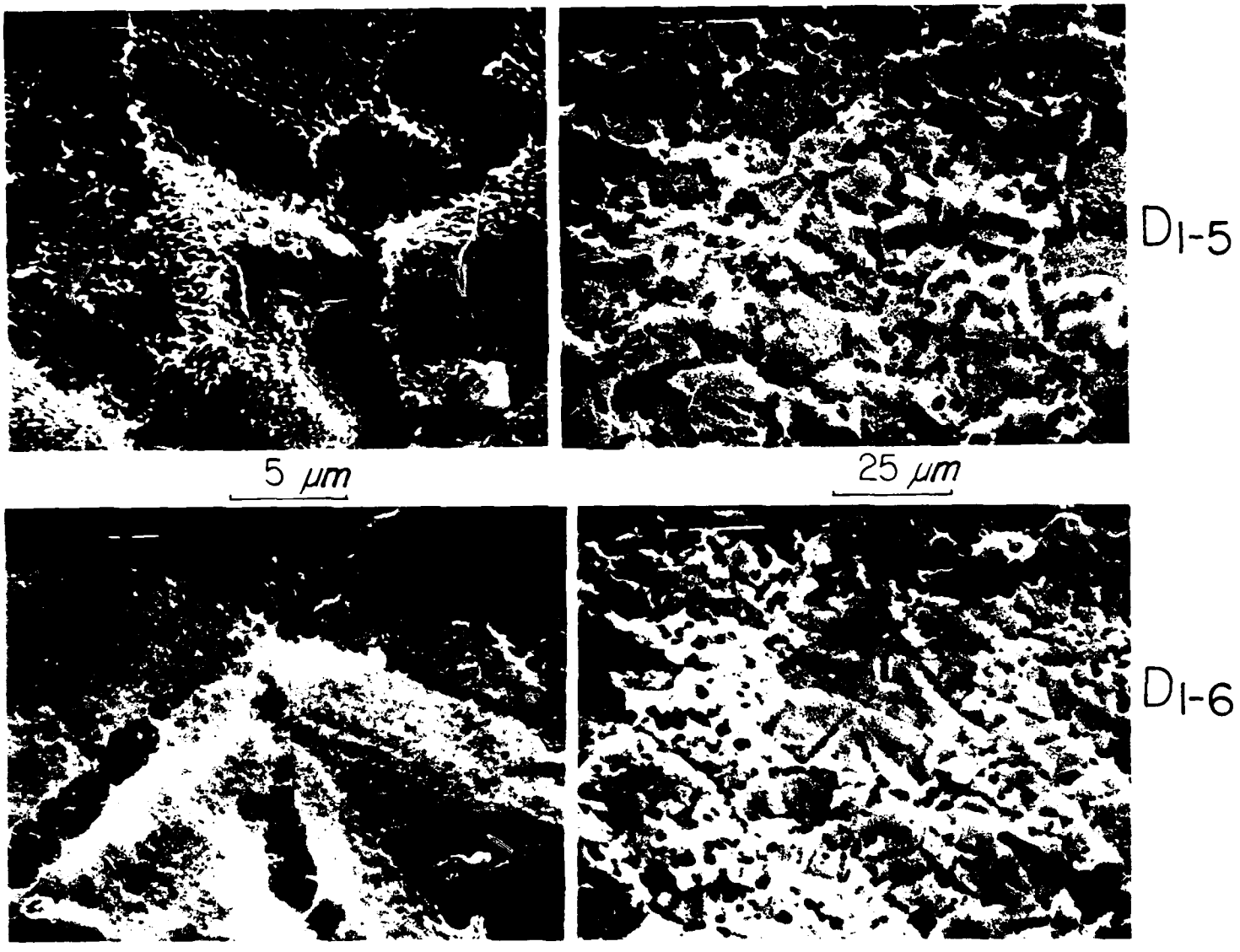

FIG. 46 S.E.M. photomicrographs of Ti-5Al-2.5Sn subjected to 1-5 and 1-6 treatments

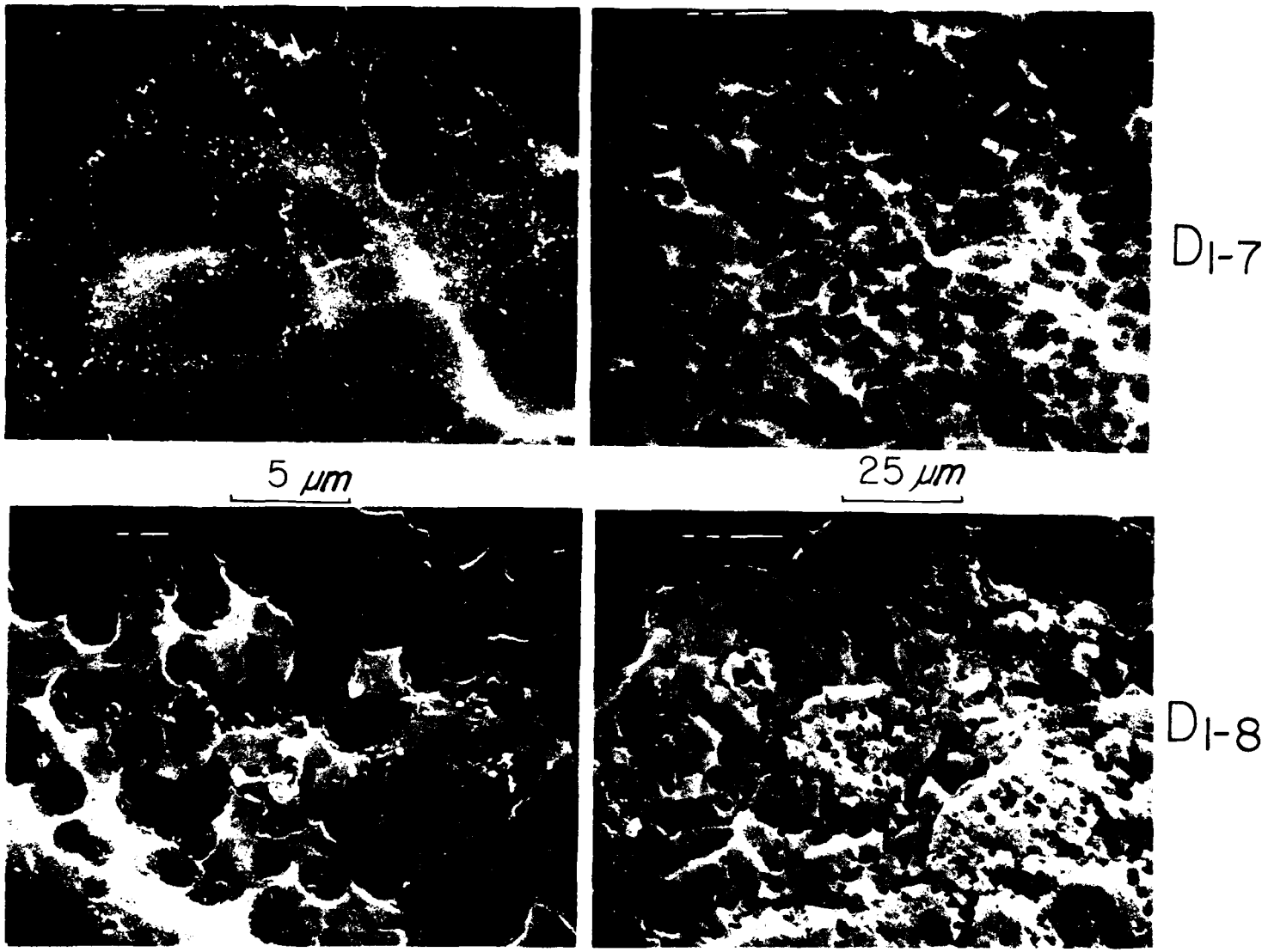

FIG. 47 S.E.M. photomicrographs of Ti-5Al-2.5Sn subjected to 1-7 and 1-8 treatments

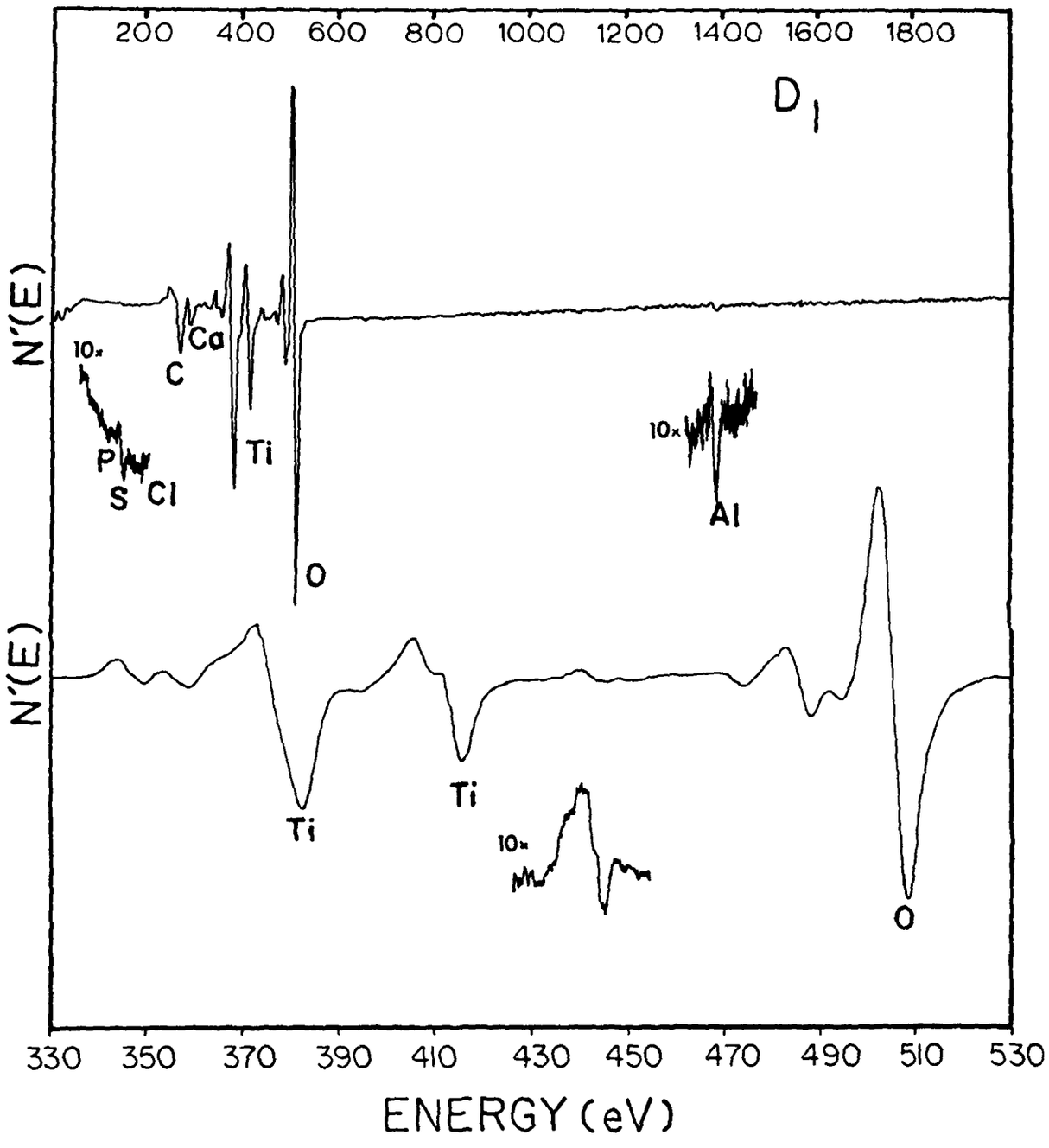

FIG. 48 A.E.S. spectra of Ti-5Al-2.5Sn subjected to 1 treatment (0-2000 eV and 330-530 eV)

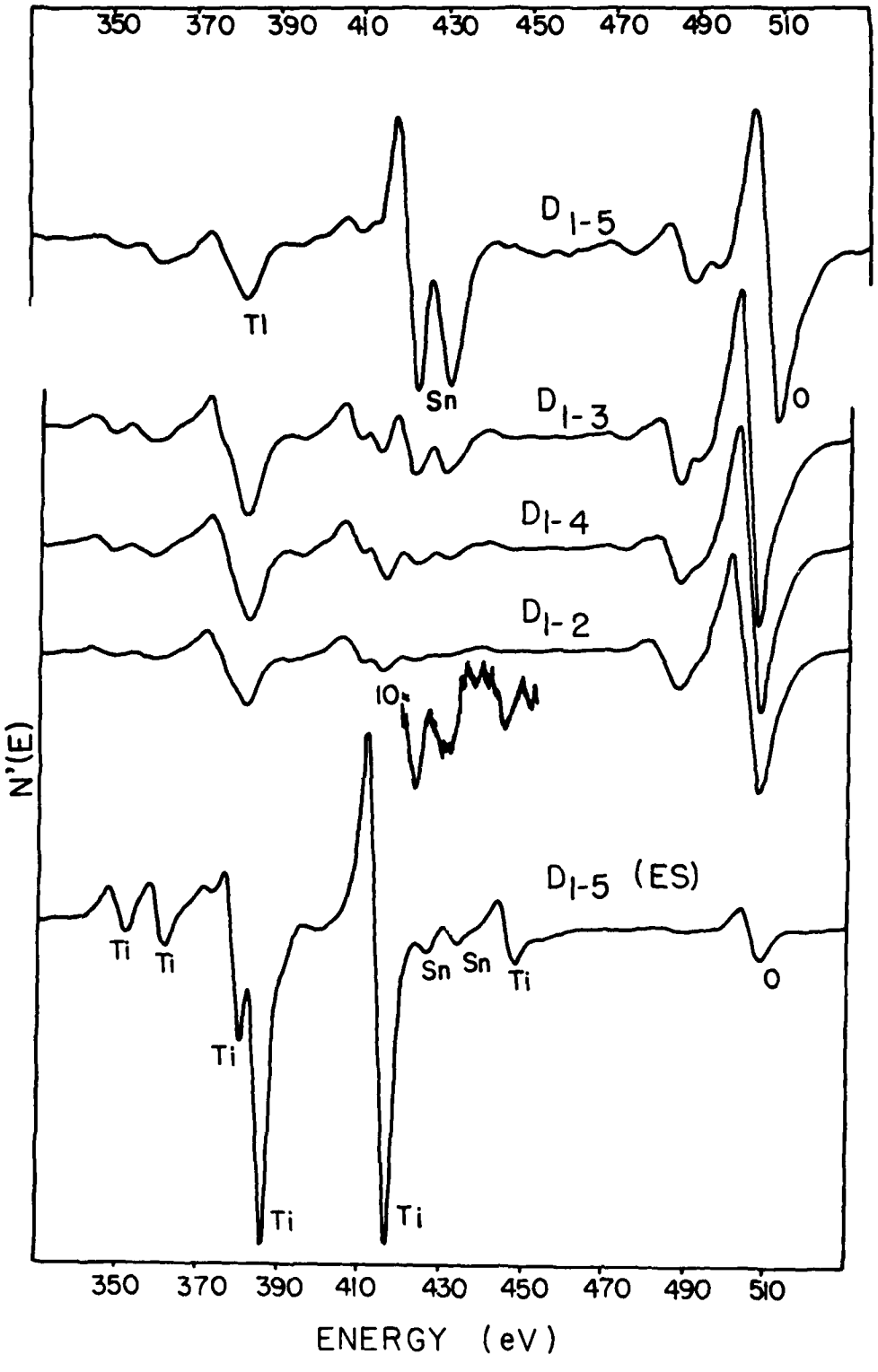

FIG. 49 A.E.S. spectra of Ti-5Al-2.5Sn subjected to 1-2, 1-3, 1-4, 1-5 treatments and Equilibrium Sputtered A.E.S. spectrum of Ti-5Al-2.5Sn (330 - 530 eV)

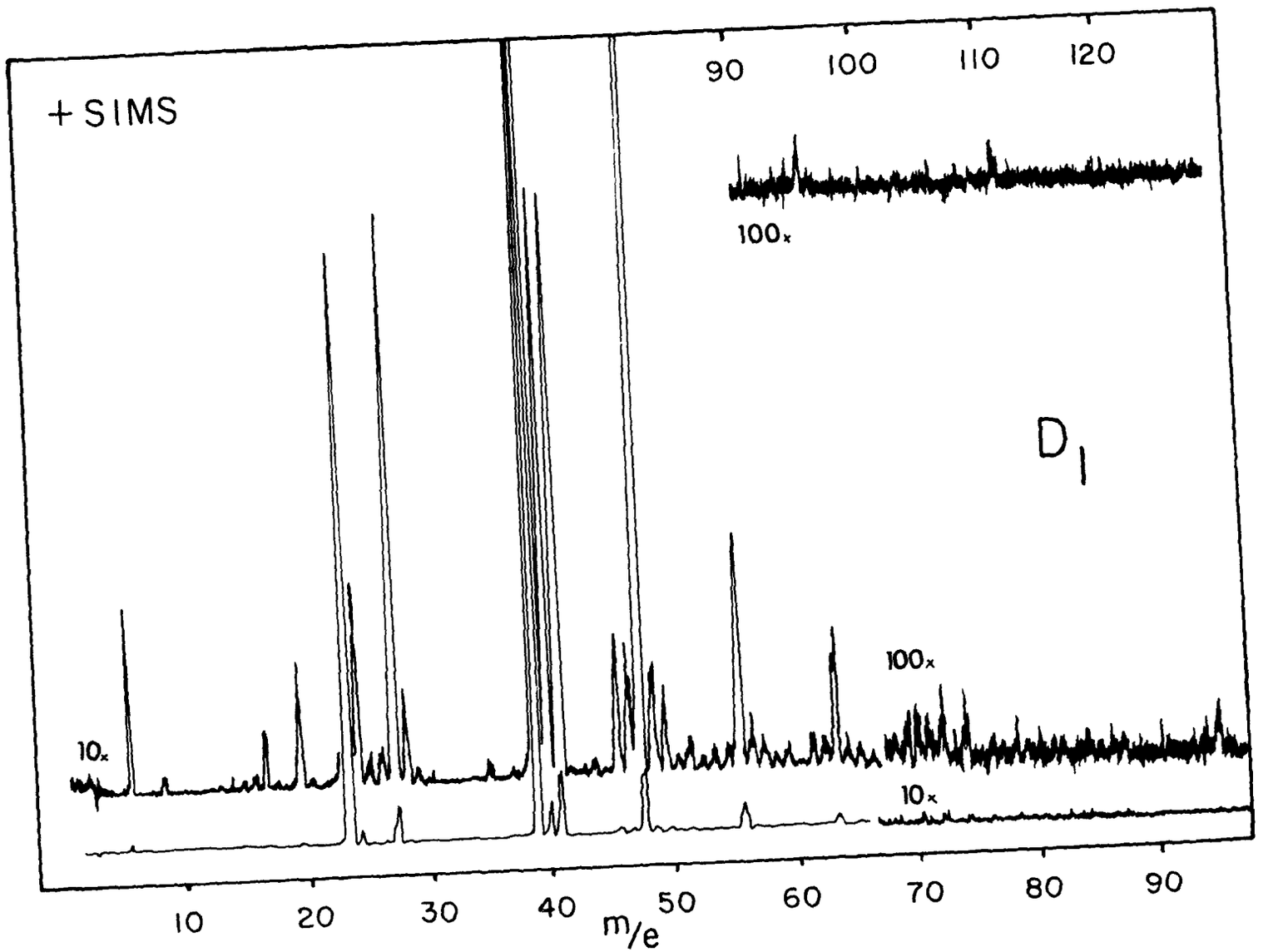

FIG. 50 Positive ion SIMS spectra of Ti-5Al-2.5Sn subjected to 1 treatment

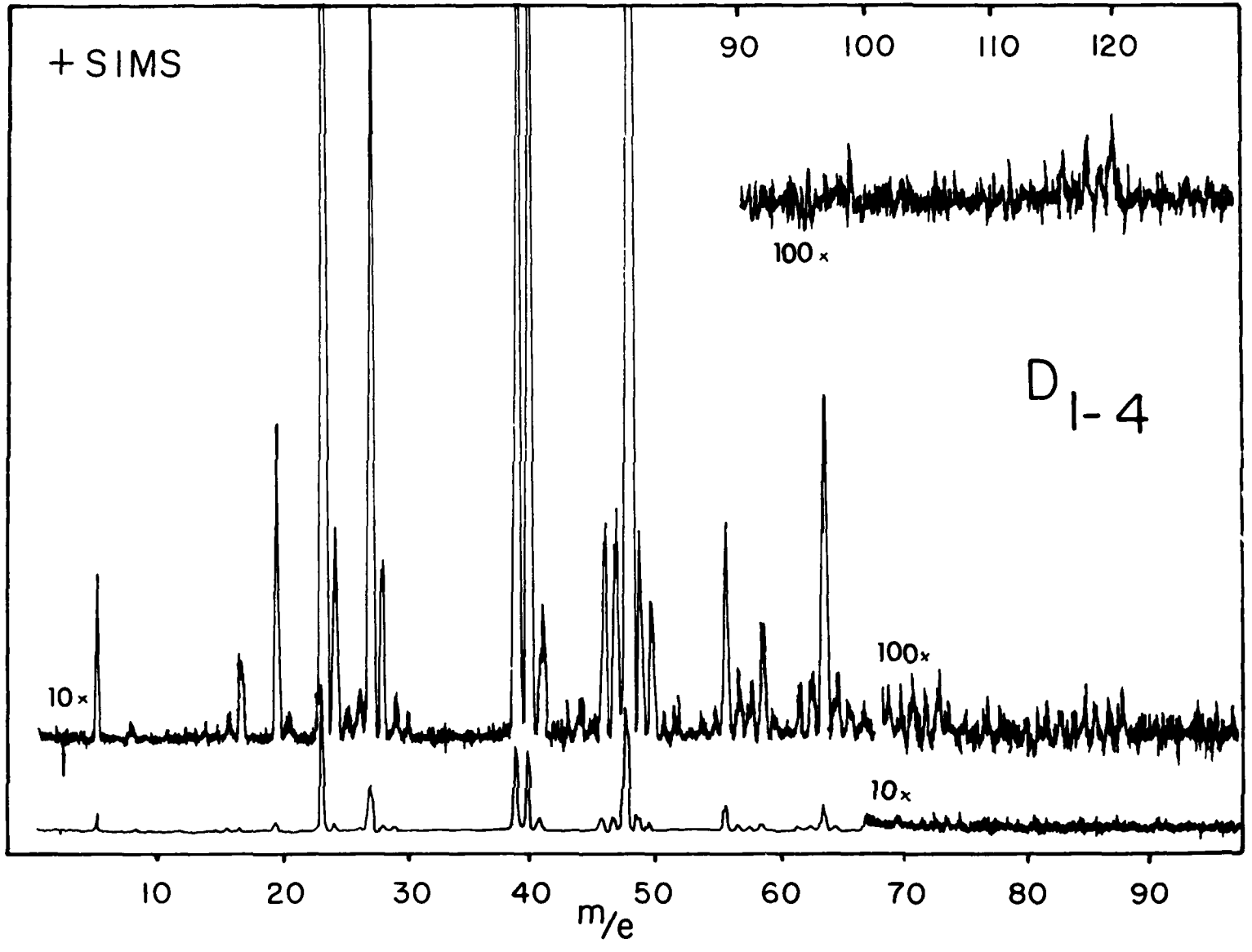

FIG. 51 Positive ion SIMS spectra of Ti-5Al-2.5Sn subjected to 1-4 treatment

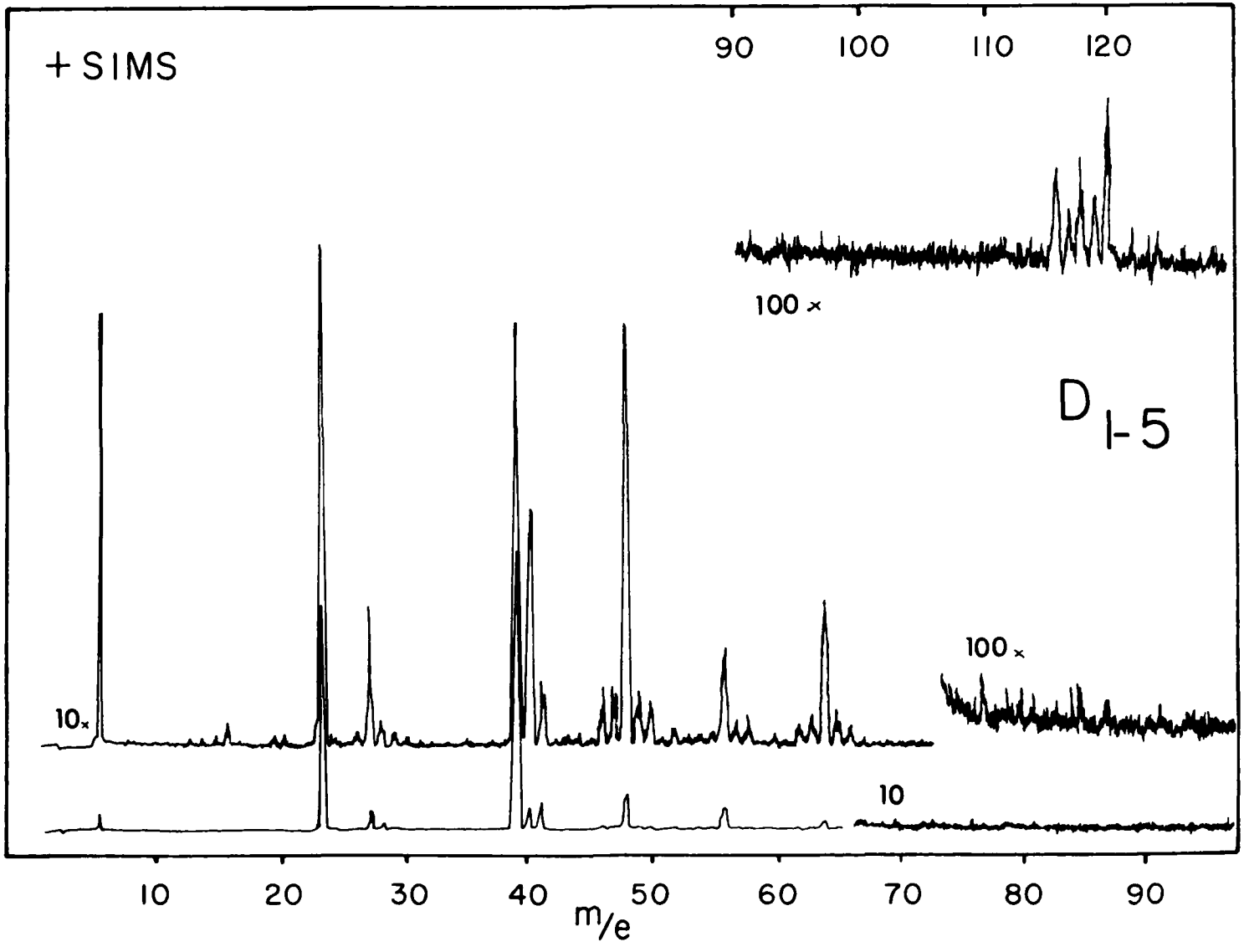

FIG. 52 Positive ion SIMS spectra of Ti-5Al-2.5Sn subjected to 1-5 treatment

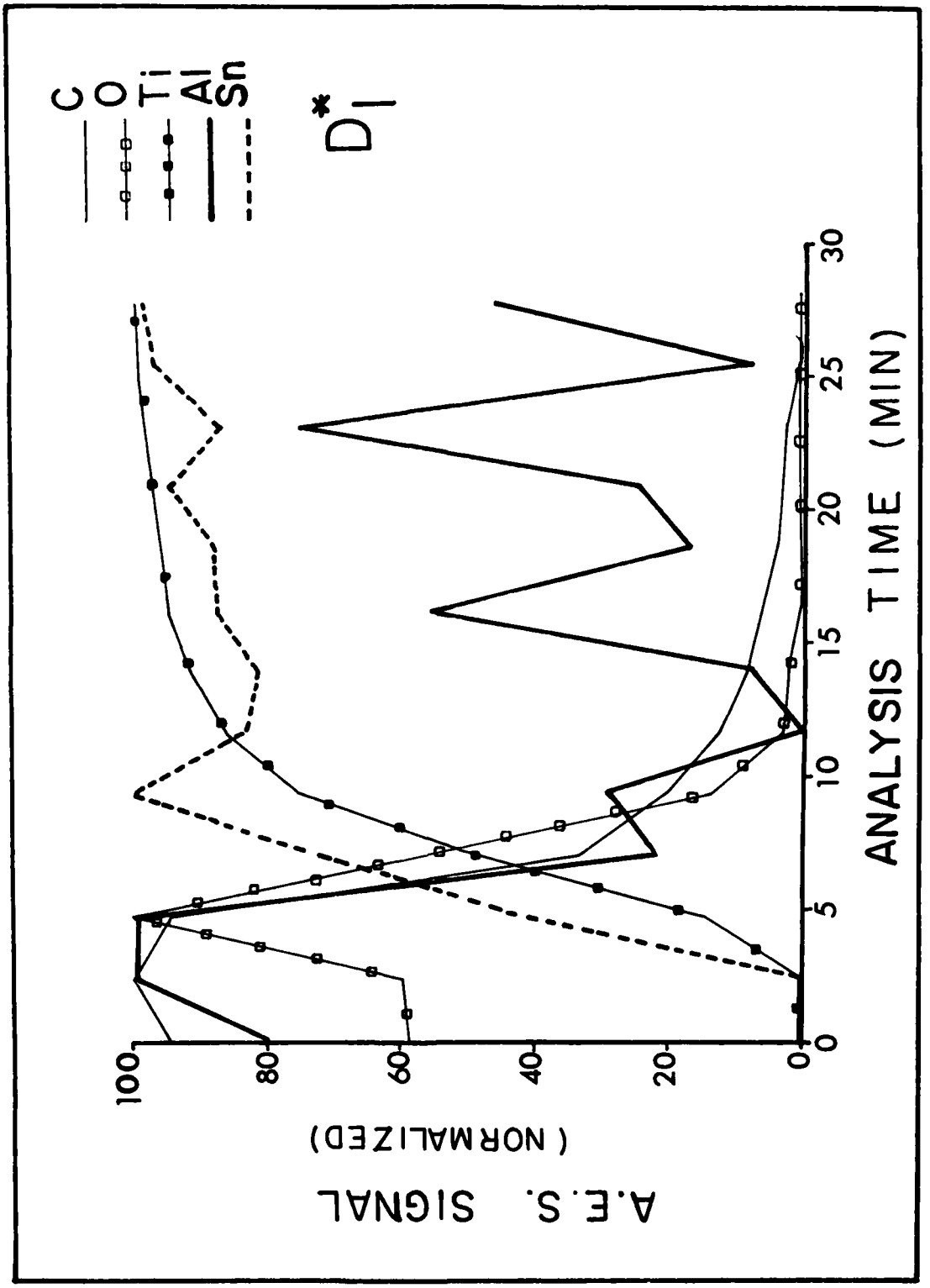

FIG. 53 A.E.S. sputter profiles of Ti-5Al-2.5Sn subjected to 1 treatment

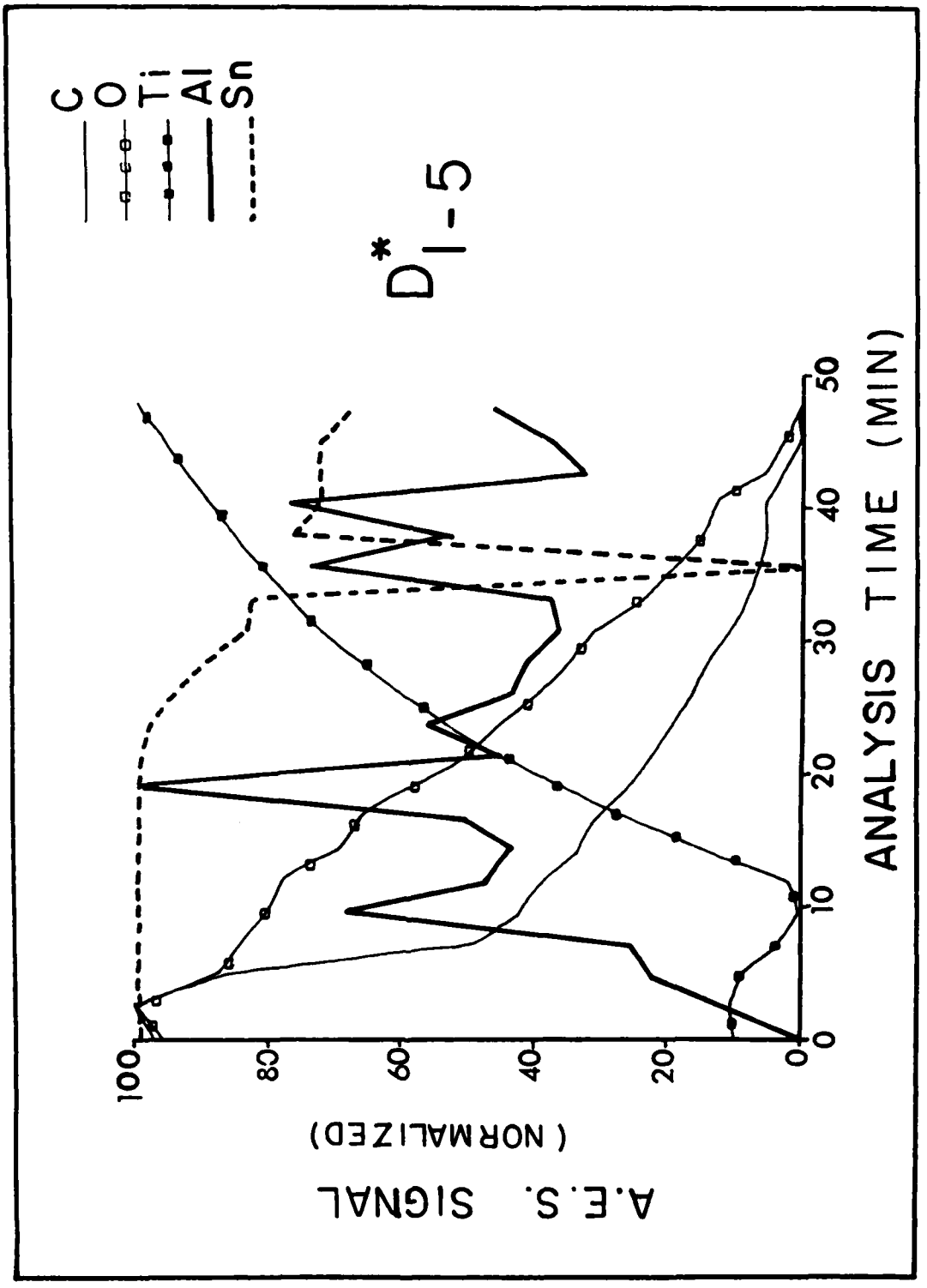

FIG. 54 A.E.S. sputter profiles of Ti-5Al-2.5Sn subjected to 1-5 treatment

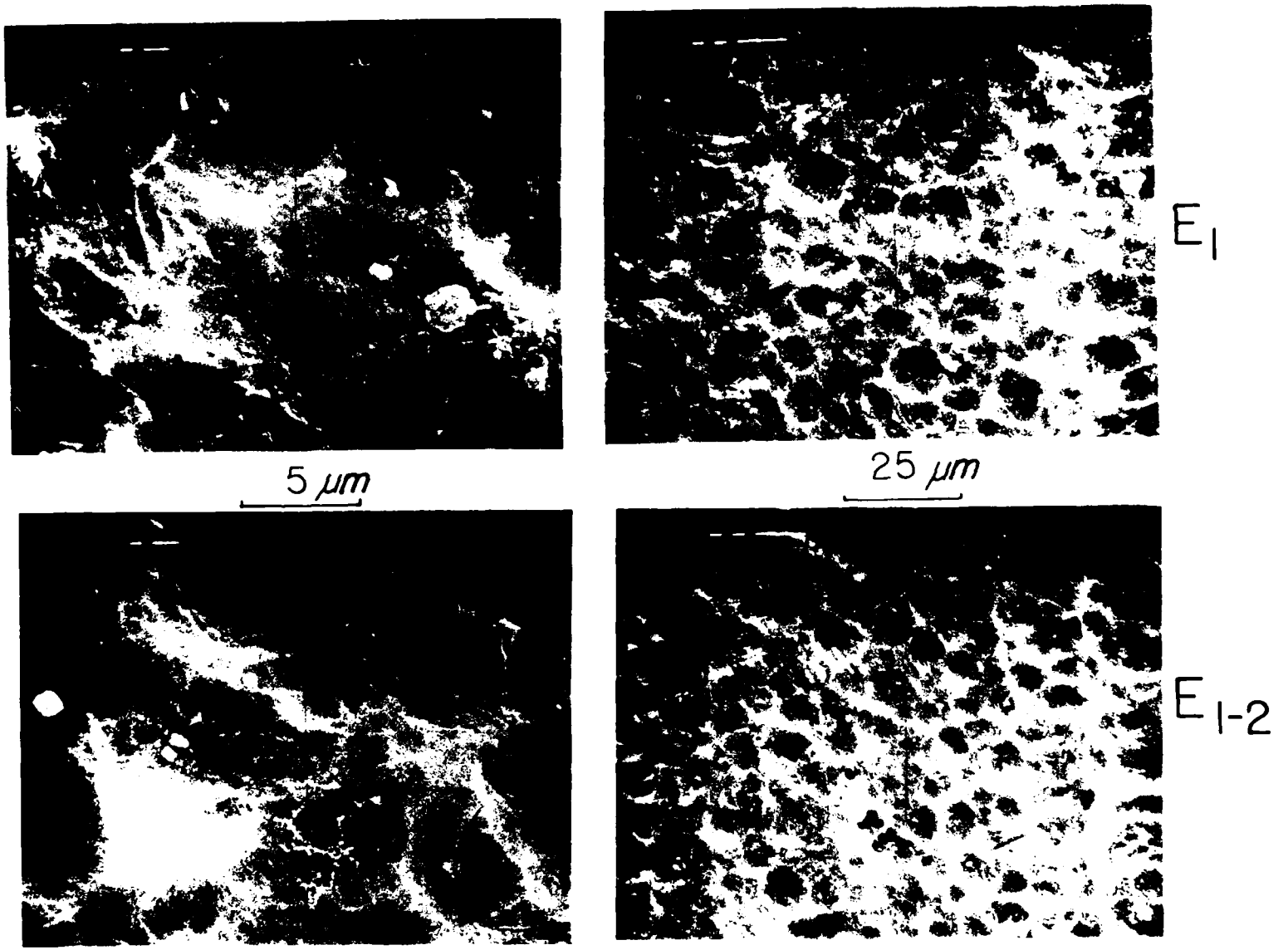

FIG. 55 S.E.M. photomicrographs of Ti-5Al-5Sn-2Mo-2Zr-0.25Si subjected to 1 and 1-2 treatments

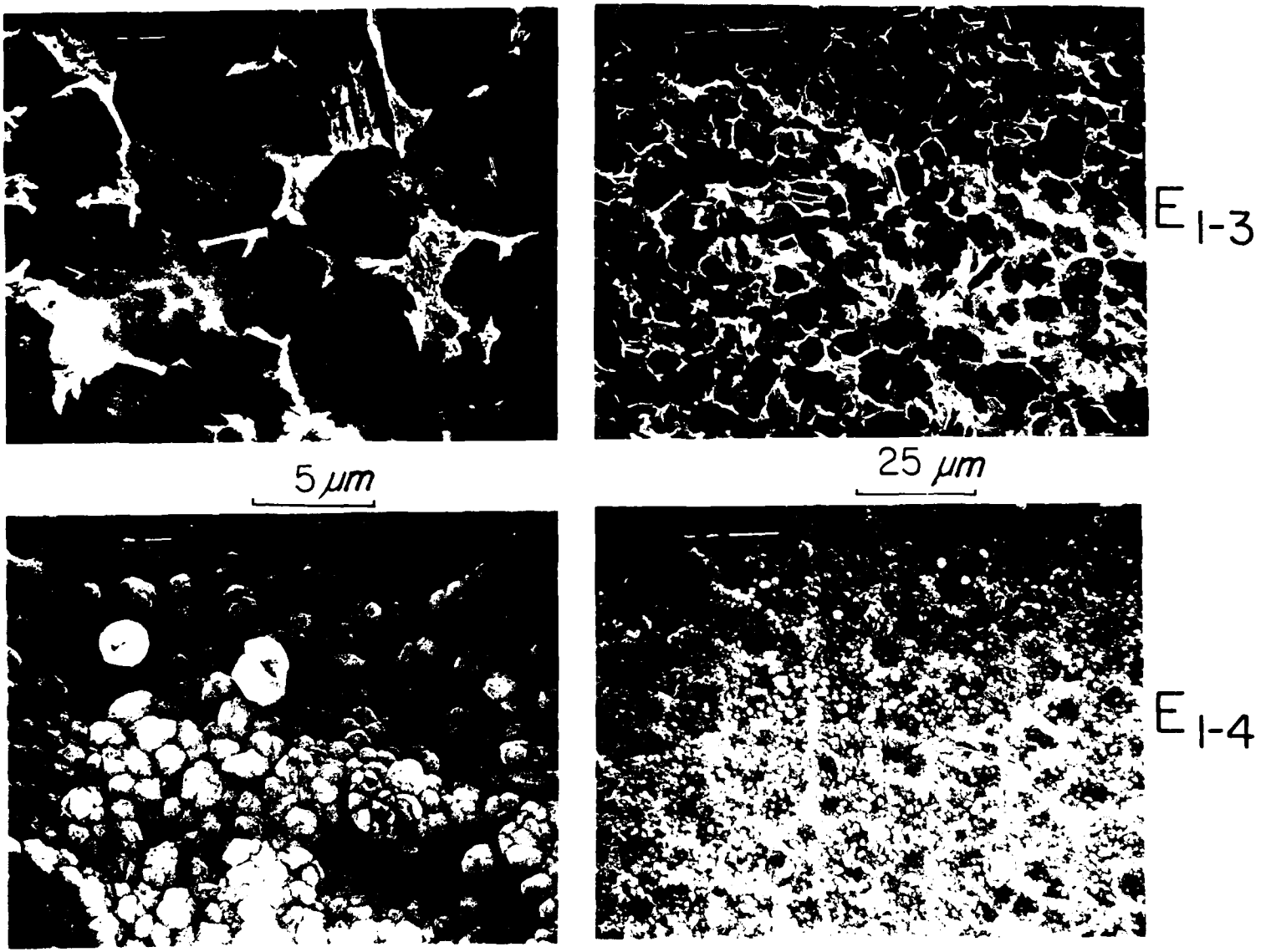

FIG. 56 S.E.M. photomicrographs of Ti-5Al-5Sn-2Mo-2Zr-0.25Si subjected to 1-3 and 1-4 treatments

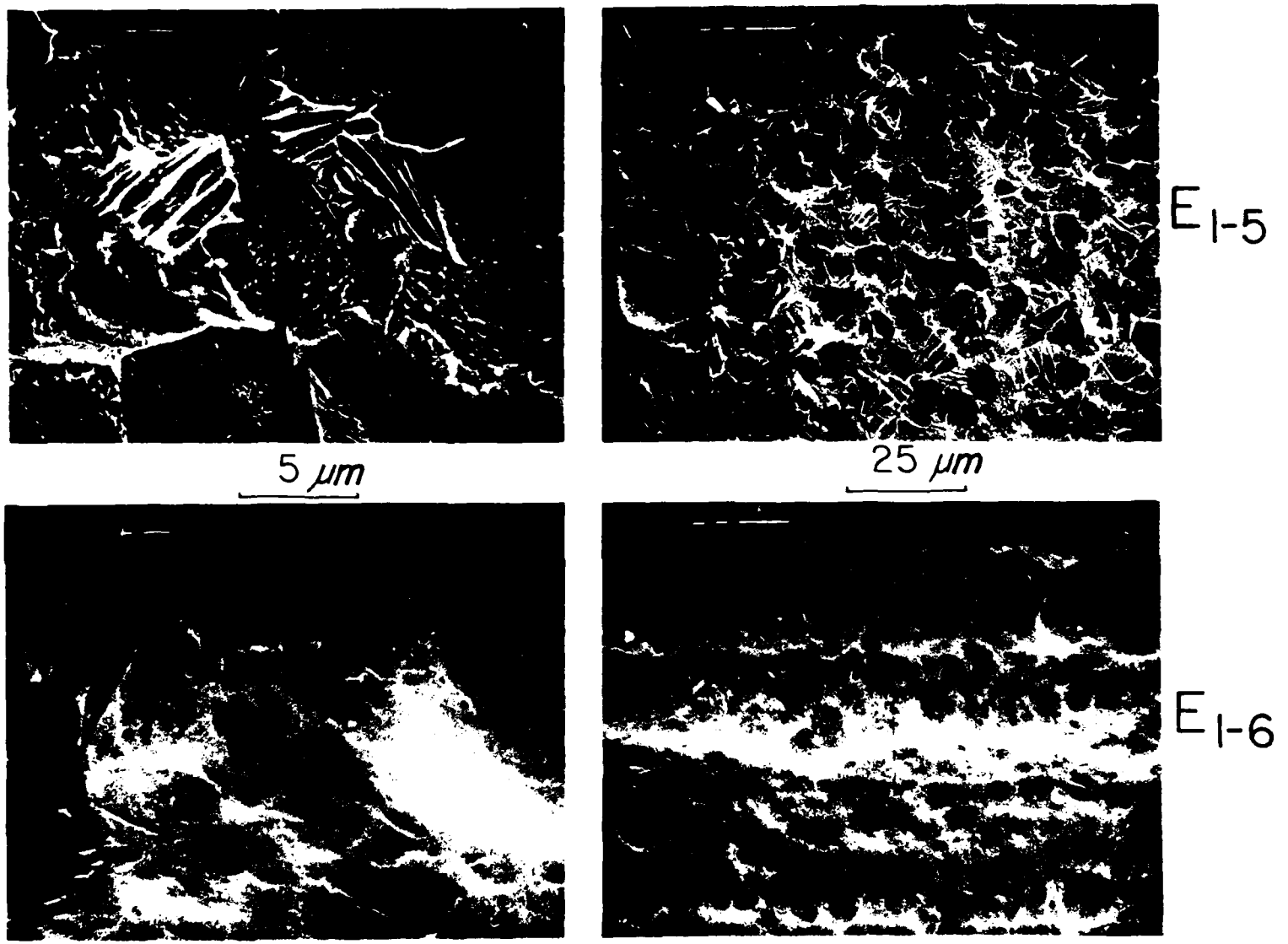

FIG. 57 S.E.M. photomicrographs of Ti-5Al-5Sn-2Mo-2Zr-0.25Si subjected to 1-5 and 1-6 treatments

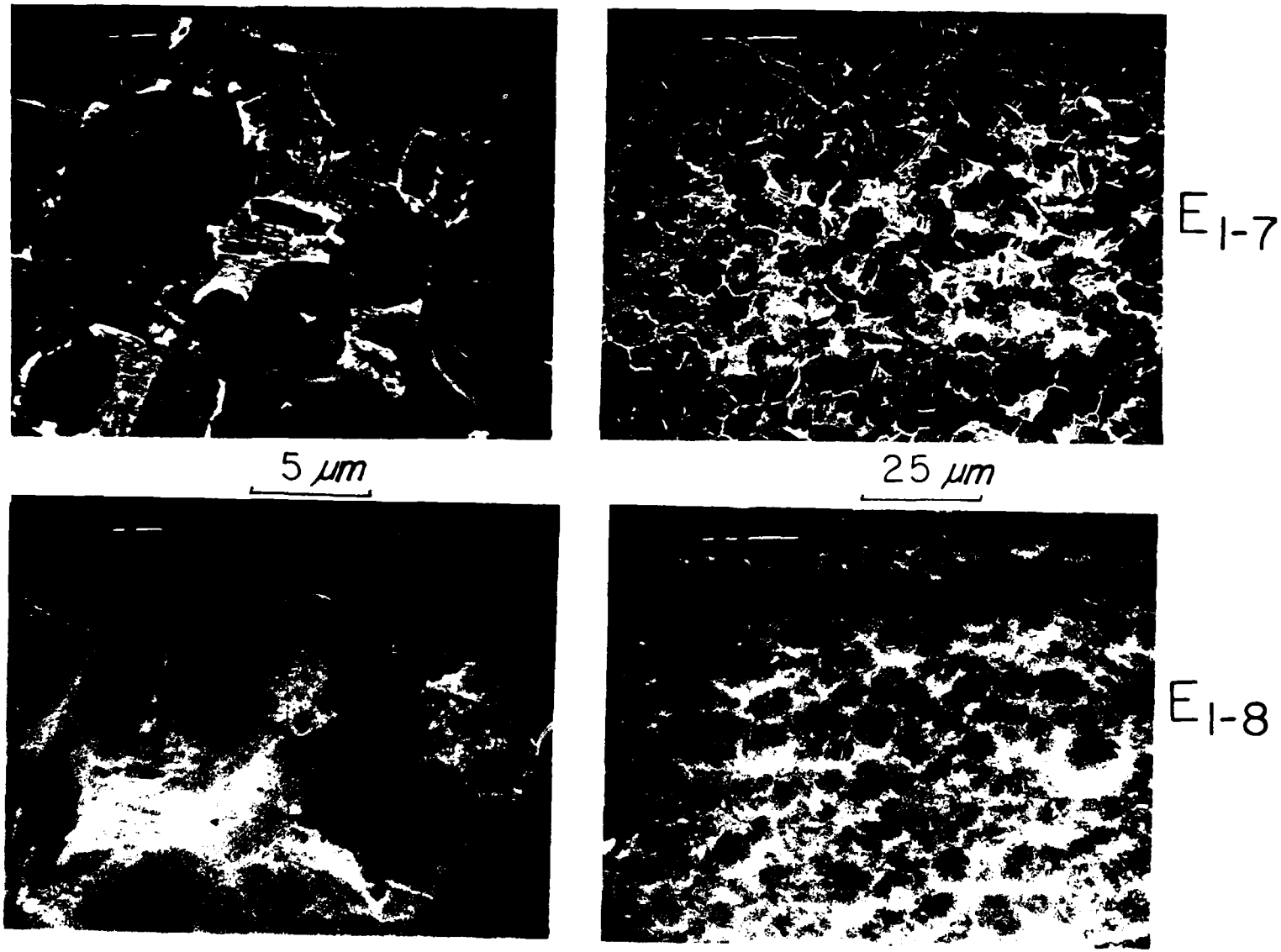

FIG. 58 S.E.M. photomicrographs of Ti-5Al-5Sn-2Mo-2Zr-0.25Si subjected to 1-7 and 1-8 treatments

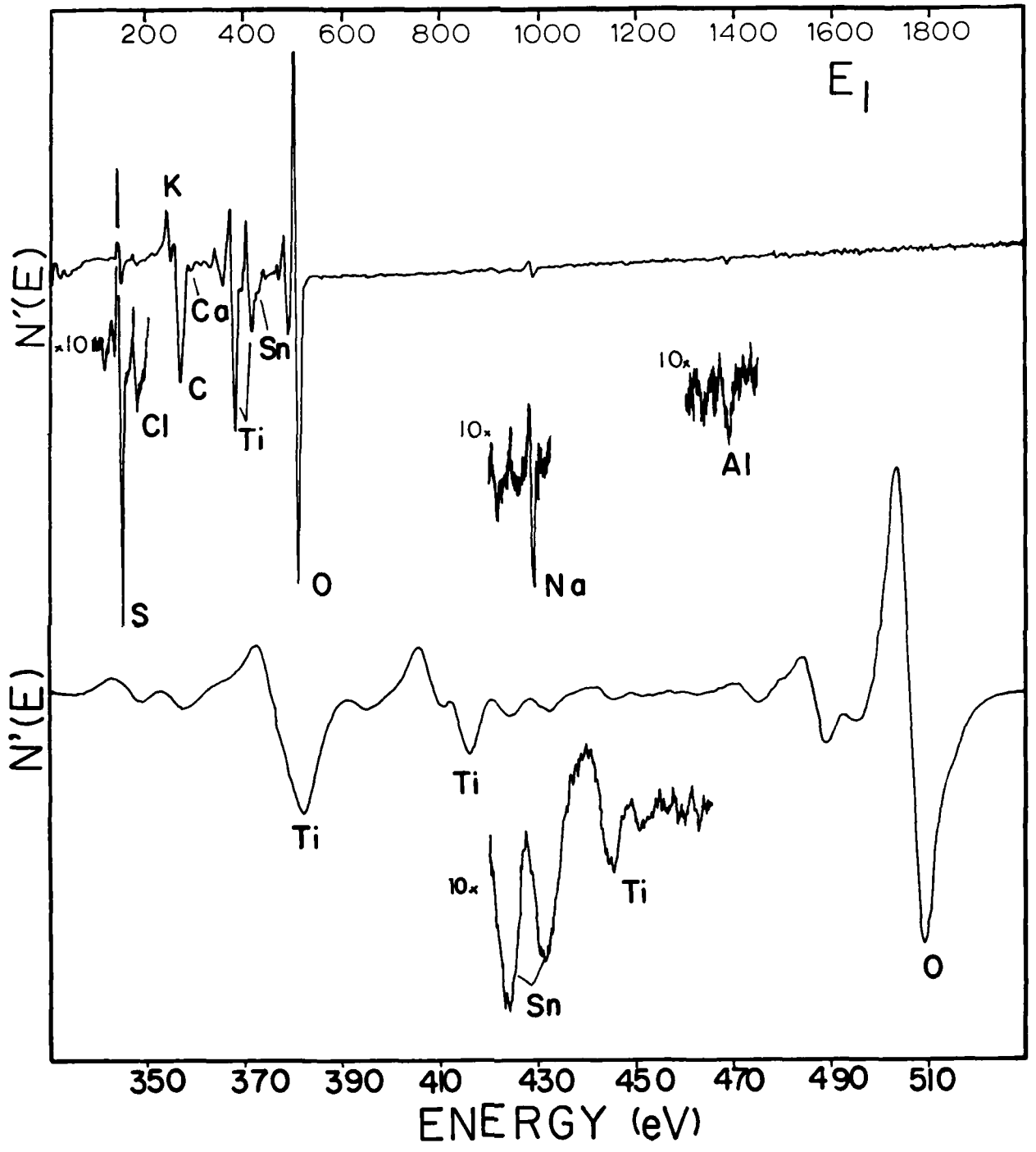

FIG. 59 A.E.S. spectra of Ti-5Al-5Sn-2Mo-2Zr-0.25Si subjected to 1 treatment (0-2000 eV and 330-530 eV)

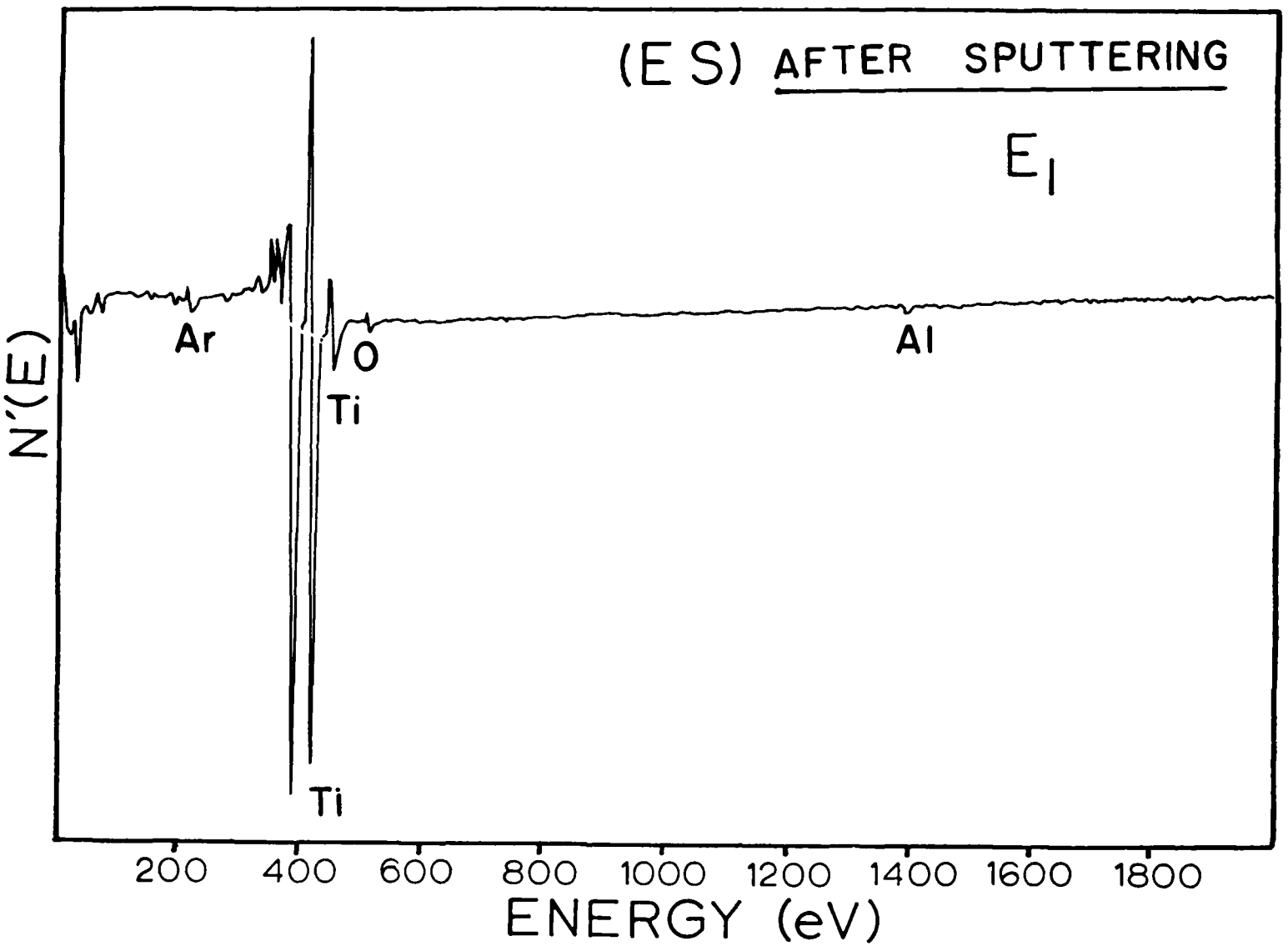

FIG. 60 A.E.S. Equilibrium Sputtered spectrum of Ti-5Al-5Sn-2Mo-2Zr-0.25Si subjected to 1 treatment (0-2000 eV)

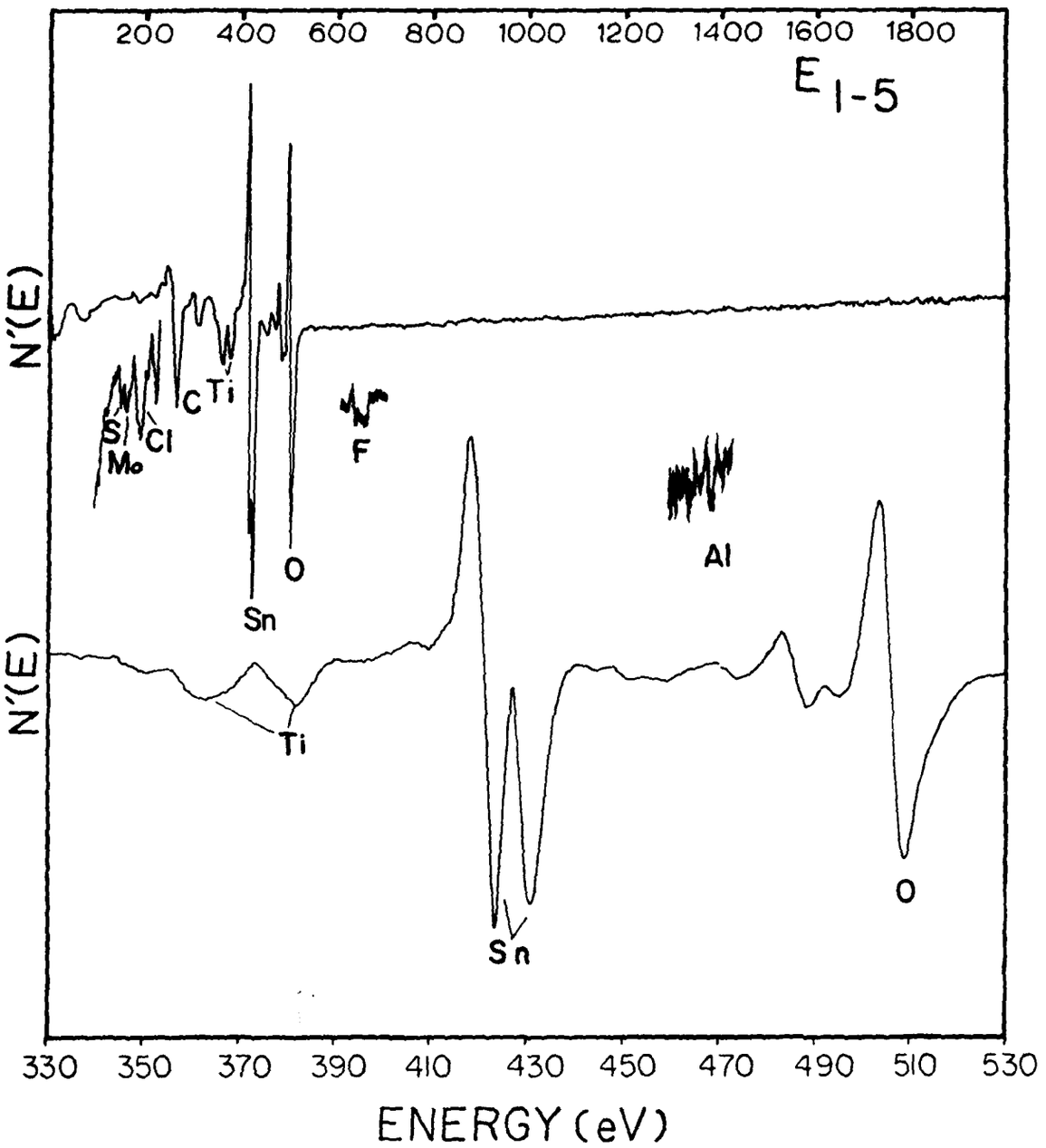

FIG. 61 A.E.S. spectra of Ti-5Al-5Sn-2Mo-2Zr-0.25Si subjected to 1-5 treatment (0-2000 eV and 330-530 eV)

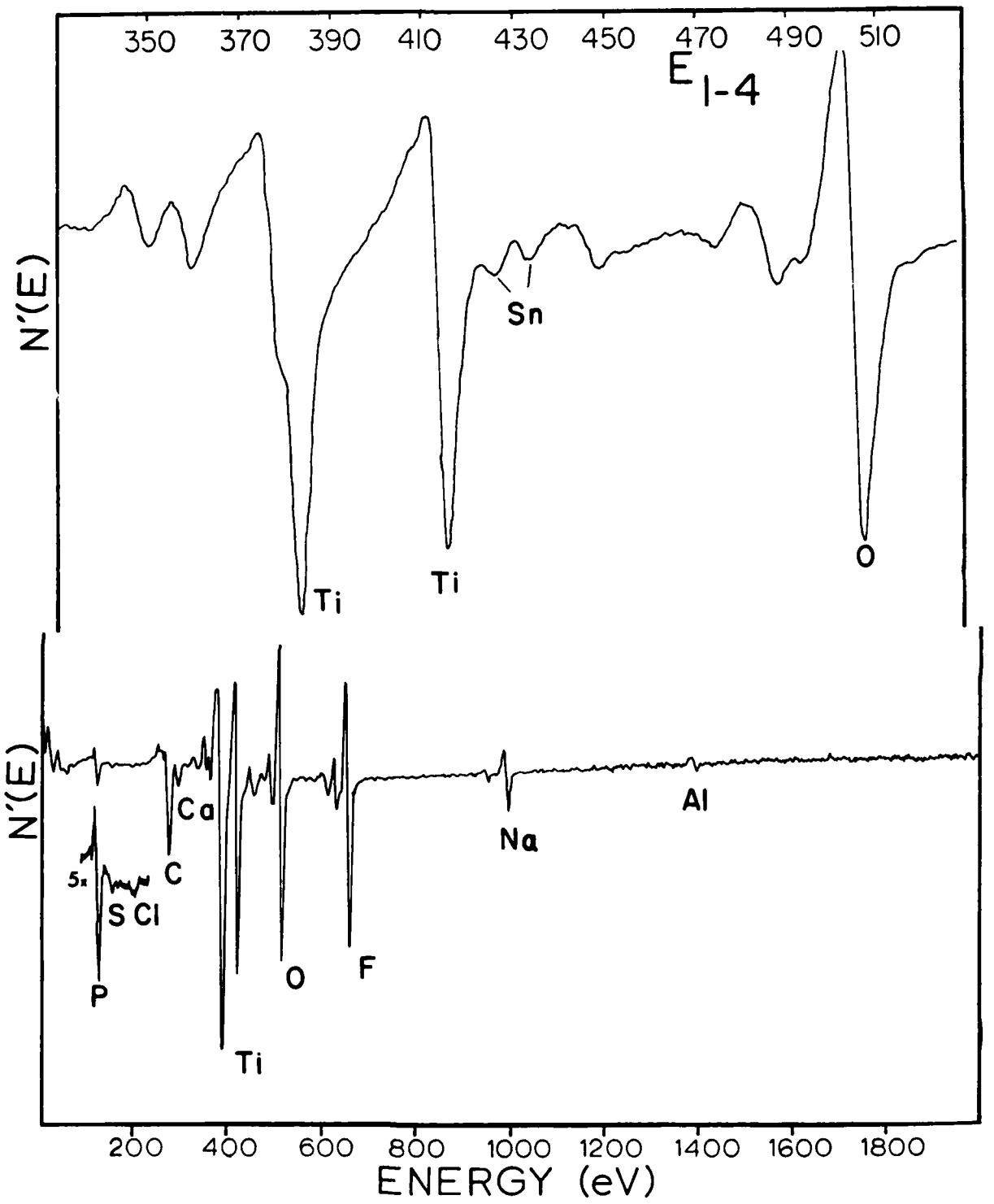

FIG. 62 A.E.S. spectra of Ti-5Al-5Sn-2Mo-2Zr-0.25Si subjected to 1-4 treatment (0-2000 eV and 330-530 eV)

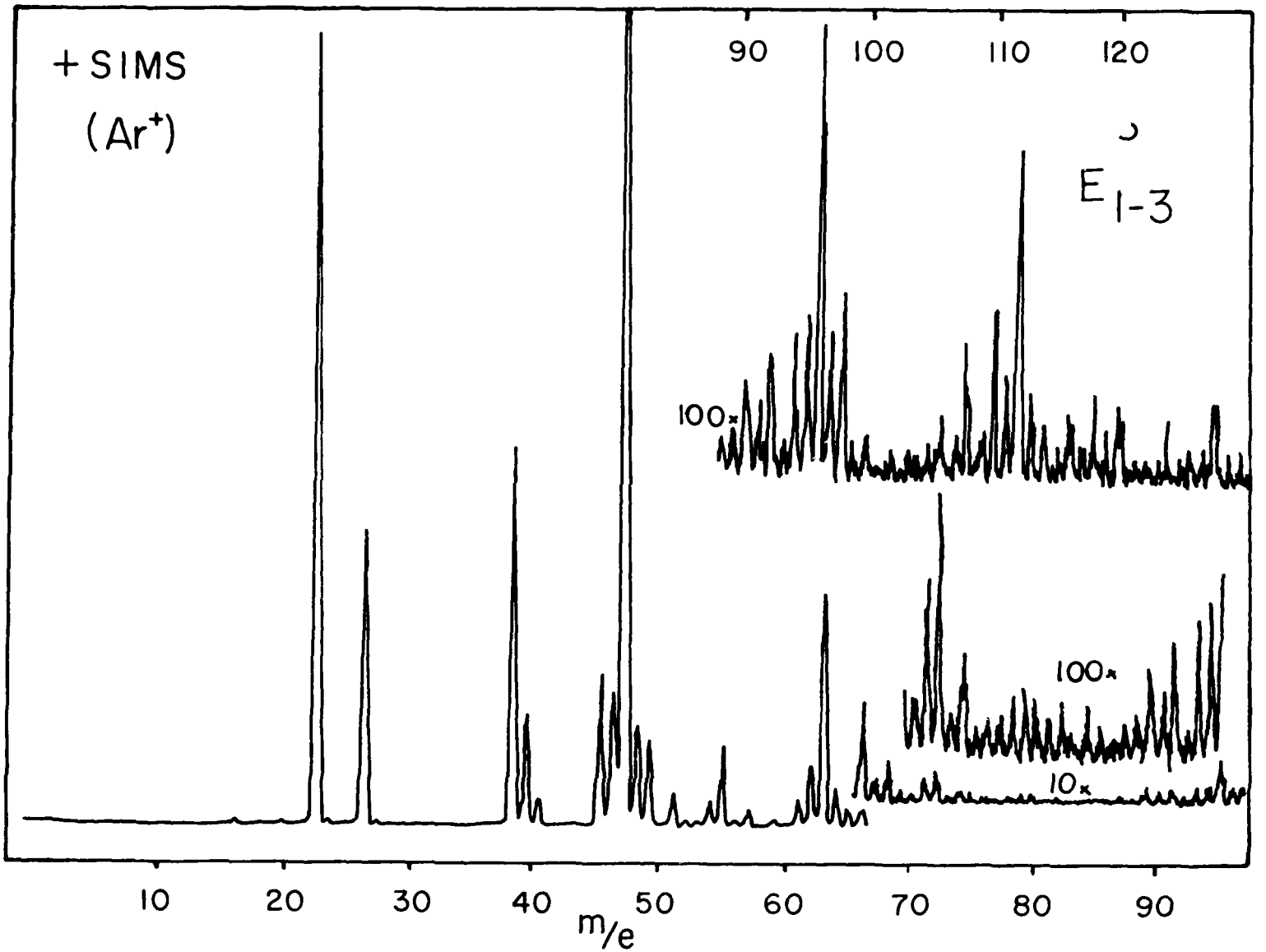

FIG. 63 Positive ion SIMS spectra of Ti-5Al-5Sn-2Mo-2Zr-0.25Si subjected to 1-3 treatment

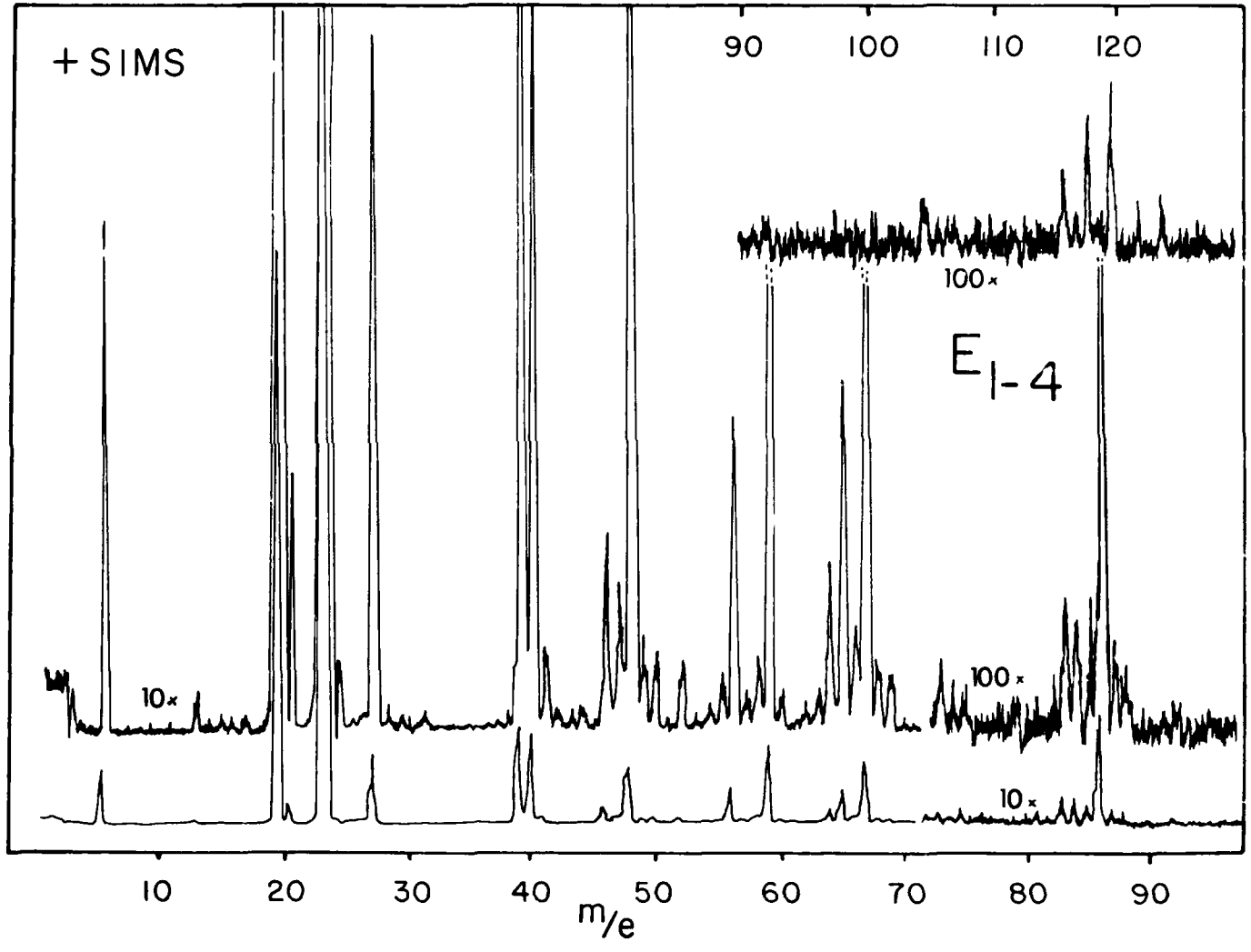

FIG. 64 Positive ion SIMS spectra of Ti-5Al-5Sn-2Mo-2Zr-0.25Si subjected to 1-4 treatment

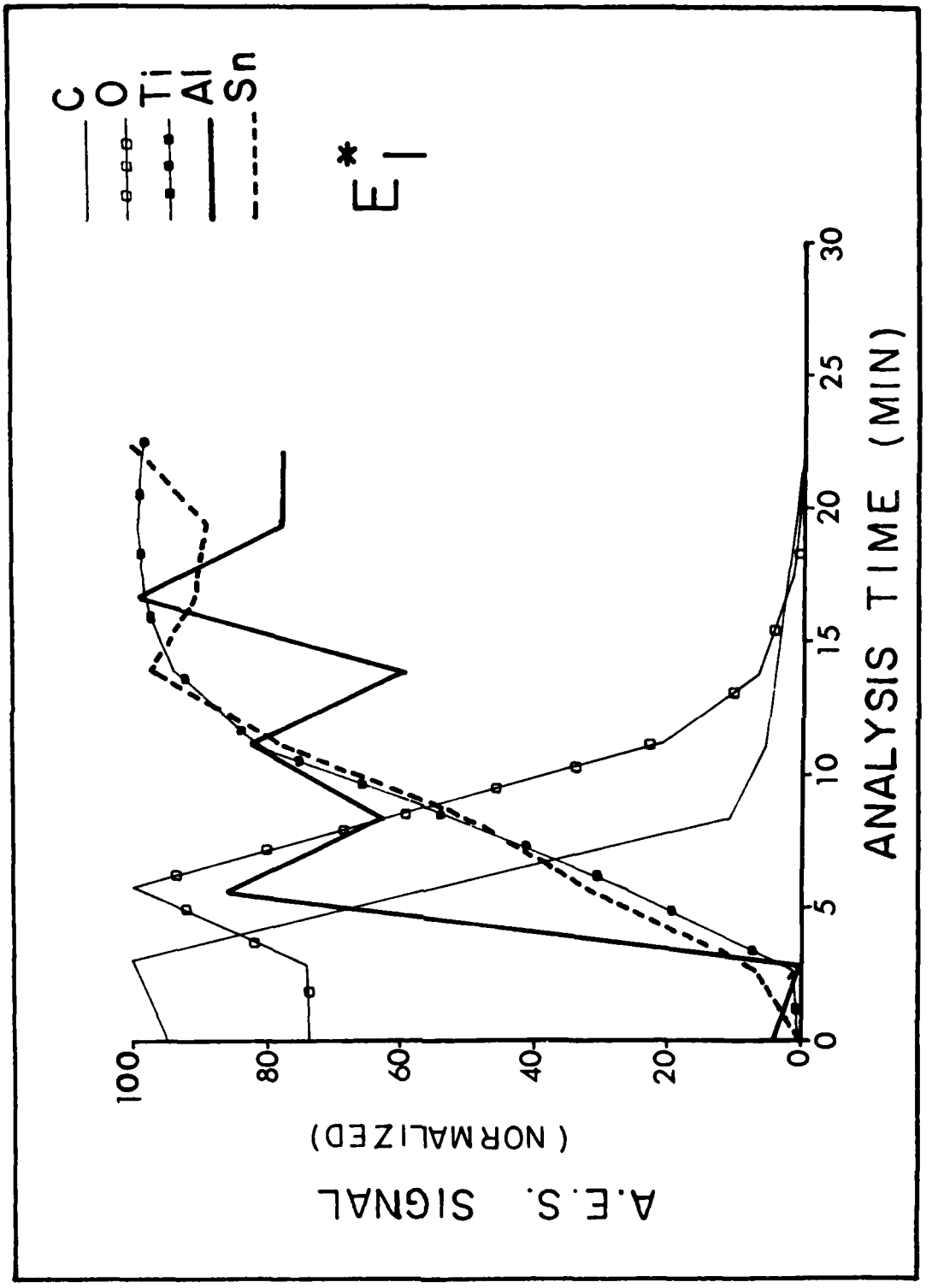

FIG. 65 A.E.S. sputter profiles of Ti-5Al-5Sn-2Mo-2Zr-0.25Si subjected to 1 treatment

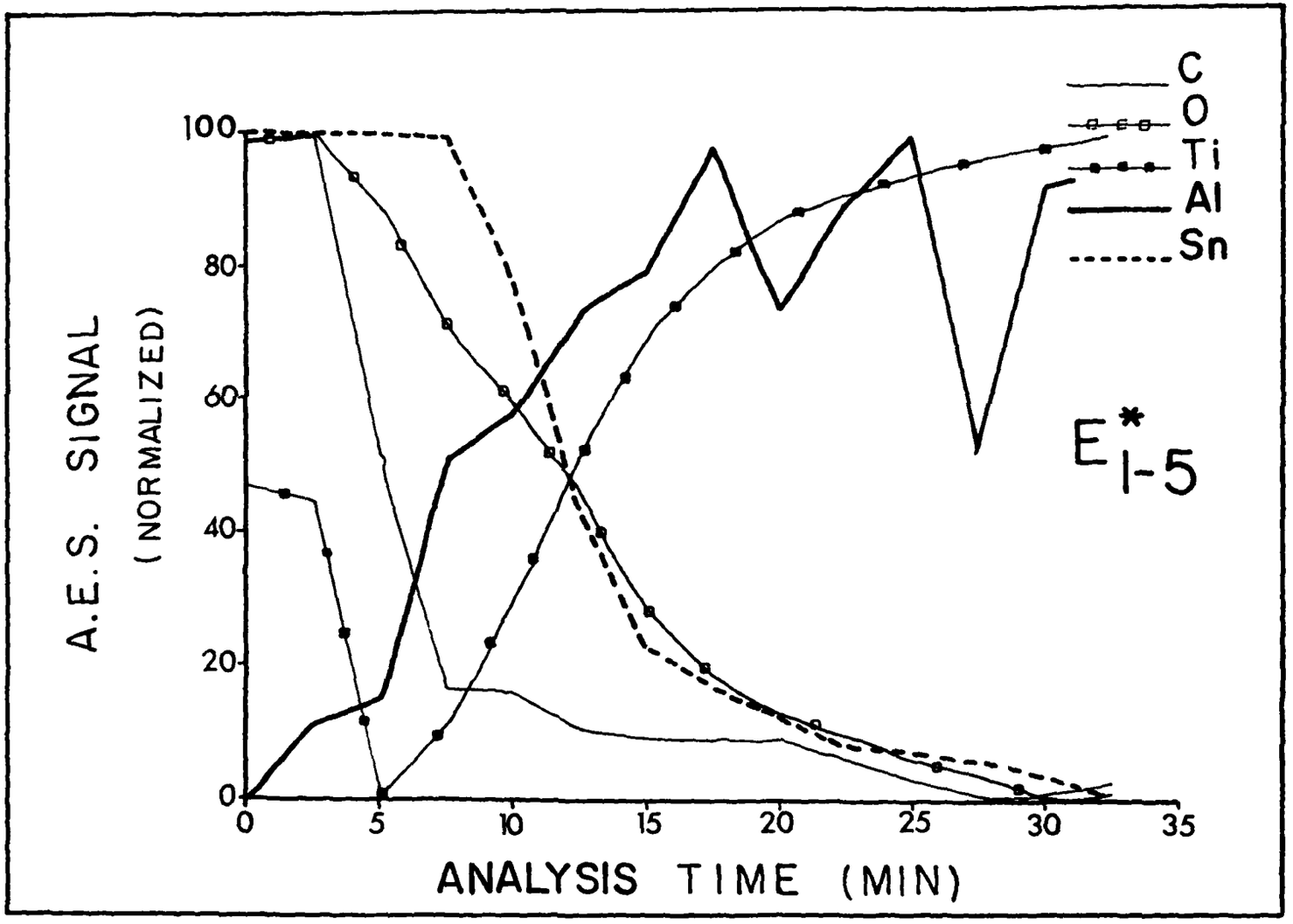

FIG. 66 A.E.S. sputter profiles of Ti-5Al-5Sn-2Mo-2Zr-0.25Si subjected to 1-5 treatment

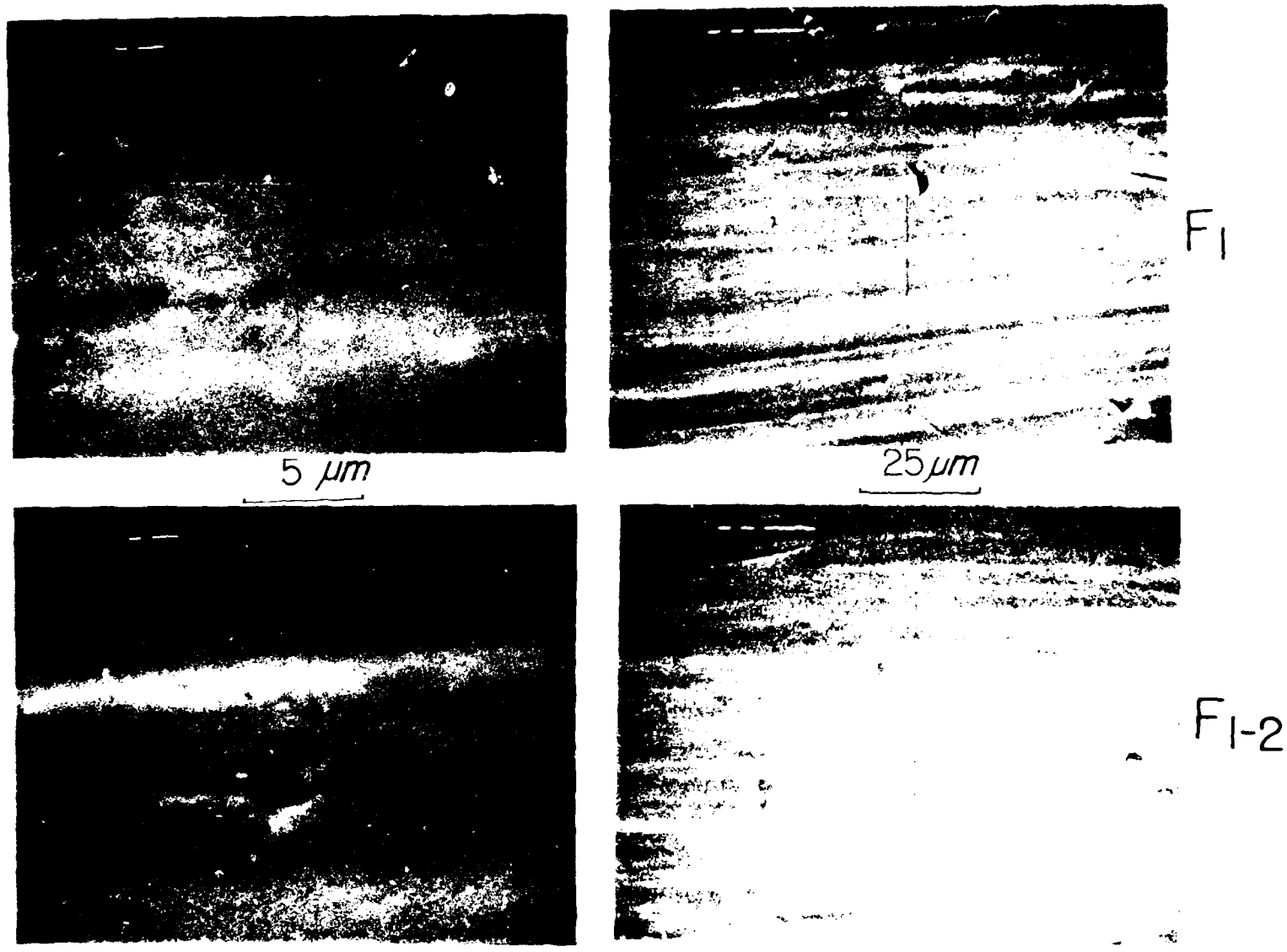

FIG. 67 S.E.M. photomicrographs of Ti-3Al-2.5V subjected to 1 and 1-2 treatments

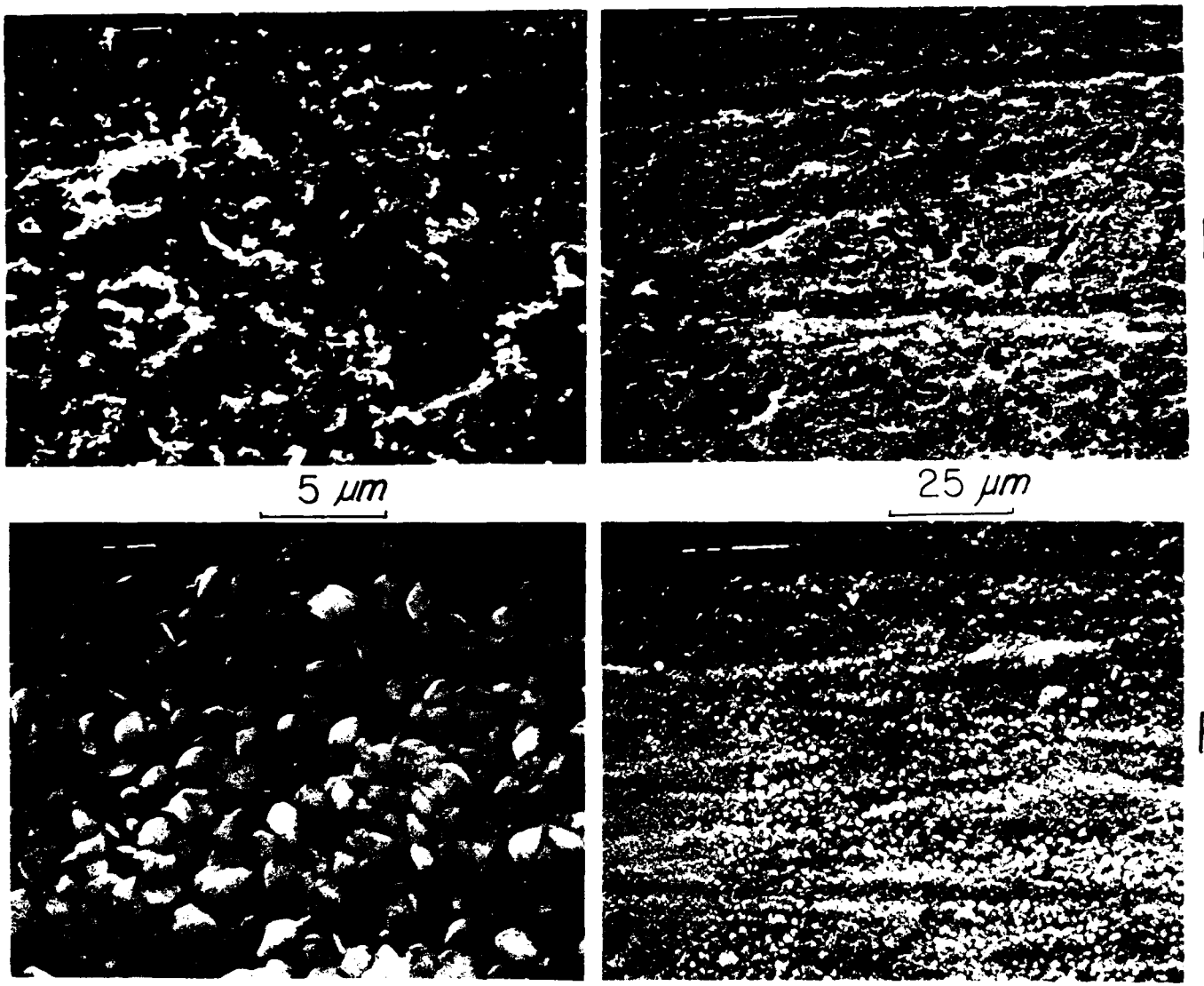

FIG. 68 S.E.M. photomicrographs of Ti-3Al-2.5V subjected to 1-3 and 1-4 treatments

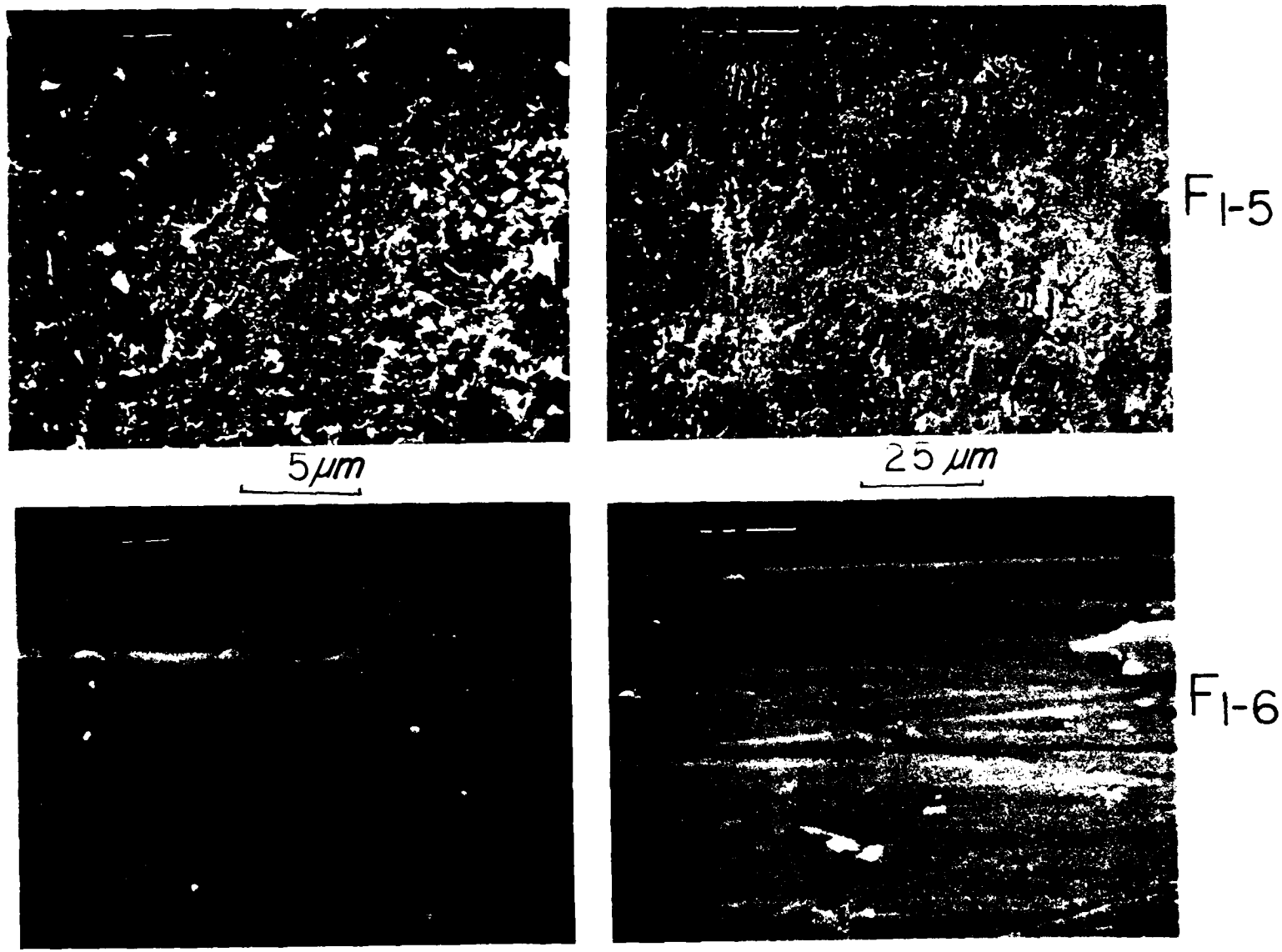

FIG. 69 S.E.M. photomicrographs of Ti-3Al-2.5V subjected to 1-6 and 1-6 treatments

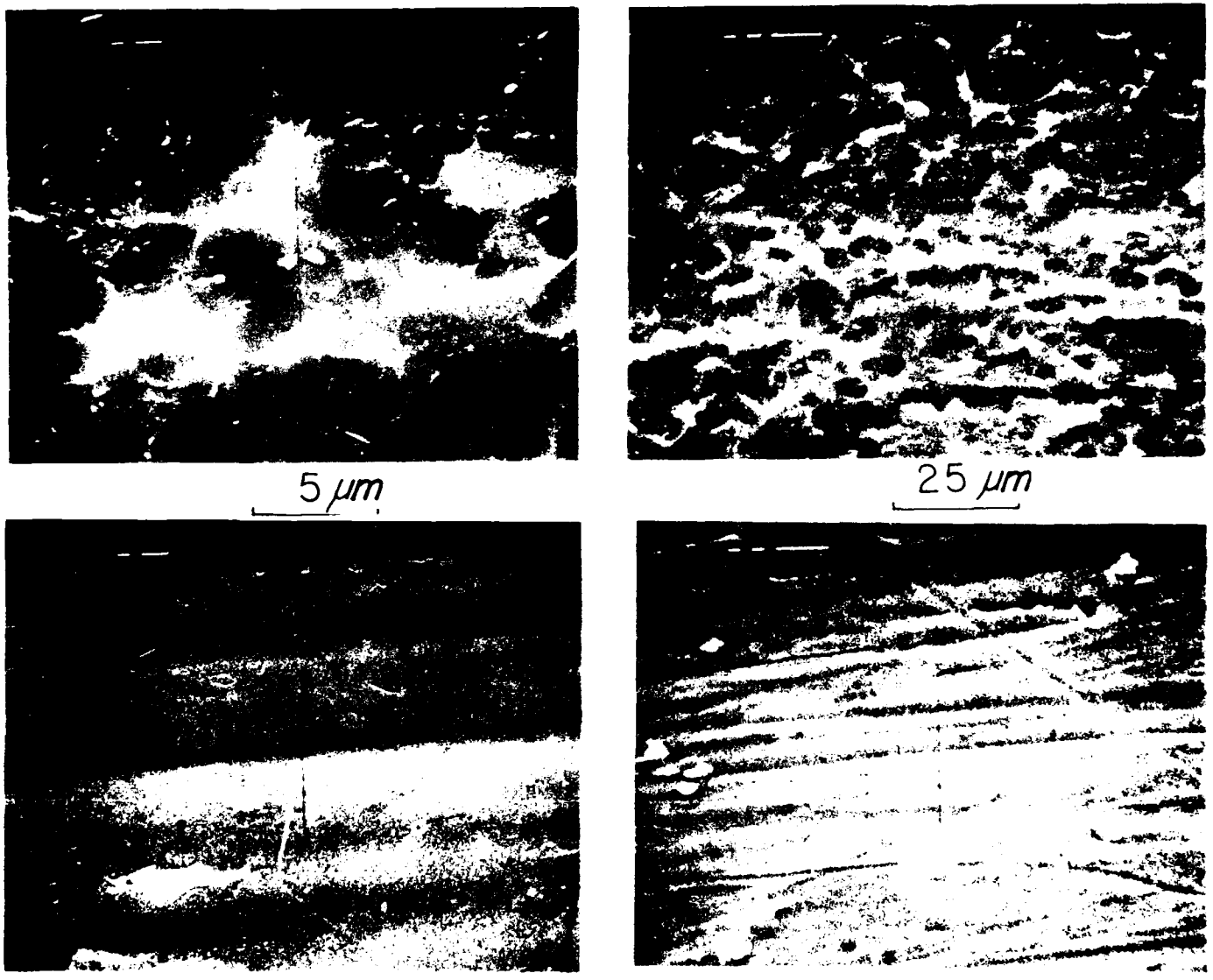

FIG. 70 S.E.M. photomicrographs of Ti-3Al-2.5V subjected to 1-7 and 1-8 treatments

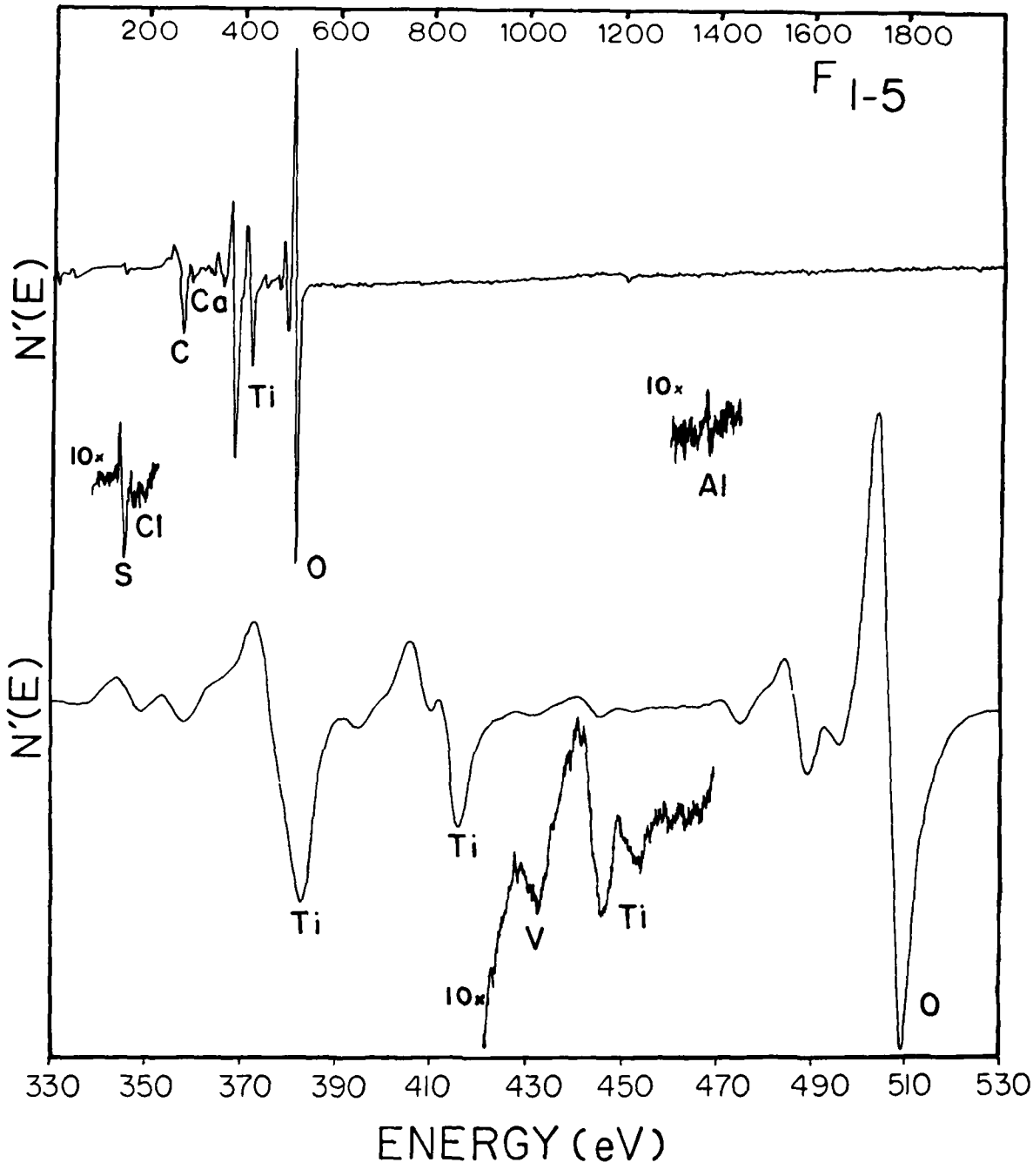

FIG. 71 A.E.S. spectra of Ti-3Al-2.5V subjected to 1-5 treatment (0-2000 eV and 330-530 eV)

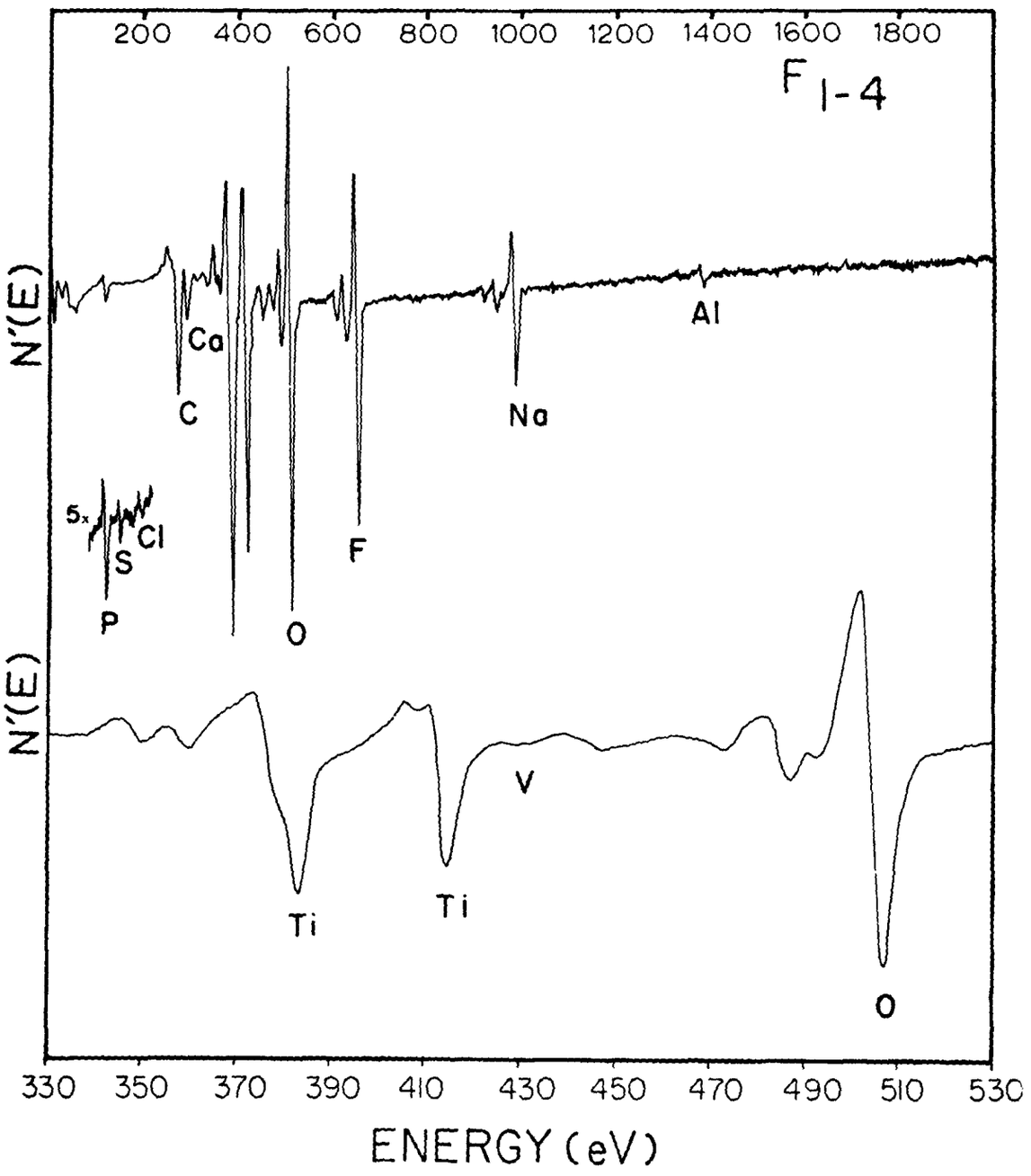

FIG. 72 A.E.S. spectra of Ti-3Al-2.5V subjected to 1-4 treatment (0-2000 eV and 330-530 eV)

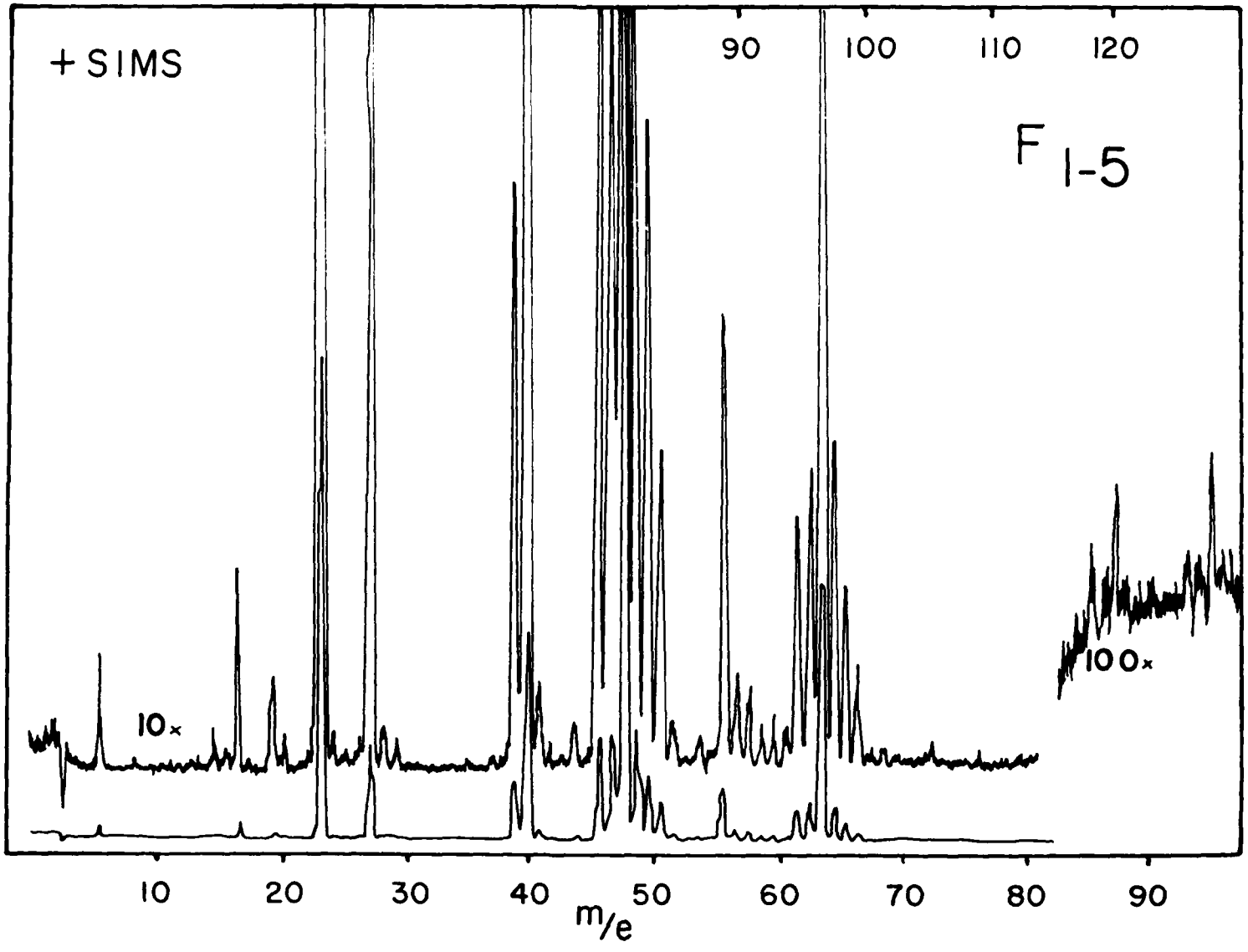

FIG. 73 Positive ion SIMS spectra of Ti-3Al-2.5V subjected to 1-5 treatment

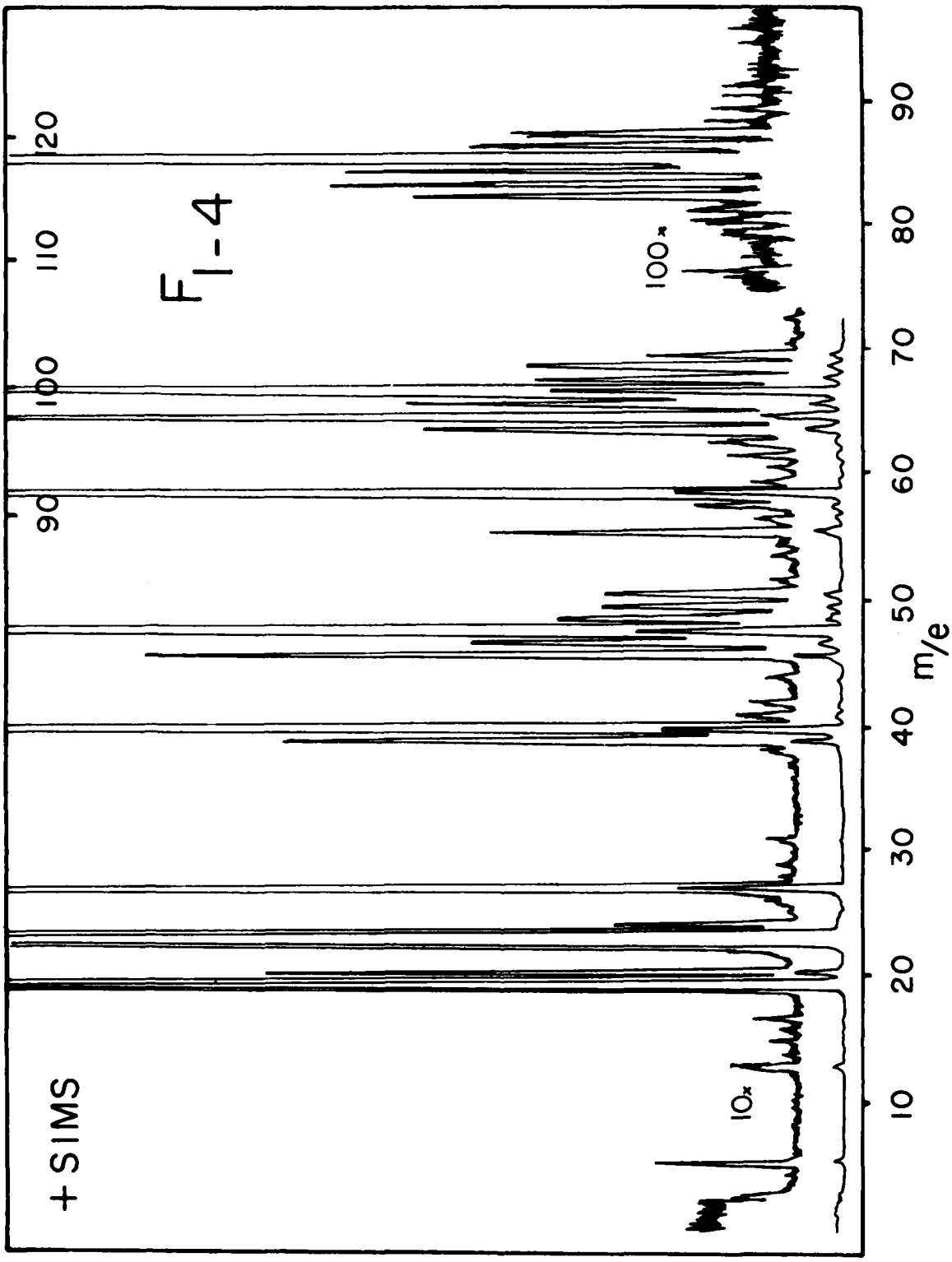

FIG. 74 Positive ion SIMS spectra of Ti-3Al-2.5V subjected to 1-4 treatment

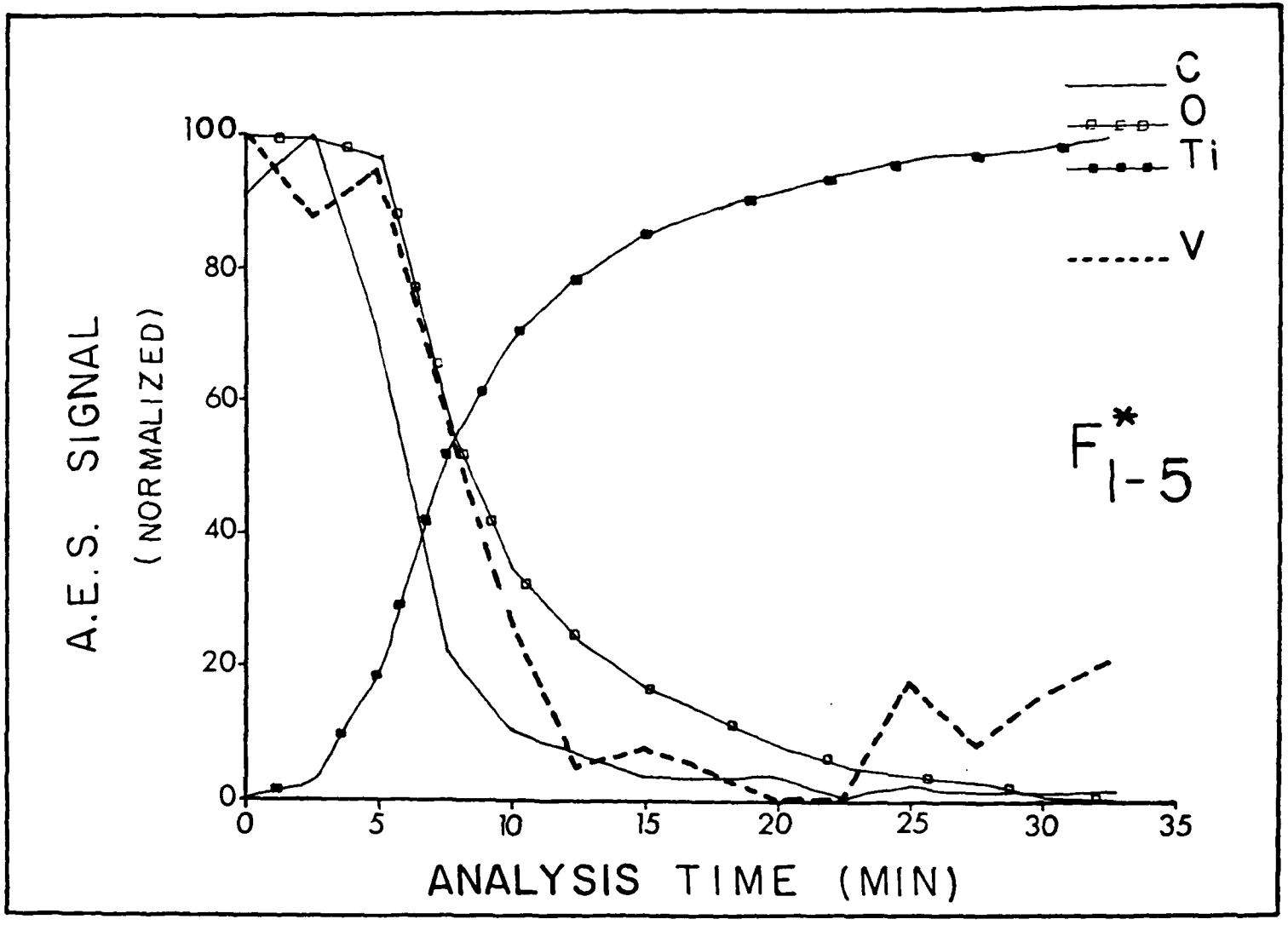

FIG. 75 A.E.S. sputter profiles of Ti-3Al-2.5V subjected to 1.5 treatment

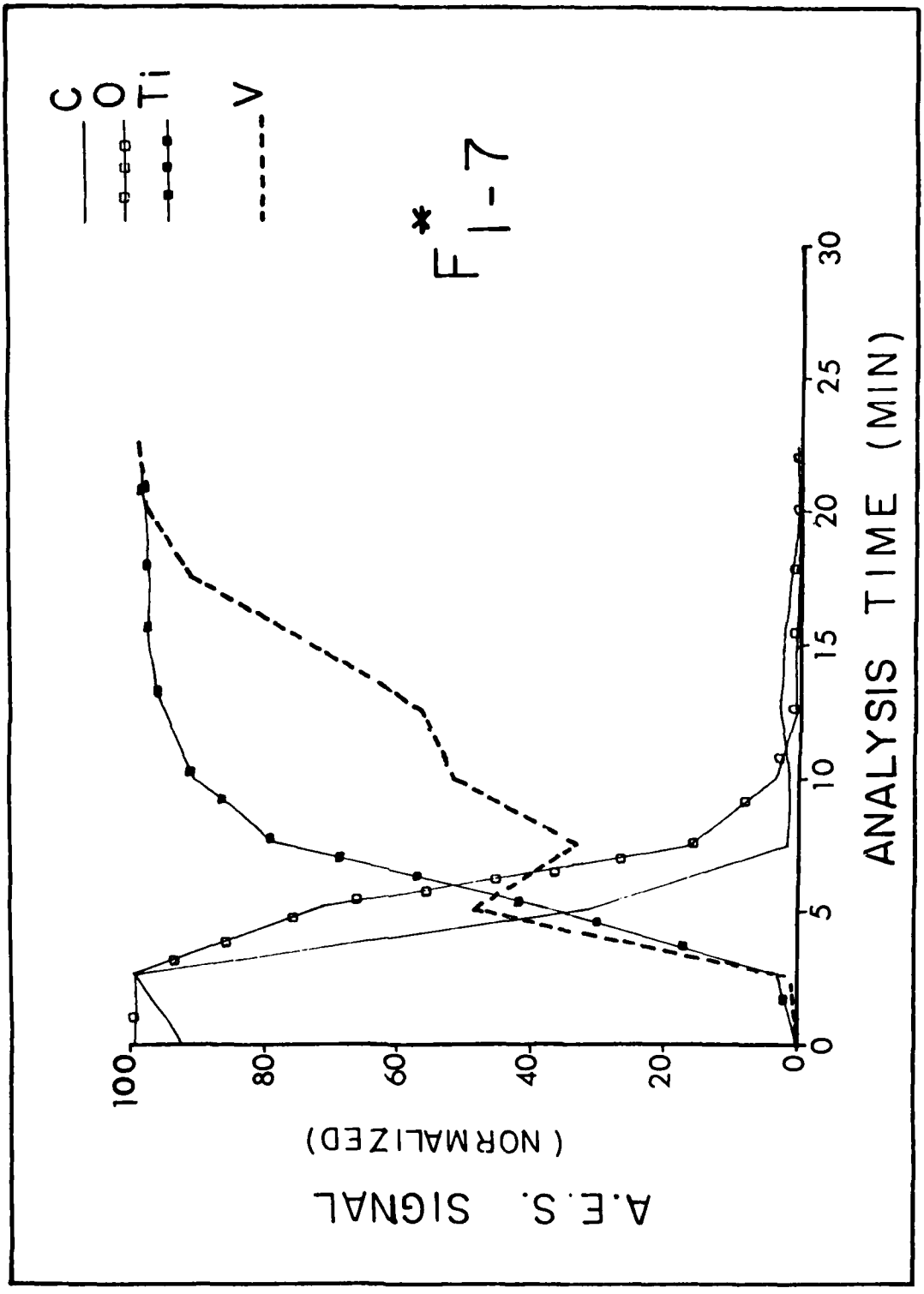

FIG. 76 A.E.S. sputter profiles of Ti-3Al-2.5V subjected to 1.7 treatment

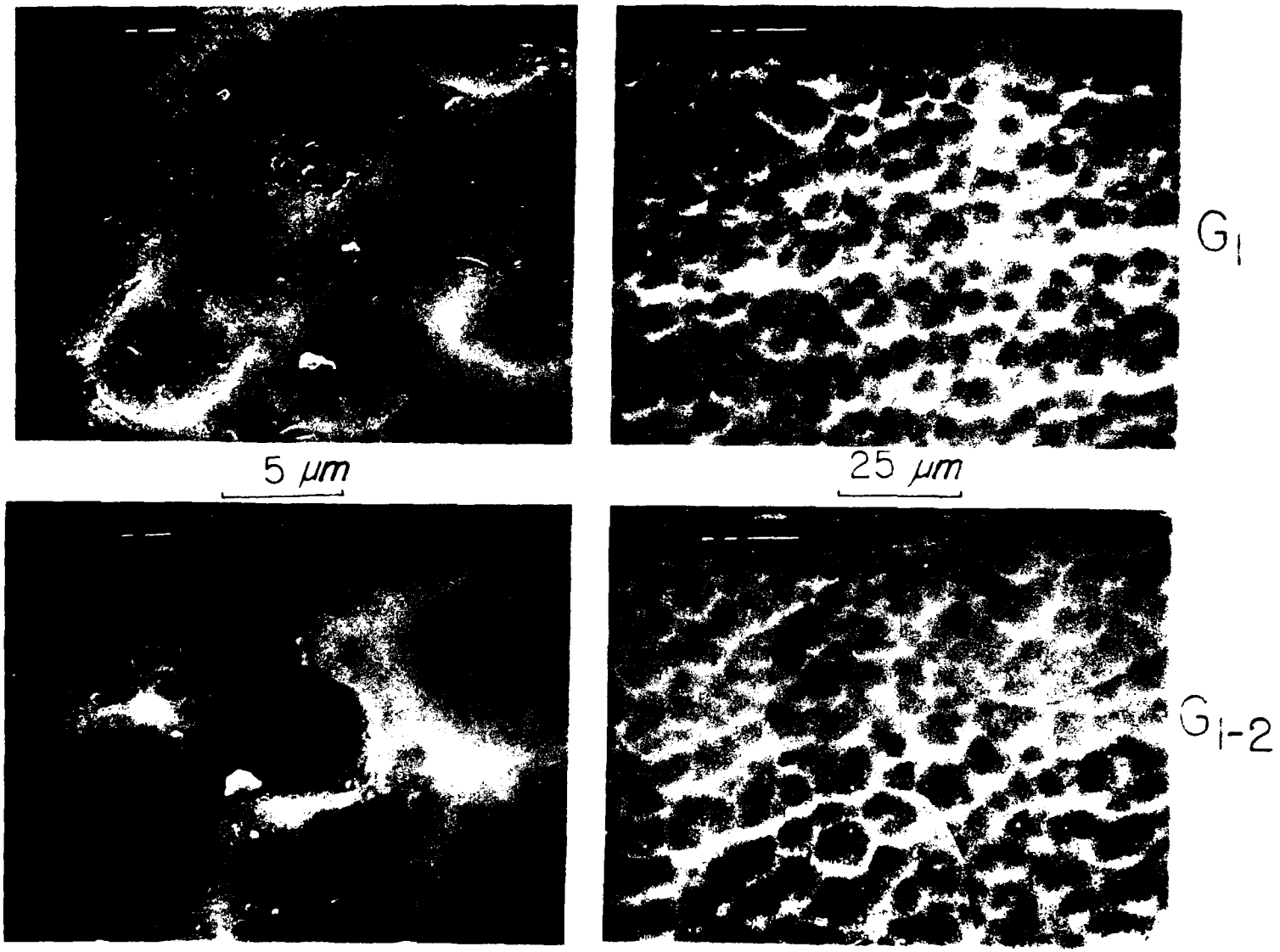

FIG. 77 S.E.M. photomicrographs of Ti-13V-11Cr-3Al subjected to 1 and 1-2 treatments

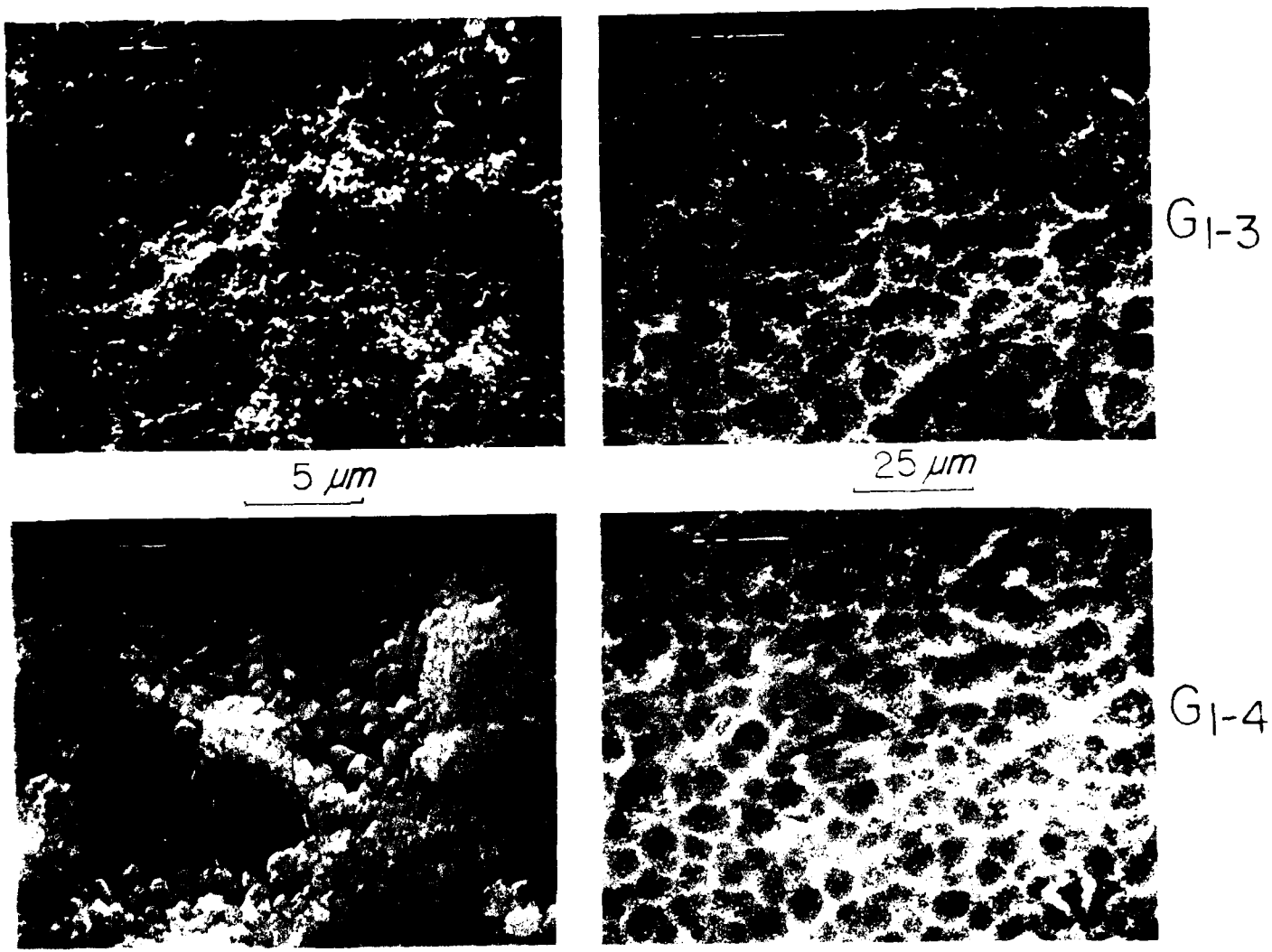

FIG. 78 S.E.M. photomicrographs of Ti-13V-11Cr-3Al subjected to 1-3 and 1-4 treatments

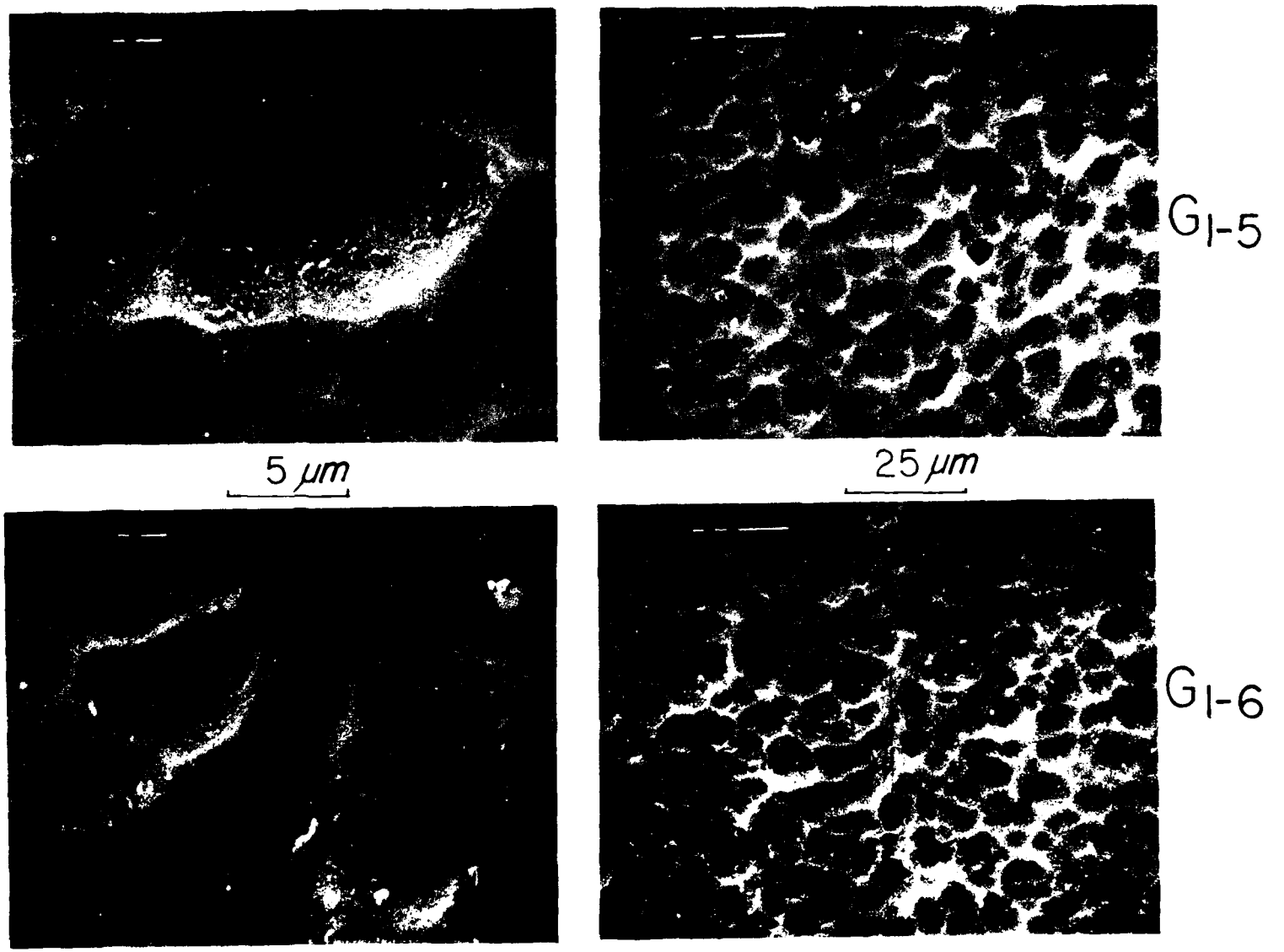

FIG. 79 S.E.M. photomicrographs of Ti-13V-11Cr-3Al subjected to 1-5 and 1-6 treatments

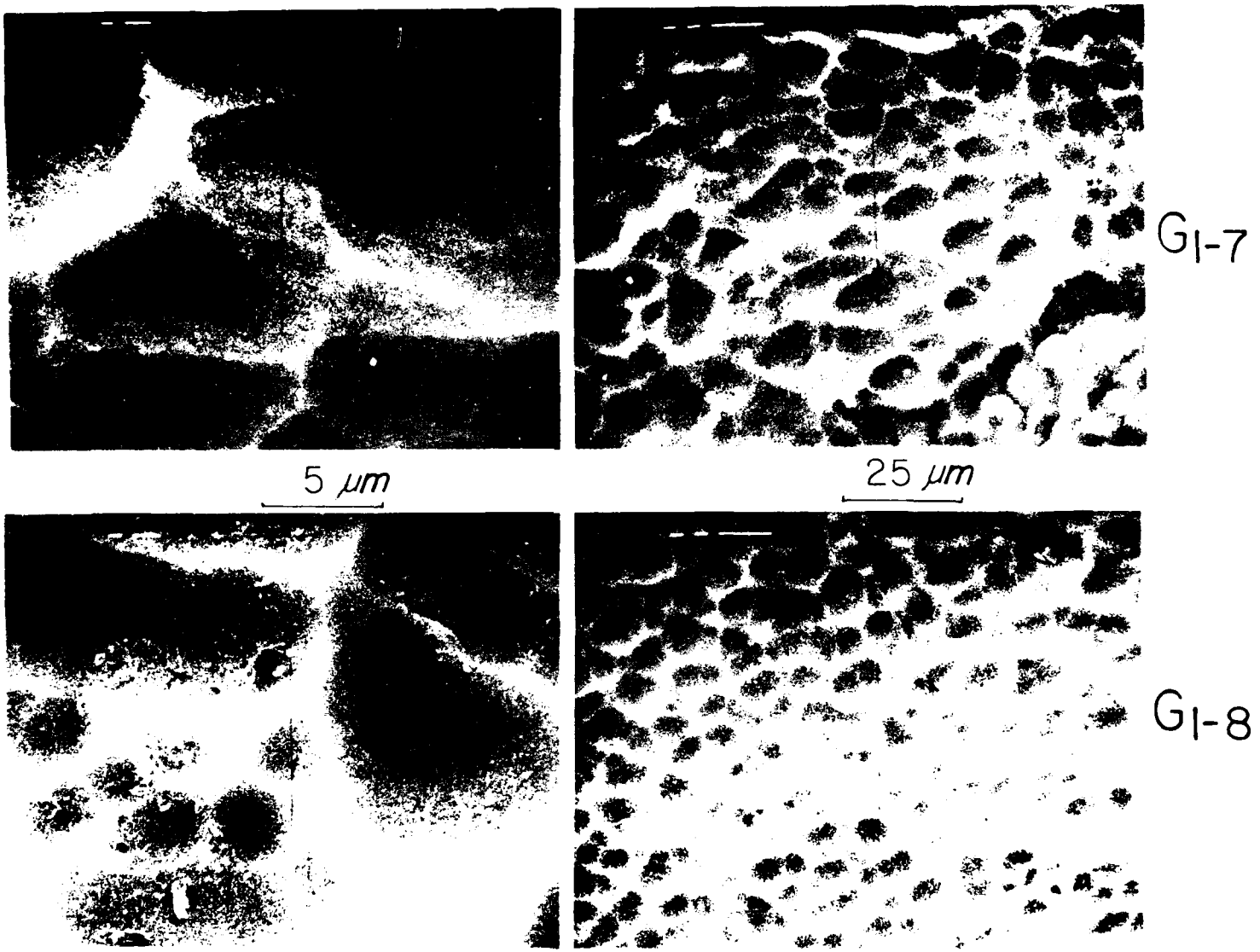

FIG. 80 S.E.M. photomicrographs of Ti-13V-11Cr-3Al subjected to 1-7 and 1-8 treatments

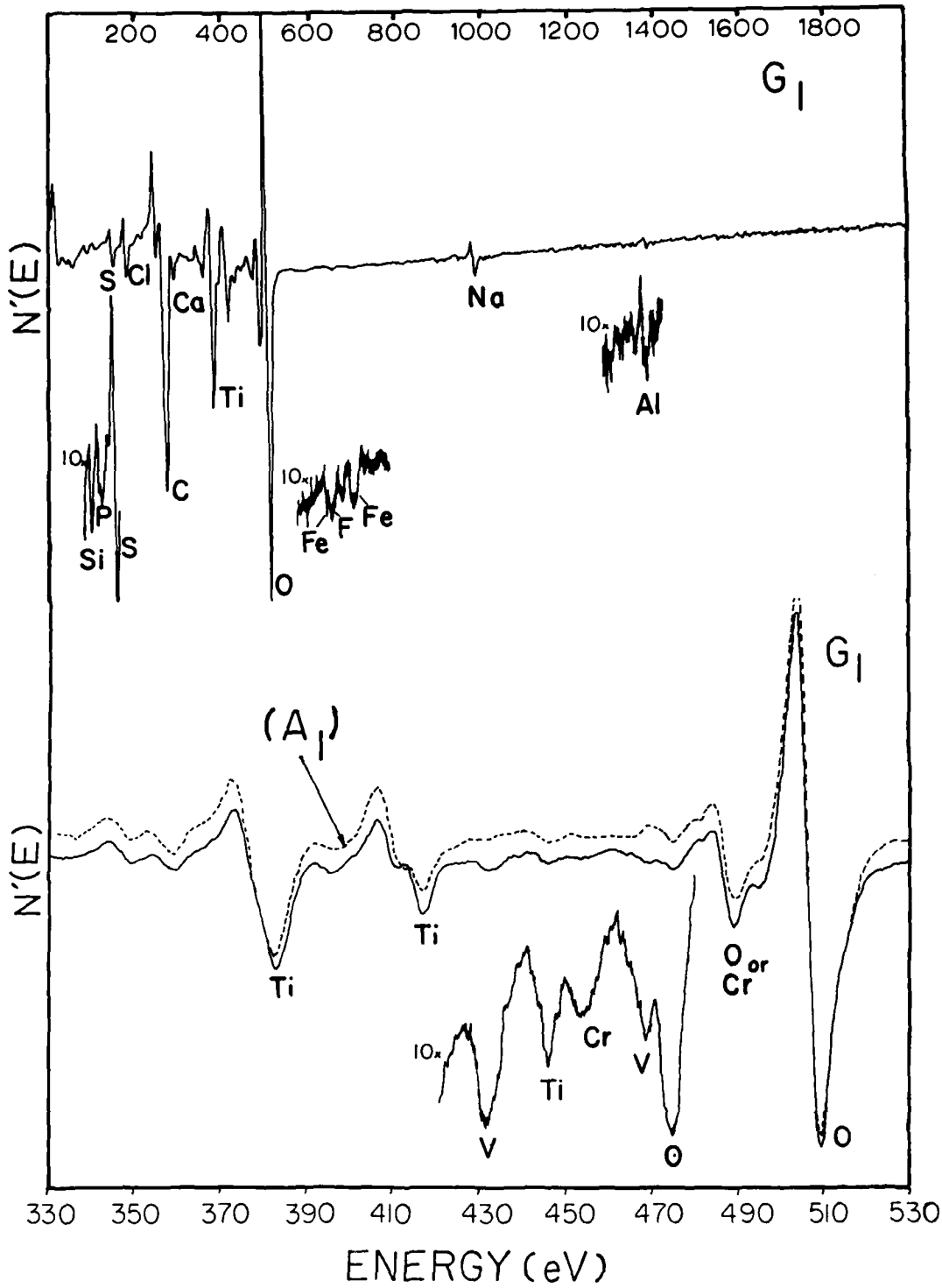

FIG. 81 A.E.S. spectra of Ti-13V-11Cr-3Al(G_1) and titanium(A_1) subjected to 1 treatment (0-2000 eV and 330-530 eV)

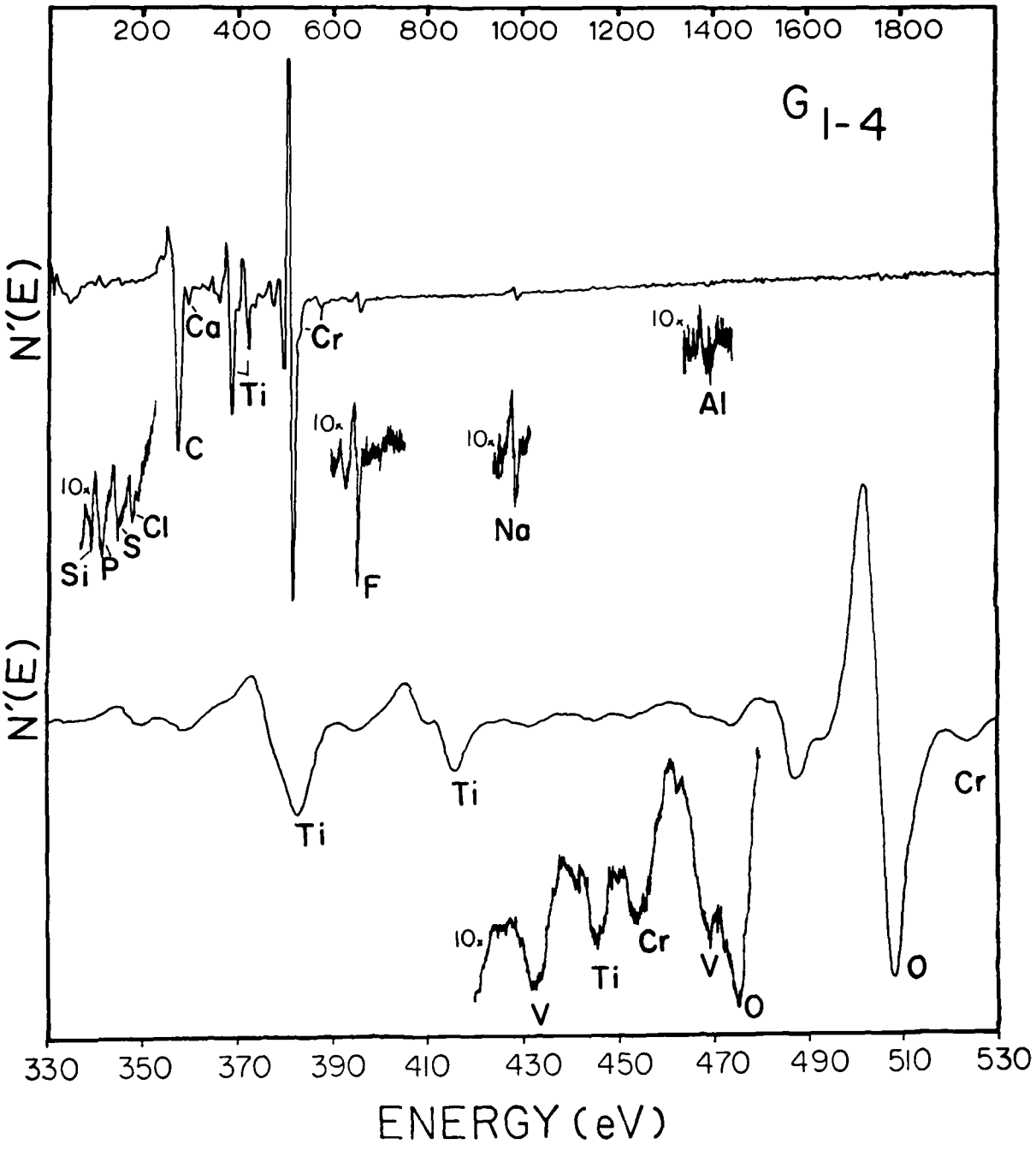

FIG. 82 A.E.S. spectra of Ti-13V-11Cr-3Al subjected to 1-4 treatment (0-2000 eV and 330-530 eV)

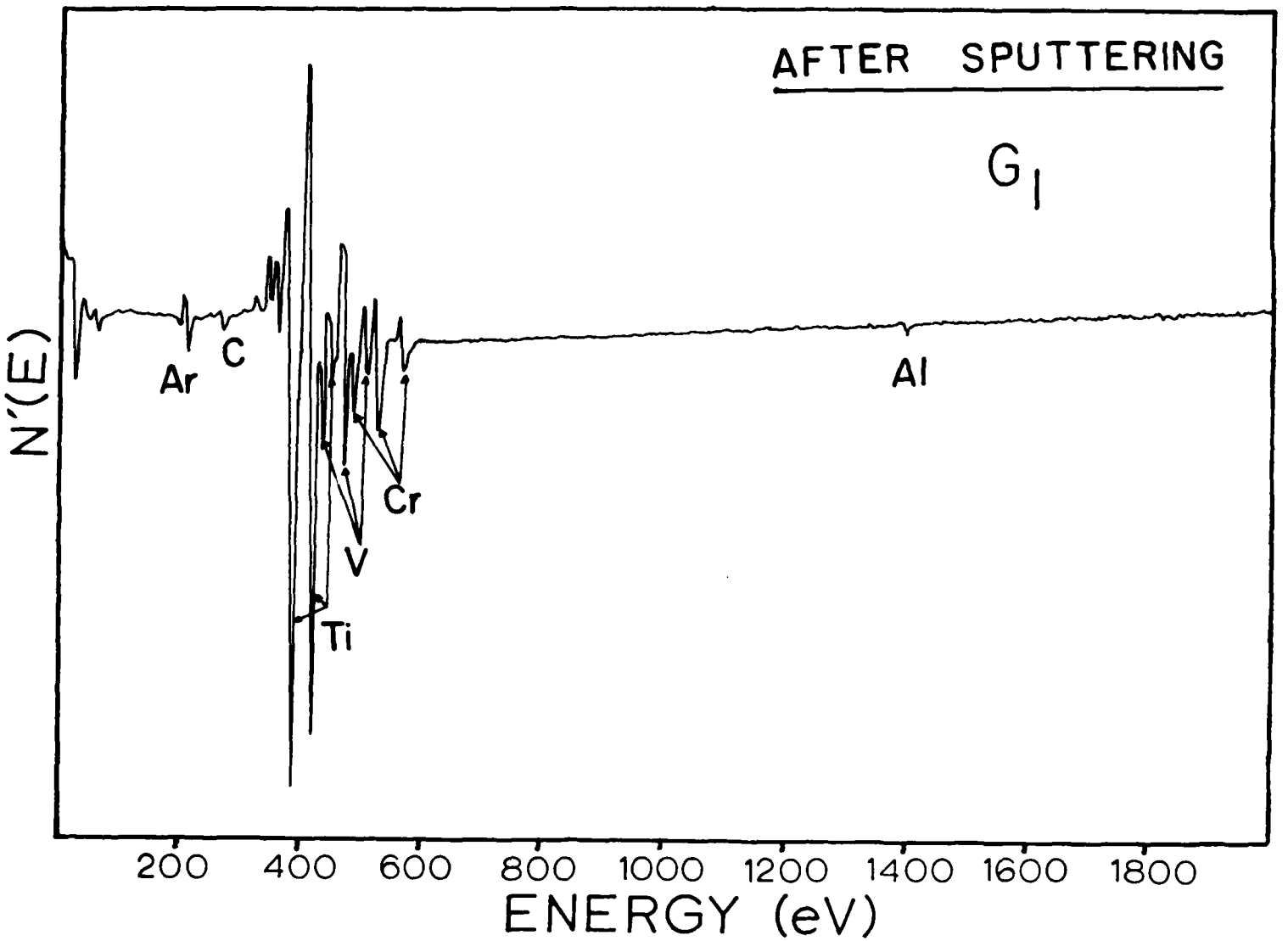

FIG. 83 A.E.S. Equilibrium Sputtered spectrum of Ti-13V-11Cr-3Al subjected to 1 treatment

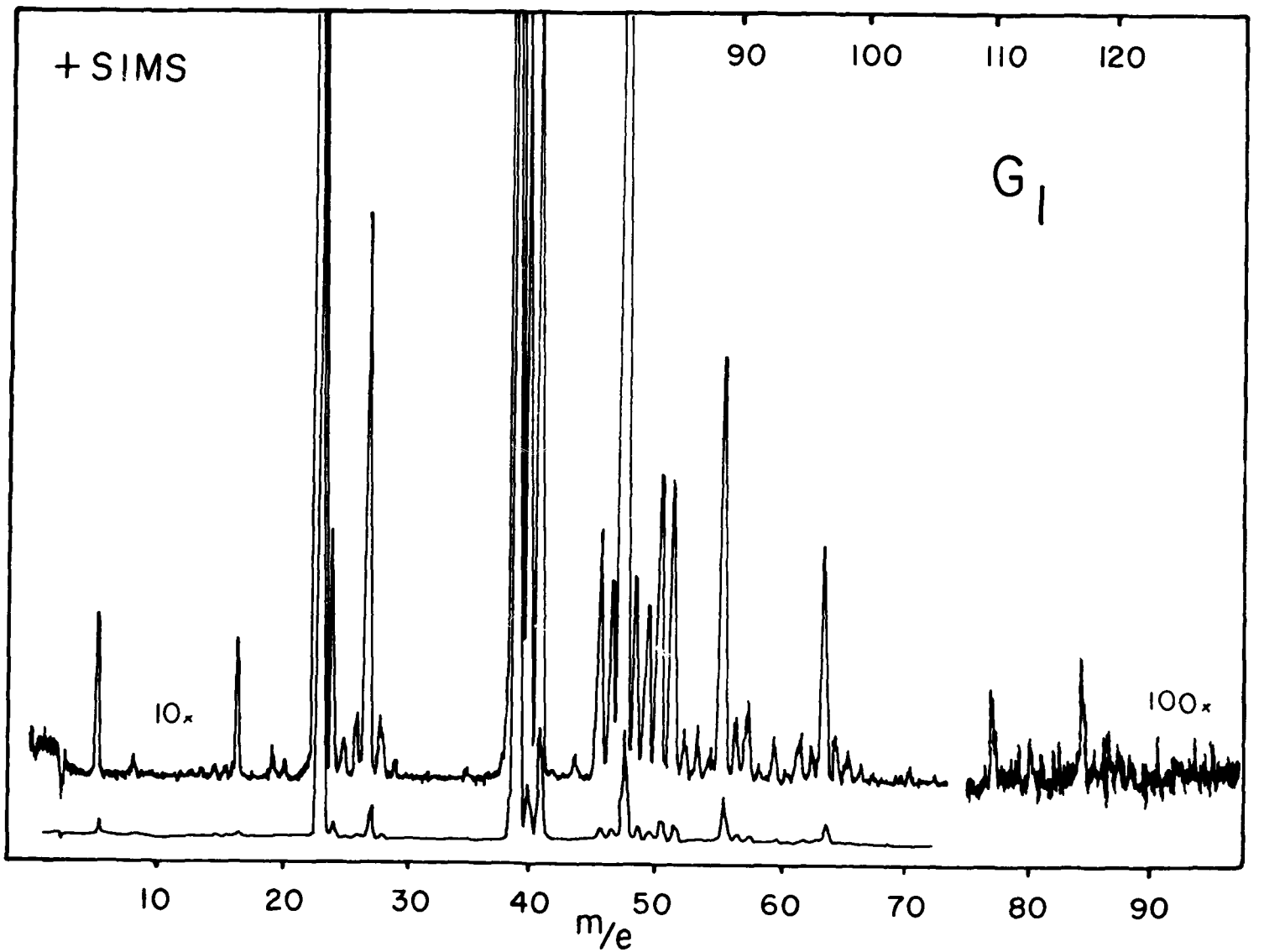

FIG. 84 Positive ion SIMS spectra of Ti-13V-11Cr-3Al subjected to 1 treatment

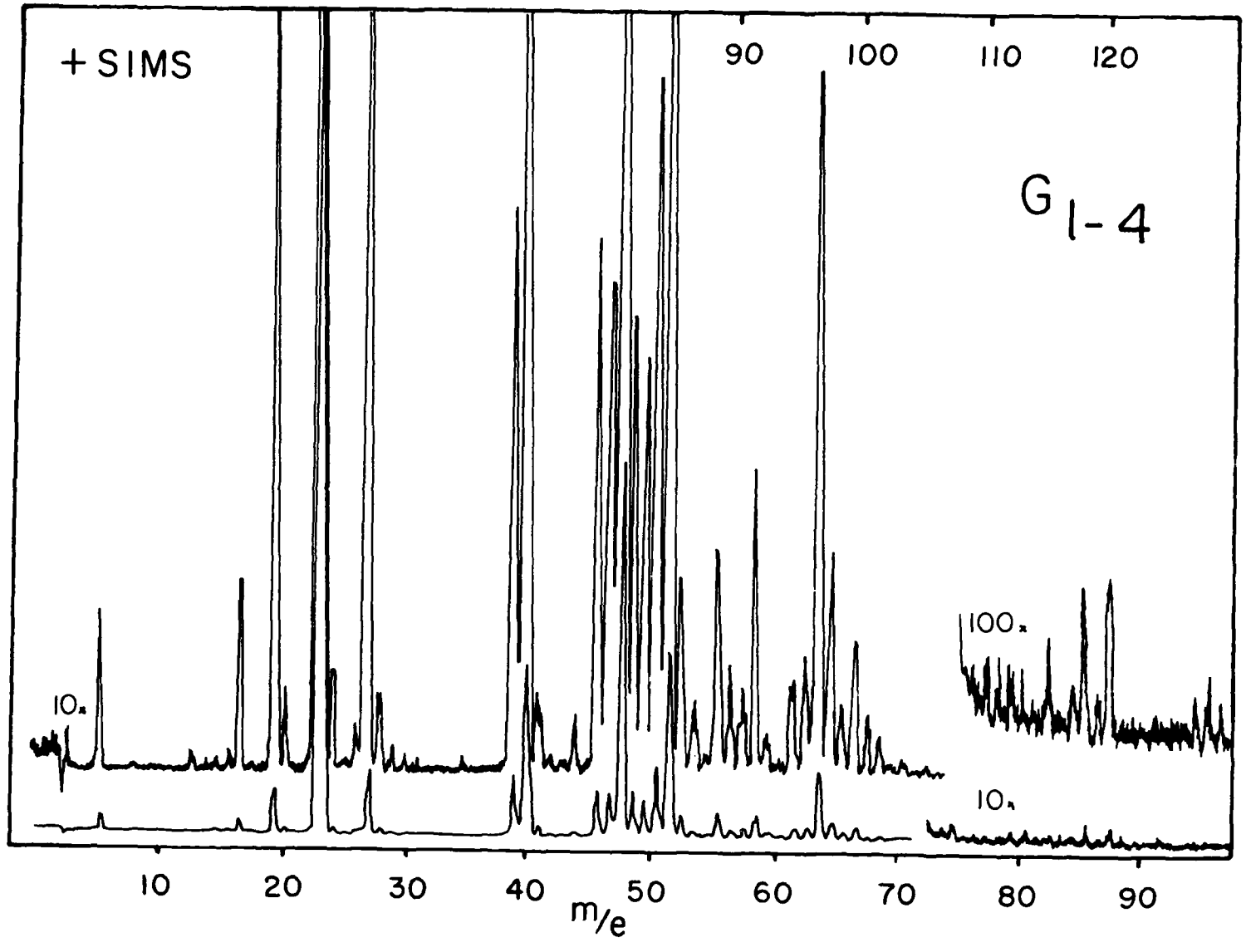

FIG. 85 Positive ion SIMS spectra of Ti-13V-11Cr-3Al subjected to 1-4 treatment

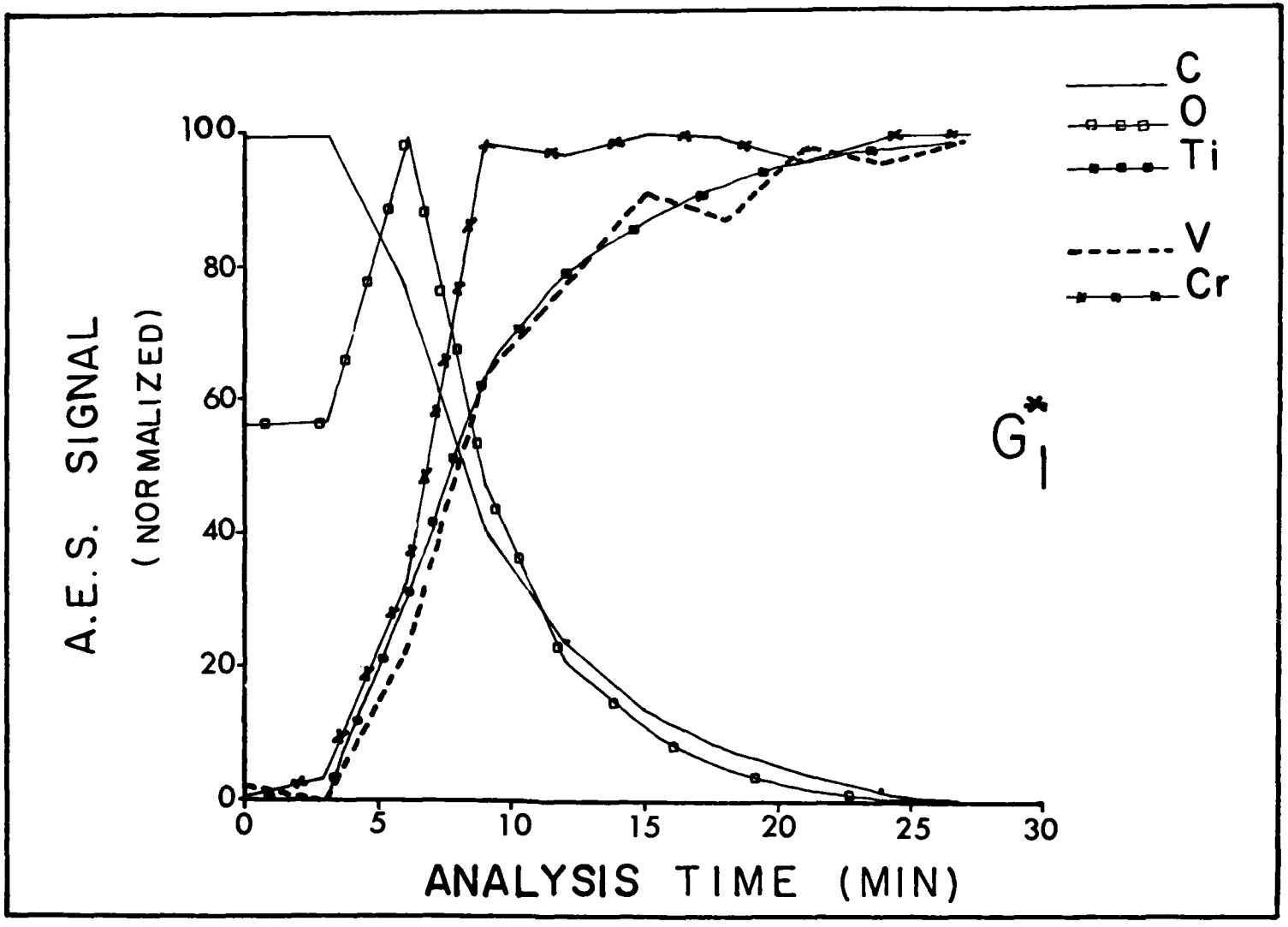

FIG. 86 A.E.S. sputter profiles of Ti-13V-11Cr-3Al subjected to 1 treatment

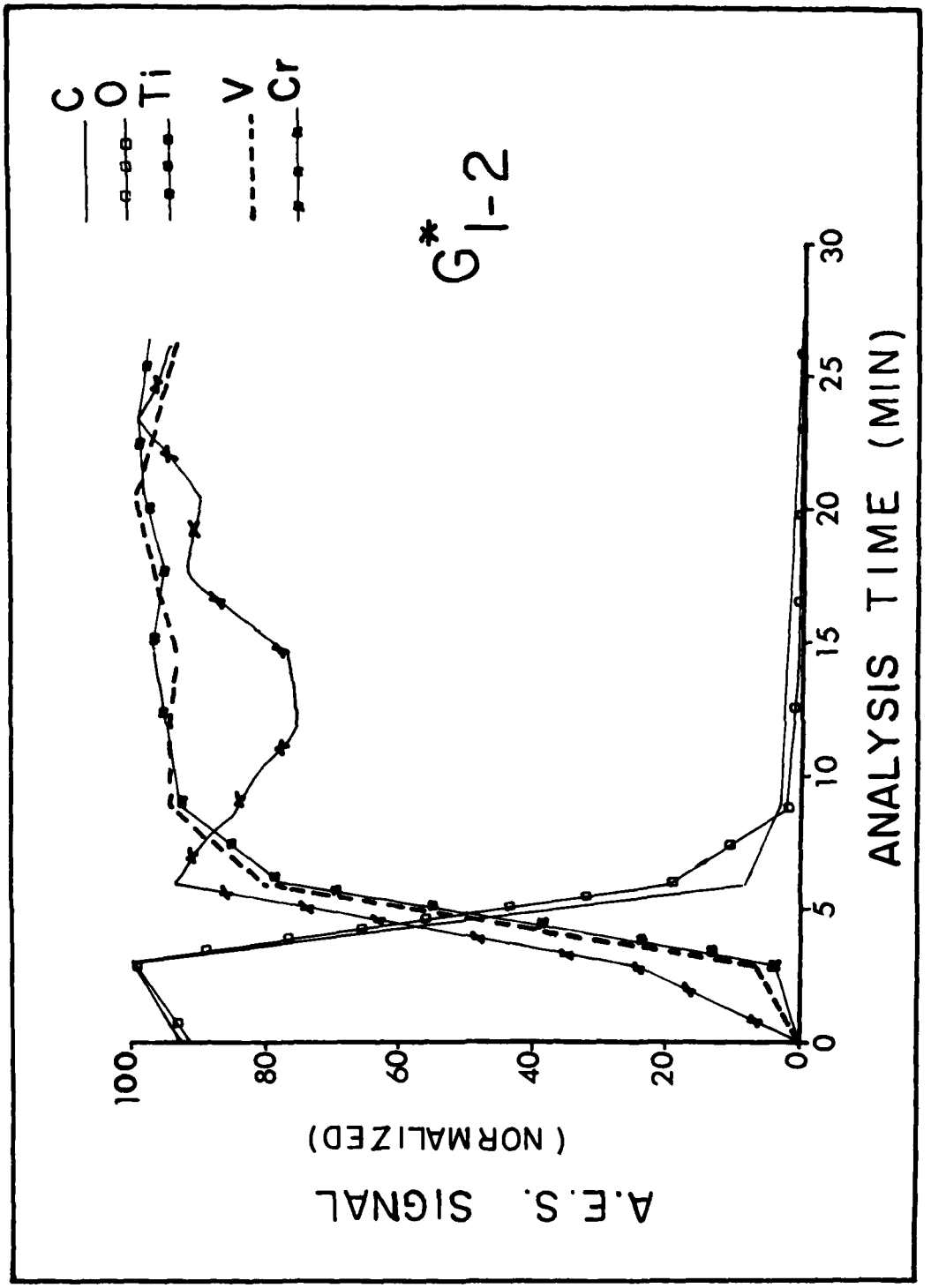

FIG. 87 A.E.S. sputter profiles of Ti-13V-11Cr-3Al subjected to 1-2 treatment

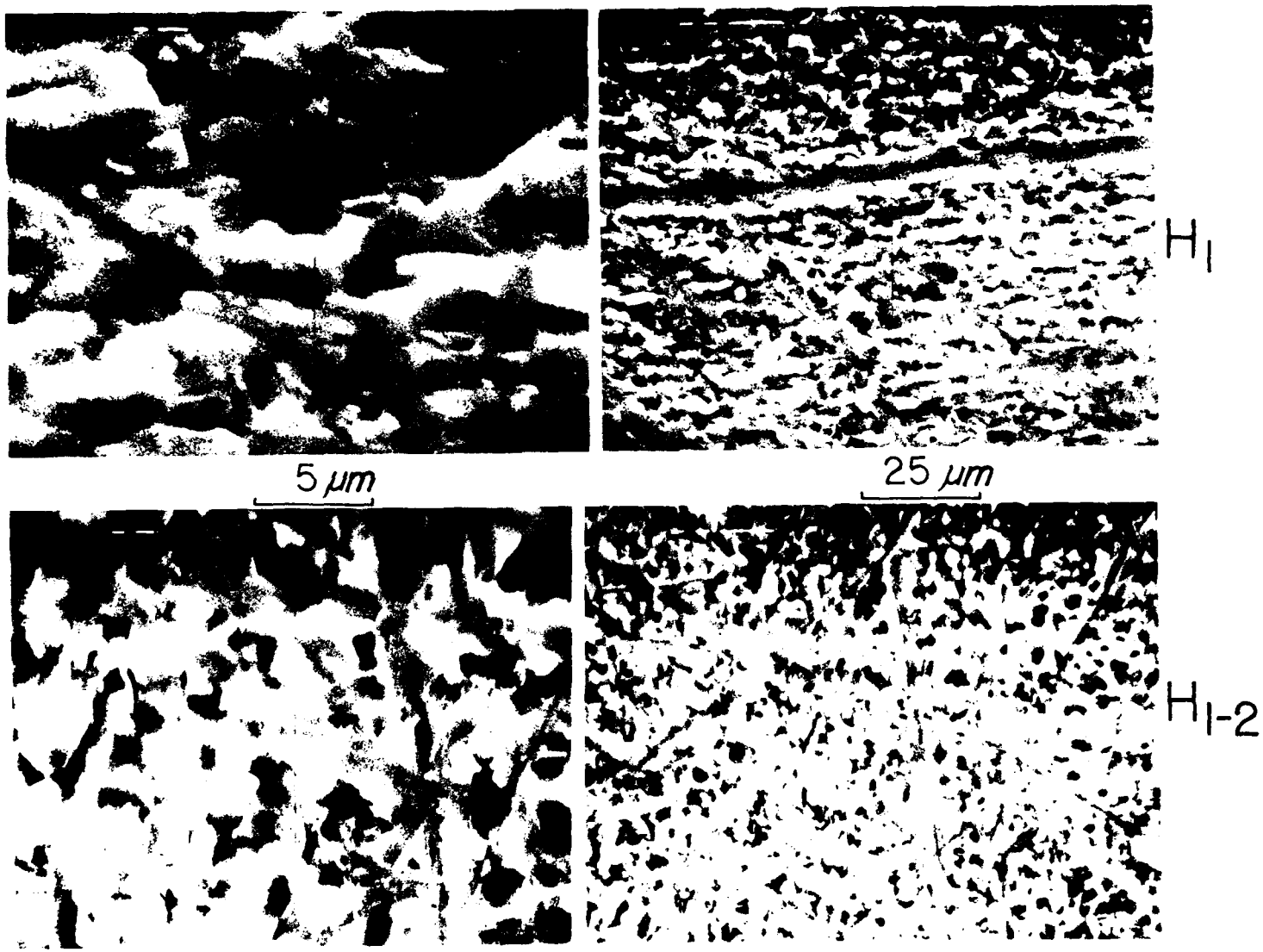

FIG. 88 S.E.M. photomicrographs of Ti-8Mn subjected to 1 and 1-2 treatments

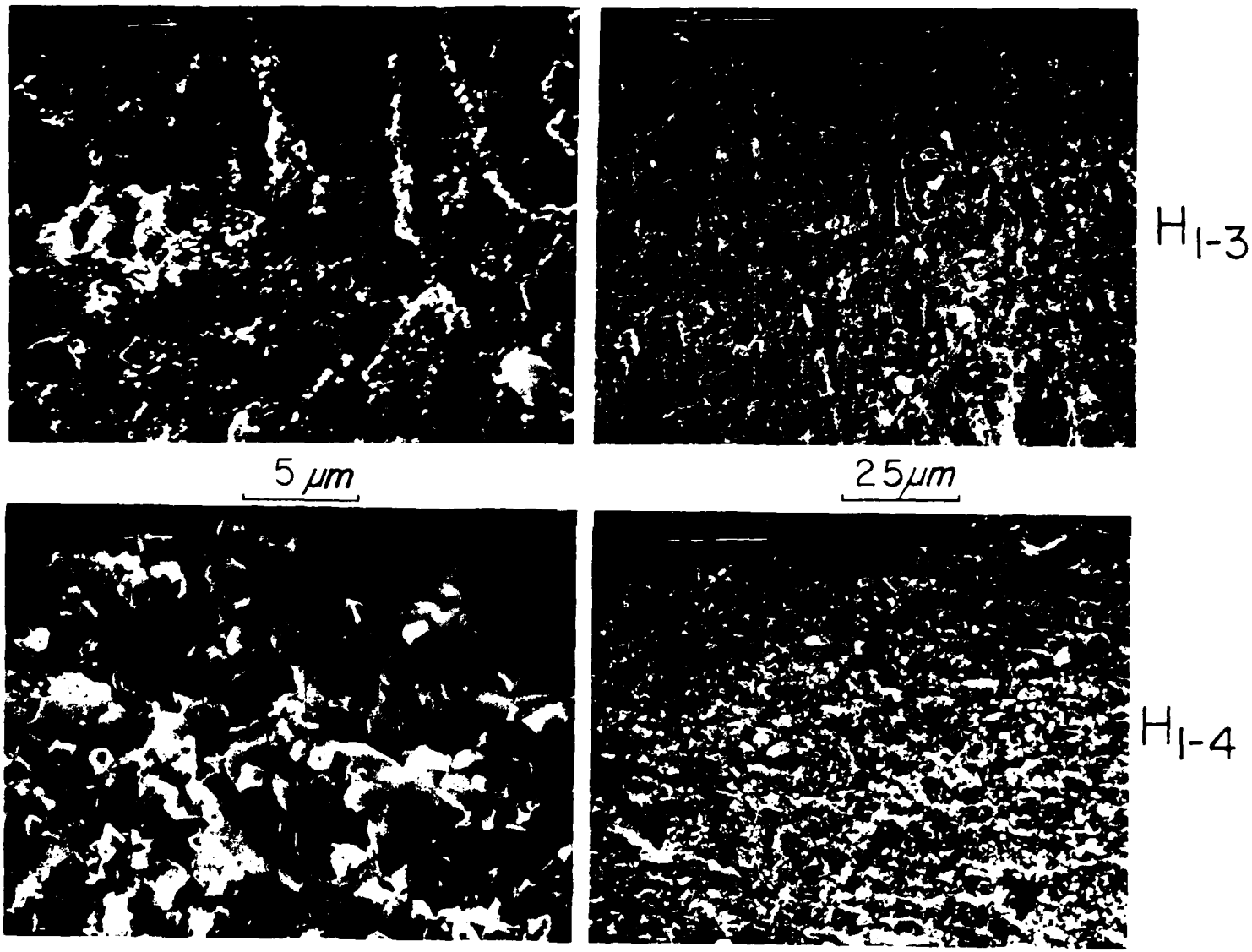

FIG. 89 S.E.M. photomicrographs of Ti-8Mn subjected to 1-3 and 1-4 treatments

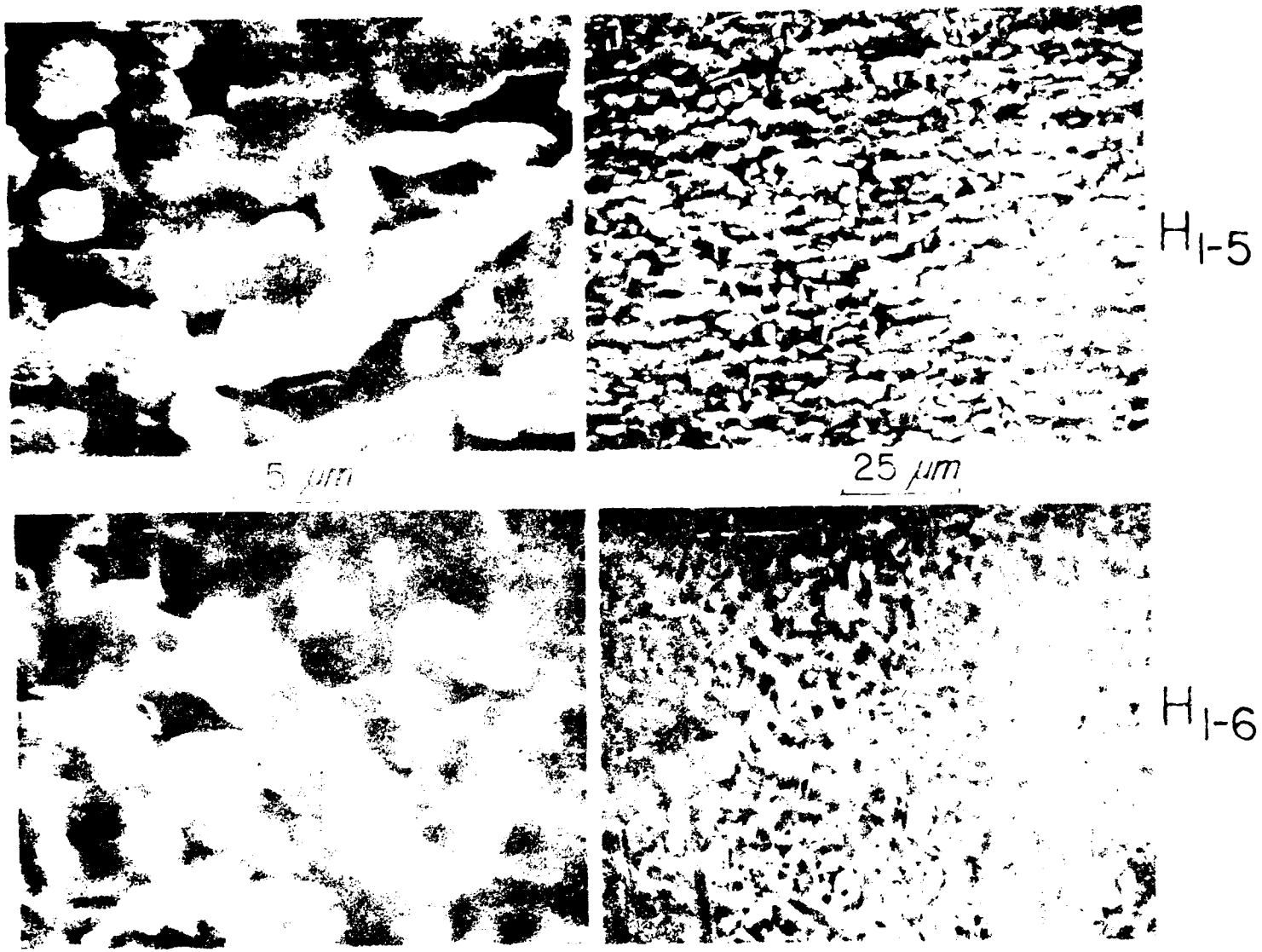

FIG. 90 S.E.M. [illegible] of [illegible] exposed to I-5 and I-6 treatments

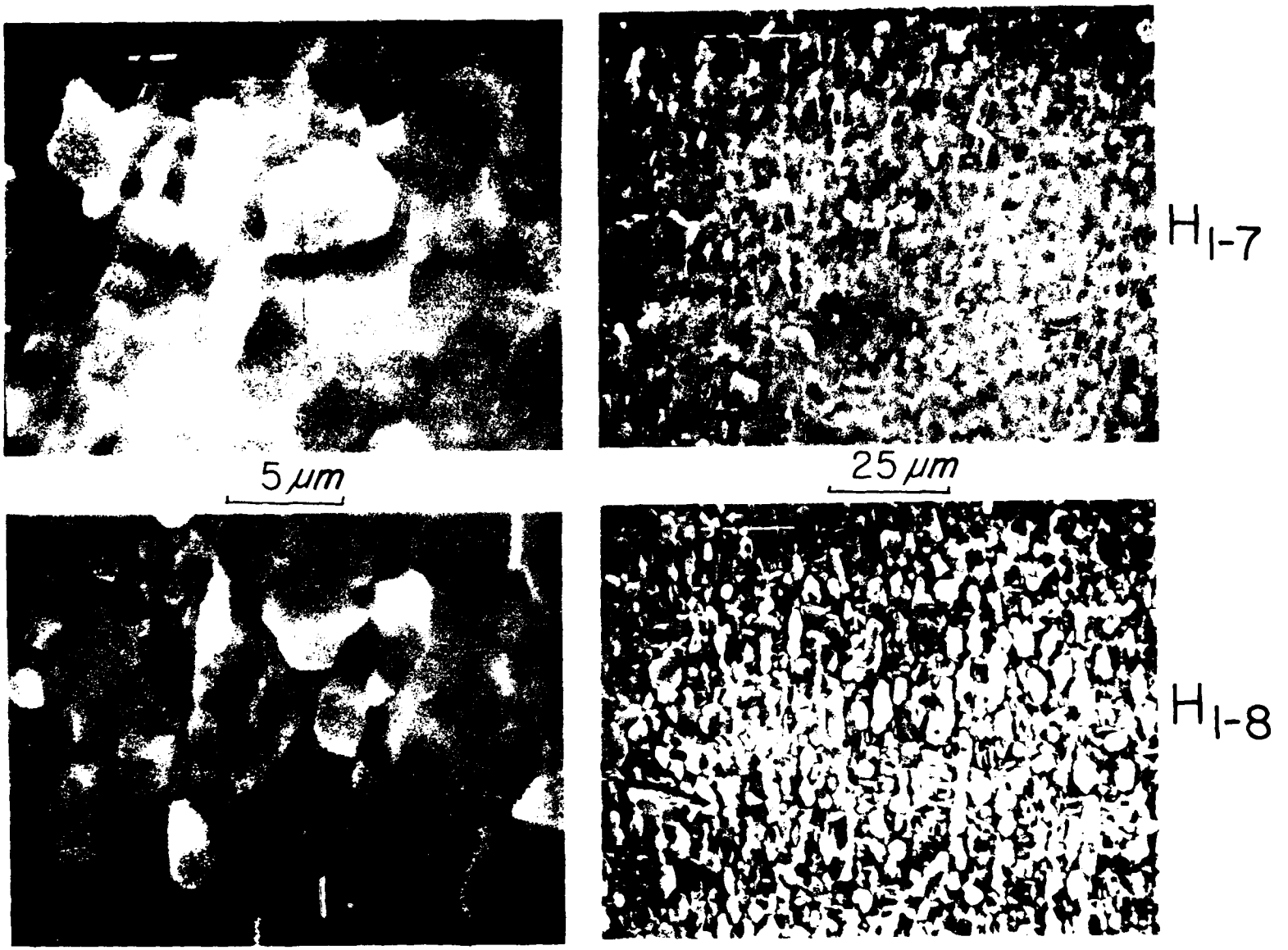

FIG. 91 S.E.M. photomicrographs of Ti-8Mn subjected to 1-7 and 1-8 treatments

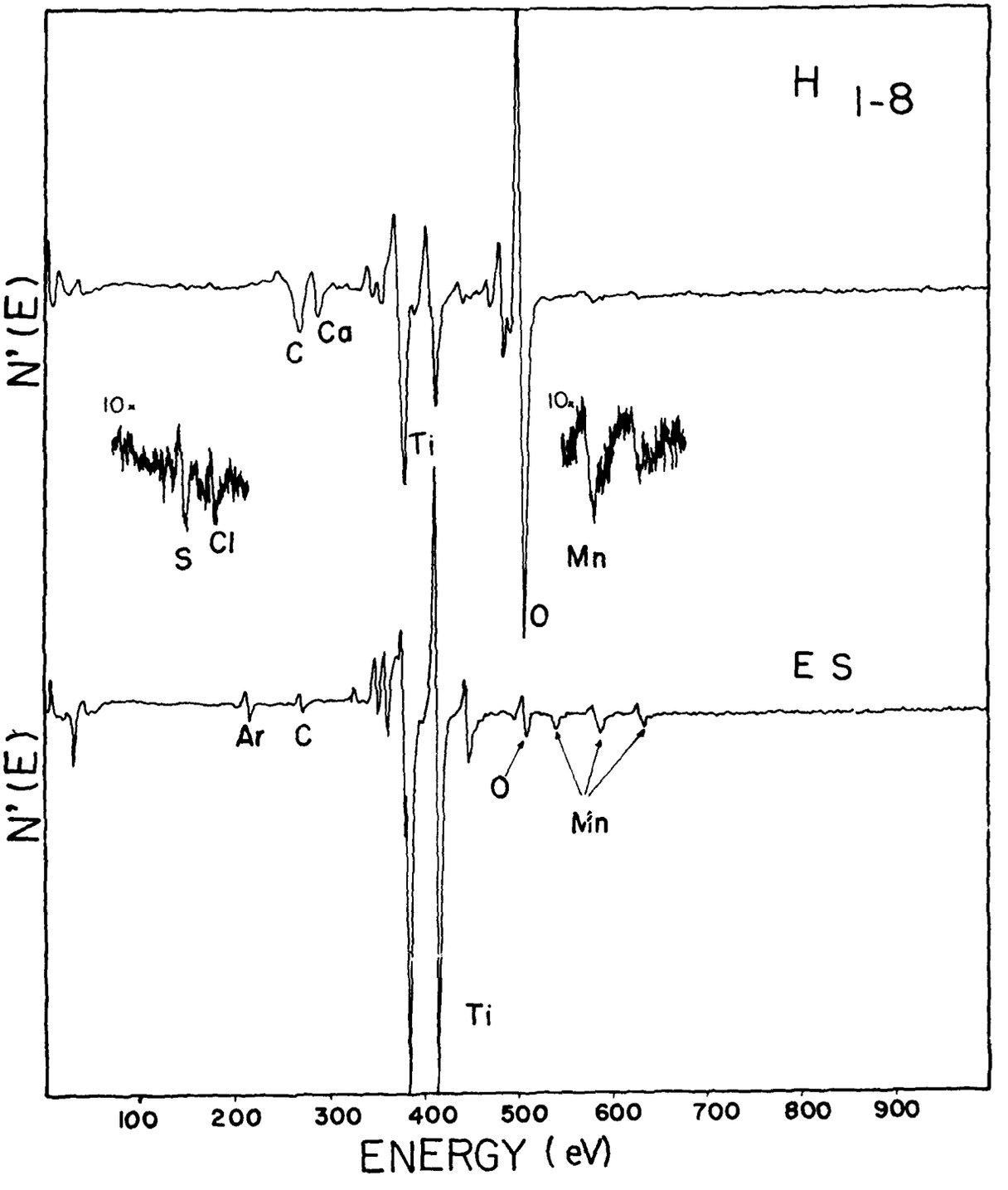

FIG. 92 A.E.S. spectra of Ti-8Mn subjected to 1-8 treatment (0-1000 eV) and Equilibrium Sputtered A.E.S. of Ti-8Mn (0-1000 eV)

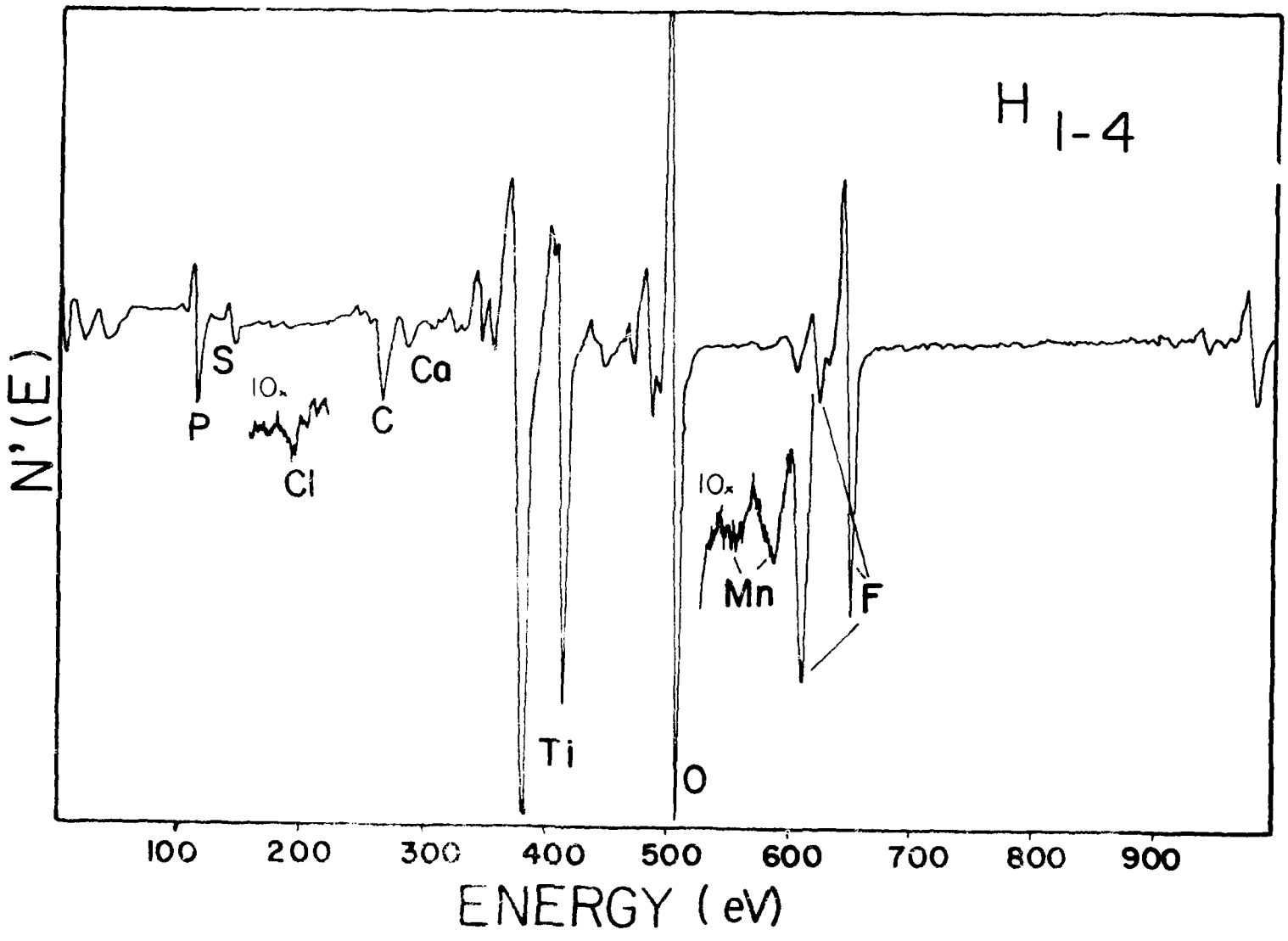

FIG. 93 A.E.S. spectra of Ti-Mn subjected to 1-4 treatment (0-1000 eV)

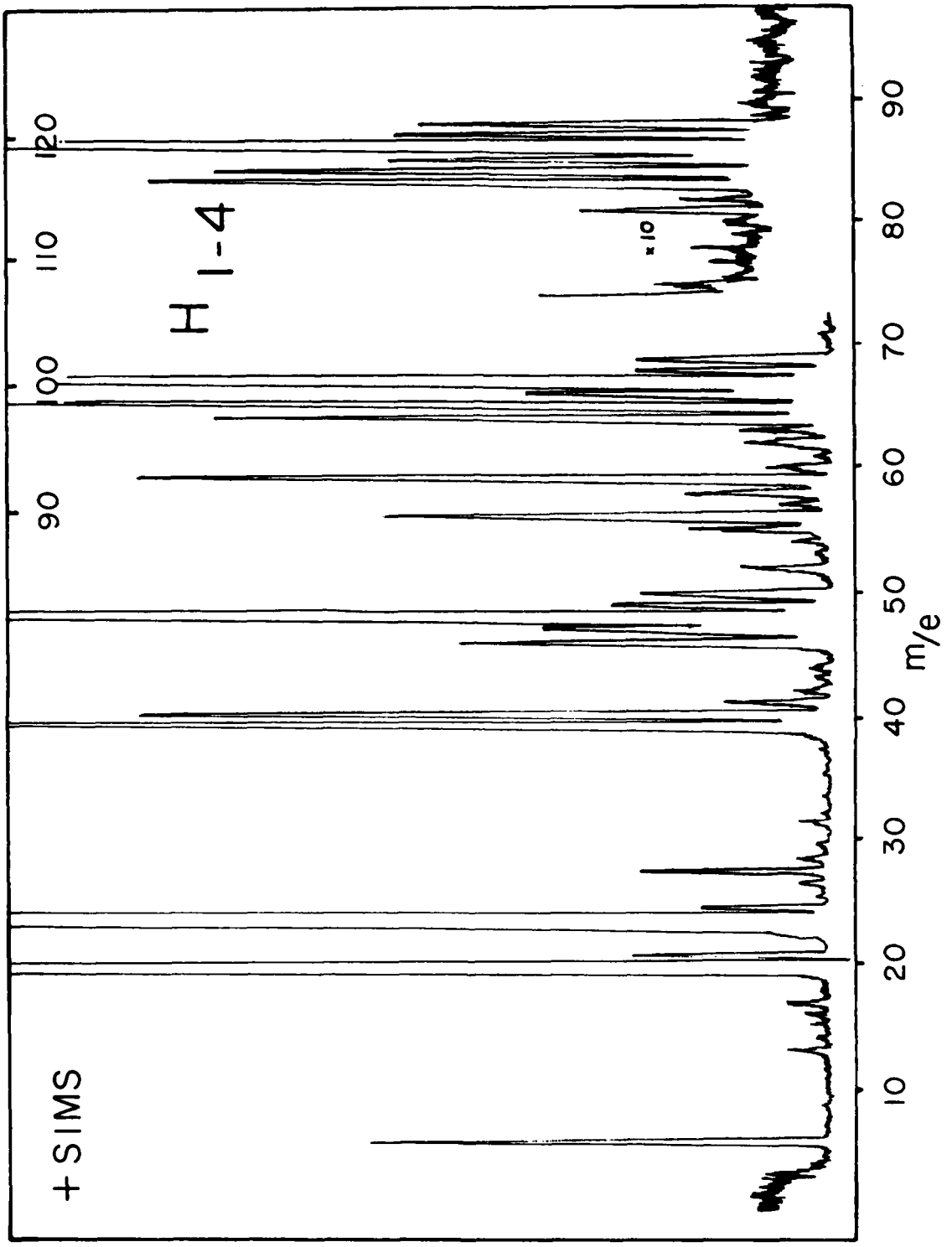

FIG. 94 Positive ion SIMS spectra of Ti-8Mn subjected to 1-4 treatment

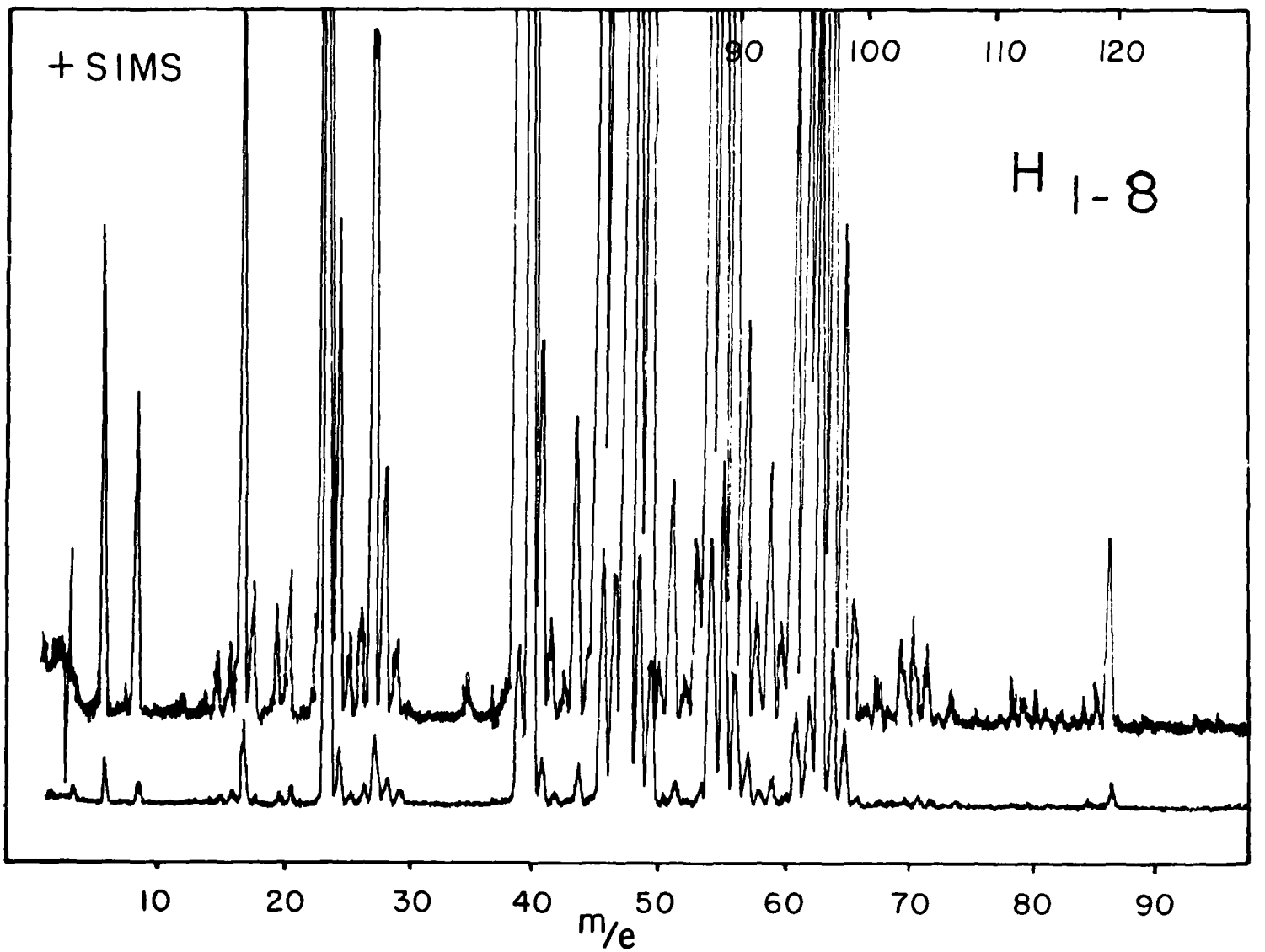

FIG. 95 Positive ion SIMS spectra of Ti-8Mn subjected to 1-8 treatment

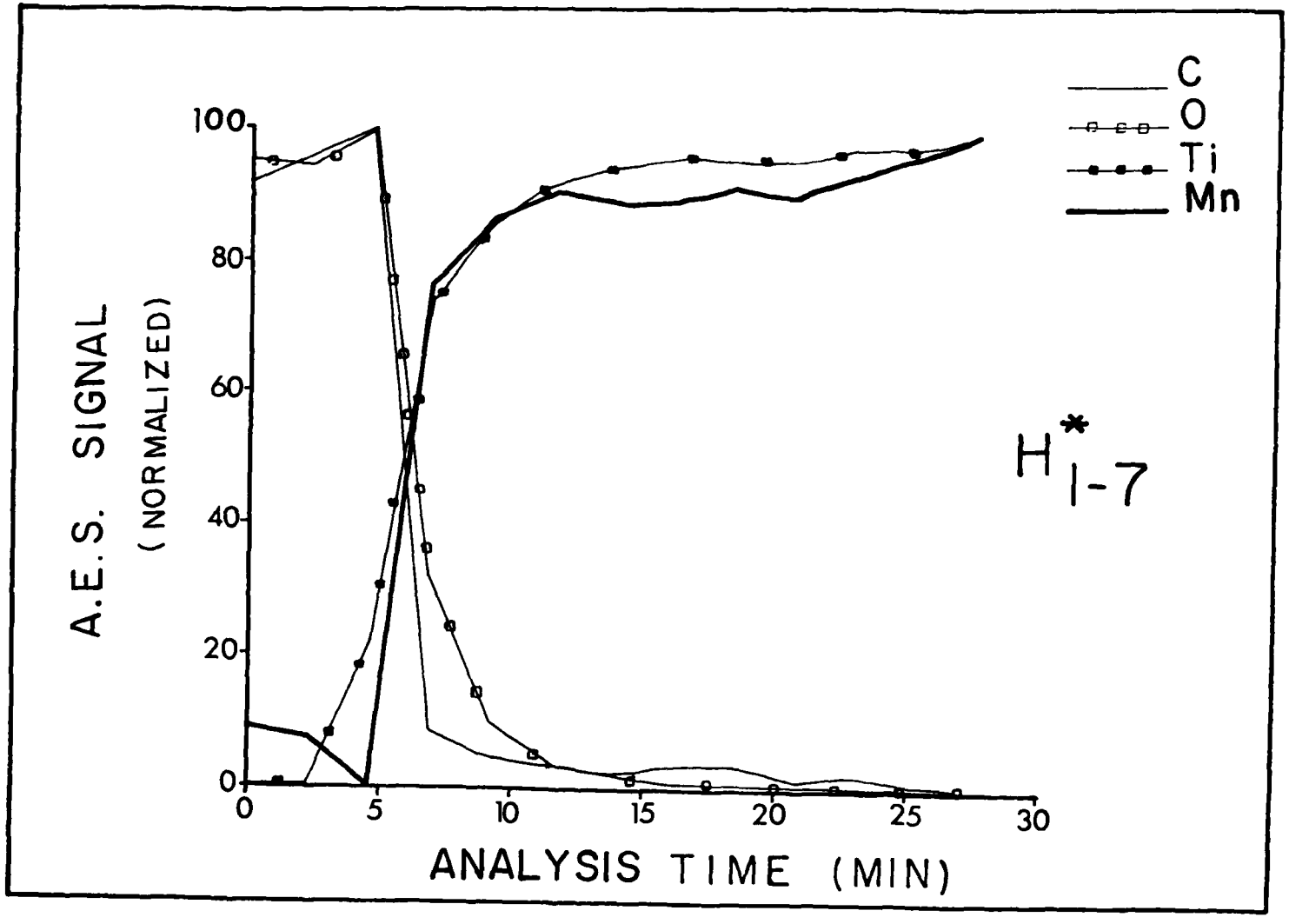

FIG. 96 A.E.S. sputter profiles of Ti-8Mn subjected to 1-7 treatment

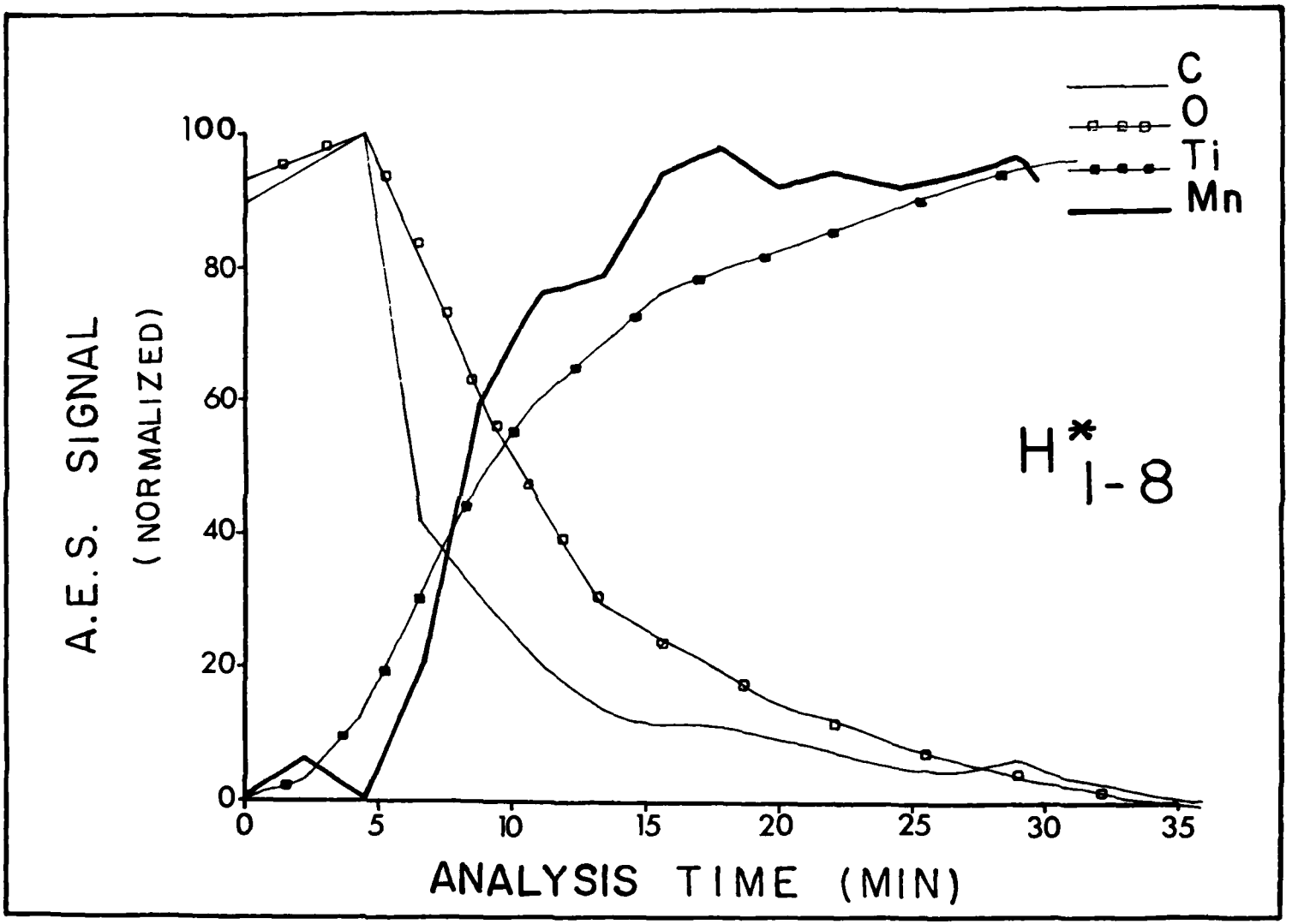

FIG. 97 A.E.S. sputter profiles of Ti-8Mn subjected to 1-8 treatment

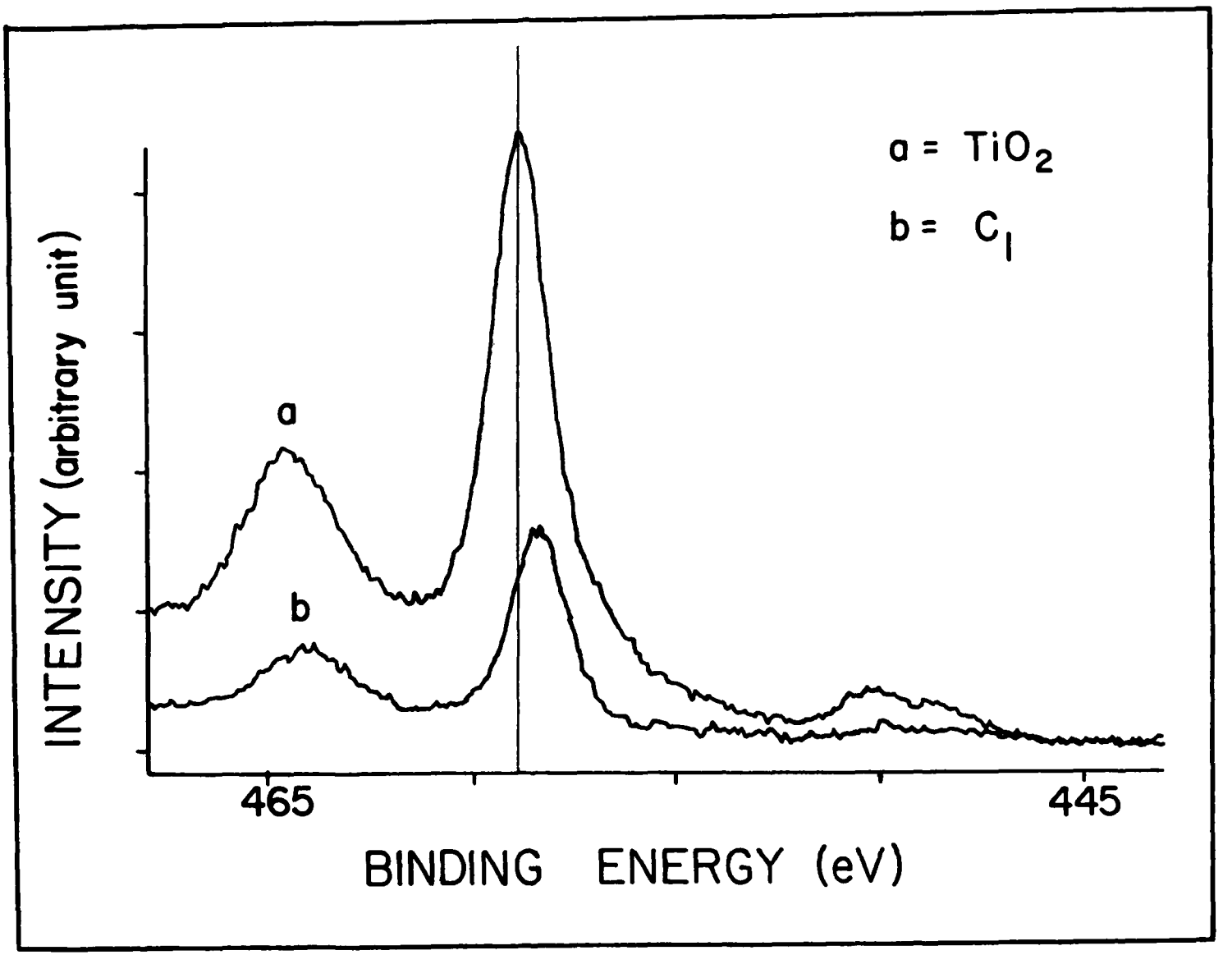

FIG. 98 X.P.S. spectra of Ti_{2p}: (a) TiO_2"standard," (b) natural oxide on degreased Ti-6Al-4V

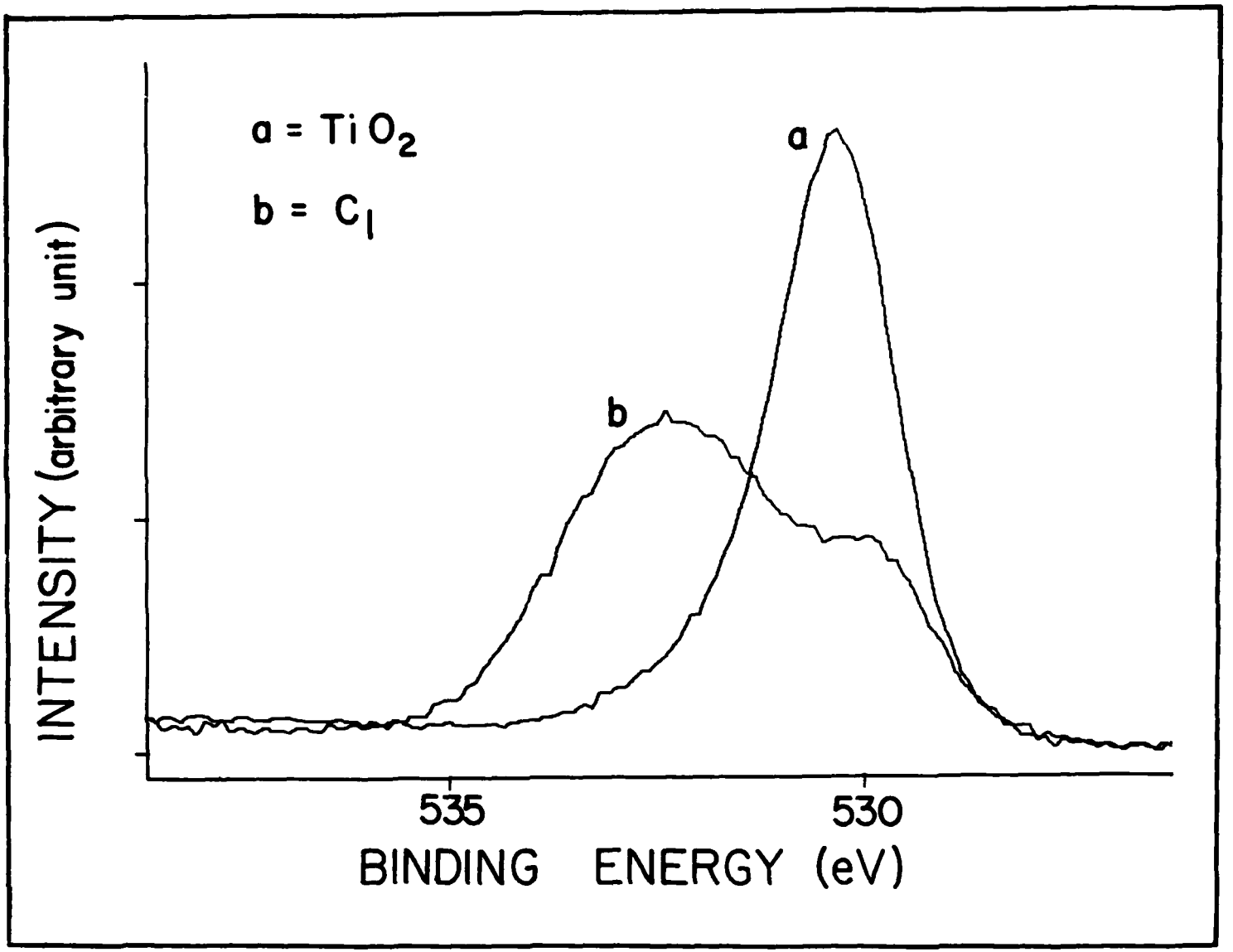

FIG. 99 X.P.S. spectra of O_1: (a) TiO_2"standard," (b) natural oxide on degreased Ti-6Al-4V

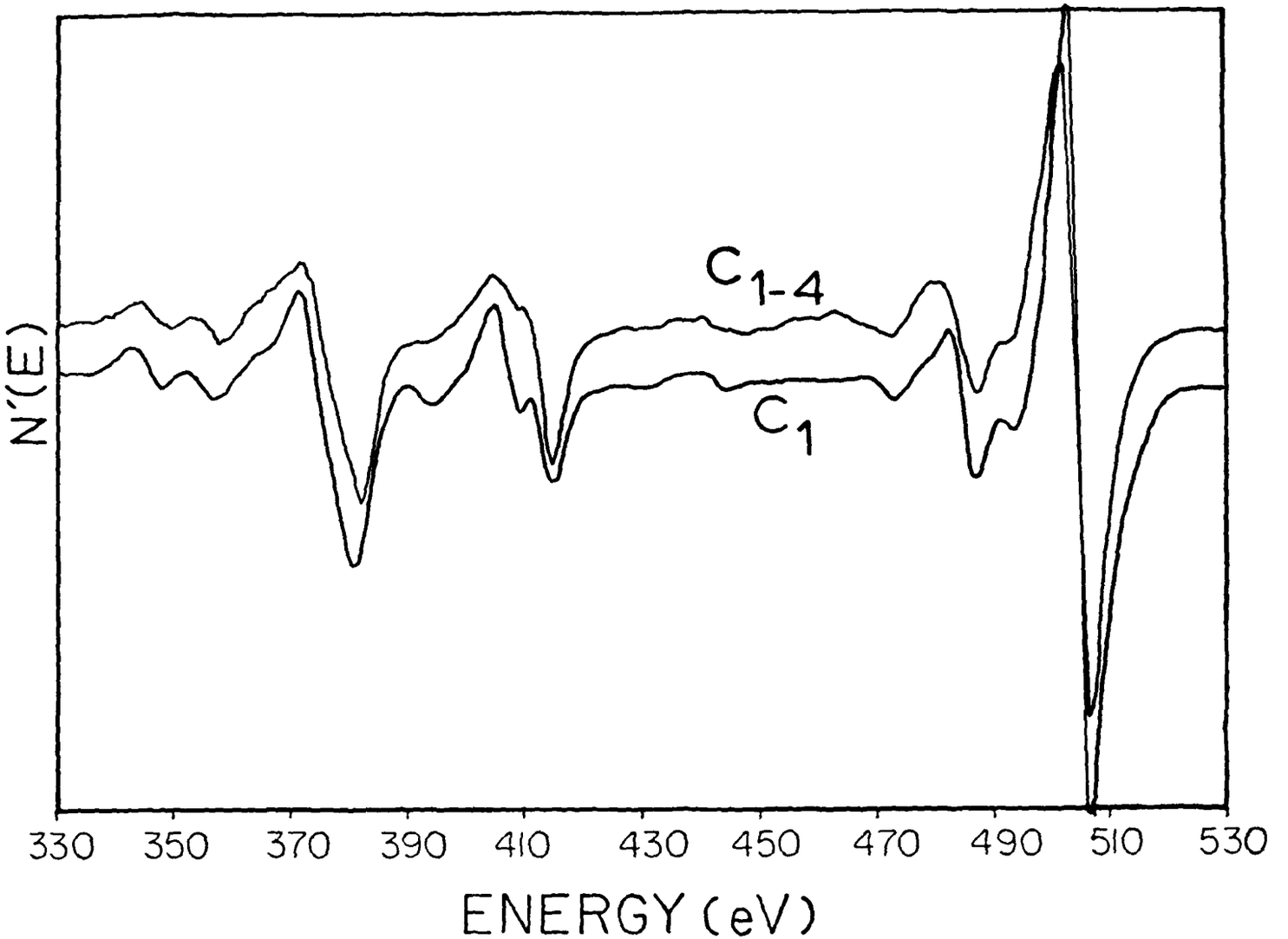

FIG. 100 A.E.S. spectra of Ti-6Al-4V subjected to degrease treatment (1) and to fluorophosphate treatment (1-4) (330-530 eV)

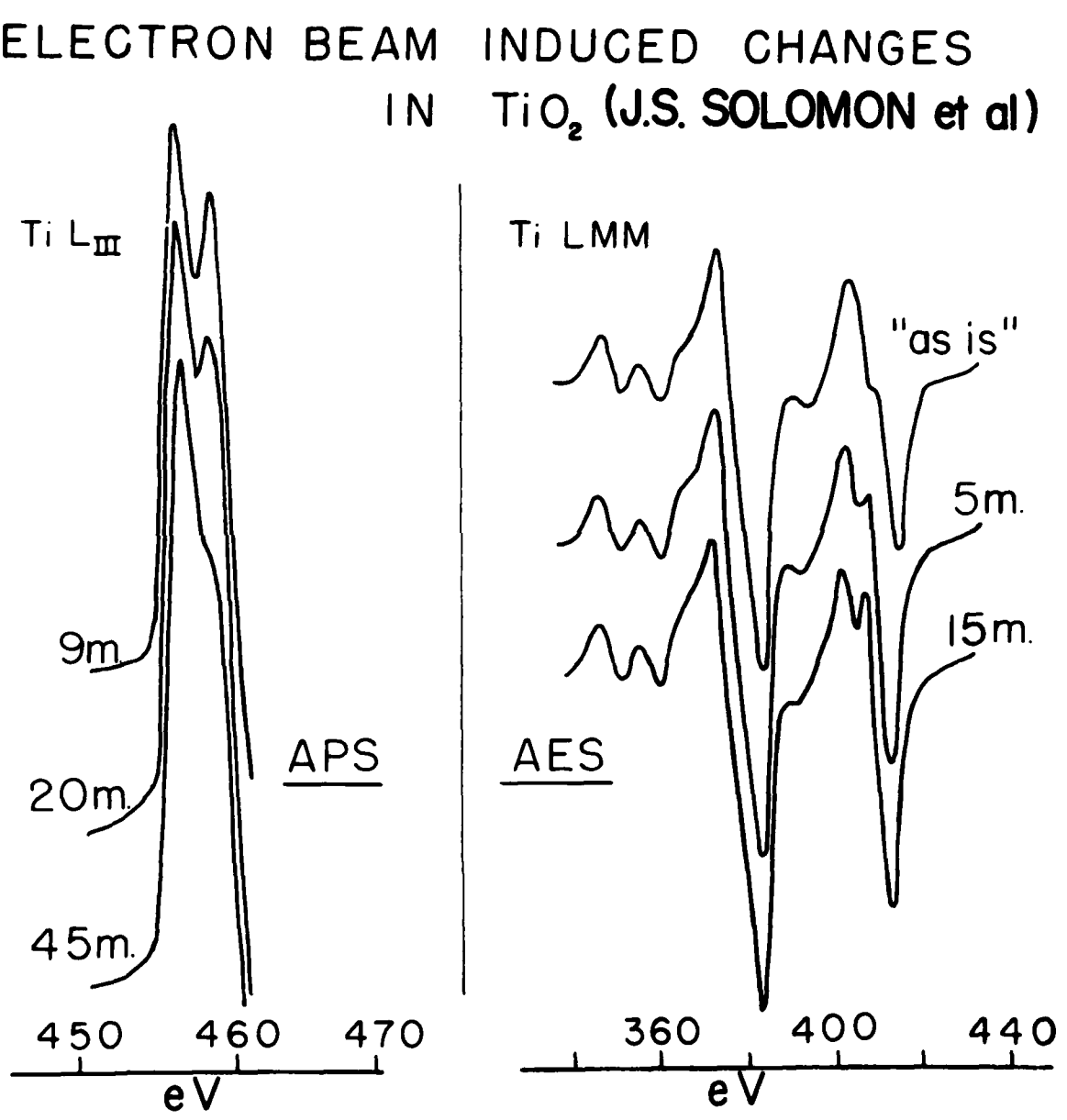

FIG. 101 A.E.S. and A.P.S. spectra of TiO_2 by J.S. Solomon et. al. (Ref. 16).

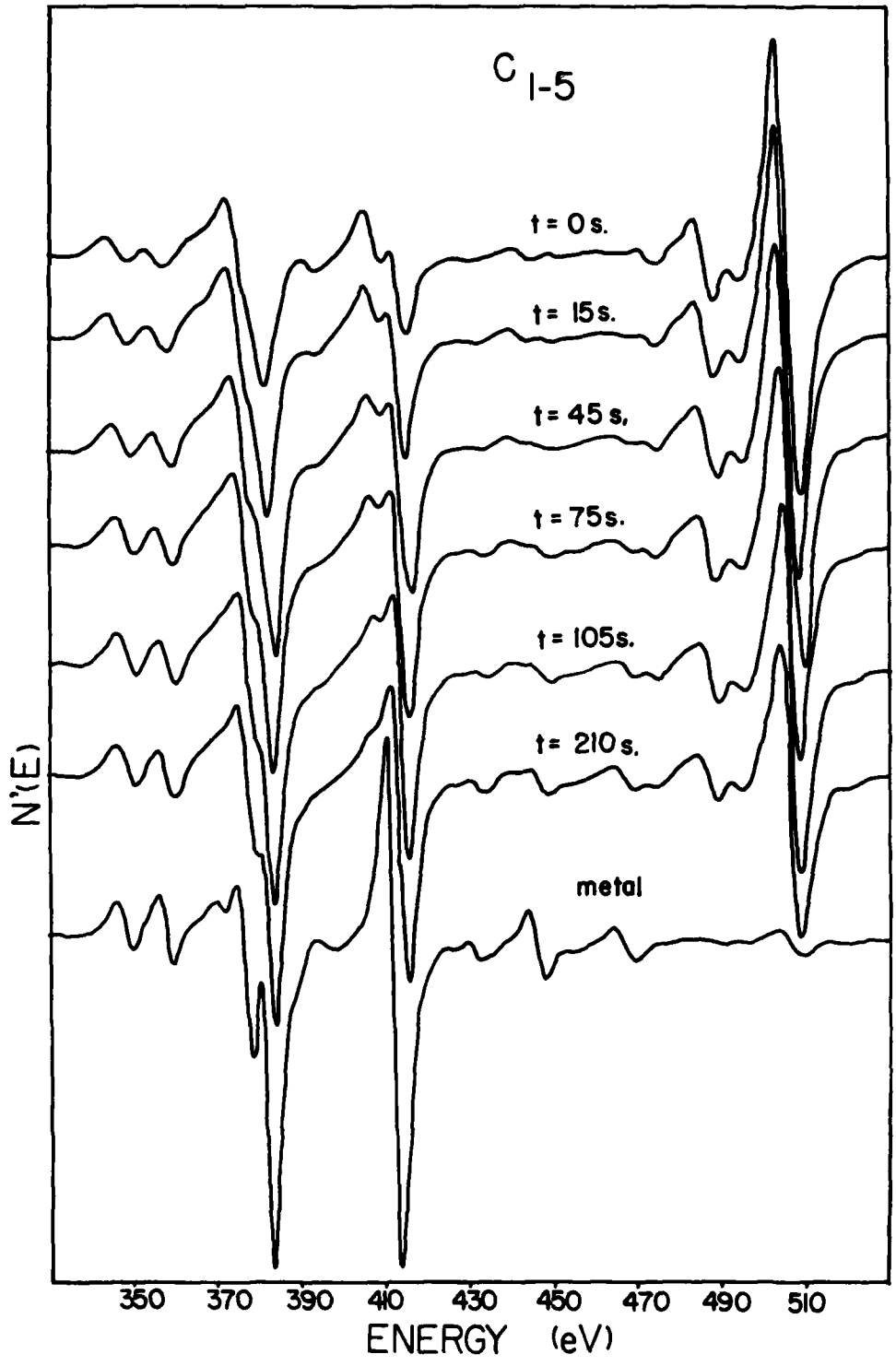

FIG. 102 AES spectra of Ti-6Al-4V subjected to 1-5 treatment at various times during sputtering (330-530 eV)

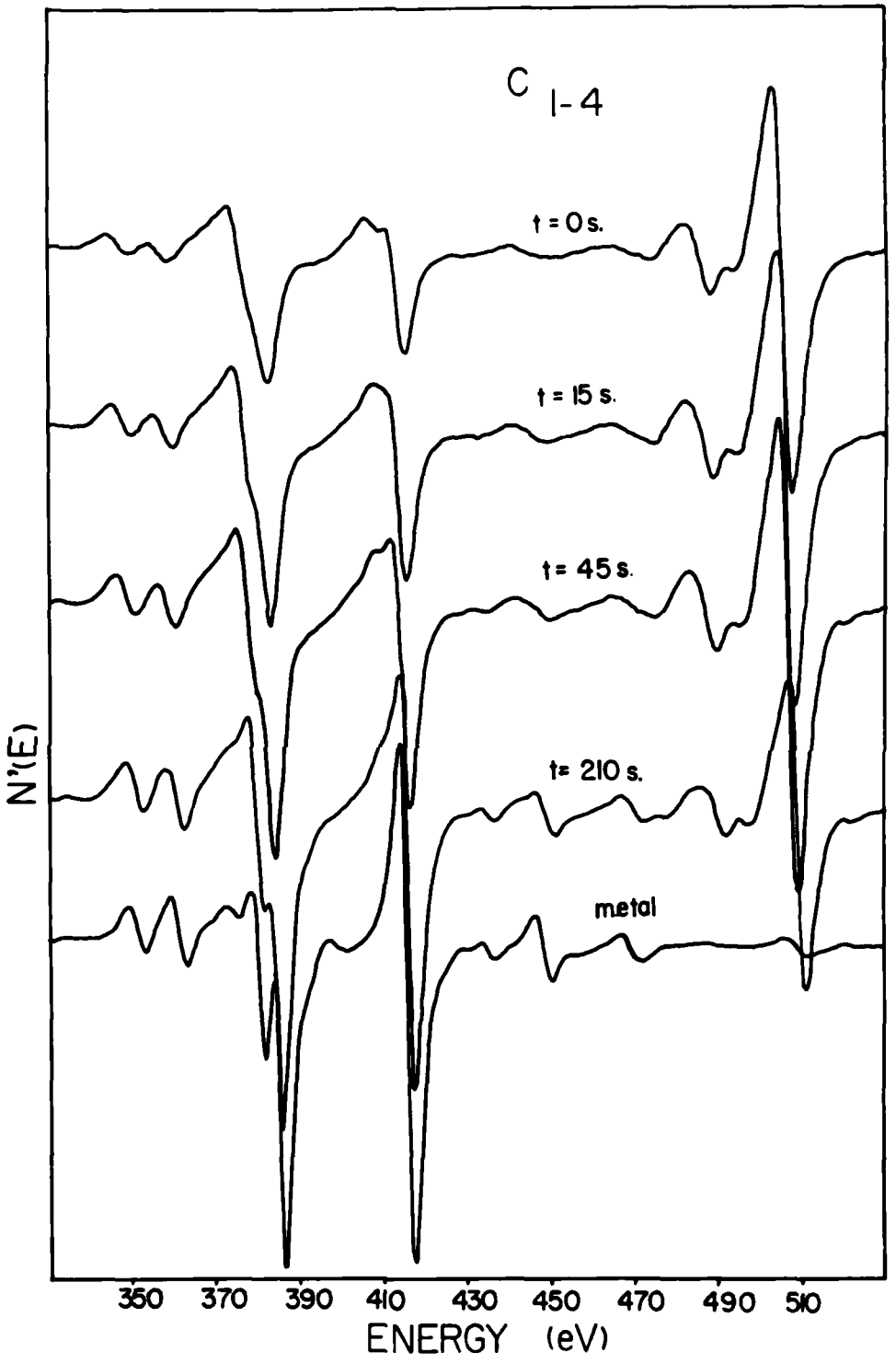

FIG. 103 A.E.S. spectra of Ti-6Al-4V subjected to 1-4 treatment at various times during sputtering (330-530 eV)

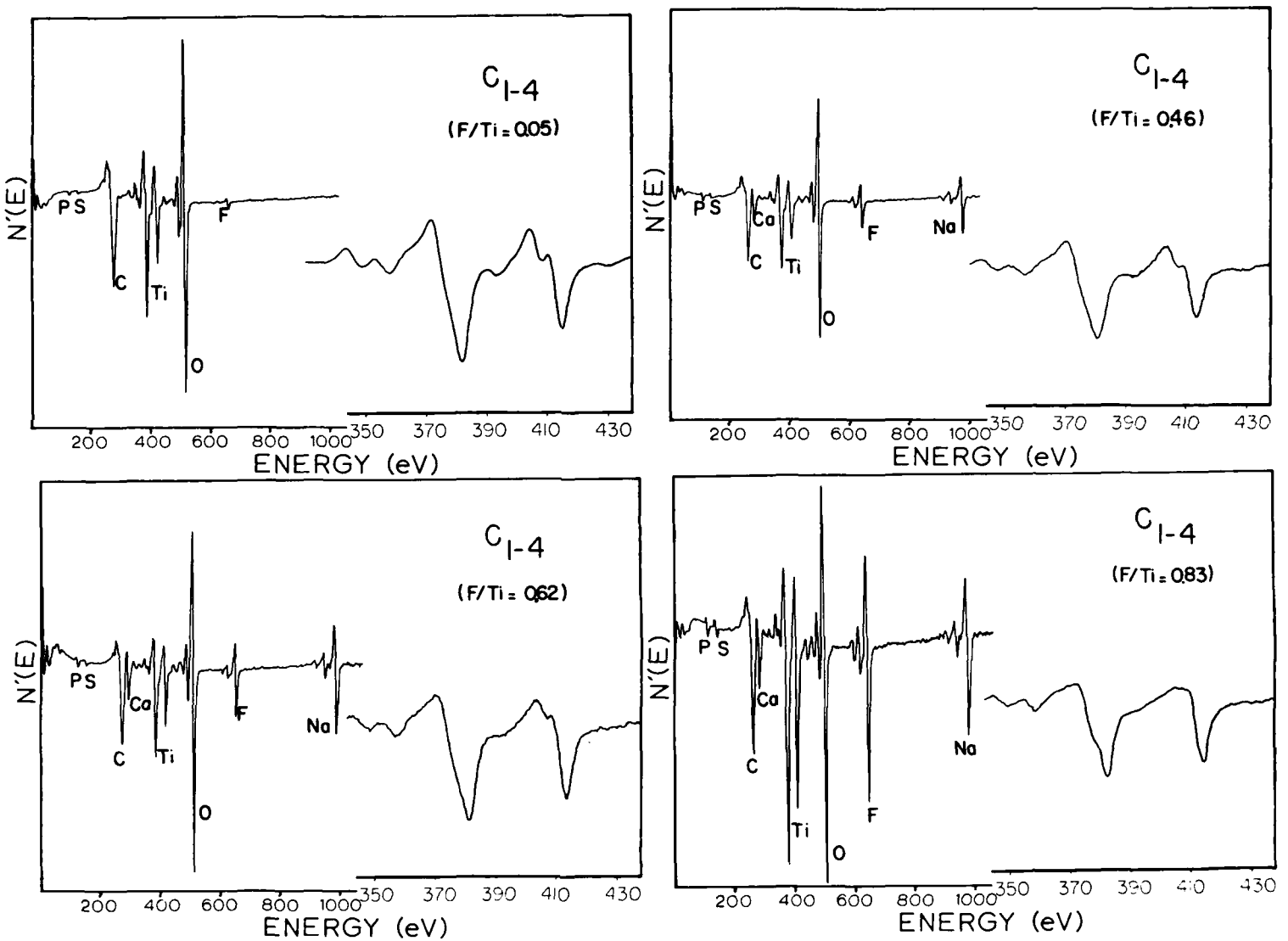

FIG. 104 A.E.S. spectra of Ti-6Al-4V subjected to 1-4 treatment in different places on the same panel

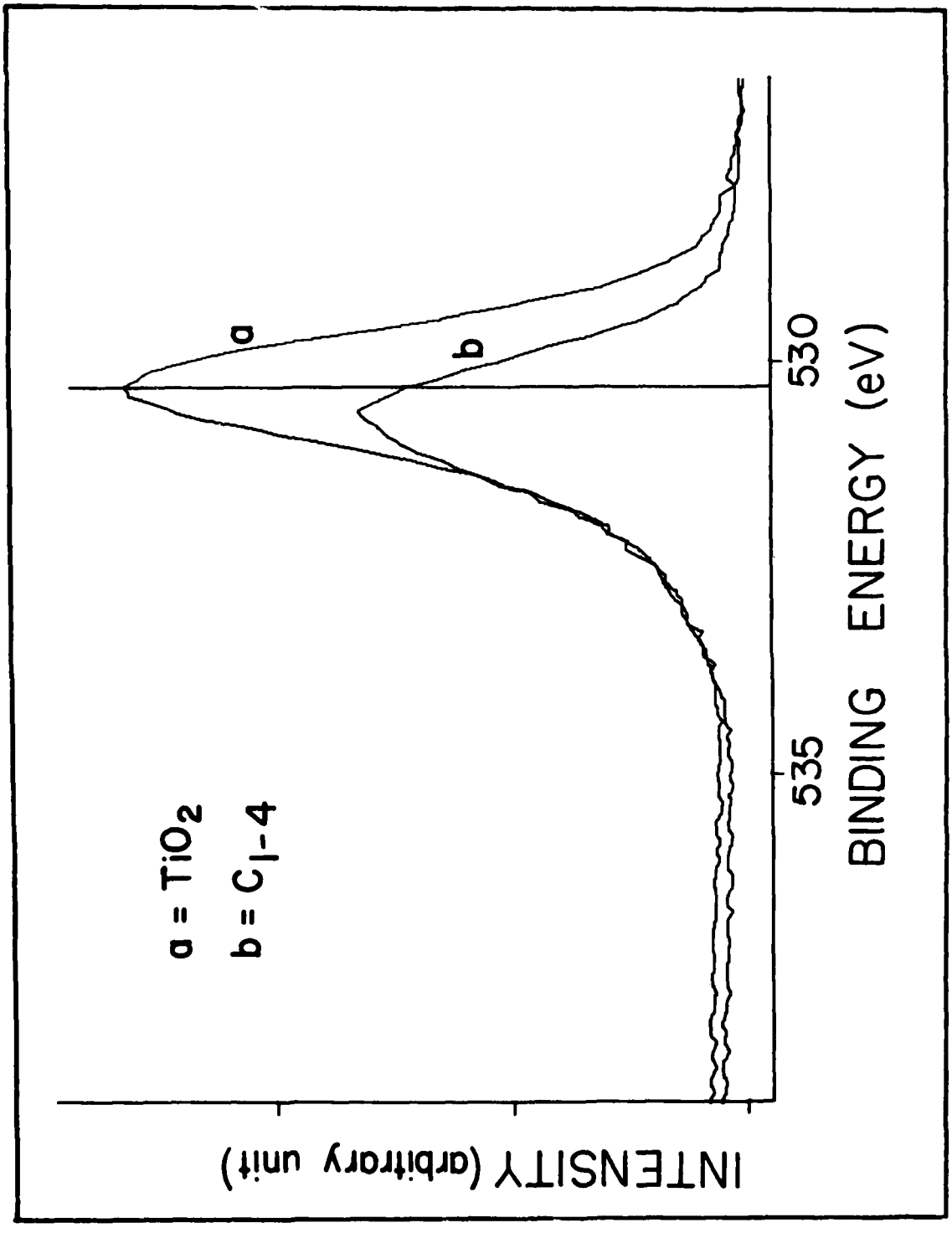

FIG. 105 X.P.S. spectra of O_{1s}: (a) TiO_2 "standard," (b) Ti-6Al-4V subjected to 1-4 treatment

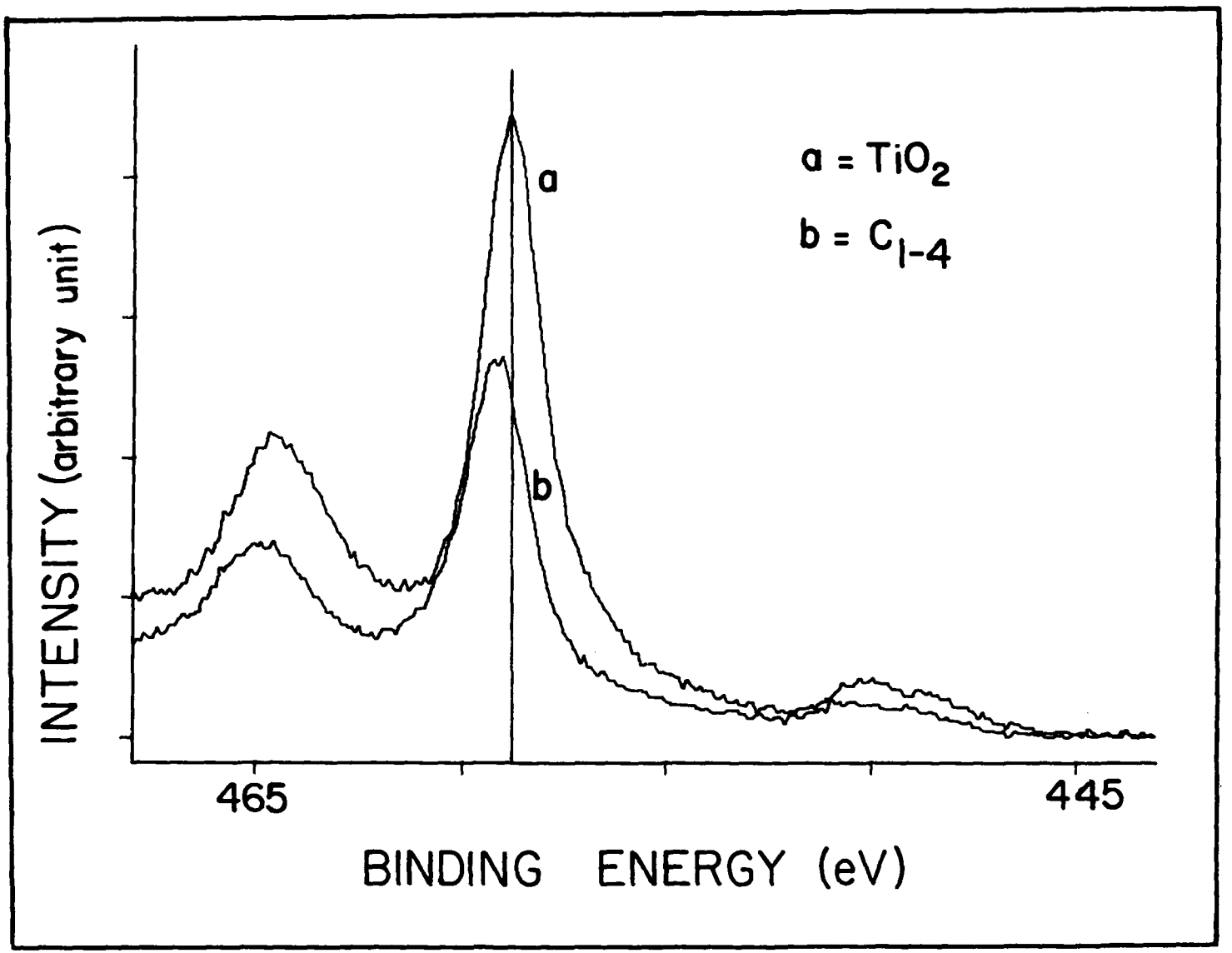

FIG. 106 X.P.S. spectra of Ti_{2p}: (a) TiO_2"standard," (b) Ti-6Al-4V subjected to 1-4 treatment

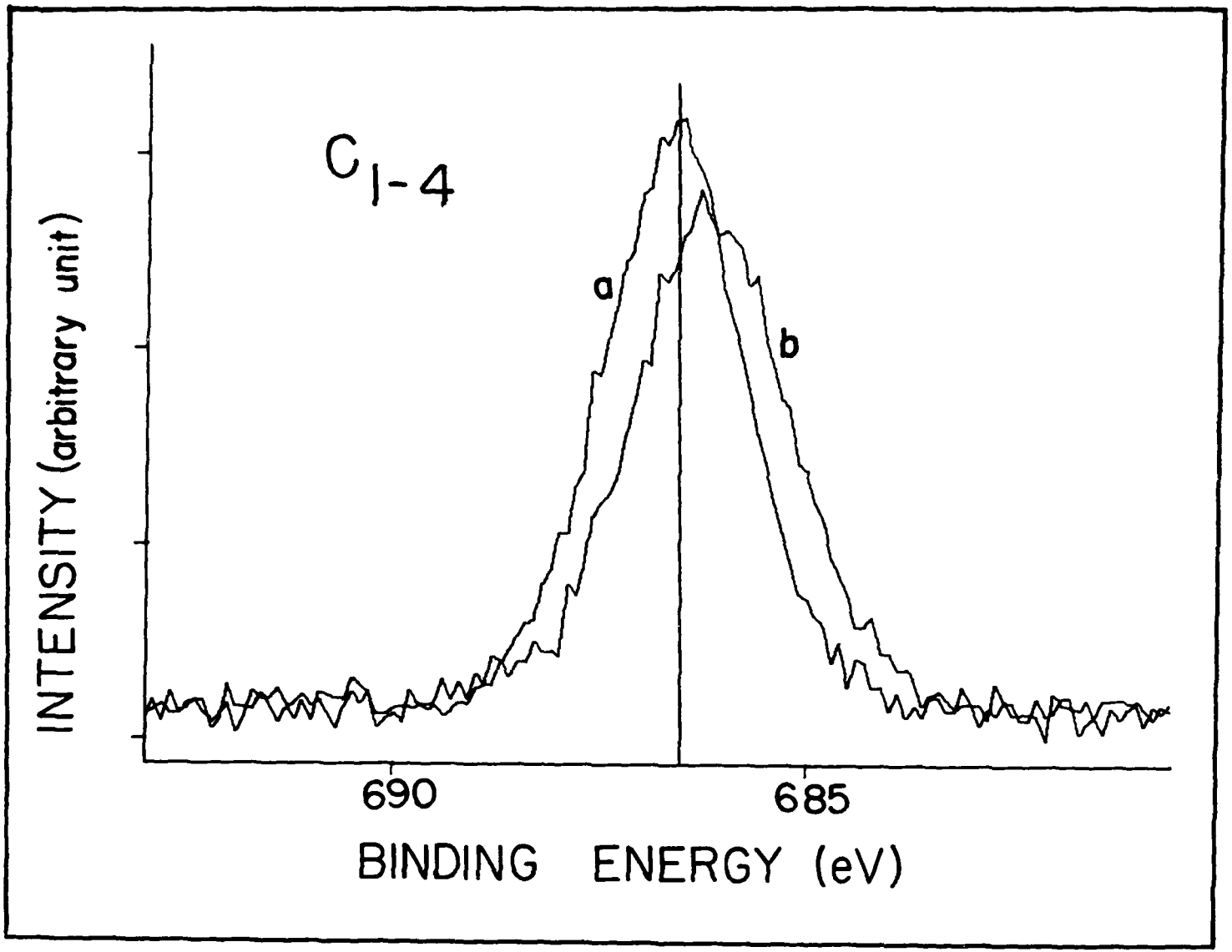

FIG. 107 X.P.S. spectra of F_{1S} from Ti-6Al-4V subjected to 1-4 treatment: (a) on the surface, (b) in the oxide layer

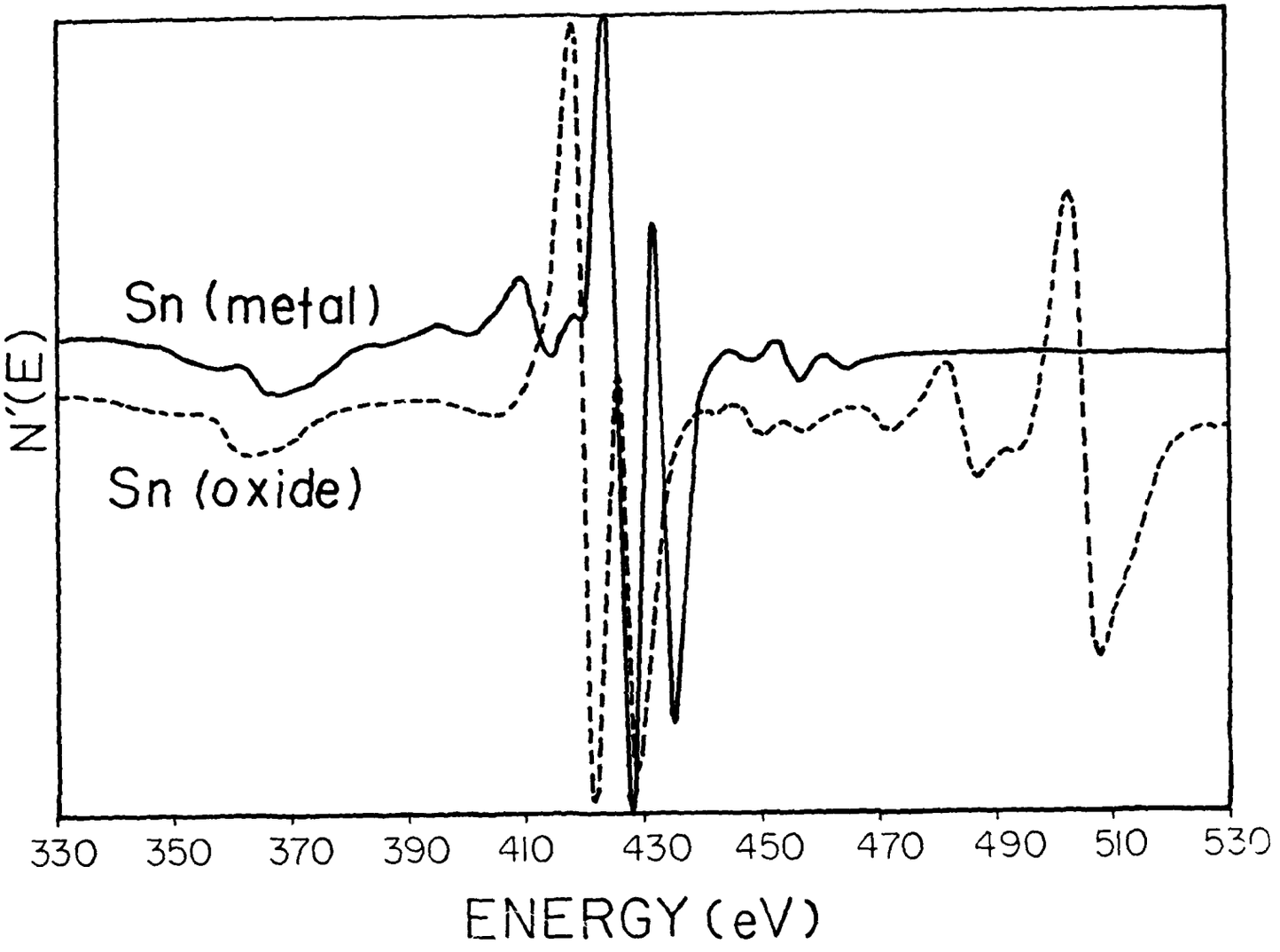

FIG. 108 AES spectra from Sn metal and $C_4H_6O_6$(1M) 20 volts anodized Sn